Copyright Warning & Restrictions

The copyright law of the United States (Title 17, United States Code) governs the making of photocopies or other reproductions of copyrighted material.

Under certain conditions specified in the law, libraries and archives are authorized to furnish a photocopy or other reproduction. One of these specified conditions is that the photocopy or reproduction is not to be "used for any purpose other than private study, scholarship, or research." If a, user makes a request for, or later uses, a photocopy or reproduction for purposes in excess of "fair use" that user may be liable for copyright infringement,

This institution reserves the right to refuse to accept a copying order if, in its judgment, fulfillment of the order would involve violation of copyright law.

Please Note: The author retains the copyright while the New Jersey Institute of Technology reserves the right to distribute this thesis or dissertation

Printing note: If you do not wish to print this page, then select "Pages from: first page # to: last page #" on the print dialog screen

ABSTRACT

METHODS TO IMPROVE THE REMEDIATION OF POLYCYCLIC AROMATIC HYDROCARBONS (PAHs) IN AEROBIC AND ANAEROBIC ENVIRONMENTS

by
Brian Wartell

Oil spills occur regularly in terrestrial environments and crude oil can contain many compounds that are highly resistant to degradation. Among these compounds are high levels of polycyclic aromatic hydrocarbons (PAHs) which are not only toxic but can also be carcinogenic and/or mutagenic. The first chapter of this dissertation includes an extensive review chapter on the variables affecting the anaerobic degradation of hydrocarbons, with a particular focus on PAHs. Electron acceptors, electron donors, temperature, salinity, pH all play key roles in determining the possibility effective of effective degradation occurring. Thus, by addressing solutions, such as biostimulation, improving environmental variables for optimal growth and enzymatic rates, and increasing the supply of the electron acceptors needed for anaerobic respiration help to remove obstacles to biodegradation. Additionally, the use of co-substrates or techniques such as bioaugmentation can further enhance this endeavor.

Aerobic hydrocarbon degradation also has its challenges, especially for complex aromatic compounds such as PAH.s Electrokinetics (EK) is a remediation technology can be used to make species more accessible such as contaminants, nutrients, electrons acceptors, and electron donors. EK technology can be used to migrate certain contaminants but can also greatly enhance the aerobic degradation of PAHs primarily by increasing bioavailability and nutrient delivery.

Studies were conducted to examine differences in electromigration rates for sand and clay. Two dyes, a red dye with anionic properties (FD&C 40) and a green dye with both anionic and cationic properties, composed of turmeric and *Spirulina* Blue were analyzed separately. The component of the green dye found to readily migrate is *Spirulina* Blue, consisting primarily of the protein pigment C-phycocyanin. The red dye in both sand and clay moves towards the anode, as predicted, and the rate between the two media was found to be approximately ten-fold. The green dye, having amphoteric qualities, can accept or donate protons, and can thus become strongly positively or negatively charged depending upon the pH of the system. It was found that due to a shifting pH gradient over time (in sand), this dye was initially anionic and thus migrated towards the anode but ceased migration after 48-72 hours due to a shift to a positive charge. Additional studies were conducted to observe how pH gradients in both sand and soil change over time. It is discovered that the rate at which the pH changes is dependent upon system variables including the current applied, which appears to absent from the literature, and that the initial semi-linear trend does not match the final gradient typically reported.

The final study investigates the potential of EK technology to enhance biodegradation. In order to do so, a sandy soil, spiked with three compounds (fluorene, phenanthrene, fluoranthene) is placed within self-designed electrokinetic setups and an initial experiment shows a high possibility of PAH degradation but is unconfirmable. A second experiment attempts to verify the general findings of the first experiment and employs the use of a surfactant (Brij-35), which is thought to increase microbial movement throughout the contaminated soil and possibly reduce the sorption of PAHs to soil particles, both thereby increasing bioavailability and degradation rates. While biological activity is

very apparent in this experiment, no degradation is observed and this may be due to a presence of carbonaceous materials (i.e. organic matter) within the soil. This yields an additional variable that must be taken into consideration in future in-situ studies or remediation projects.

Overall it is found that many factors need to be taken into consideration for both aerobic and anaerobic biodegradation of PAHs. Increasing favorable growth conditions and increasing bioavailability can greatly help with this endeavor. Electrokinetics is an efficient means of ensuring this takes place but very specific designs or methods may be needed and pH gradients and extremes are found to provide significant obstacles to certain implementation but the results found in these experiments may be helpful to shed light on means of maintaining biological or chemical degradation experiments in an in-situ environment.

METHODS TO IMPROVE THE REMEDIATION OF POLYCYCLIC AROMATIC HYDROCARBONS (PAHS) IN AEROBIC AND ANAEROBIC ENVIRONMENTS

by
Brian Wartell

A Dissertation
Submitted to the Faculty of
New Jersey Institute of Technology
in Partial Fulfillment of the Requirements for the Degree of
Doctor of Philosophy in Environmental Engineering

Department of Civil and Environmental Engineering

December 2018

APPROVAL PAGE

METHODS TO IMPROVE THE REMEDIATION OF POLYCYCLIC AROMATIC HYDROCARBONS (PAHS) IN AEROBIC AND ANAEROBIC ENVIRONMENTS

Brian A. Wartell

Dr. Michel C. Boufadel, Dissertation Advisor — Date
Professor of Civil and Environmental Engineering, NJIT

Dr. Lucia Rodriguez-Freire, Dissertation Co-Advisor — Date
Assistant Professor of Civil and Environmental Engineering, NJIT

Dr. Lisa B. Axe, Committee Member — Date
Professor of Chemical and Materials Engineering, NJIT

Dr. Sunil Saigal, Committee Member — Date
Professor of Civil and Environmental Engineering, NJIT

Dr. Thomas Olenik, Committee Member — Date
Professor of Civil and Environmental Engineering, NJIT

Mr. Stewart Abrams, Committee Member — Date
Vice President and Principal, Langan Engineering

BIOGRAPHICAL SKETCH

Author: Brian A Wartell

Degree: Doctor of Philosophy

Date: December 2018

Undergraduate and Graduate Education:

- Doctor of Philosophy in Environmental Engineering,
  New Jersey Institute of Technology, Newark, NJ, 2018

- Master of Science in Environmental Sciences,
  Rutgers, the State University of New Jersey, New Brunswick, NJ, 2009

- Bachelor of Arts in Biology,
  Brandeis University, Waltham, MA, 2007

Major: Environmental Engineering

Journal Publications:

Brian A. Wartell, Michel C. Boufadel, Lucia Rodriguez-Friere, Lisa Axe. A Review of the Effect of Multiple Variables on the Anaerobic Degradation of Hydrocarbons. *Journal of Hazardous Materials* (pending submission).

Brian A. Wartell, Michel C. Boufadel, Lucia Rodriguez-Friere, Lisa Axe, Stewart Abrams, Ali Ciblak. A Study in Electrokinetic Migration Rates in Sand and in Clay. *Journal of Contaminant Hydrology* (pending submission).

Brian A. Wartell, Michel C. Boufadel, Lucia Rodriguez-Friere, Lisa Axe. The Electromigration of C-Phycocyanin in Sand and the Discovery of Changing pH Profiles over Time. *Journal of Contaminant Hydrology* (pending submission).

Wen Ji, Lin Zhao, Michel C. Boufadel, Kenneth Lee, Cosan Daskiran, Wenxin Ye, **Brian A. Wartell**. Characterizing Turbulent Properties for a WAF Experiment Using Particle Image Velocimetry (in preparation).

Brian A. Wartell., V. Krumins, J. Alt, K. Kang, B.J. Schwab, and D.E. Fennell, 2012. Methane production from horse manure and stall waste with softwood bedding. *Bioresource Technology*, 112, pp.42-50.

Presentations and Conference Proceedings:

Brian A. Wartell, Michel Boufadel. Presentation. The Use of Electrokinetics to Enhance Chemical and Biological Remediation of Contaminated Sands and Soils. International Research Conference: 20th International Conference on Polluted Soil and Groundwater Remediation, WASET. Boston, MA. 2018.

Brian A. Wartell, Donna Fennell. Presentation. Feasibility of Horse Waste Digestion for Renewable Energy. Biocycle's 50th Anniversary International Conference, San Diego, CA. 2009.

Brian A. Wartell, Valdis Krumins, Robin George, Jeffrey Alt, Bryan Schwab, Kathleen Kang, Donna E Fennell. Conference Proceedings. Anaerobic Digestion of Equine Stall Waste. ASABE Annual International Meeting, Providence, RI. 2008.

Brian A. Wartell, Donna Fennell. Presentation. The Effect of Softwood Bedding on Anaerobic Digestion of Equine Waste. The Journal of Solid Waste Technology and Management: 23rd ICSWM, Philadelphia, PA. 2008

Personal Biography:

Brian Wartell has known he has wanted to pursue a career in science since he was a child and has aspired to get a degree with an environmental focus. Brian obtained his Bachelor's in Biology and Brandeis University with a minor in Chemistry and a Concentration in Environmental Studies. He then attend Rutgers University to attain his Master's Degree in Environmental Sciences. After a break of several years, he sought to obtain a Ph.D., which would enable him to meet his overall goal of becoming a research professor.

Brian aims to one day run and manage a University laboratory whereby he can design pollution-remediation and other environmentally-related experiments, while also having the ability to teach, another long-term passion of his.

To my Mother

My rock, my ear, and whom I turn to for advice

To my Father

For his encouragement and support

To my Friends

For their unwavering support, reassurance, and interest

To my Teachers and Professors

I could not have gotten this far without you. Thank you for you wisdom.

ACKNOWLEDGEMENTS

First and foremost, I am forever grateful to Dr. Michel C. Boufadel, my research advisor and mentor, who greatly supported me throughout my PhD studies.

Second, to Dr. Lucia Rodriguez-Freire, my co-advisor, and someone who helped me out immensely if Dr. Boufadel was not available and for providing me with valuable insights. Third, to Marilyn Quiles, for without her hard work with finances paperwork, and so many logistics, my goals could not be achieved.

I would like to thank all of my peers who have been a listening ear and a source of enjoyment and relief when deed, especially Maedeh Soleimanifar, who was immensely helpful in so many ways along my journey.

I am very grateful to the additional members of my doctoral dissertation committee:
Dr. Lisa B. Axe, Dr. Sunil Saigal, Dr. Thomas Olenik, and Dr. Stewart Abrams who generously gave their precious time and expertise to read and improve my work.

I owe so much of this success, of course, to Dr. Donna Fennell, who provided me with invaluable experience while performing Master's Degree research and who helped me along the way with confidence, training, publications, and paving the way towards a Ph.D, as well as being a good friend.

The faculty and staff of the Civil and Environmental Engineering Department and the administrative staff at the New Jersey Institute of Technology are gratefully recognized as well.

TABLE OF CONTENTS

TABLE OF CONTENTS

TABLE OF CONTENTS

Chapter **Page**

TABLE OF CONTENTS

Chapter **Page**

TABLE OF CONTENTS

TABLE OF CONTENTS

Chapter **Page**

TABLE OF CONTENTS

Chapter **Page**

LIST OF TABLES

LIST OF TABLES

LIST OF FIGURES

LIST OF FIGURES

LIST OF FIGURES

LIST OF FIGURES

LIST OF DEFINITIONS

Alternant vs. Non-Alternant Structure	Pertaining to ringed aromatic hydrocarbons, where 'alternant' refers to a compound not containing an odd-membered ring and the molecule can be divided into two sets so that no two atoms of the same set are directly linked.
Amphoteric	Can either accepting or donating protons, thereby causing the compound to function as an acid or base, depending upon the pH
Anhydrous	Not containing water
Bioavailability	The proximal access or ability of an organism to come in contact with a substance, also known as "bioaccessibility".
Biodegradation	The overall process of the breakdown of a compound through biological means
Biofilm	A consortium of bacterial cells joined together, often upon a surface
Bioremediation	The technology of using biological organisms to remediate contaminants
Biostimulation	Increasing the growth or activity of microorganism through chemical means, such as added electrons donor or nutrients
Biotransformation	The processes whereby a substance is changed via biological means
Chemotrophic	Obtaining energy via the oxidation of electrons donors (organic or inorganic molecules)
Current Density	The electrical current flowing per unit cross-sectional area of a medium
Electrokinetics	A remediation technology using an applied current and voltage, comprised of three basic phenomena: Electromigration, Electroosmosis, and Electrophoresis
Electrolysis	The decomposition of water into hydrogen and oxygen via the use of an electrical current
Facultative	Having the ability to operate in a dual-capacity. A facultative aerobe is a primarily anaerobic organism that can function under aerobic conditions.

Flux	The amount of a substance that changes per unit per time via a particular process
Halophilic	Thrives under high-salt conditions
Isoelectric Point	pH at which a molecule carries no net electrical charge, above or below which, it obtains a particular charge or set of charges
Mesophilic	Thrives at warm (~20-40°C) temperatures
Mineralization	The conversion of an organic substance to a basic compound, in reference to degradation, usually referring to CO_2.
Most Probable Number (MPN) test	Designed to give an estimate of the number of organisms of a particular type present
Polarity Reversal	The process of switching the anode and cathode by reversing the outputs from the power supply
Psychrophilic	Thrives at low (< 15°C) temperatures
Recalcitrant	Not easily degraded
Surfactant	A substance possessing hydrophobic and hydrophilic properties that reduces the surface tension of a liquid in which it is dissolved
Terminal Electron Acceptors	A molecule that accepts an electron during chemical oxidation and can function as a supplement. Organisms can obtain energy by transferring electrons from an electron donor to an electron acceptor. A terminal electron acceptor is specifically one that is utilized during cellular respiration or photosynthesis
Thermophilic	Thrives at high (> 40°C) temperatures
Voltage Gradient	The voltage applied over a distance or cross-sectional area
Weathering	A combination of physical and biological process that affects the properties of a substance over time. (Volatile components tend to be most prone to weathering.)
Zeta Potential	The electric potential at the plane where a liquid flows relative to the particle

CHAPTER 1

INTRODUCTION

1.1 The Need for Crude Oil Remediation and the Recalcitrance of Polycyclic Aromatic Hydrocarbons (PAHs)

Crude oil spills and the resulting contamination cause major adverse impact on the environment and the local economy [1]. Crude oil is toxic to both aquatic and terrestrial life and can greatly affect nearly all organisms, ranging from bacteria to large fish, birds, mammals, and even humans [2]. The risk to ecosystems is substantial and the threat to humans is great as many components of crude oil, especially polycyclic aromatic hydrocarbons (PAHs), can be carcinogenic or mutagenic. Even very low levels of some of these contaminants are harmful [3].

Large oil spills in aquatic environments are somewhat infrequent but of immense consequence when they occur [4]. Particular spills of note in salient environments are the Exxon Valdez oil spill in Alaska [5] and the Deepwater Horizon in the Gulf of Mexico [6]. There are also many terrestrial spills that occur on a relatively frequent basis, as a result of transporting oil inland using pipelines, tankers, trucks, and railcars. On average, there are about 10,000 terrestrial oil spills in the United States each year, amassing approximately 40,000 tons of oil. Nearly half (45%) of these spills originate from pipeline bursts and leaks, and 35% of these spills occur at production facilities [7] (see Figure 1.1). Crude oil that is released onto soils and sediments can migrate deep within the sediment column or if in an aquatic environment can be prone to subsequent sedimentation after the oil binds to sediments in the water column and sinks to the bottom of the water body. Many technologies and strategies have been employed to improve remediation and approaches

include removal, isolation, and the transformation or breakdown of the contaminants, known as degradation. Degradation can occur through physical, chemical, or biological means, and often all three play a role. However, techniques that are much less invasive than dredging or soil removal such as chemical oxidation and bioremediation are often preferred [8, 9]. Bioremediation is a technology currently used to remediate PAHs contamination that does not have the limitations that are associated with many other pollutant removal methods [10], namely it is often more economical, less disruptive, more eco-friendly, and generally safer than traditional methods [11] such as chemical or physical methods [12]. In place of bioremediation, the term "biodegradation" is often used, and this term specifically refers to the process of degradation taking place rather than the overall approach or technique.

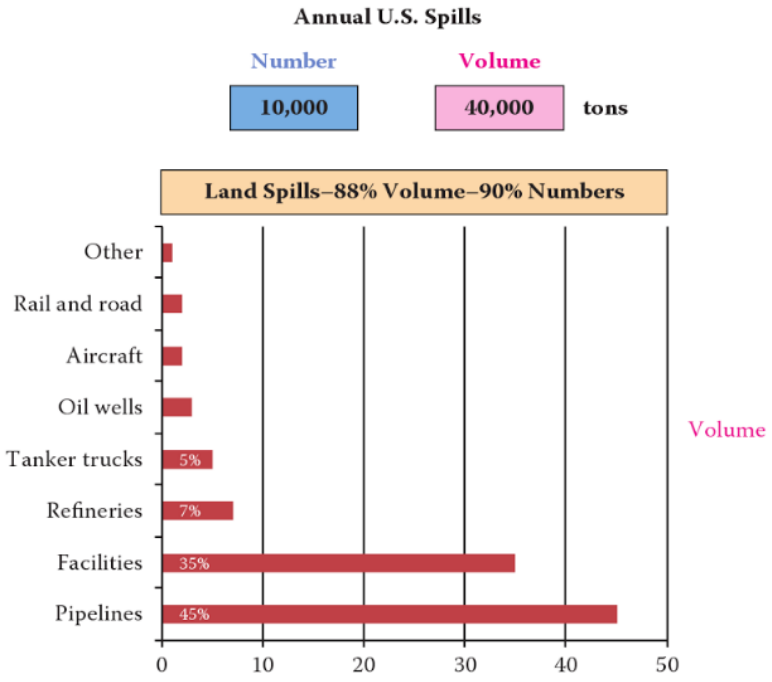

Figure 1.1 Representation of average spill types for the United States per year.
Source: [7]

A common component of crude oils are polycyclic aromatic hydrocarbons (PAHs). PAHs are a class of organic compound consisting of two or more fused benzene rings and at times, also pentacyclic molecules, arranged in various structural configurations (Figure 1.2). PAHs in the environment tend to be highly recalcitrant, especially under anaerobic conditions and can persist for long periods of time in an environment due to their hydrophobic nature, adsorption properties and low solubility [13, 14]. As a result of this, PAHs tend of accumulate more in sediments than in water [15, 16] and in order for PAH degradation to occur most efficiently, it must take place in the aqueous phase [17], which can often not be the case if sorbed to deep soil or sediment particles. PAHs constitute a few percent of oils, but due to their toxic nature, a lot of effort has been dedicated to understanding their biotransformation in the environment [18]. PAHs are also used or are byproducts of numerous industrial processes including wood treatment sites [14, 19]. More than 1,000 dry metric tons of hazardous sludge waste are produced annually by wood treatment plants and one of the primary hazards is coal tar creosote, consisting of approximately 85% PAH by composition [20]. Van Zuydam [21] cites a study of contaminated soil resulting from wood treatment facilities and electricity production facilities where PAHs such as anthracene, fluorene, naphthalene and fluoranthene were found at levels as high as 0.64 mg/kg (0.1 mg/kg is the EPA limit).

PAH structure can be crucially important when determining biodegradability. Factors influencing biodegradability and solubility include the number of rings [17, 22] (typically, as the number of (benzene) rings increases, the solubility of the PAH decreases [23]) as well as the angularity vs linearity of the molecule, alternant vs. non-alternant structure, planarity, symmetry, and the presence and location of substituents [17]. Planar

PAHs tend to be less reactive (i.e., less soluble) than non- planar PAHs [24]. Alternant PAHs that are symmetrical and planar often require a relatively high energy of solubilization due to their ability to fit closely in a lattice and therefore tend to be less soluble [22].

PAHs tend to have a high adsorption coefficient and the adsorption capacity has been shown to increase for compounds like phenanthrene with decreasing sediment particle size [25, 26]. Consequently, PAHs tend to be prone to sequestration, thereby limiting bioavailability [17]. Bioavailability is defined herein as the direct access to the molecule to be degraded by a microorganism [27]. The variables affecting organism-contaminant interactions include the chemical and physical properties of a PAH molecule and are highly dependent upon the specific organism that can be species-specific [28, 29]. For example, a particular strain may not contain the appropriate enzyme to alter a PAH's structure, or a consortium of different microorganisms may lack the enzymatic diversity to fully mineralize the contaminants [30]. The toxicity of a particular PAH may also reduce the functionality of the proteins that produce the necessary enzymes [31]. Seasonal factors such as temperature and moisture content can also affect the ease at which the PAH molecule can be accessed or utilized [30]. PAHs are also more readily degraded by certain microbial populations, such as those adapted to the ongoing presence of PAHs and hydrocarbons. This depends upon enzymatic abilities, previous exposure to PAHs and hydrocarbons, tolerance to toxicity, and feasible pathways [10]. PAHs may also not be degraded due to insufficient nutrients or electron acceptors present for microorganism growth or needed metabolic activity [17]. Colder soil (underground) temperatures may severely limit microbial or enzymatic activity [32] (although to what extent is debated [33])

and soil pH not only affects microbial activity and growth [34] but can also influence the mobility of metals and nutrients [35].

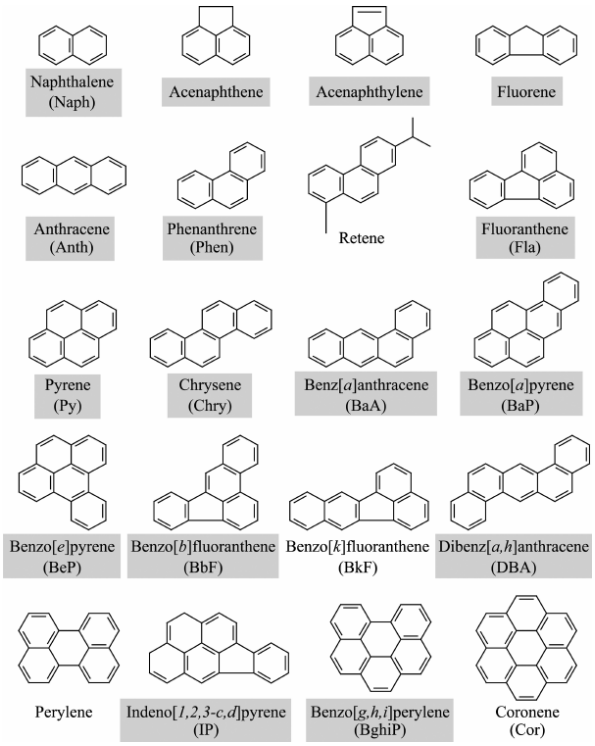

Figure 1.2 Configurations of common Polycyclic Aromatic Hydrocarbon (PAH) compounds.
Source: [36]

Most PAHs can be readily biodegraded under aerobic conditions (i.e., in the presence of oxygen), if sufficiently high concentration of nutrients are available [37, 38]. Bacteria tend to prefer aerobic conditions for PAH degradation of PAHs and often do so via oxygenase-based metabolism (using either a monooxygenase or dioxygenase enzyme)[10] , which leads to intermediates that eventually are often mineralized to CO_2 (Figure 1.3), or simple hydrocarbons including metabolic compounds such as pyruvate or succinate [39]. However, there are many factors that can limit the success of aerobic

biodegradation including low bacterial populations or diversity and other variables that affect growth and metabolic rates (e.g., temperature, oxygen levels). Additionally, there are difficulties of both nutrient transport and bioavailability of the contaminants to the organisms, especially if the PAHs are not in the aqueous phase where the bacteria are primarily located [40]. Because of their recalcitrance and resistance to degradation, PAHs may persist for long periods of time in an environment. This is especially due to their hydrophobic nature, adsorption properties and low solubility [13, 14] and therefore are difficult to remediate even with current chemical and biological techniques.

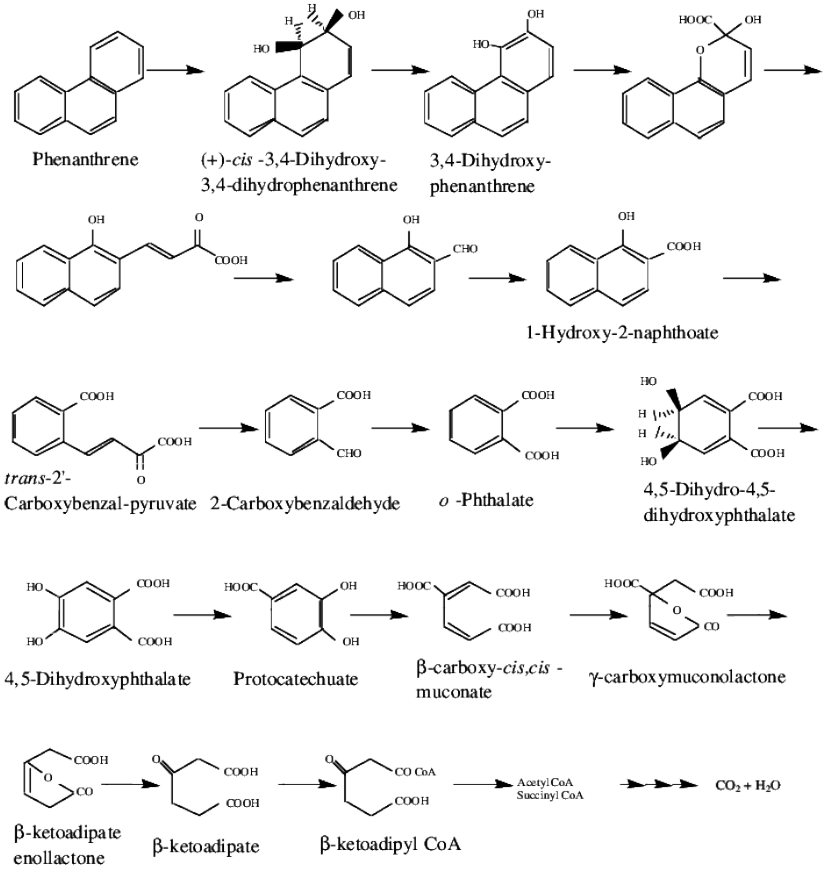

Figure 1.3 A degradation (catabolic) pathway of phenanthrene via the aerobic organism *Nocardioides* sp. KP7.
Source: [41].

1.2 Increased Recalcitrance under Anaerobic Conditions

Although most PAHs can be degraded relatively quickly under aerobic conditions, in an anaerobic environment (i.e., lacking oxygen), such as deeply-buried oil, PAHs could reside for decades or longer [42]. The organisms present in deep soils and sands are largely anaerobic bacteria and archaea, and research has shown that they have the ability to degrade certain oil components (alkanes, single ring aromatics, and some two-ring aromatics). However, they have not been shown to readily biodegrade most polycyclic aromatic hydrocarbons (PAHs) [43]. In part, this is due to more selective and slower enzymatic processes than those used by aerobic organisms [44]. Yet, many researchers claim that bioavailability is often the primary obstacle to anaerobic degradation [45]. This is due to the inability of the typical enzymes used by these organisms to effectively utilize "aged" PAHs [46]. The aging of PAHs is defined as the reaction over time with soil components and the formation of covalent bonds and subsequent complexes [47].

Anaerobic bacteria are chemotrophic organisms (utilize chemical energy) that derive energy from the coupling of oxidation and reduction (redox) reactions. These reactions stimulate phosphorylation (electron transport and substrate-level) yielding the formation of ATP, providing the microorganisms with energy [48]. Anaerobic bacteria specifically utilize alternative terminal electron acceptors such as sulfate, nitrate, iron, or manganese, in lieu of oxygen [49] and can utilize organic or inorganic substrates as electron donors. PAHs are carbon-based organic molecules and can therefore be utilized as one of these substrates [17].

Successful anaerobic degradation of PAHs has been largely limited to compounds containing three or fewer rings. One membered-ring compounds such as benzene and toluene have been shown to degrade under a wide variety of anaerobic conditions and

numerous studies have cited the ability of anaerobic bacteria to degrade biphenyl, naphthalene and 2-methylnaphthalene [44, 50], although 1-methylnaphthalene has proven to be more recalcitrant [17]. These compounds, as well as phenanthrene are capable of being utilized as a sole carbon source under anoxic and often, anaerobic conditions [44]. Among PAHs containing three rings, phenanthrene has been the most successfully degraded and often the only compound to be mostly degraded under sulfate-reducing conditions [46]. One of the exceptions is Tsai et al. [51] who observed 88% and 65% degradation of fluorene and phenanthrene, respectively, under sulfate-reducing conditions. They noted, however, that degradation rates were reduced when these PAHs were combined.

With the exception of phenanthrene, the number of studies reporting successful biodegradation of three-ringed PAHs are still relatively few and when it does take place, is often under artificially-induced lab conditions or at a very slow degradation rate [44, 52]. Reports of PAHs containing four or more rings being degraded under anaerobic conditions are even scarcer, though they do occur. Some of this degradation occurs via facultative anaerobes (i.e., aerobic bacteria active under anaerobic conditions) such as several *Mycobacterium* species [53] reports which are capable of transforming pyrene and benzo[a]pyrene [53]. A summary of experiments demonstrating anaerobic PAH degradation potential is seen in Table 1.1. The addition of specific co-substrates and electron donors (biostimulation) has been suggested in order to bolster the ability of anaerobic degradation to succeed in a realistic time-frame [54]. The presence of these compounds improves microbial growth and can activate necessary enzymes [55], thereby reducing the lag phase and improving overall degradation rates [56]. However, the

implementation of these stimulants as well as nutrients is often quite difficult in *in-situ* environments due to accurate delivery and the subsequent lack of availability of these compounds to the organisms [57].

Table 1.1 A Summary of Anaerobic Degradation (>50%) of PAHs Containing Three or More Rings (excluding phenanthrene)

Compound	# of Rings	Percent Degraded	Source
Fluorene	3	100%	[58]
Fluorene	3	88%	[51, 58]
Fluorene	3	30-60%	[59, 60]
Anthracene	3	100%	[61]
Anthracene	3	34 - 55%	[62]
Fluoranthene	4	100%	[58, 63-65]
Pyrene	4	100%	[51, 60]
Pyrene	4	30-70%	[59]
Pyrene	4	95%*	[66]
Various	3-4	59 - 92%	[67]
Various	3-4	>80%	[68]
Benzo[a]pyrene	5	70-84.2%	[63-65]

*Conducted under artificial conditions in a microbial fuel cell (MFC)

1.3 Basics of Electrokinetics and Its Usage to Enhance Biodegradation

Both aerobic and anaerobic biodegradation of PAHs encounter the difficulties of both nutrient transport and bioavailability (proximal access) to the organisms of the contaminants. Many studies have claimed that bioavailability is the primary obstacle to anaerobic degradation of PAHs but also plays a major role in the extent of degradation under aerobic conditions [45, 46]. A recently developed technology, known as electrokinetics (EK or EK-BIO for "electrokinetic bioremediation") has been found to transport efficiently nutrients or other chemicals in the subsurface (see Chapters 3-7).

Electrokinetics can further enhance bioremediation and be used as an effective tool to enhance degradation rates and its efficiency [69]. Electrokinetics is a remediation technology defined by the implementation of a direct current applied to or within subsurface porous media in order to prompt specific forms of transport. The core principles by which it works are: Electromigration, electroosmosis, and electrophoresis [70].

Electromigration is the movement of ions due to the presence of the applied electric current. This process directs the negatively charge ions towards the anode and positively charged ions towards the cathode. Electroosmosis is the bulk movement of fluid through pores and occurs when a direct current is applied to a media containing some charge, such as most soils. In most soils, which carry an overall negative charge due to the presence of clay particles, a double boundary layer is formed and the fluid in the soil flows from anode to cathode. If a media were to possess a positive charge, the flow would be in the reverse direction [71]. Electrophoresis is the movement of charged colloidal particles (dissolved or suspended) in the pore fluid [57] and is dependent upon their electric charge or zeta potential, where zeta potential is defined as the electric potential at the plane where the liquid flows relative to the particle [57, 72]. Electrophoresis can also be used to transport microorganisms throughout the media and can therefore greatly enhance bioavailability [73].

An electrokinetic system operates by utilizing the electrochemical differential between an anode and a cathode and electrolysis occurs via the following reactions (Equations 1.1 and 1.2).

$$2H_2O - 4e^- \rightarrow O_2 + 4H^+ \quad (1.1)$$

$$2H_2O + 2e^- \rightarrow H_2 + 2OH^- \quad (1.2)$$

For bioremediation purposes, electrokinetics can effectively make contaminants, nutrients, electrons acceptors, and electron donors more accessible by causing them to flow and spread throughout the media [74] However, the rate at which compounds are transport relies heavily on the nature of the compound of interest as well as the media through which it is being transported [75].

One example of successful degradation enhancement via EK is a study by Xu et al. [76] who used electrokinetic processes to circulate key nutrients (e.g., nitrate, ammonium) throughout the system and a series of polarity reversals to keep pH values balances. The EK apparatus cell consisted of a polyethylene cylindrical chambers in which natural soil was placed and two similar chambers functioning as the anodic and cathodic chambers, respectively were placed on either end. At each of the two junctions, a graphite plate of 5 mm thickness was placed, functioning as an electrode and the system was connected to a direct current power supply, to which was also connected a pumping system. The combination of the electric current and the pumping system allowed for greater distribution of the nutrients. In their experiment, they observed 70-90% degradation of phenanthrene (200 mg/kg) in 20 days ($k \approx .04\ d^{-1}$), a faster degradation rate than reported for many similar non-EK experiments [77, 78].

Electrokinetic technology can also be used to help remediate anaerobic environment, primarily by generating an aerobic system [79]. Aerobic biodegradation is far more efficient and versatile than anaerobic biodegradation [80] and there are more thermodynamically favorable ways for biodegradation of the PAHs to take place [79].

Degradation under anaerobic conditions, if it occurs, can be have degradation rates of at least a magnitude lower than under aerobic conditions [34, 81]. Electrolysis at the anode (Equation 1.1) produces oxygen gas (O_2) and can be used as a means to ensure sufficient aeration if the system is already aerobic. In order to convert an aerobic system to anaerobic, oxygenating compounds, such as peroxide can be injected into the system and transported via electrokinetic processes [82].

1.4 Use of Surfactants

For both aerobic and anaerobic systems, physical obstacles such as nutrient and contamination migration as well as bioaccessibility pose large barriers to the effectiveness of biodegradation that actually takes place. Surfactants have been proposed to aid with this as they can help mobilize both the contaminant and the nutrients [83, 84]. Surfactants are amphiphilic, specifically possessing a hydrophilic tail and a hydrophobic head. These qualities cause a reduction in surface tension and can increase PAH mobility (e.g., in soil) [85]. Surfactants often form micelles, (a collection of surfactant molecules aggregated in water, forming a spherical shape) [86]. Micelle formation enables PAHs to partition within the micelle's hydrophobic core thereby increasing the solubility of these hydrocarbons in the liquid phase [87].

Research studies on PAH-contaminated soil suggest that use of surfactants is most beneficial when biodegradation is limited by poor bioavailability. The use of surfactants in soils has shown to enhance PAH bioavailability [88] and certain surfactants can increase degradation efficiency and reduce the time required for complete biodegradation to occur. [87]. The ability of surfactants to remove PAHs from soils has been known for decades, an example of which is Bourbonais et al. [89] who found that the use of an anionic

surfactant and anionic/non-ionic blend increased PAH recovery above basic flushing techniques by 49 to 99% and 80 to 90%, respectively. The use of surfactants in electrokinetic systems was demonstrated to assist in the removal of phenol from porous media. Cicek and Govind [90] reported 92% and 99% removal using the cationic surfactant CTAC in kaolin clay and silica sand, respectively and 85-90% removal from silica sand using the non-ionic surfactant Triton-X [91]. Niqui-Arroyo and Ortega-Calvo [92] demonstrated that the implementation of a nonionic surfactant (Brij 35) in an electrokinetic setup increased creosote biodegradation from 79% to 90%. Even without the aid of a surfactant, electrokinetic phenomena alone were able to increase bioavailability and improve degradation rates approximately four-fold (~20% to 79%).

An additional benefit of the use of surfactants is that is resolves the issue of microbes tending to attach to sediment and organic matter particles (which can reduce bacterial transport) [57]. Due to a surfactant's surface-active properties, the bacterial attachment to porous media (e.g., soil) can be reduced by altering the steric, electrostatic, and hydrophobic interactions between the organism's cell surface and the media. This often generates a partial repulsion between the bacteria and the media grains, enabling enhanced transport of bacteria [93]. Wick et al. [94] found that Brij 35 enhanced electrokinetic dispersion of bacteria as much as 80%. Brij 35, like many other nonionic surfactants, has the particular advantage that it is essentially nontoxic to most PAH-degrading microorganisms [95]. Yet, surfactant efficiency for the desorption of PAHs is highly dependent upon soil composition, PAH properties, and the surfactant's structure [96] as well as the degradation ability prior to surfactant use and the organisms' sensitivity to the presence of the surfactant [88]. PAH desorption will only be sufficiently enhanced,

however, if the surfactant concentration exceeds the critical desorption concentration (CDC). The CDC is defined as the specific surfactant concentration PAH desorption is equal to the initial desorption in water [96]. Surfactants are also more effective at desorbing PAHs soils when they possess a higher organic carbon content and a lower clay content [96].

1.5 Objectives

The primary objective of this Ph.D. research was to establish an understanding of the electrokinetic process and study its use in improving physical, chemical, and biological conditions under which bacteria can degrade designated three-ringed PAHs (fluorene, phenanthrene, fluoranthene) to a significant degree and short time frame. The research focused predominantly upon aerobic systems and utilized both soil and sand media although an extensive literature review on anaerobic hydrocarbon degradation was performed as well and is present as Chapter 2.

The secondary objectives of this research were:

1) To investigate different rates of electrokinetic phenomena, primarily electromigration, and to compare dyes with different charge properties and how their migration rates changed accordingly (Chapters 4-5).

2) To look at pH gradients within an electrokinetic system and how they change over time and the effects of polarity reversals and other mitigating factors (Chapters 4-5).

3) To investigate whether the electrokinetic process, both with and without the aid of a surfactant, would enhance bioavailability of the PAHs present (fluorene, phenanthrene, fluoranthene) and its effect on the extent of biodegradation of these compounds (Chapters 6-7).

4) To improve electrokinetic methods to more effectively deliver electron donors, nutrients, and surfactant to the target organisms in the system (see Chapters 6-7).

5) To investigate the effectiveness of electrokinetics to convert an anaerobic environment aerobic through the use of peroxide (see Appendix).

CHAPTER 2

A REVIEW OF THE EFFECT OF MULTIPLE VARIABLES ON THE ANAEROBIC DEGRADATION OF HYDROCARBONS

2.1 Background

Oil spills are becoming more frequent in both marine and terrestrial environments due to increased exploration and growing demand [97]. According to a data contained within the Energy-Related Severe Accident Database (ENSAD) between 1974 and 2010 there were 1213 spill incidents yielding a total of 9.8 million tons of oil. Although fewer in number of incidences, oil spills as a result of exploration and production caused great release oil into the environment than pipelines, storage, or refineries. Among these, the greatest oil release was due to tanker spills, accounting for approximately 75% of the total spills by volume over this time period. In addition, there were 888 ship incidents, 113 storage and refinery spills, and 118 pipeline leaks and bursts, resulting in the release of 6,000,000 tons of oil, 870,000 tons of oil, and 750,000 tons of oil, respectively [98, 99]. The vast majority of oil spills specifically release crude oils into the environment [98]. The composition of crude oil is highly variable and is the most complex type of oil [100]. It can contain thousands or even tens of thousands of different hydrocarbon compounds [101, 102]. Due to the toxicity and difficulty to remediate these compounds, enhanced biodegradation was proposed as a solution because it is a process occurring naturally in many environments [103, 104].

Oil pollution can seep far into the subsurface, including sediment columns or beach shorelines [105] . While oil components often biodegrade aerobically readily (within a year), deeply buried oil could reside in an anaerobic environment (i.e., lacking oxygen) for

decades [38, 106]. The organisms present in these environments are largely anaerobic bacteria and archaea, and research has shown that they have the ability to degrade certain oil components (alkanes and single ring aromatics) [107]. However, they have not been shown to readily biodegrade many complex hydrocarbons, including most polycyclic aromatic hydrocarbons (PAHs) [108]. PAHs are a common component of crude oil, especially "heavier" oils, and are especially resistant to degradation under anaerobic conditions [109]. They tend to accumulate and persist and there is much interest in their removal due to their potentially harmful effects to both environmental and human health [110]. Although biodegradation is a cost-effective and less intrusive means of remediation than most alternatives [111], anaerobic degradation is often slow, has reduced enzymatic capabilities, is more prone to nutrient limitation and the pathways are often poorly understood.

The ability of anaerobic organisms to degrade hydrocarbons was elucidated in the 1980s but reports of hydrocarbon degradation in the absence of oxygen have appeared regularly since the 1940s [112, 113]. Anaerobic bacteria utilize alternative electron acceptors such as sulfate, nitrate, iron, manganese, or carbon dioxide [114] (Figure 2.1). Anaerobic bacteria have also been found to utilize uncommon electron acceptors such as vanadium, cobalt, and even uranium [115]. The electron acceptors are converted to a reduced form, and this reduction helps provide for the metabolism and/or respiration of the organism [49]. Sulfate-reduction appears to be the most successful anaerobic process in degrading complex hydrocarbons such as polycyclic aromatic hydrocarbons (PAHs) [51, 116] though successful biodegradation of these and other hydrocarbons has also been shown under nitrate-reducing and iron-reducing conditions [117].

Despite having a lower redox potential and Gibbs Energy value than denitrification or iron-reduction (Tables 2.1 and 2.5), sulfate-reduction appears to be more successful largely due to the diverse enzymatic capabilities associated with sulfate-reducing bacteria [118]. Under sulfate-reducing conditions, compounds that have been shown to be degraded include cycloalkanes [119], phenols [120], and at times, multi-ringed compounds such as phenanthrene and anthracene [44], which were long-thought to be resistant to degradation [121, 122]. The following sections present a comprehensive review of the current knowledge pertaining to the biodegradation of hydrocarbons under anaerobic conditions. The aim of this review is to highlight key factors affecting the extent of degradation, the variables involved, and understanding potential methods to optimize the remediation of complex hydrocarbons.

This compendium of data is of importance as it is more comprehensive than many other similar reviews. Many articles recently published on this subject focus on pathways, molecular approaches, or tend to be environment or compound-specific. There are numerous review papers focusing only upon alkanes or only PAHs and many focus solely on remediation in soil or seawater. The few papers that are quite broad in their scopes have not been categorized or focused in the specific method which this paper is organized. Additionally, the bulk of these papers have been published over five, and many times over ten years ago with very few appearing in the last several years, and therefore an update is warranted. Examples of successful hydrocarbon degradation under various conditions are shown in Table 2.2.

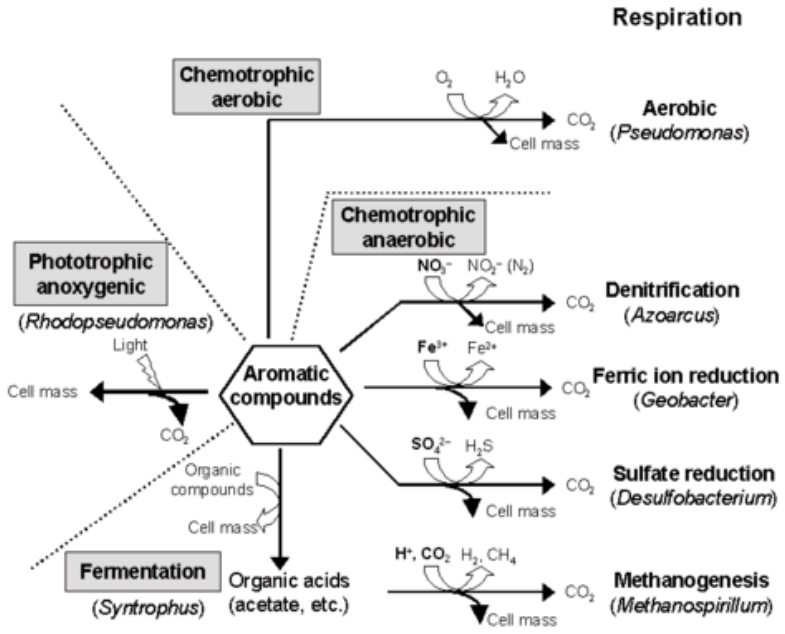

Figure 2.1 Respiration mechanisms for bacterial degradation of aromatic pollutants. *Source*:[123].

Table 2.1 The Utilization of Electron Acceptors in Soils, Equilibrium Potentials, and Measured Potentials of These Reactions in Soils

Reaction	*Eh* at pH 7 (V)	Measured Redox Potential in Soils (V)
O_2 disappearance		
$\frac{1}{2}\,O_2 + 2e^- + 2H^+ = H_2O$	0.82	0.6 to 0.4
NO_3^- disappearance		
$NO_3^- + 2e^- + 2H^+ = NO_2^- + H_2O$	0.54	0.5 to 0.2
Mn^{2+} formation		
$MnO_2 + 2e^- + 4H^+ = Mn^{2+} + 2H_2O$	0.4	0.4 to 0.2
Fe^{2+} formation		
$FeOOH + e^- + 3H^+ = Fe^{2+} + 2H_2O$	0.17	0.3 to 0.1
HS^- formation		
$SO_4^- + 9H^+ + 6e^- = HS^- + 4H_2O$	−0.16	0 to −0.15
H_2 formation		
$H^+ + e^- = \frac{1}{2}H_2$	−0.41	−0.15 to −0.22
CH_4 formation (example of fermentation)		
$(CH_2O)_n = n/2\ CO_2 + n/2\ CH_4$	,,	−0.15 to −0.22

Source: [124].

Table 2.2 Examples of Conditions for Anaerobic Hydrocarbon Degradation and Representative Organisms

Source of Organisms and/ or Contaminants	Representative Organisms	Classification	Respiration Type	Source
Soil from former coal gasification site	Consortium (incl. *Peptococcaceae (Pelotomaculum)* , *Clostridiacae*, *Syntrophaceae*, *Desulfotomaculum*)	Family (Genus)	Sulfate-reducing	[125]
Gasoline contaminated site	Not specified	-	Sulfate-reducing	[126]
Petroleum- contaminated harbor sediments	Not specified	-	Sulfate-reducing	[58]
Wastewater sludge	Not specified	-	Sulfate-reducing	[127]
PAH-adapted consortium from river sediment	Not specified	-	Sulfate-reducing	[67]
Marine sediments	Not specified	-	Sulfate-reducing	[128]
Coal tar waste bioremediation site	Deltaproteobacteria (incl. *Desulfotomaculum, desulfobactrium, desulfobacula*	Class (Genus)	Sulfate-reducing	[129]
Coal tar waste bioremediation site	Betaproteobacteria (incl. *Thauera aromatica* which is a *pseudomonad* strain, *azoarcus, mangetospirillum*)	Class (Genus)	Nitrate-reducing	[129]
Artificial	*Betaproteobacteria* (hxn1, ocn1), *Gammaproteobacteria* (hdn1)	Class	Nitrate-reducing	[130, 131]
PAH-polluted soil and sediment w/ sludge	Not specified		Nitrate-reducing, iron-reducing, sulfate-reducing, manganese-reducing	[131]
Two distinct sites: former gas station, clean freshwater swamp	Not specified	-	Nitrate-reducing	[102, 132]
Unknown	Ebn1, related to *thauera,* (other strains tested didn't grow on ethylbenzene)	Genus	Nitrate-reducing	[133]
N/A - Review article	*Azoarcus, thauera, magnetospirillum*	Genus	Nitrate-reducing	[134]
N/A - Review article	*Georgfuchsia toluolica*	Species	Nitrate, Fe(III), or Mn(IV) or toluene reducing	[134]
Contaminated marine sediment	Unidentified, related to *Pseudomonas*	-	Nitrate-reducing	[77, 135, 136]
PAH-contaminated river sediment	Strain M-1, related to *Paracoccus denitrificans*	Genus	Nitrate-reducing	[136]
PAH-contaminated river sediment	Many, mostly Beta and Gamma Proteobacteria	Genus, Species	Nitrate-reducing	[137]
Spiked contaminated river sediment	Not specified	-	Nitrate-reducing, Sulfate-reducing, methanogenic	[68]

Spiked contaminated river sediment	*Pseudomonas* (facultative anaerobe)	Genus	Nitrate-reducing, sulfate-reducing	[138]
Contaminated river sediment	Too many to list	Genus, Species	Nitrate-reducing, sulfate-reducing	[139]
Contaminated river sediment	Unidentified Alpha-Proteobacterium (related to Phyllobacteriaceae*; Parvibaculum*), *psuedomonas stutzeri, psuedomonas* sp. 42, *ochrobactum anthropi, thauera* sp., *rhizobium*	Genus, Species	Nitrate-reducing, Sulfate-reducing, methanogenic	[140]
Artificial	*Aromatoleum aromaticum* ebn1, *Georgfuchsia toluolica* G5G6, and an *Azoarcus*-dominated mixed culture	Genus, Species	Nitrate-reducing, iron-reducing, manganese-reducing	[141]
Marine sediments	*Desulfuromonas palmitatis*	Genus, Species	Iron-reducing, sulfate-reducing	[142]
Enrichment culture	*Peptococcaceae,* Deltaproteobacteria, *actinobacteria, clostridia, desulfobulbaceae*	Phylum, Class, Family	Iron-reducing	[143, 144]
Multiple sources	Too many to list	-	Syntrophic relationships (incl. SRB, methanogens)	[144]
Enrichment culture	Peptococcaceae, - similarities to *Aromatoleum aromaticum* and *Geobacter metallireducens*	Family	Iron-reducing	[145]
Contaminated paddy soil	Bacillaceae, Peptococcaceae, and *Methanobacterium*	Family	Iron-reducing	[146, 147]
Former manufacturing and gas plant site	Unidentified gram-positive "N49" from Peptococcaceae family similar to *Thermincola carboxydiphila* , (also cites *Geobacter, Desulfitobacterium, Georgfuchsia,* Peptococcaceae)	Family	Iron-reducing	[147]
Enrichment culture	Thermoanaerobacteraceae	Family	Iron-reducing	[148]
Spiked field soil - artificial conditions	*Geobacter* spp. And GOUTA19 spp.	Genus	Iron-reducing, sulfate-reducing	[149]
Spiked contaminated river sediment	*Methylotenera, Gallionella, Ralstonia, Dechloromonas, Desulfobacterium, Geobacter, Syntrophobacter, Desulfovirga, unknown Gammaproteobacteria, Acidobacteria, Chlorobi, Chloroflexi, Clostridium, Verrucomicrobia, Bacteroidetes, Planctomycetes, Nitrospira*	Genus	Iron-reducing	[66]
Spiked river sediment	Not specified	-	Manganese-reducing	[150-152]
Colomac Mine groundwater	*Pseudomonas, thiobacillus, geobacter*	Genus	Manganese-reducing (cold temperature)	[152]
Marine sediment	*Desulfobacterales*, organisms related to *Clostridiales*	Genus	Multiple, co-substrate usage	[54]
Petroleum contaminated soil	Mostly Gamma-Proteobacteria primarily *Escherichia*	Genus	Multiple, co-substrate usage	[153, 154]
Contaminated wastewater	Organisms related to *Syntrophus* and *Smithella*	Genus	Methanogens, co-substrate usage	[154]

Petrochemical effluent	*Pseudomonas fluorescens, Haemophilus* sp., and some unidentified strains	Genus, Species	Multiple, co-substrate usage	[155]
Mangrove sediment	*Clostridium pascui*	Species	Multiple, co-substrate usage	[156]
Unspecified	Geobacter, *Geothrix,* and *Wolinella*	Genus	Multiple, humic substances usage	[157]
Hydrocarbon seeps	*Esulfovibrio* spp., *desulfonatronum* spp., *desulforhabdus* spp., and *desulfotomaculum* spp. At 40°c, *thermodesulfovibrio* spp. At 50°c, *thermodesulfovibrio* spp. and *thermacetogenium spp*. At 60°c, thermacetogenium spp. and *archaeoglobus* spp. At 70°c and 80°c, *archaeoglobus* spp .	Genus, Species	Primarily sulfate-reducing, (high-temperature)	[158]
Enrichment culture	Multiple (e.g., 28bb2t, 8aa2 and *desulfobacter psychrotolerans* dsm 17155, and *desulfobacula*)	Genus, Species	Primarily sulfate-reducing, (high-temperature)	[159]
Unspecified	*Desulfatibacillum aliphaticivorans*	Species	Primarily sulfate-reducing, (high-temperature)	[160]
Unspecified	*Lysinibacillus fusiformis* BTTS10	Species	Primarily sulfate-reducing, (high-temperature)	[161, 162]
Antarctic Seawaters	Many, primarily *Arthrobacter* and *Rhodococcus*	Genus	Unspecified (low-temperature)	[163]
Arctic sediment	*Desulfofrigus marinus, desulfofrigus fragile, desulfofaba gelida, desulfotalea psychrophila, desulfotalea arctica*	Species	Primarily sulfate-reducing, (low-temperature)	[164]
Oil-contaminated Antarctic soil	*P. Stutzeri*	Species	Unspecified (low-temperature)	[165]
Oil reservoir	*Dietzia*	Genus	Unspecified - highly pH tolerant	[166, 167]
Sludge	*Methanosaeteta* sp. *Methanobacterium beijingense*, *Deltaproteobacteria, Nitrospira*, *Synergistes, Chloroflexi, Spirochaetes*	Phylum, genus	salinity	[167, 168]
Shantou Bay, China	*Pseudomonas* sp. JP1	Genus, species	Non-specific, halotolerant	[168]
Unspecified	Too many to list, primarily *Arhodomonas aquaeolei, Marinobacter lacisalsi, Halomonas axialensis*, and *Kocuria flava, Haloferax elongans and Halobacterium salinarum,*	Species	Multiple, halotolerant/halophilic	[169]
Hypersaline lakes	Multiple *pseudomonas*	Genus	Non-specific, halophilic	[170]

2.2 Use of Alternative Electron Acceptors in Anaerobic Degradation

2.2.1 Sulfate-Reduction

Most alkanes have been shown to degrade completely under sulfate-reducing conditions along with some aromatics, primarily by the activity of sulfate-reducing bacteria (SRB) [117] such as *desulfatibacillum*, *desulfatiferula*, *desulfosarcina, desulfococcus, desulfobacula, desulfovibrio, smithella,* and *firmicutes* [139, 171-173]. Abu Laban et al. [125] noted that a concentration of 10mM of sulfate (960 mg SO_4/L) was optimal for the biodegradation of benzene and Coates et al. [58] similarly found that the PAHs naphthalene ($C_{10}H_8$) and phenanthrene ($C_{14}H_{10}$) could be completely mineralized to carbon dioxide when SRB were provided with 10 mM of sulfate. Tsai et al. [127] obtained like results when analyzing the optimal sulfate concentrations for the degradation of phenanthrene and found the highest rates to occur at a sulfate level of 1.1 mM (1064 mg SO_4/L).

However, Dou et al. [126] found that although BTEX (benzene, toluene, xylene, ethylbenzene) degradation rates increased with corresponding increases in sulfate concentration, a maximum level was reached after which degradation rates began to decline, possibly due to a buildup of toxic sulfide [174]. The maximum concentration reached for benzene, *o*-xylene, and *p*-xylene was 5.2 mM (50 mg SO_4/L), whereas it was 8.3 mM (80 mg SO_4/L) for *m*-xylene and 10.4 mM (100 mg SO_4/L) for toluene and ethylbenzene [126]. With respect to minimally efficient sulfate levels, Chang et al. [67] demonstrated that even levels above 20 mM (192 mg SO_4/L) could be effectively utilized to degrade certain PAH compounds and Plante [128] showed full utilization of 28 mM (269 mg SO_4/L) sulfate levels, the average concentration of sulfate in seawater [175]. It therefore appears that ideal sulfate concentrations can vary greatly depending upon the

environment, the population count, and the particular species of SRB present. Yet, it is understood that if sulfide levels reach very high concentrations (a product of sulfate-reduction), sulfide can be toxic to microorganisms, including SRB [176].

2.2.2 Nitrate-Reduction

The nitrate-reduction process occurs when nitrogen or nitrate is utilized as the sole electron acceptor. Often, organic compounds are used as electron donors and at times the sole carbon source [177]. This process can occur via two pathways. One of the two pathways , known as denitrification, takes place via the conversion of nitrate to atmospheric nitrogen via nitrite (Equation 2.1) [178]. In the other pathway, known as nitrogen assimilation, hydrocarbons are coupled with nitrogen cycling via the reduction of nitrate to ammonia and subsequent nitrification processes (Equations 2.1 and 2.2) [129].

$$NO_3^- \rightarrow NO_2^- \rightarrow NO \rightarrow N_2O \rightarrow N_2 \quad (2.1)$$

$$NO_3^- \rightarrow NH_2OH \rightarrow NH_3 \rightarrow \text{organicN} \quad (2.2)$$

Many hydrocarbons have been shown to be able to be degraded under denitrifying conditions. For example, pristane ($C_{19}H_{40}$), a long-chained alkane, can be degraded with nitrate as the electron acceptor [179]. Zedelius et al. [130] identified three bacterial strains (*Betaproteobacteria* strains HxN1 and OcN1 and *Gammaproteobacteria* strain HdN1) able to grow under anoxic denitrifying conditions by coupling the alkane oxidation to CO_2 with NO_3^- being reduced to N_2. They also suggested that nitrogen–oxygen species are relatively strong oxidants and therefore may activate enzymatic mechanisms not possible under

sulfate-reducing or methanogenic, thereby allowing a special means of alkane activation [130].

However, the effectiveness of denitrification and relative degradation rates can vary significantly even within a given environment depending upon which hydrocarbons are present. Langenhoff et al. [131] showed that under the same denitrifying conditions, toluene underwent partial degradation whereas no degradation occurred for benzene. Since then, many researchers such as Burland and Edwards [132] and Atashgahi et al. [180] successfully reported degradation of benzene under nitrate-reducing conditions. The genera *Dechloromonas and azoarcus* of the class *Betaproteobacteria* are most commonly cited as successful benzene degraders [181, 182]. Recent papers have cited in addition to many other *Betaproteobacteria,* members of the classes *Ignavibacteria, Anaeroineae* and some strains of *Bacillus* (within the class *Bacilli*). *Ignavibacteria* and *Anaeroineae* are typical anaerobic bacteria with thermophilic tolerance while *Bacilli* are either obligate aerobes, in these instances, facultative anaerobes [182, 183].

Nearly all reported toluene-oxidizing nitrate-reducers also belong to the class *Betaproteobacteria* and many are facultative anaerobes. Examples of common genera reported are *Geobacter, Azoarcus,* and *Thuera* [184]. Nitrogen-reducing bacteria capable of fully degrading ethylbenzene have been reported and nearly all are *Betaproteobacteria.* They include the species *Aromatoleum aromaticum*, *Georgfuschia toluolica*, and members of the genus *Azoarcus* [133]. Notwithstanding, the ability of anaerobic bacteria to degrade ethylbenzene is not as ubiquitous as the ability to oxidize benzene or toluene [134]. Despite its similar chemical structure to toluene, ethylbenzene degradation usually occurs via a

different pathway and most strains capable of utilizing ethylbenzene are members of the *Rhodocyclales* order (primarily genera *Azoarcus* and *Aromatoleum*) [134, 184, 185].

Weelink et al. [134] reported that toluene and *m*-xylene are the most likely BTEX compounds to be degraded under denitrifying conditions. Other substituted toluenes such as *o*-xylene and *p*-xylene have particular stability due to their resonance structure and are therefore difficult for organisms to dearomatize [186]. The use of benzoyl-CoA reductases, chiefly 4-methylbenzoyl-CoA reductase is needed by an anaerobic organism to catalyze the de-aromatization process [187]. For this reason, early studies (pre-2000) insisted that para-alkylated toluenes (e.g., p-xylene) were fairly recalcitrant under denitrifying conditions. In recent years, more examples of p-xylene utilizing strains have appeared, including the strain *Denitratisoma oestraiolicum* [188]. Yet, to-date, there appears there are no reports of a pure nitrate-reducing culture capable of utilizing p-xylene as a sole carbon source [189]. Additionally, Meckenstock et al. [190], among others, found that the presence of *m*-xylene can inhibit the degradation of *o*- and *p*- xylenes. One of the only studies indicating the ability for *o*-xylene degradation to take place under nitrate-reducing conditions is a paper by Dou et al. [126]. They used a consortium of facultative anaerobes (e.g., *Pseudomonas*, *Microbacterium*, *Bacillus*) obtained from gasoline-contaminated soil and found *o*-xylene to be degradable at levels ≤ 50 mg *o*-xylene/L. They found degradation to be much more favorable in the presence of toluene by inhibited by ethylbenzene. They also observed inhibitory effects of ethylbenzene towards p-xylene degradation, but to a lesser extent [126].

PAHs such as naphthalene, phenanthrene, and pyrene are reported to be degraded and can sometimes be completely oxidized to CO_2 under denitrifying conditions [191].

Langenhoff [192] found that naphthalene could be transformed under denitrifying conditions in a soil-water system but that it may have been part of a co-metabolic process. The concentration levels of nitrate may also play a role in effective degradation capability. Lu et al. [135] found that both degradation rates and overall degradation of naphthalene (10 mg/L) occurred at high nitrate levels (1 and 5 mM), with greater degradation occurring at 5 mM (96.3% versus 91.7%, respectfully). However, at very low nitrate levels (< 0.4 mM), the efficiency of naphthalene degradation was seen to decrease significantly due to insufficient nitrate supply. They also found high levels of phenanthrene to be inhibitory (30 mg/L with a nitrate concentration of 5 mM) as only 20.2% of the phenanthrene was degraded. Yang et al. [136] studied pyrene (30 mg/L) rather than phenanthrene but found somewhat contradictory results to that of Lu et al. [135]. They discovered that 2 mM nitrate concentrations led to better degradation rates than at 5mM and far better than at 8 mM. It was also noticed that high concentrations of NO_2^- and NO_3^- could inhibit maximum growth and be toxic to the microbial population. Their study also did not show any inhibition due to high substrate levels, despite the same equivalent PAH load (i.e., 30 mg/L) [136]. This distinction may not be substrate-related but rather one or several of other variables such as culture source (river sediment vs marine sediment) and diversity (single species vs consortium).

Dou et al. [193] showed that naphthalene (30 mg/L) could degrade well under denitrifying conditions but that there seemed to be a boundary or threshold, as complete mineralization only occurred at naphthalene levels below 30mg/L. In their experiment, they observed no lag phase when the culture was inoculated with sufficient nutrients. Mihelcic and Luthy [194], though, encountered an acclimation period before significant

degradation of acenaphthene and naphthalene (1-3 mg/L) would occur under denitrifying conditions. However, they concluded based on additional findings that presence or absence of an acclimation period may very much be contingent upon the environment from which the cultures were taken. Rockne and Strand [81] showed that the presence or absence of a lag time may also depend on the accumulation concentration and nature of metabolic intermediates. Their research studied the ability of nitrate-reducers to degrade naphthalene, biphenyl, dibenzofuran, and phenanthrene at concentrations of 5, 2.5, 3, and 0.7 mg/L, respectively. The amount of nitrate provided was consistently 3.5 mM. In their study, they discovered that lag times and enhanced degradation are not necessarily exclusive as naphthalene and phenanthrene began to degrade immediately but biphenyl, despite having a lag time, had the greatest overall removal rates (dibenzofuran did not degrade). They also found that the degradation rate of naphthalene under nitrate-reducing conditions (2.4 mg /g of VSS day^{-1}) was twice as large as the degradation of phenanthrene (1.1 mg /g of VSS day^{-1}).

Biochar, a rich carbon source, has been shown to increase the stimulation of biodegradation under nitrate-reducing conditions as it helps retain the nitrate present thereby encouraging the growth of nitrate-reducers [137, 195]. Biochar has charged surface groups that can function in the capacity of electron donors or acceptors [196] and these properties give it a strong affinity toward aromatic hydrocarbons and has a high adsorption capacity for compounds like phenanthrene. Success in degradation rates were only seen when biochar and nitrate were added as the ability of biochar alone to remove PAHs from a system was found to be insufficient [137].

Anaerobic degradation of hydrocarbons can occur via two processes. They can generate energy coupling substrate oxidation (e.g., a hydrocarbon) to respiration via the reduction of a non-oxygen terminal electron acceptor (e.g., sulfate, nitrate) or they can generate energy via a fermentation pathway. These organisms, some bacteria and some archaea, are called fermentative degraders [197]. Under reducing conditions, fermentative degradation, which often converts a hydrocarbon into acetate and hydrogen gas, can accompany denitrification (see Section 2.2.6). This is most likely to occur if hydrogen-consuming microorganisms are present or in the presence of highly oxidized molecules [191].

Ambrosoli et al. [191] investigated the potential benefit of adding supplemental electron donors, acetate and glucose, to soil contaminated with biphenyl, phenanthrene, fluorene, and pyrene. Microorganisms were taken from paddy soil and incubated under anaerobic conditions with different variables. They found that what NO_3^- was not supplied, the addition of either glucose or acetate led to enhanced degradation (see Section 2.3). They explained that the addition of these electron donors led to co-metabolic degradation by respiratory and fermentative microorganisms. Yet, when nitrate was added, degradation rates were slightly-to-moderately reduced.

Yuan and Chang [68] similarly noticed that the addition of electron donors, while beneficial under methanogenic and sulfate-reducing conditions, negatively impacted degradation rates under nitrate-reducing conditions. Their results specifically examined the effect of lactate, pyruvate, and acetate. They explain that the presence of the electron donors promotes the growth of methanogens, which outcompete the nitrogen-reducing bacteria and do not perform well in the presence of nitrate. In contrast, certain substrates

such as benzoate have been shown to increase degradation rates of naphthalene when utilizing nitrate as an electron acceptor, though rates were not as strong as under sulfate-reducing conditions [131]. The positive contribution from benzoate may be due to its presence activating benzoyl-CoA reductase, which was shown to have a 70-78% genetic similarity to the key enzyme used in naphthalene degradation, naphthoyl-CoA [44]. However, these and other studies [68, 198] have shown that degradation can indeed occur under denitrifying conditions even if not always as efficient as under sulfate or metal-reducing conditions.

Lu et al. [45] found that two- and three-ringed PAHs degraded at a faster rate under nitrate-reducing condition than under sulfate-reducing conditions whereas Keller et al. [182] found benzene degradation rates to be similar under both conditions. Nitrate-reduction has a far greater energy yield per mole of substrate than anaerobic processes using other electron acceptors (Table 2.3) as well as a greater redox potential (Table 2.1). Thus, there is a correlation not only to the feasibility of biodegradation under these conditions, but also indirectly, the rate. The rate constant for degradation is dependent upon the activation energy as seen in the Arrhenius equation (2.3), which is a function of the enthalpic component of the Gibbs Free Energy. The extent of nitrate-reduction is determined by the amount of nitrate present, and therefore only when the concentration of nitrate surpasses the amount of sulfate, will significant nitrate-reduction take place, assuming all other environmental conditions are in place and the ideal organisms are present [199].

Wang et al. [139] demonstrated that significantly different bacterial populations can degrade hydrocarbons under nitrate-reducing versus sulfate-reducing conditions. In fact,

De Weert et al. [140] studied the effect of both nitrate-reducing and sulfate-reducing environments on the degradation of nonylphenol from a bacterial population taken from river sediment. Their results showed that under none of these conditions was the branched form of nonylphenol degraded, seemingly a result of its steric hindrance. The linear form of the molecule, though, was degraded under nitrate-reducing but not under sulfate-reducing conditions. They attributed this to a lack of sulfate degraders present in the sample and the inability of nitrate-reducers to degrade this compound under sulfate-reducing conditions as the degradation pathways differ [140]. Hidaka et al. [200] isolated a strain (*Desulfotignum* YB01) capable of degrading sulfate in a nitrate-rich environment and cited several others strains (e.g., *Arcobacter*) capable of nitrogen-reduction and simultaneous sulfate-oxidation, working in tandem with sulfate-reducing strains such as *Desulfotignum.*

$$k = Ae^{-\frac{E_A}{RT}} \tag{2.3}$$

,where k is the rate constant, A is the pre-exponential factor, E_A is the activation energy (J mol^{-1}), R is the universal gas constant (J K^{-1} mol^{-1}), and T is temperature (K).

Table 2.3 Standard Free Energy Changes and Calculated Possible Synthesis of ATP per Mole of Aromatic Hydrocarbons Oxidized to CO_2 with Different Electron Acceptors

Electron acceptors, oxidized/reduced	Stoichiometric equation	$\Delta G^{0'}$, kJ	Estimated ATP, mol
Benzene			
CO_2/CH_4	$C_6H_6 + 10.5\ H_2O + 3.75\ CO_2 \rightarrow 6\ HCO_3^- + 3.75\ CH_4 + 6\ H^+$	−106	1.5
SO_4^{2-}/HS^-	$C_6H_6 + 3\ H_2O + 3.75\ SO_4^{2-} \rightarrow 6\ HCO_3^- + 3.75\ HS^- + 2.25\ H^+$	−186	2.7
Ferrihydrite/Fe^{2+}	$C_6H_6 + 30\ Fe(OH)_3 \rightarrow 6\ HCO_3^- + 30\ Fe^{2+} + 18\ H_2O + 54\ OH^-$	−525 to −1,104	7.5–15.8
MnO_2/Mn^{2+}	$C_6H_6 + 15\ MnO_2 + 24\ H^+ \rightarrow 6\ HCO_3^- + 15\ Mn^{2+} + 12\ H_2O$	−2,104	30.1
NO_3^-/N_2	$C_6H_6 + 6\ NO_3^- \rightarrow 6\ HCO_3^- + 3\ N_2$	−2,978	42.5
Naphthalene			
S^0/HS^-	$C_{10}H_8 + 30\ H_2O + 24\ S \rightarrow 24\ HS^- + 10\ HCO_3^- + 34\ H^+$	−40	0.6
CO_2/CH_4	$C_{10}H_8 + 18\ H_2O + 6\ CO_2 \rightarrow 10\ HCO_3^- + 6\ CH_4 + 10\ H^+$	−157	1.2
SO_4^{2-}/HS^-	$C_{10}H_8 + 6\ SO_4^{2-} + 6\ H_2O \rightarrow 10\ HCO_3^- + 6\ HS^- + 4\ H^+$	−286	4.1
Ferrihydrite/Fe^{2+}	$C_{10}H_8 + 48\ Fe(OH)_3 \rightarrow 10\ HCO_3^- + 48\ Fe^{2+} + 28\ H_2O + 86O\ H^-$	−828 to −1,754	11.9–25.1
MnO_2/Mn^{2+}	$C_{10}H_8 + 24\ MnO_2 + 38\ H^+ \rightarrow 10\ HCO_3^- + 24\ Mn^{2+} + 18\ H_2O$	−3,355	47.9
NO_3^-/N_2	$C_{10}H_8 + 1.2\ H_2O + 9.6\ NO_3^- \rightarrow 10\ HCO_3^- + 0.4\ H^+ + 4.8\ N_2$	−4,752	67.9
2-Methylnaphthalene			
SO_4^{2-}/HS^-	$C_{11}H_{10} + 6.75\ SO_4^{2-} + 6\ H_2O \rightarrow 11\ HCO_3^- + 6.75\ HS^- + 4.25\ H^+$	−287	4.1
Ferrihydrite/Fe^{2+}	$C_{11}H_{10} + 54\ Fe(OH)_3 \rightarrow 11\ HCO_3^- + 54\ Fe^{2+} + 32\ H_2O + 97\ OH^-$	−896 to −1,938	12.8–27.7
Phenanthrene			
SO_4^{2-}/HS^-	$C_{14}H_{10} + 8.25\ SO_4^{2-} + 9\ H_2O \rightarrow 14\ HCO_3^- + 8.25\ HS^- + 5.75\ H^+$	−341	4.9

Source: [44]

There are many other key variables that may also play a role in the effectiveness of nitrate-reduction. One of these factors is the molar carbon-to-nitrogen ratio. High C/N values have been reported to stimulate degradation rates where Yang et al. [136] found degradation efficiency to increase linearly with C/N values, where C/N was defined as a molar ratio of pyrene-C to (NO_3^--N+NO_2^--N) measured from 0.1 to 0.6 (Figure 2.2). Another factor affecting nitrate-reduction is the environment where degradation is taking place. In most marine sediments, nitrate-reduction plays a minor role and Mn(IV) reduction, Fe(III) reduction, and sulfate reduction are the primary terminal electron-accepting processes [58]. One other factor is weathering. "Weathering" is a terminology applied to oils such as crude and can include the phenomena such as evaporation, dissolution, emulsification, and photo-oxidation [201]. Bregnard et al. [202] demonstrated that weathered diesel fuel could be at least partially be degraded under denitrifying

conditions and that the degradation process was enhance by agitation and other factors. Pietroski et al. [203] found that in coastal marsh soil, weathered oil impacted denitrification rates less than fresh oil implying more degradative activity could be present under nitrate-reducing conditions.

Successful biodegradation of high-molecular-weight PAHs (> 4 rings) is limited. Qin et al. [65] studied the effect of nitrate-addition rates of the biodegradation of benzo(a)pyrene (BaP) by *Microbacterium sp*. under denitrifying conditions. They found that in addition to nitrate, the bacteria could utilize nitric (NO) and nitrous (N_2O) oxides (products of denitrification) as electron acceptors. The highest BaP removal was seen at a ratio of 1:33 of BaP:Nitrate and that the C/N ration also played a role in the degradation efficiency.

Although nitrate (NO_3^-) has been extensively studied for its applicability towards denitrification, there seems to be a disagreement as to the role nitrite (NO_2^-) plays with respect to denitrification rates. Nitrite, which also functions as an electron acceptor can build up within a system as a results of the denitrification process and can compete with nitrate for substrate electrons [178]. Zedelius et al. [130] found that under nitrate-reducing conditions, the addition of nitrite above 5mM slightly reduced alkane degradation and sometimes created a lag phase not present before. They posited that at certain concentrations, nitrite can be inhibitory. This is consistent with the research of Dou et al. [193] who observed that accumulating nitrite levels did not seem to have an inhibitory nor a stimulatory effect on naphthalene degradation at a concentration of 1.1 mM (50 mg NO_2^- /L)

A third possibility of the effect of nitrite was observed by Yang et al. [136] that nitrite could actually stimulate or enhance the denitrification process (by functioning as a key electron donor) when utilizing pyrene (30 mg/L) as an electron donor. The NO_2^- levels of at which this occurred was 2mM and 5mM. They also studied relative ratios of NO_3^- to NO_2^- at concentrations of ranging from 0 to 10 mM each with extremes at 0 mM NO_3^- / 5 mM NO_2^- and 10 mM NO_3^- / 0 mM NO_2^-. Their results showed that altering nitrate and nitrite concentrations and their respective ratios significantly influenced the efficiency of pyrene degradation and that nitrite could induce complete denitrification, where the strongest degradation rates occurred at 2mM NO_3^-/ 2mM NO_2^- and 5mM NO_3^-/ 2mM NO_2^-, (98% and 87% degraded, respectively) followed by 10mM NO_3^-/ 0mM NO_2^- (60-85%). Thus, it was concluded that nitrite acted as a factor leading to the higher degradation rates but was not wholly necessary to achieve decent degradation. They also found that high concentrations (8mM) of either NO_3^- or NO_2^- proved somewhat inhibitory. High NO_3^- concentrations (≥8 mM) can cause the denitrification process to be inhibited before the NO_2^- reduction step occurs [136].

The bacterial reduction of NO_3^- to NO_2^- can often occur more rapidly and dominantly than NO_2^-reduction. Therefore, a buildup of nitrite can often occur, creating inhibitory problems. Ge et al. [178] adds that the stronger activity of NO_3^- reductase (competition for electrons) outcompetes the functioning of the NO_2^- reductase, leading to more nitrite accumulation than nitrite reduction. They also demonstrated that increasing the C/N ratio (from 1 to 15) led to enhanced nitrite buildup effectively decreasing successful degradation. Yang et al. [136] notes that's when both nitrate and nitrite levels

are low (≤ 5mM) a mild increase in the C/N ratio can reduce nitrite buildup and subsequently enhance degradation (Figure 2.2).

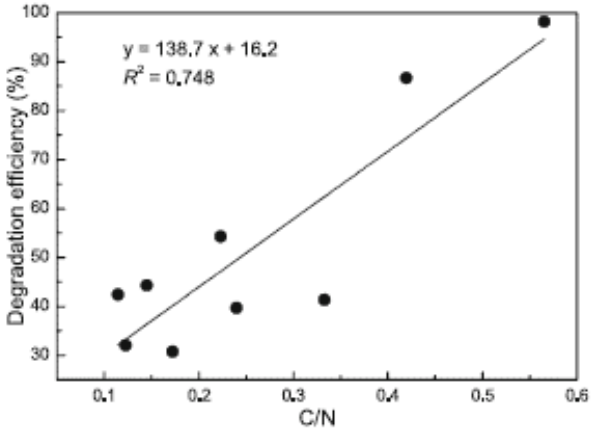

Figure 2.2 Data from Yang et al.[136] showing the relationship between (pyrene) degradation efficiency and C/N ratios.

Source: [136].

Another method of controlling NO_2^- is to maintain useful levels of ammonium ions; Musat et al. [204] found that nitrate reduction had a high correlation to the depletion of ammonium ions in the system. However, they found that a larger quantity of ammonium was consumed than could be accounted for by the assimilation process and it was found to be oxidized via the utilization of nitrite as an electron acceptor. It was therefore concluded that the addition of ammonium would lead to nitrite depletion, often rapidly. This was qualified to be true where there was sufficient substrate such as the cyclohexane present in their experiment. One additional finding was that the presence of N_2O disturbed this process of complete denitrification [204]. The denitrification process and the correlated biodegradation rates can also be enhanced or impaired by the addition of particular substrates or compounds.

2.2.3 Effect of Nitrate on Sulfate-Reducing Conditions

The effect of nitrate addition to enhance the degradation activity of sulfate-reducing bacteria (SRB) has been studied by numerous researchers. Keller et al. [182] studied a benzene-contaminated aquifer. Although some benzene had degraded via SRB, sulfate levels were depleted, in addition to an accumulated presence of sulfide. They proposed that by adding nitrate, sulfides could be oxidized back to sulfate using nitrate as the electron acceptor, thereby replenishing sulfate in the aquifer. During this period of sulfide oxidation, some benzene could also be degraded via denitrifiers. They explain that benzene degradation coupled to nitrate reduction is more energetically favorable than sulfate reduction but by having the pathway shift to utilize nitrate as the terminal electron acceptor, nitrite is produced which greatly inhibits SRB activity [182].

Nitrate is especially inhibitory to SRB at high concentrations. He et al. [205] reported that elevated nitrate levels ($\geq$70 mM NO_3^-) can inhibit sulfate reduction activity and may be due to induced osmotic stress. Similarly, Van den Brand et al. [206] found nitrate levels of 35.6 mM (500 mg NO_3^- N/L) to inhibit sulfate-reduction. This often occurs as nitrate suppresses the production of hydrogen sulfide, thus limiting SRB activity. Nitrate-reduction is more energetically favorable than sulfate-reduction and as a result nitrate-reducing organisms can outcompete sulfate-reducing bacteria when utilizing a substrate [207]. Yet, while higher levels of nitrate may be detrimental to the sulfate-reducing process [208], low levels of nitrate (1-10 mM) may be beneficial as it can repress toxic sulfide buildup without significantly inhibiting the sulfate-reduction process [209]. Additionally, bacterial growth is dependent upon an adequate supply of nitrogen for metabolic activity and cell multiplication [210] as the presence of nitrogen is key for any biodegradation to occur and is primarily used in organisms to form proteins and nucleic

acids and thus essential for growth [211]. Without ample nitrogen, microorganisms are unable to significantly increase their biomass and biodegradation would be limited [212].

It has been reported that one of the major causes of ineffective SRB activity and thus poor sulfate reduction, is the lack of nitrogen as a nutrient [213], but since the addition of nitrate appears detrimental under sulfate-reducing conditions, compounds such as NH_4^+, NH_4Cl, HNO_3, tri-nitrotoluene, aniline, corn liquor, urea, peptone, and chitin are all reported to have served as nitrogen sources for SRB. SRB, in conjunction with fermentative bacteria, can metabolize these compounds to NH_4^+, amines, and amino acids, and eventually nucleic acids and enzyme co-factors which help promote growth as well as allow for degradation pathways. Although there are many potential nitrogen sources, NH_4^+ (ammonium) has been reported as the dominant form of nitrogen to be readily utilized by SRB [210].

2.2.4 Effect of Sulfate on Nitrate Reduction

Wong and Lee [214] showed that the addition of sulfate and sulfide under nitrate-reducing conditions increased overall methane production and caused the nitrate reduction pathway to shift from a denitrification process to the dissimilatory nitrate reduction to ammonia (DNRA). Additionally, it is reported that sulfur compounds such as sulfide, the primary product of sulfate-reduction, can also inhibit denitrification or disrupt its efficiency as it can be oxidized easily in co-reactions of the nitrate reduction pathway [130]. In an attempt to utilize both sulfate and nitrate as electron acceptors while increasing degradation efficiency, Zhang et al. [215] created an approach of utilizing acetate and iron-reduction (Figure 2.3). The addition of acetate stimulated SRB growth, which lead to the reduction of SO_4^{2-} to S^{2-}. Some this S^{2-} was then oxidized to S^0 (elemental sulfur) by ferric iron

(Fe^{3+}) which was provided via the mineral akaganeite. As part of this process Fe^{3+} was reduced to Fe^{2+}, which reacted further with residual S^{2-} to form acid volatile sulfide (AVS). During the overall sulfate reduction process, TPH biodegradation occurred. Following this, (nitrate) NO^{3-} was injected and the reduced sulfur compounds (S^0 and AVS) were then oxidized by certain denitrifying species (e.g., *Denitrificans*, *Sulfurimonas*) and sulfur-oxidizing species such as *T. sulfidophilus* and *T. nitratireducens*. The SRB initially stimulated via the acetate were largely *Desulfobacterales* and *Desulfuromonadales* and were indigenous to the marine sediment used in this study [215].

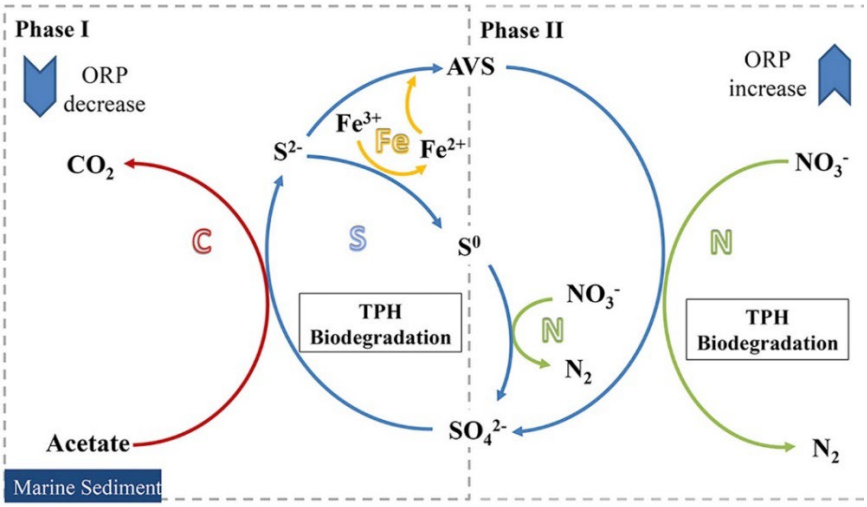

Figure 2.3 Schematic illustrating the proposed mechanism utilized by Zhang et al.[215] for applying sequential sulfate reduction and denitrification combined with an iron-based mineral and acetate.

Source: [215].

2.2.5 Metal-Reduction

Metals such as iron and manganese can be utilized by microorganism through a process known as dissimilatory metal reduction. It was originally thought that these metals

primarily functioned as key protein components, assisting in electron transfer to terminal acceptors. However, it has now been well-documented that microorganisms can use these metals as the actual terminal electron acceptors [216] (Table 2.4). Metal-reduction enables the creation of electrochemical gradients, providing the chemical energy needed for growth [217]. This specifically occurs by coupling the oxidation of electron donors (e.g., hydrocarbons) to metal reduction [218]. Vodyanitskii [219] points out that metal-reduction sometimes may occur only when organic matter is scarce or depleted but in the presence of abundant organic matter (including the hydrocarbons), other TEAs such as sulfate and nitrate may be utilized.

Table 2.4 Dissimilatory Metal-Reducing Microorganism (DMRM) Coupling Aromatic Hydrocarbon Oxidation with Metal Reduction

Species	Classification	Reduced Metals	Reference
Geobacter metallireducens	(Gram Negative) *Deltaproteobacteria Geobacteraceae*	Benzene-Fe(III) Toluene-Fe(III)	[220-222]
Geobacter strain "Ben"		Benzene-Fe(III) Toluene-Fe(III)	[222]
Geobacter grbiciae		Toluene-Fe(III)	[223]
Geobacter toluenoxydans		Toluene-Fe(III)	[224]
Georgfuschia toluolica	(Gram Negative) *Betaproteobacteria Rhodocyclaceae*	Toluene-Fe(III) or Mn(IV) Ethylbenzene-Mn (IV) Toluene-Mn(IV)	[141, 225]
Azoarcus sp.- dominated microbial consortium		Ethylbenzene-Mn (IV)	[141]
Desulfitobacterium aromaticivorans	(Gram positive) *Clostridiales Peptococcaceae*	Toluene-Fe(III) o-xylene-Fe(III)	[224]
Culture N49[a]		Naphthalene-Fe(III) 1-methylnaphthalene-Fe(III) 2-methylnaphthalene- Fe(III)	[147]
Ferroglobus placidus	*Archaeoglobales Archaeoglobaceae*	Benzene-Fe(III)	[226]

[a]Culture N49 is composed of 90% of a bacteria species from the *Peptococcaceae* family

2.2.5.1 Iron, Fe. Among active redox (reduction-oxidation) metals, iron is the most prevalent [227] and ferric iron (III) is often considered the most abundant terminal electron acceptor, particularly for the oxidation of organic matter [141]. In soils and sediments, iron-reduction (Fe^{3+} to Fe^{2+}) occurs mainly through the activities of iron-reducing bacteria, a natural process that can be utilized to enhance in-situ remediation [227]. Numerous studies have indicated that Fe(III)-reducing bacteria are capable of degrading petroleum hydrocarbons [131, 142] and may be able to oxidize electron donors more effectively even than sulfate-reducing bacteria (SRB) due to more favorable redox potentials (Table 2.1). However, this may very much depend on the environment and population sizes [142]. Iron-reducing conditions have shown to be particularly effective for the biodegradation of BTEX compounds, including from petroleum-contaminated aquifers [141] and harbor sediments, especially when combined with sulfate-reducing conditions [142].

Jun et al. [218] successfully demonstrated the ability to degrade BTEX contaminants including the more recalcitrant *o*-, *m*-, and *p*-xylenes under iron-reducing conditions, and showed that the bacterial reduction of iron (0.1 g/L iron oxides) coupled with the oxidation of BTEX hydrocarbons follows a first-order kinetic model. The oxidation rate constant was shown to increase in the order benzene < toluene < ethylbenzene < xylenes. In their study, they also found that the degradation efficiency increased with increasing concentration of co-substrate (citric acid). However, the ability to degrade these compounds was limited by concentration. Extremely high BTEX concentrations were shown to inhibit iron-reducing activity with the ideal microbial activity occurring at BTEX concentration of 100 mg/L [218]). More often, the ratio of contaminant to iron is much less than 1 [228], but other monoaromatic compounds such as

m- and–*p*-cresol, phenols, and benzoate have also been shown to be effectively degraded under these conditions [108, 224].

Co-substrates such as acetate function as supplement electron donors and have been long-established as facilitating the iron-reduction process [221] and can be also very useful in mediating the role of iron in other microbial processes. Kunapuli et al. [143] investigated an iron-reducing enrichment culture with benzene as the sole carbon and energy source, and found evidence of iron-reducers involved in a syntrophic relationship. They proposed that benzene was being degraded via syntrophic interactions wherein benzene was oxidized via iron-reduction, producing H_2 that served as an energy source for other anaerobic organisms present including various *Desulfobulbaceae* and methanogens [143, 144]. The anaerobic degradation of benzene can form benzoate and phenol as metabolic intermediates [229]. Abu Laban et al. [145] observed iron-reducing bacteria capable of degrading benzoate, 4-hydroxybenzoate, and phenol. Zhuang et al. [146] also observed benzoate degradation but specifically by the methanogens present in the system. In their experiment they utilized iron oxides in the form of hematite and magnetite and found that the addition of iron oxides increased methanogenic benzoate degradation by 25–53%.

Kleeman and Meckenstock [147] identified gram-positive iron-reducers (*Desulfobacteriaceae*) capable of degrading benzene but found that the culture could grow solely on 1-naphthoic acid, 2-naphthoic acid, 1-methyl-naphthalene, and 2-methyl-naphthalene, but could not grow on 1-naphthol, 2-naphthol, phenanthrene, anthracene, indane, or indene. The ability of these microorganisms to utilize 1-naphthoic acid and 2-naphthoic acid illustrates the pathway used to degrade 1-methyl and 2-metyl-naphthalene, as these are primary metabolites for these compounds, respectively. As the focus of the

study was largely genomic, the amount of each compound degraded was not reported although it was noted that at least mineralization to CO_2 occurred [147]. The discovery of 1-methyl-napthalene degradation is particularly intriguing as under many conditions it tends to be more difficult to anaerobically degrade than naphthalene alone or 2-methyl-naphthelene [17] . This phenomenon is echoed by Marozava et al. [148] who discovered iron-reducing bacteria capable of using 1-methyl-naphthalene as the sole carbon and electron source, but proposed that its degradation pathway is different than naphthalene or 2-methyl-napthalene and thus more difficult to achieve by most iron-reducing or sulfate-reducing microorganisms [152]. They hypothesize that in both iron-reducing and sulfate-reducing microorganisms, there are fewer genes capable of metabolizing 1-naphthylmethyl succinate than those capable of metabolizing 2-naphthylmethyl succinate (Figure 2.4).

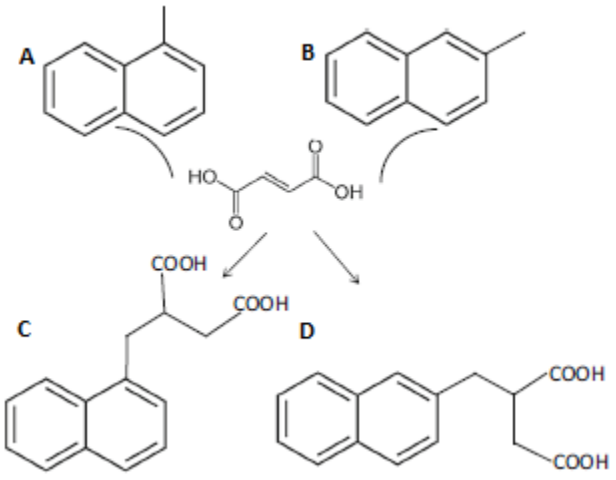

Figure 2.4 Proposed initial degradation step for a) 1-methyl-naphthalene and for b) 2-methyl-naphthalene, yielding c) 1-naphthylmethyl succinate and d) 2-naphthylmethyl. Succinate.

Source: [148].

It has been implied in numerous papers that anaerobic degradation of PAHs containing 3 or more rings can take place under iron-reducing conditions but Li et al. [230] was not successful. They examined mangrove sediment contaminated with PAHs and monitored the effects of iron [Fe(III)] amendment on the biodegradation of four PAHs (fluorene, phenanthrene, fluoranthene, pyrene) under low-oxygen (2 ± 0.3% O_2) and non-oxygen (0% O_2) conditions. For all conditions and PAH types, the iron amendment did not show significant improvement towards biodegradation rates. Coates et al.[58] is one of several papers claiming that utilizing both iron-reducing and sulfate-reducing conditions can increase the success of overall hydrocarbon degradation.. Recently, Müller et al. [149] investigated biostimulating iron-reducing and sulfate-reducing bacteria with ammonium acetate and a derivative of acid-mine waste containing high levels of iron and sulfate (the acetate functioned as an electron donor and the mine waste as electron acceptors). The stimulation increased microbial growth and led to successful and faster degradation of benzene and naphthalene.

Yan et al. [66] investigated the degradation of pyrene and phenanthrene in freshwater sediment under three kinds of treatments (amorphous ferric hydroxide, sediment microbial fuel cell (SMFC), combination of ferric addition and 'SMFC employment'). The combination treatment yielded the highest removal efficiencies of phenanthrene (99.47 ± 0.15%) and pyrene (94.79 ± 0.63%), while the SMFC treatment alone was more successful than just the Fe(III) amendment.

Due to its prevalence, especially in terrestrial environments, and the diversity in which iron-reducers abound, the possibility of hydrocarbon degradation partially or fully under iron-reducing conditions seems promising for future cleanup initiatives. Although

successful degradation has been mostly limited to monoaromatic and some diaromatic compounds [148], there is much effort and hope that this iron-reductive process can also be used to at opportunely attacked other hydrocarbons such as PAHs [147].

2.2.5.2 Manganese, Mn. Another naturally occurring metal that is promising for hydrocarbon degradation is manganese. Manganese can occur in the form of reduced-soluble or adsorbed Mn(II) as well as insoluble Mn(III) and Mn(IV) oxides and the oxidation of manganese has been reported by various microorganisms such as *Leptothrix*, *Pedomicrobium*, *Caulobacter, Arthrobacter*, *Oceanospirillum, Georgfuschia*, and *Azoarcus* [231, 232]. Mn(IV), present as a manganese oxide (MnO), is naturally-occurring and widely distributed in groundwater, where it can be reduced microbiologically, allowing for the degradation of alkanes and monoaromatic compounds. Villatoro-Monzón et al. [150, 151] observed BTEX degradation in anaerobic sediment under Fe(III) and Mn(IV) reducing conditions. They conducted two studies, and in both instances found the degradation rate under manganese-reducing conditions to proceed faster than under iron-reducing conditions for all BTEX compounds.

In both studies, the greatest discrepancy was seen by benzene degradation. In the first study, benzene (5 mg/L) was degraded at 0.8 μmol l^{-1} d^{-1} under Mn(IV) reducing conditions but only 0.08 μmol l^{-1} d^{-1} under Fe(III) reducing conditions. Among all of the BTEX compounds under Fe(III) reducing conditions, they found ethylbenzene to degrade fastest (0.19 μmol l^{-1} d^{-1}), only slightly less than under Mn(IV) reducing conditions (0.20 μmol l^{-1} d^{-1}). In their second study, benzene (3.5 mg/L) degraded in 80 days under Mn(IV) reducing conditions as compared to 710 days under Fe(III) reducing conditions. As can be

seen in Table 2.3, manganese-reduction is more thermodynamically favorable and generates more ATP than iron-reduction per mole of substrate [44].

Langenhoff et al. [233] observed the oxidation of toluene in manganese-rich sediment columns via the reduction of Mn(IV). The strains tested were able to grow on toluene in the presence of manganese oxide under anaerobic conditions. They found that adding organic ligands such as oxalic acid and nitrilotriacetic acid (NTA) would increase degradation rates. Organic ligands can stimulate metal reduction by complexing with the metals or metal oxides and allowing for increased solubility [233, 234]. Yeung et al. [152] investigated petroleum-contaminated Colomac Mine groundwater in the Northwest Territories, Canada and found anaerobic bacteria using nitrate, manganese (IV), iron (III) and sulfate as electron acceptors to degrade the hydrocarbons present.

Jimenez et al. [235] point out that in that in some environments such as those heavily of sandstone, although iron and manganese oxides could work well as electron acceptors for degrading hydrocarbons in oil, it is unlikely they would be responsible for any significant compositional changes in oil accounting for their limited availability. Therefore, the metals naturally present in an environment and the acclimation of the bacteria may prove to be a vital factor in the success of this technology. Additionally, the presence of other heavy metals, such as lead, cadmium, copper, and zinc may inhibit degradation ability due to their toxicity and their tendencies to decrease microorganism activity [68]. Surprisingly, researchers have found the ability of certain anaerobic organisms to reduce even heavy metals such as molybdenum and chromium (VI) while using hydrocarbons as the main carbon source [236, 237]. The potential of these organisms is still largely to be explored.

2.2.6 Syntrophic Relationships and Methanogesis

Complete mineralization of organic molecules (e.g., hydrocarbons) to CO_2 and methane is often achievable through a partner-dependent metabolic partnership known as syntrophy [238]. Syntrophic processes can occur in most environments where methanogenic conditions are favorable, such as sewage treatment plants, freshwater sediments, landfills, and rice paddies. This co-metabolism usually occurs in the presence of alternative electron acceptors, primarily sulfate, nitrate, and iron and occurs when the primary anaerobic organisms (e.g., sulfate-reducers) produce long-chain fatty acids such as formate and acetate. A second type of organism (e.g., acetogens, methanogens) then converts these molecules to methane, removing the buildup of these acids [43] (See Figure 2.5). This enables further degradation of the initial contaminant to take place be helping to regulate pH and balance the system thermodynamically [55].

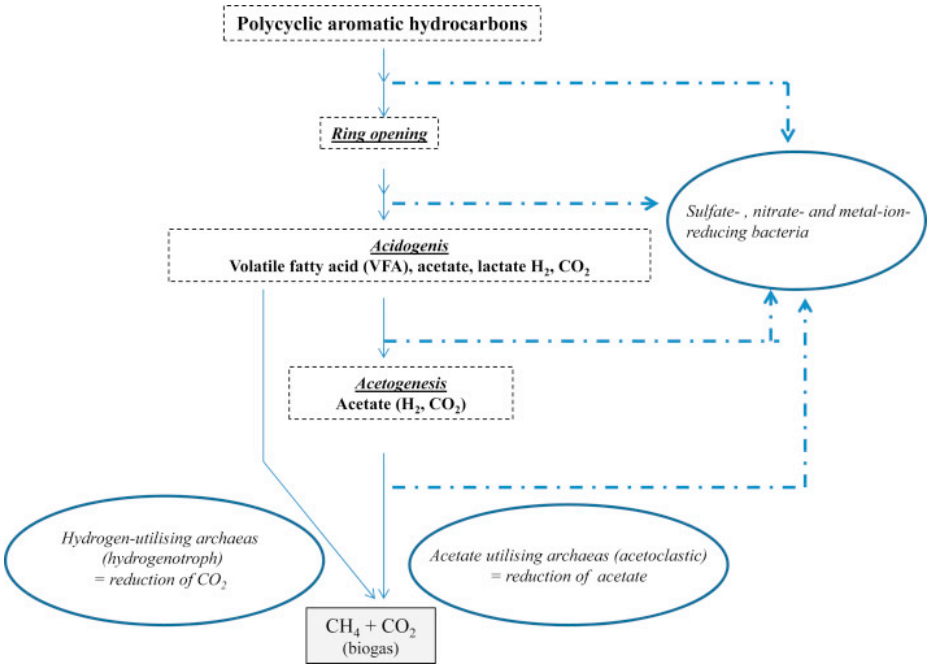

Figure 2.5 Diagram illustrating the syntrophic anaerobic biodegradation of PAHs.
Source: [239].

Sulfate-reducing bacteria (SRB) are the most ubiquitous anaerobic bacteria to have syntrophic relationships with methanogens. Although methanogens alone are capable of degrading smaller hydrocarbons, they often work together with SRB to complete the mineralization of more complex hydrocarbons (e.g., long-chained alkanes and monoaromatics) to CO_2 [240]. This is process can also work sequentially as upon the depletion of sulfate, a system may become favorable to methanogenic conditions [241]. Callaghan et al. [242] discovered that the SRB *Desulfatibacillum alkenivorans AK-01*, normally solely capable of n-alkane biodegradation, was found in the absence of sulfate to produce methane from hexadecane when the strain was co-cultured with a formate/H_2-utilizing methanogen [144]. Some strains such as certain *desulfomaculum* are fully dependent upon syntrophy and cannot utilize sulfate but rather grow alongside methanogens. Microorganisms of this nature are typically found in rich hydrocarbon-containing environments such as petroleum reservoirs [243]. Though hydrocarbon degradation may take place under sulfate-reducing conditions via only one or several strains, microorganisms (e.g., archaea) responsible for degradation under methanogenic conditions tend to be more complex and diverse [244].

Table 2.5 Estimated Stoichiometry and Gibbs Free Energy for Reactions Relating to Syntrophic Hydrocarbon Degradation Coupled to Methane Production

		$\Delta G°'$ (kJ/mol)	$\Delta G'$ (kJ/mol)
Methane-producing reactions			
Acetotrophic	$CH_3COO^- + H_2O \rightarrow HCO_3^- + CH_4$	−31.0	−15.6
Hydrogenotrophic	$4H_2 + HCO_3^- + H^+ \rightarrow CH_4 + 3H_2O$	−135.6	−38.5
Syntrophic hydrocarbon oxidations to acetate and H_2			
Toluene	$C_7H_8 + 7H_2O \rightarrow 3.5CH_3COO^- + 3.5H^+ + 4H_2$	+113.6	−40.9
Naphthalene	$C_{10}H_8 + 10H_2O \rightarrow 5CH_3COO^- + 5H^+ + 4H_2$	+101.1	−90.2
Hexadecane	$C_{16}H_{34} + 16H_2O \rightarrow 8CH_3COO^- + 8H^+ + 17H_2$	+470.8	−91.3
Overall conversion of hydrocarbons to methane			
Toluene	$C_7H_8 + 7.5\ H_2O \rightarrow 4.5CH_4 + 2.5HCO_3^- + 2.5H^+$	−130.5	−134.1
Naphthalene	$C_{10}H_8 + 10\ H_2O \rightarrow 6CH_4 + 4HCO_3^- + 4H^+$	−189.5	−206.9
Hexadecane	$C_{16}H_{34} + 16\ H_2O \rightarrow 12.25CH_4 + 3.75HCO_3^- + 3.75H^+$	−353.5	−380.0

Source: [144]

2.3 Biostimulation via Co-Substrates

Biostimulation is an effective strategy to stimulate microorganism and their ability to degrade hydrocarbons. Biostimulation can involve electron acceptors such as nitrate or sulfate, can employ nutrients such as nitrogen and phosphorus, or utilize the addition of co-substrates [245, 246]. Zhang and Lo [54] researched the effectiveness of methanol (20mM) and acetate (10 mM) as co-substrates for the C_{10}–C_{40} hydrocarbons in marine sediment. Their study showed found that both substances increased total degradation, but that acetate performed more favorably than methanol. Untreated samples only had a TPH removal of 25-35%, whereas treatments where acetate or methanol was added had TPH removals of 50-75% and 25-65%, respectively (Methanol was far more effective in facilitating the degradation of alkanes $\leq C_{30}$). Microbial populations also differed between the two treatment studies. In the sediment where acetate was added, the dominant bacteria

were from or related to the order *Desulfobacterales,* whereas for the methanol treatment, bacteria were from or related to the order *Clostridiales* [54]. Li et al. [247] added glucose to a microbial fuel cell as a co-substrate to soil contaminated with petroleum hydrocarbons and found the total hydrocarbon degradation rate to be increased by 200%. Paulo et al.[248] found that the ability of methanogens to convert 1-hexadecene to methane increased threefold and sevenfold with the addition of lactate and yeast extract, respectively.

Numerous studies have indicated that the supplementation of electron donors such as short-chained volatile fatty acids can have a positive result on PAH degradation rates Chang and Yuan [67, 68, 155, 156]. Yuan et al. [155] found that the addition of acetate, glucose, pyruvate, or yeast extract, could enhance phenanthrene (5 mg/L) degradation, with complete degradation occurring in within only 28h. They determined optimal conditions at pH 7.0 and 30°C. Similarly, Chang et al. [67] noticed the enhancement of PAH degradation by the addition of acetate, lactate, or pyruvate as electron donors. They reported full degradation of phenanthrene, pyrene, and anthracene (all at 32 mg/kg of soil) in 37d, 42d, and 93d, respectively, and 95% and 75% degradation in 93d for fluorene and acenaphthene, respectfully. Optimal conditions were found to be pH 8.0 and 30°C [67]. However, they found that this augmentation (specifically, acetate, lactate, and pyruvate) enhanced PAH degradation rates under methanogenic and sulfate-reducing conditions but actually was inhibitory under nitrate-reducing conditions [68]. Lei et al. observed that phenanthrene degradation under sulfate-reducing conditions was enhanced by the addition of either ethanol or acetic acid but had no significant effect under nitrate-reducing conditions. They also noticed that degradation would occur without the addition of these

co-substrates but only after a lag phase of 14 weeks (Figure 2.6). The addition of ethanol and acetic acid also were found to be significantly effective for phenanthrene but not for other PAHs tested [46].

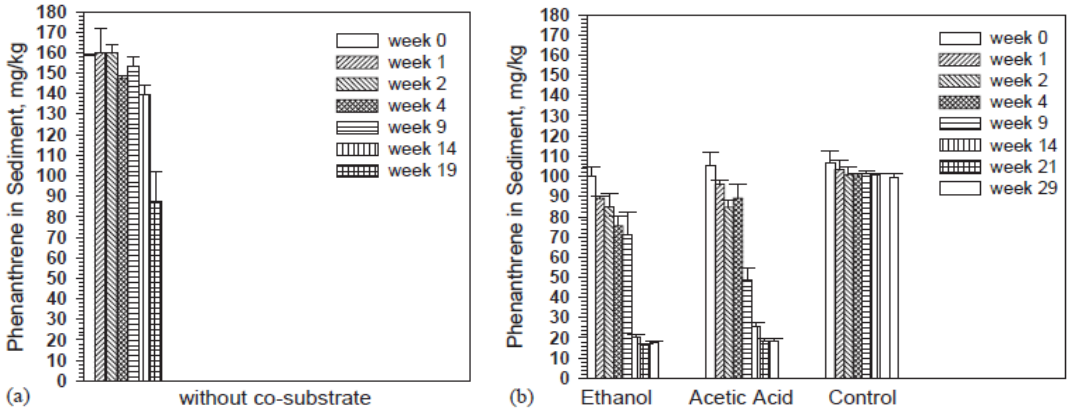

Figure 2.6 Biodegradation of phenanthrene under sulfate-reducing conditions.
Source: [46].

Bach et al. [249] took a unique multidimensional approach towards biostimulation. They tested a variety of biostimulating agents (urea and phosphate in the form of slow-release fertilizer (SRF), dextrin, yeast extract (YE), Tween 80, and lactate) and all except dextrin were found to improve degradation rates of PAHs over unamended systems. The PAHs used were phenanthrene, anthracene, fluoranthene, pyrene, chrysene, and benzo[a]pyrene. Phenanthrene was best degraded with the amendment of SRF, lactate, or YE. Anthracene, pyrene, and most pronouncedly fluoranthene degradation rates were greatest with the lactate amendment. Chrysene was best degraded with the amendment of Tween 80 and Benzo[a]pyrene was best degraded with the amendment of SRF. Their research also showed even greater degradation potential when combining Tween 80, lactate

(0.01-10 μg PAH/kg dry sediment/day), which had rates up to 8.2 times that of untreated sediment [249].

Adelaja et al., [250] successfully supplemented microbial fuel cells with microcrystalline cellulose along with mineral and nutrients to enhance the biodegradation of phenanthrene, although, Quantin et al. [251] attempted to use cellulose for this purpose and got poorer results. They conducted a batch experiment to measure the anaerobic degradation of 11 PAHs in polluted river sediment, and whether the addition of fresh cellulose would have an effect on degradation rates. Cellulose addition stimulated both anaerobic respiration and greatly stimulated microbial activity but had no real effect on PAH dissipation or degradation. There many key differences between these studies but primarily include that Adelaja et al., [250] conducted degradation experiments using a microbial fuel cell, used microcrystalline cellulose, and provided carbonate, an additional carbon source. In contrast, Quantin et al. [251], who conducted their study ten years earlier, used typical batch reactors, used shredded cellulose filters, and did not add any additional carbon sources.

In addition to volatile fatty acids (propionate, butyrate, valerate) and simple organic acids such as lactate, anaerobic organisms have also been discovered to be capable of using reduced humic substances (HS) as electron acceptors [252] and electron donors [157]. Humic substances occur in a wide variety of environments including aquifers and lake sediments [253] and can function as an electron acceptor under anaerobic conditions to oxidize certain organic compounds, including simple hydrocarbons [252]. HS can also function as electron donors by pairing with alternative electron acceptors such as nitrate or fumarate, a common intermediate in anaerobic degradation pathways [254] and thereby

enhance the ability for microorganisms to reduce other electron acceptors, such as insoluble Fe(III) oxides, which may be less accessible. This process occurs via the shuttling of electrons between humic-reducing microorganisms and the metal complex [252].

Related to this, Sayara et al. [255] discovered that compost derived from the organic fraction of municipal solid wastes (OFMSW) was capable of improving PAH degradation in contaminated soil, although results varied. The efficiency of the compost may be related to the humic acid (HA) present as part of the total organic matter. It has been reported that HA are beneficial as they increase the bioavailability of the PAHs. This takes place as HA have been shown to decrease the adsorption coefficient between the hydrocarbon and soil particles this increasing hydrocarbon solubility in the groundwater and allowing for greater degradation rates [255, 256]. An illustration of this can be seen in Equation 2.3.

$$S_w^* = S_w(1 + C_{ha}K_{ha}) \tag{2.3}$$

where, S_w^* and S_w are the solubilities of the hydrophobic organic compounds (e.g., hydrocarbons) in soil and (ground)water, respectively. C_{ha} is the humic acid (HA) concentration (g/mL of water) and K_{ha} is the partition coefficient of the compound between HA and water [256]. Additionally, Coates et al. [157] claims that a metabolism that utilizes humic substances can give organisms competitive advantages in environments that would normally require other organic compounds as both a carbon and energy source.

2.4 Temperature

One of the key factors affecting degradation rates is temperature. The influence of temperature on the biodegradation rate is actually quite complex and is dependent upon a

large variety of factors such as the composition and physical state of the hydrocarbons, the microbial community, the water content (if in soil), and the type and abundance of nutrients present [257]. Temperature is also capable of altering a hydrocarbon's chemical properties (via evaporation or other weathering processes) [258] and can greatly affect the metabolic rates of the representative organisms [101].

Bargiela et al. [259] examined the degradation rates of a crude oil spills in both aerobic and anaerobic waters. These areas were chronically contaminated with crude oil and they found that the adaptation and gene expression of the organisms present increased with increasing temperatures (13°C to 26°C). They also discovered an increase in catabolic biodiversity (i.e., the number of pathways utilized for pollutant degradation) with increasing temperature. However, as catabolic diversity increased, the microbial diversity was found to decrease, regardless of factors such as the geographical location and other environmental factors. They reported that sites with lower temperatures (13-16°C) contained the highest bacterial diversity while having the lowest diversity of catabolic genes. Bargiela et al. also compared the two chronically contaminated sites with the Deepwater Horizon spill site (DWH) and found two items of importance. One discovery was that there were more hydrocarbon degraders present in the chronically polluted site than at DWH implying a prior-contaminated site will have organisms more adept at targeting the pollutant and they also discovered that the gene expression and number exhibited by the organisms by the DWH was very low and that their general species diversity was fairly high, consistent with the characteristics of a low temperature environment (The DWH site investigated was 3°C). Additionally, they found that the

enzymatic activity of microorganisms with at least 20 pollutants, was impacted by temperature [259].

The notion that although overall degradation rates may increase with rising temperature, the overall bacterial and archaeal diversities can significantly decrease, complicates methods towards biodegradation applications [158]. The diversity of sulfate reducing bacteria appears to be especially affected by temperature, as various different genera and species tend to be abundant at different temperature levels [158, 159]

Methanogens are important hydrocarbons degraders and are often found in subsurface environments contaminated crude oil hydrocarbons or petroleum. However, methanogens are primarily adept at degrading (oxidizing) shorter-chained alkanes ($\leq C_8$) [260]. Dolfing et al. [260] examined the effect of temperature on methanogenic alkane degradation on the alkane length versus its free energy yield. They discovered that energy yields increase with increasing temperature and that the energy yield per temperature change was noticeably much greater for longer chained hydrocarbons (up to C_{80}). Focusing the study on hexadecane ($C_{16}H_{34}$), a medium-length hydrocarbon, they found that this trend was apparent for the partial oxidation of alkanes to H_2 and acetate and the full oxidation of alkanes to H_2 and CO_2. In contrast, the oxidation of alkanes solely to acetate became less energetically favorable as temperatures increased. Their conclusion was that at least for hexadecane, there is an overall increase in the energy yield from methanogenic degradation with increasing temperature, thus making biodegradation more favorable [260]. This phenomenon may especially be true with thermophilic methanogenesis. *Methanothermobacter Tm2*, a particular strain of thermophilic methanogen, was capable of growth on oil hydrocarbons between 55 and 80°C, and optimally at 65°C, but no growth

occurred above 85°C or below 45°C [261]. However, for each organism, at a certain point the necessity to keep it biologically sound overrides the thermodynamic favorability of the degradation process and therefore biodegradation ability rapidly decreases [260].

Cheng et al. [158] also noted a similar upper threshold for thermophilic organisms. They investigated the sulfate consumption by mesophilic and thermophilic organisms taken from high-temperature hydrocarbon seeps from 40˚C to 90˚C. They found that sulfate consumption rates began to decline above 40°C and consumption stopped above 80°C. This may have been due to the loss of co-metabolizing mesophilic organisms at the higher temperatures. And while the rate of sulfate consumption does not directly reflect the rate of hydrocarbon degradation, there is often a very strong correlation between the two as hydrocarbon degradation is often coupled with sulfate reduction [158, 159].

Many other researchers have noted similar trends with respect to sulfate-reducing bacteria. For example, Cravo-Laureau et al. [160] discovered a species of sulfate-reducing bacteria (obtained from marine sediment) that grew solely on hydrocarbons optimally from 28-35˚C. Similarly, Chang et al. [67] found that there was not much difference between a 30°C and 40°C system temperature but that based on numerous studies, 30°C appears to be optimal. This was true for numerous PAHs tested, including phenanthrene. Adelaja et al. [250], who specifically focused on phenanthrene and benzene, found that degradation rates among anaerobic organisms improved somewhat upon a system increase from 30°C to 40°C but were reduced by an even greater degree when the temperature reached 50°C. A temperature of 40°C was regarded as optimal as this slightly elevated temperature the activation energy needed to drive the oxidation process is lowered [250]. Many researchers have reached a similar conclusion, namely that the highest degradation rates occurred in

the range of 30°C to 40°C and where exactly the optimum lies is largely dependent upon the species and environmental factors. In aquatic environments, however, the threshold appeared to be lower, with maximum degradation rates occurring between 20°C-30°C in fresh water environments and 15°C-20°C in marine environments [161].

Sayara et al. [240] found that the capacity for degradation under mesophilic conditions was higher than under thermophilic conditions. Notwithstanding this, thermophilic conditions did result in better biodegradation rates when low concentrations of PAHs were used. This is because high temperatures often increase the desorption of PAHs and their solubility, affecting general bioavailability. Roussel et al. [162] suggests that at higher temperatures, the presence of significant substrate concentrations is detrimental to some SRB. However, for some organisms (e.g., certain strains of SRB and some archaea), they found that bacterial cell numbers were stimulated by substrate addition at all temperatures, including above 70°C. This response could be applicable to oil reservoirs, which are high-temperature and high-substrate environments [162].

In addition to the research on elevated temperatures, much has been studied on lower temperatures, both for psychrophilic and mesophilic organisms. In a review by Margesin and Schinner [262], it was observed that cold habitats often have a significant population of psychotrophic hydrocarbon-degrading microorganisms. Yet, despite adaptation to cold temperatures, the growth rate of psychotrophic organisms is still quite low and therefore even under ideal conditions, a lag time may occur before degradation takes place.

Modern studies have shown that while metabolic rates of mesophilic organisms can be greatly reduced at low temperatures [263], the degradation rates in a naturally cold

environment (<10°C) are often not that different than more mild temperatures (15-25°C) [262]. This may largely be due to the normalized metabolic rates of the psychrophilic organisms present in these environments [264]. However, Rodriguez-Blanco et al. [264], who studied the degradation of crude and diesel oils in seawater microcosms, noted that although degradations rates were similar irrespective of temperature for crude oil, by diesel oil degradation rates were found to be higher at 25°C than at 10°C or 4°C. This was confirmed to occur without any changes in microbial cell counts [264].

Daniel Delille [33], a researcher who has collaborated with Dr. Rodriguez-Blanco was surprised to find that in contrast to prior reports, reducing a system's temperature from 20°C to 10°C did not reduce biodegradation efficiency. It is proposed that this was due to analyzing rates from a chronically cold system (Antarctic seawater) but that a more temperate system, and consequently, mesophilic organisms, may in fact be adversely affected far greater by declining temperatures. He mentions the research of Michaud et al. [163] which found that the biodegradation efficiency was higher at 20°C than at 4°C for two psychrotrophic Antarctic marine organisms which is in strong contrast to his own findings. He suggests, therefore, that whether or not colder temperatures will adversely affect degradation rates in an environment largely depends on which organisms are present and a variety of environmental factors [33]. Van Stempvoort et al. [265] studied the effects of temperature on hydrocarbon degradation by analyzing sulfate-reduction rates. They reported that low groundwater temperatures (5-6°C) in a naturally cold environment (Alberta) did not have significantly different hydrocarbon degradation rates in comparison to warmer groundwater sites in California (15-20°C). Eriksson et al. [266] investigated how temperature affected PAH degradation specifically under nitrate-reducing conditions

and determined that it also did not have a significant impact on degradation rates.. They reported that in all anaerobic cultures (inoculated with different soil samples), the extent of removal of all PAH compounds were very similar at both low and moderate temperatures (7°C, 20°C).

Knoblauch and Jorgensen [164] investigated the growth rates and sulfate-reduction rates of five psychrophilic bacteria isolated from Arctic sediments (*Desulfofrigus marinus, desulfofrigus fragile, desulfofaba gelida, desulfotalea psychrophila,* and *desulfotalea arctica*). They found all strains capable of growing at -1.8°C, the freezing point of sea water, but grew optimally (T_{opt}) at specific temperatures. The strain of *D. gelida* grew best at 7°C, strains of *D. marinus* and *D. psychrophila* grew best at 10°C, and *D. fragile* and *D. arctica* grew best at 18°C. All of these temperatures well above the in-situ temperatures of their habitats (-1.7°C and 2.6°C). In their experiments, the highest sulfate-reduction rates occurred at 2–9°C above the T_{opt}, despite the fact that growth yields remained relatively constant between -1.8°C and T_{opt}. The exception was for two strains with growth yields peaking at the lowest temperatures, about 0°C. Their results indicated that this type of SRB (psychrophilic) tend to be adapted to permanently low temperatures by their relatively high growth rates and growth yields for in-situ conditions [164]. However, organisms which are merely psychrotolerant grow and metabolize most efficiently at temperatures above 20°C [267].

Colder temperatures, in addition to possibly affecting degradation rates metabolically can also reduce bioavailability by increasing sorption between hydrocarbons and soil particles[32] . This decreased ability to remove hydrocarbons from frigid soil is

the reason why environments such as Antarctic soils are rarely subject to biodegradation and difficult to remediate, despite being chronically contaminated in certain areas [268].

Ongoing exploration of oil reserves in the Arctic and Sub-Antarctic, as well as increased scientific research in Antarctica, have led to increased risk of oil pollution in often otherwise, pristine and sensitive environments [269]. As of 2015, there were approximately 200 reported sites in Antarctica [270]. Other indications of anaerobic hydrocarbon degradation at these temperatures have not been reported although anaerobic organisms expressing genes utilized in hydrocarbon degradation pathways have been in Arctic and Antarctic environments [270].

Recently, several strains of anaerobic bacteria have been found capable of producing biosurfactants (rhamnolipids). Biosurfactants can increase bioavailability in harsh cold environments [271] and are quite stable at a wide range of pH values, salinity, and temperature. Biosurfactants also possess lower toxicity and are more readily biodegradable than most commercial surfactants [272]. However, only one anaerobic strain has been capable of producing biosurfactants below 10°C [272]. *Pseudomonas aeruginosa* SG, a facultative anaerobe was reported by Zhao et al. [273] to be able to produce a rhamnolipid biosurfactant. Though, this ability was inhibited by the presence of sulfide, a compound often found by oil production as a result of sulfate-reduction.

2.5 The Effect of pH

The pH of seawater tends to be slightly alkaline whereas soil and freshwater environments can have a wide range of pH values. It has generally been observed that oil degradation rates increase with increasing pH reaching an optimal state between 7.0 and 8.0 [161]. The effect that pH has on degradation rates is co-dependent upon the effect on the substrates as

well as the effect of metabolic activities of the organisms [274, 275]. Hambrick et al. [276] found that the pH of a sediment played a very important role in determining the population of hydrocarbon degraders. They observed that mineralization rates were greatest at pH 8.0 and lowest at pH 5.0 and that these mineralization rates were directly related to the oxidation-reduction potential of the system. Langenhoff [192] noticed a similar observation. Studying toluene degradation under manganese-reducing conditions, he found that maximum degradation rates occurred near pH 7.0 and that no degradation occurred below a pH of 4.9 or above a pH of 8.8. Wang et al. [166] researched a strain known to be tolerant to a wide variety of temperatures and salinity and could grow at pH vales between 6 and 12. However, they established, like other researchers, that the optimal pH value was around 8.

The majority of research on the effect of pH on hydrocarbon degraders has been limited to the methanogenic and sulfate-reducing communities and few if any papers published have reported its effect on nitrate or metal-reducing organisms. Sulfate-reducing bacteria (SRB) have been noted to be found at not only extreme temperatures but also at a very wide range of pH values [277] including highly acidic or alkaline environments [278, 279]. Yet, most SRBs that are not extremophiles still have greater resistance to changes in pH than most other anaerobic bacteria [277].

In contrast to SRBs, methanogens appear to be more sensitive to changes in pH [260, 280]. O'Flaherty et al. [280] with the optimal pH range usually between 7.0 and 7.5. Monitoring changes in pH is crucial, even for neutral environments as imbalances as a result of biochemical processes may shift the pH into a potentially unfavorable state, most often towards acidic pH values. pH can decrease due to an abundant production of CO_2,

H_2S, or simple organic acids during anaerobic biodegradation [281], much as increases in pH can also occur via nitrate reduction to ammonia leading to an ammonia buildup [282, 283]. Methanogens are especially sensitive to changes in pH and are crucial to the biodegradation process. Dolfing et al. [260] found that both the process of hexadecane oxidation and the conversion of hexadecane to acetate are dependent upon the pH and that both processes become increasingly energetically favorable as pH increases.

2.6 The Effect of Salinity

Although much research has been spent on the effect of salinity on hydrocarbon biodegradation, it has primarily pertained to aerobic organisms or environments. Nevertheless, it appears well agreed upon that with the exception of halophilic organisms, salinity levels well above the norm for a particular environment yield negative results on the degradation rates of the tested compounds and of the organisms' metabolism in general. For example, Minai-Tehrani et al. [284] observed that at both a 30 g/L and 50 g/L NaCl concentration, PAH and overall crude oil degradation activity was reduced, and to a greater degree at the 50 g/L level. They also noted an intriguing discrepancy between certain PAHs and other crude oil compounds. The overall biodegradation rates of the crude oil at 0 g/L NaCl were higher than at 10 g/L NaCl but the reverse was true (i.e., 10 g/L NaCl had higher rates) for many of the PAH compounds such as phenanthrene, anthracene and pyrene but not for fluoranthene and chrysene. These results were observed under aerobic conditions; however, it is assumed that a similar trend may be true for anaerobic organisms.

Adelaja et al. [250] looked at microbial fuel cells (MFCs) and conducted batch tests focusing on the effect of salinity of the anaerobic degradation of phenanthrene and benzene. They found that at salinity levels up to 15 g/L degradation rates were 60-90% but

worsened significantly (20-25% degradation) when the salinity was raised to 25 g/L. They concluded that salinity levels of 10 g/L appeared to be the optimal salinity level for the biodegradation of these two compounds. O. Lefebvre [285], a strong contributor to this field, also tested along with his colleagues the effect of salinity on the anaerobic degradation rates in MFCs. Their results showed that the addition of up to 20 g/L NaCl showed to be beneficial towards the biodegradation process but that 40 g/L NaCl was quite detrimental. They also concluded the 20 g/L of NaCl was indeed the optimal concentration for these bacteria [285]. In partial contrast, a previous study by Lefebvre [167] showed that concentrations of NaCl above 20 g/L inhibited acidogenesis to some degree but methanogenesis was shown to be inhibited by NaCl concentrations of as low as 5 g/L and cited literature that sodium concentration exceeding 10 g/L will strongly inhibit methanogenesis. However, Nicholson et al. [286] cited sources that methanogens were capable of surviving in hypersaline environments such as the Dead Sea. This shows that the detrimental effect salinity upon methanogenesis depends strongly upon which organisms are involved. Other researchers have demonstrated that tolerance to hypersaline environments can also be exhibited by other anaerobic organisms. Liang et al. [168] investigated a facultative anaerobe that showed its strongest degradation ability at 10-20 mg/L total salinity (akin to its natural environment) and was able to partially degraded fluoranthene and benzo[a]pyrene. Wang et al. [166] reported a hardy strain of *Dietzia*, a facultative anaerobe, that was capable of significant growth of C_6-C_{20} alkanes with salinity levels up to 20 mg/L NaCl, the equivalent of 3.4 M.

Recently, Al-Mailem et al. [169] utilized halophilic strains from an area with concentrations of about 4 M NaCl (~233 g/L). Brusa et al. [170] and his colleagues studied

mixed cultures obtained from water/brine interfaces in deep hypersaline anoxic basins in the eastern Mediterranean Sea. They found eight strains capable of completely degrading toluene six to ten days. They were supplemented with yeast extract and grew in the presence of NaCl concentrations of up to 100 g/L but also at much lower concentrations, indicating that they are halotolerant rather than halophilic.

Several researchers such as Le Borgne et al. [287] noted that although as a general rule, metabolic activity and diversity decreases with increasing salt concentration, the metabolization of hydrocarbons over an extended period of time tends to increase, suggesting that microbes can adapt to high salt concentrations. It is not known if this is true as well for anaerobic organisms.

Environments with high salinity are often thought of as aquatic, such as seas and oceans. However, study on the remediation on saline contaminated lands is often overlooked. Soils with high degrees of salinity represent around 40% of the world's lands and contaminated saline soil, including saline-alkali soil, is a common occurrence and as oilfields tends to be located in coastal areas [288]. The saline conditions often limit bacteria activity due to the salts' unfavorable high osmotic potential [288].

In addition to affecting the organisms metabolically or biochemically, the effect of salinity can also hamper biodegradation due to physical restraints. Tremblay et al. [289] showed that the PAHs sorbed to suspended particulate matter (taken from a depth of 20 m) tends to increase with salinity and that salinity has a very significant effect on the partition coefficient (Kp). Sorption/desorption constants were observed to increase significantly with increasing salinity but no significant differences were found between sorption and desorption equilibrium constants (Kd) [290]. Another concern is that salts may reduce the

effect of humic acid or other organic matter. Humic acid has been shown to enhance the solubility of some PAHs which would potentially increase biodegradation rates [291]. Yet, high salt concentrations can increase sorption factors and reduce the availability of compounds like humic acid, thereby restricting the solubility of these PAHs [289]. A recently developed alternative to ordinary bioremediation techniques for saline environments is the use of bioelectrochemical degradation, a technology that utilizes the inherent conductivity of the soil present to function as a microbial fuel cell in-situ [288].

2.7 Conclusion

The world of anaerobic organisms and their role in biodegradation of hydrocarbons is still far from well understood. They have been shown often to be resilient and capable of degrading many types of hydrocarbons under a wide variety of conditions. Yet, certain branched alkanes and most PAHs still provide an obstacle. Enhancements such as electron donors, favorable growth conditions, and the proper consortia of bacterial and archaeal strains may pave the way to finding means of increasing biodegradation potential. A summary of optimum concentrations for electron donor under sulfate-reducing and nitrate-reducing conditions is seen in Table 2.6.

Anaerobic degradation can take place under a variety of different conditions and every environment present a unique challenge. The presence of sulfur in many sediments and marine environments necessitates the enhancement of sulfate-reduction while more fertile areas with plant growth might utilize nitrate-reduction. Organisms in rocky and barren environments might reduce metals instead. However, the ample supply of both primary electron acceptors and supplemental electron donors (co-substrates) are crucial for proper degradation to take place. Temperature and salinity play vital roles and

bioavailability is always a concern. Nevertheless, given the diversity of metabolic and catabolic genes, and the increasing discovery of unique enzymatic properties of anaerobic organisms, it may in fact be that anaerobic conditions are not as limited in its degradation capacity as once thought.

Table 2.6 Optimum Concentrations of Electrons Donors Added for Hydrocarbon Degradation

Compound	**Electron Acceptor**	**Conc.** (mM)	**Conditions**	**Ref.**
Benzene	Sulfate	10	Sulfate-reducing	[126]
Toluene, Ethylbenzene	Sulfate	10.4	Sulfate-reducing	[126]
o- , *p*-xylene	Sulfate	5.2	Sulfate-reducing	[126]
m-xylene	Sulfate	8.3	Sulfate-reducing	[126]
Naphthalene	Sulfate	10	Sulfate-reducing	[58]
Phenanthrene	Sulfate	10	Sulfate-reducing	[58]
Phenanthrene	Sulfate	11.1	Sulfate-reducing	[127]
Phenanthrene, Pyrene, Anthracene, Fluorene, Acenaphthene	Sulfate	20	Sulfate-reducing	[67]
Naphthalene	Nitrate	5	Nitrate-reducing	[135]
Acenaphthalene	Nitrate	5	Nitrate-reducing	[135]
Pyrene	Nitrate	2	Nitrate-reducing	[136]
Naphthalene	Nitrate	<2.14	Nitrate-reducing	[193]
Alkanes	Nitrite	5	Nitrate-reducing	[130]
Pyrene	Nitrite	2, 5	Nitrate-reducing	[136]

Nevertheless, it is well understood that aerobic conditions and the use of aerobic organisms to degrade PAHs is far more effective than its anaerobic counterpart. This does not mean, though, that aerobic degradation always occurs or does not have hindrances in its degradation rates or that extent of mineralization that takes place. One technology currently being studied in detail to improve the efficiency of aerobic degradations is electrokinetics. Numerous studies pertaining to general migrations, patterns, operational variable, and attempt at enhance PAH biodegradation are seen in Chapters 3-7.

CHAPTER 3

AN INTRODUCTION TO ELECTROKINETICS AND ITS APPLICABILITY TO CONTAMINANT REMEDIATION

3.1 Background

Many technologies have been applied to remediate groundwater and soil contaminants [292]. Approaches include removal, isolation, and the transformation or breakdown of the contaminants [120]. Degradation can occur through physical, chemical, or biological means, and often all three play a role. Electrokinetics is a remediation technology whereby a DC voltage is applied to the subsurface porous media in order to enhance the transport of specific compounds [293] The core principles by which it works are: electroosmosis, electrophoresis, and electromigration. Electroosmosis is the bulk movement of fluid (i.e., water), electromigration is the movement of ions in solution based upon charge, and electrophoresis is the movement of suspended particles in the pore fluid [57]. Electrokinetics results in the electrolysis of water via the following reactions (Equations 3.1 and 3.2).

At the anode:

$$2H_2O - 4e^- \rightarrow O_2 + 4H^+ \tag{3.1}$$

At the cathode:

$$2H_2O + 2e^- \rightarrow H_2 + 2OH^- \tag{3.2}$$

When sodium chloride or other chloride-based salts are used as the primary electrolyte, chlorine gas (Cl_2) can also be generated at the anode [294] via Equation 3.3. Cl_2 production depends on the amount of chloride ions initially added, as well as pH and temperature of the anode reservoir. The specific rate at which chloride ions are oxidized

is dependent upon the electric current and can be described by Faraday's law (Equation 3.4) [295].

$$2Cl^- - 2e^- \rightarrow Cl_2 \tag{3.3}$$

$$I = F\sum_{i=1}^{N} j_i z_i \tag{3.4}$$

where F is Faraday's constant, j_i (mol/s) is the ion flux contributing to the flow of electrical current I (A), and z_i is the number of participating ions in the reaction. While Cl_2 generation can be a concern in marine environments [295], exceedingly few papers cite this is a concern under normal laboratory conditions, where NaCl are usually at levels near 1 g/L. The only instances of relevance generally presented in the literature under these conditions is when hydrochloric acid is used as a (pH) conditioning agent [296].

3.2 Uses of Electrokinetic Technology

Electrokinetic technology has been employed for a variety of environmental cleanup method since the early 1990s, including the removal of heavy metals, low molecular weight (LMW) hydrocarbons, and early attempts at biodegradation [70, 297-300]. Some successful pilot and in-situ studies have also been performed prior to 2000, including an electro-bioreclamation project to capture diesel fuel [301], a contaminant transport technology known as Lasagna used to remove chlorinated pollutants such as trichloroethylene [302], and the distribution of ammonium nitrate and other nutrients via EK to stimulate biodegradation [303, 304].

More recently, EK technology has become far more widespread and broader in its applications. In 2009, Reddy and Cameselle [69] published a scientific book entitled "Electrochemical Remediation Technologies for Polluted Soils, Sediments and

Groundwater", which highlights the use of EK technology to remove and/or remediate contaminants such as heavy metals, chlorinated organic compounds, herbicides, and hydrocarbons such as PAHs [293]. With respect to hydrocarbons solely, earlier studies focused primarily upon alkanes and monoaromatics [57] whereas in the mid-2000s, studies emerged successfully using EK to enhance biological and chemical degradation of PAHs with 2 or 3 rings, largely naphthalenes and phenanthrene [305]. In the last ten years, studies employing EK, chiefly as a means of enhancing biodegradation, have been conducted and successfully demonstrated the ability to enhance the removal of PAHs with four or more rings, including benzo[a]pyrene [306] and high-molecular-weight (HMW) PAH mixtures [307]

One of the biggest challenges to successful EK-based remediation is the tendency of a system to quickly reach extreme pH values thereby reducing effective techniques, primarily biodegradation [308]. [Xu et al. [76] utilized the combination of electrolyte circulation and frequent polarity reversal (every 12h) in an EK system to successfully remove phenanthrene from a clayey soil. This dual technique obviated the need of buffers and kept pH values between 7.0-7.6, an ideal range for most PAH-degrading bacteria. Wand allowed for 80% of an initial concentration of 200/mg/kg phenanthrene to be degraded. Wang et al. [307] used bacteria from soil at a coking plant to degrade PAHs (artificially spiked) via the EK process. Total PAH concentration added was 91.4 mg/kg and were predominantly high-molecular-weight (HMW) compounds (4+ rings). The native soil bacteria were supplement with an additional strain of *L. theobromae*, a strain shown to efficiently degrade many PAHs. Similar to Xu et al's study [76], Wang et al. [307] utilized the circulation of a mixed electrolyte solution and frequent (daily) polarity

reversal. This technique maintained pH levels at 7.5-8.3 over the course of the 200-day experiment. Their results showed that the EK system led to far greater than the control setup, which was identical to the EK setup minus the electrodes and power source (i.e., no bacterial inhibition, and presence of pumped electrolytes). Total PAH degradation rates in the EK system ranged from 48-58%, in comparison to the control, in which only 25-34% PAH degradation was observed. The greatest difference observed between these two systems was for the HMW PAHs.

Li et al. [308] studied the effect of an EK system on pyrene degradation. They did not utilize an electrolyte circulation but instead employed a systematic technique whereby the polarity was reversed every 2 hours. This polarity reversal maintained the pH at a value of 7.2 and led to increased bacterial growth an improved degradation, with nearly 56% of the pyrene removed over 42 days. In their study, the used a bacterial culture shown to be capable of pyrene degradation and included *Acinetobacter baumannii, Bacillus pumilus, Pseudomonas putida, Pseudomonas nitroreducens* and *Bordetella* sp. Additionally, no reservoir was utilized in this study and the electrodes were placed directly in the edges of the soil, which was kept at a moisture level of 30%. Huang et al. [309] conducted a very similar study investing the potential of EK technology to improve the bioremediation of benzo[a]pyrene (50 mg/kg). After a period of 40 days, greater than 40% of this compound was degraded, nearly twice the amount degraded under non-EK conditions.

The use of EK technology to remove PAHs from soil is not limited to bioremediation techniques. Alcántara et al. [310] utilized electrolyte circulation combined with the surfactant Tween 80 (1%) and 0.1M Na_2SO_4 in order to flush three PAHs from the soil. The PAHs studied were fluoranthene, pyrene, and benzanthracene added at 500

mg of each compound per kg of soil. The soil utilized in the study was 85% kaolin. In their study, they used a depolarization technique to mitigate the development of strong pH shifts and maintain pH values around 7. This resulted in the removal of 45% and 57% of the pyrene and fluoranthene, respectively. No significant benzanthracene removal was seen although it underwent a migration towards the cathode, implying an eventual removal were the experiment allowed to continue for a longer duration. The overall duration of the experiment was 23 days. The strong removal and migration of the PAHs was attributed to the strong electroosmotic flow obtained in the system, further strengthened by the regulation of the pH [310].

While the overall objective of this dissertation is focuses upon hydrocarbons such as PAHs, the electrokinetic process can be used to remediate many other classes of pollutants, especially heavy metals. Alshawabkeh, an early contributor to the EK field, worked with others to conduct a pilot-scale study [311] to extract lead from contaminated sand and sandy soil. Using electromigration, 85% of the lead in sand was removed, and using a combination of electromigration and electroosmosis, 70% of the lead in the sandy soil (clayey sand) was removed. Average lead transport values observed in these experiments were around 0.4 cm/day at a voltage gradient of 1 V/cm. Initial lead concentrations of lead in the two media were 3041 mg/kg and 1187 mg/kg, respectfully and final values were reported to be approximately 500 mg/kg and 400 mg/kg. Colacicco et al. [312] used EK technology to remediate marine sediments co-contaminated with heavy metals and PAHs.

3.3 Conclusion

EK technology has been successfully employed to remediate contaminants such as heavy metals, toxic dyes, and hydrocarbons. Efforts are constantly being made to enhance efficiencies of this technology and further understand its possibilities. In the following chapters, experiments were conducted to demonstrate migration patterns in both sands and clay for compounds with different ionic properties and behavior was analyzed to determine change in system pH values and relevant gradients. Additionally, aerobic biodegradation studies were conducted with soils spiked with Polycyclic Aromatic Hydrocarbons to investigate how the electrokinetic process could enhance biodegradation rates.

CHAPTER 4

A STUDY IN ELECTROKINETIC MIGRATION RATES IN SAND AND IN CLAY

4.1 Introduction

Electrokinetics (EK) can be used to remediate pollutants chemically and biologically. EK can transport compounds such as persulfate and permanganate which produce oxygen radicals and also can effectively make contaminants, nutrients, electrons acceptors, and electron donors more accessible as a means of enhancing biodegradation [299, 313] . Though, the rate at which compounds are transported relies on the media through which it is being transported and heavily upon the nature of the compound of interest [314].

Different subsurface media (e.g., sand, soil) may favor one or several specific electrokinetic principle over the others. Electromigration has been shown to be the dominant process in sand, whereas both electromigration and electroosmosis are considerable in clay. Yet, most electrokinetic experiments and implementations have been utilized solely in clay and fine-grained soils rather than sands [293] particularly for non-ionic compounds and heavy metals [91]. There are two reasons for this: 1) Though electromigration occurs more rapidly than electroosmosis in clay soils, electroosmosis appears to be a less energy-demanding process 2) Sands often have other more cost-efficient methods of cleanup available, such as enhancement of the hydraulic gradients through pumping. Consequently, in-situ EK in sands is less cost-efficient than in clay soils and less frequently studied [315]. Electromigration, however, is primarily reserved for the migration of charged species and electroosmotic processes are needed for non-ionic and hydrophobic compounds such as many components of crude oil. The phenomena of

electroosmosis is largely absent in sand due to its very low surface charge density [70] and thus the implementation of electroosmotic phenomena seemingly cannot be used within sand. Part of the purpose of this experiment, therefore, was to test this theory and confirm the absence of the electroosmotic process in fine-grained sand.

With respect to clay, Alshawabkeh [314] reports that per electric gradient of 1V/cm, electroosmotic rates range from 0.01 - 10 cm/d and electromigration rates from 0.5 - 10 cm/d, both of which tending towards the higher rates. Electroosmotic rates in sand have not frequently been reported but have been shown to be negligible as Lindgren et al. [298] estimated it to be only 0.24 cm/d and Alshawabkeh [314] reported an even lower value of less than 0.05 cm/d. Electromigration rates in sand, however, are often in the range of 10 cm/d and can be at least 20 cm/d depending on the power put into the system and other variable factors such as ionic strength [314, 316]. Electromigration in clay should be observable but noticeably much slower than the rate in more permeable materials such as sand [296].

In addition to utilizing EK phenomena such as electromigration to enhance nutrient delivery, it can also be used to migrate contaminants, depending upon the properties of the pollutants and the environmental and system variables [57]. Ionic and non-ionic dyes can be used as a means of modeling contaminants and their particular migrational patterns [317, 318] and due to varying properties, specific dyes can be used to predict how certain contaminants will migrate.

Two dyes, an anionic red dye and a green dye with both anionic and cationic properties, were studied in these experiments. The red dye was a food coloring primarily consisting of FD&C Red 40 and the green dye, also a food coloring, contained a mixture

of turmeric and *Spirulina* Blue. FD&C 40 (Figure 4.1), a red food coloring, is a strongly anionic dye. Anionic dyes such as FD&C 40, can be used to mimic anionic chemicals or metals in solution and can give an estimate for their electromigration rates [319]. The electromigration of this dye is especially similar to that of chromium (VI) when compared at a similar concentration, in both sands and in clay [320] and was studied on multiple occasions by Lindgren et al. [298, 321] and was used as a basis of study by Reddy et al.to remove chromium, nickel, and cadmium for clays via the EK process [322, 323]. Pazos et al.[324] studied a kaolin clay polluted with the predominantly anionic dye Lissamine Green B (a.k.a. Acid Green 50) as a means of evaluating the ability of EK phenomena to remove organic pollutants from soils. They found that by using sodium phosphate as a processing fluid, the electroosmotic flux was greatly enhanced, leading to 94% dye removal in 2 days. FD&C Red 40 also possesses similar properties to other predominantly anionic dyes such as Reactive Blue 19. These dyes are commercial textile dyes and have been found to be highly toxic to both aquatic and human life [325].

The green dye utilized in this study contained turmeric and *Spirulina* Blue, a blue coloring obtained from the cyanobacteria *spirulina platensis*. As turmeric tends to adhere to sand or soil particles, this blue component is the only migrating component of the green dye, and is primarily comprised of the pigment-protein C-phycocyanin [326, 327]. *Spirulina* Blue, or specifically the compound C-phycocyanin, is regarded as an amphoteric compound, meaning it has sufficient ability to both donate and accept electrons. The presence of several terminal amine groups (Figure 4.1) allows for a wide variety of behavior within a media, dependent upon environmental variables, predominantly pH and thus C-phycocyanin can function as an anionic, non-ionic, or cationic dye depending upon

the pH at the location of the dye (see Chapter 5). The isoelectric point (pI), or the point at which this molecule is neutral (has no effective charge) can range from 4.6-5.2 [328] but is often found to be around 4.8 [329].

This type of dye can be used to analyze migration abilities for the removal of other amphoteric compounds, that are quite toxic in nature, such as Congo Red [330] and Acid Blue dyes [331]. Analysis of C-phycocyanin's behavior may also prove useful in modeling migration patterns of emerging hormone contaminants such as sulfonamides and tetracyclines [332-334]. This is in addition to N-heterocyclic compounds such as quinoline that are produced for applications in products such as pharmaceuticals and disinfectants [335]. Quinoline at concerning levels has been discovered in soils, surface water, and coastal areas, and is highly resistant to biodegradation [336]. Ren et al.[336] found that electrokinetics can be a useful alternative to other remediation methods for quinoline removal but that the efficiency of removal was partially depending upon the pH gradient, and that its migration was enhanced by the addition of a buffer to the anodic chamber (Na_2CO_3), which also increased conductivity and subsequent electroosmotic flow within the soil.

Unlike the red dye's applicability, with is limited to certain heavy metals and some strongly anionic compounds, the migrational patterns of Spirulina Blue (C-phycocyanin) are broader in scope, including a possible approach towards PAH remediation. The amphoteric nature of this compound can assist with this in two possible ways. Some surfactants, especially those used to flush PAHs sorbed to subsurface media, tend to be amphoteric in nature and may migrate within groundwater in a similar manner to the dye used in this study [337]. Additionally, some PAHs can be transformed, chemically or

photochemically to derivatives containing nitro- and amino- groups thereby sometimes obtaining semi- zwitterionic or amphoteric qualities [338]. Most aromatic amines, which can include some substituted PAHs, tend to have pKas below 5.5, and can thus be in a protonated state at significantly lower pH values, thus being prone to electromigration [339].

One purpose of this study was to compare the electromigration rates of FD&C Red 40 in both sand and clay. Another purpose of this experiments was to compare migration of two different dye types.

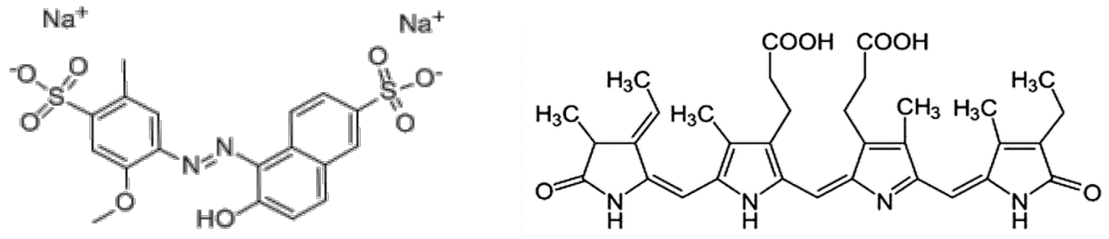

Figure 4.1 Molecular structure of FD&C Red 40 (left) and C-Phycocyanin (right).

The main objectives of this study were to investigate different rates of electrokinetic phenomena, primarily electromigration, and to compare these two different dyes and how their migration rates and patterns changed accordingly. It was expected that the red dye would move fairly rapidly, via electromigration, towards the anode in sand and similarly but at a slowly rate in clay. The green dye (specifically the *Spirulina* Blue as the turmeric stays in place) was not predetermined as to its behavior but these studies were conducted to see their migration behavior and how it might change with respect to pH as results of the dye's amphoteric properties. Electromigration was expected in the sand and either electromigration or electroosmosis was anticipated to occur in the clay.

Experiments were performed in self-designed setups (Figure 4.2). Four separate studies were conducted to measure these scenarios.

4.2 Materials and Methods

4.2.1 System Design

Two identical Electrokinetic (EK) apparatuses (Figure 4.2) designated as “System 1” and “System 2” were constructed consisting of the following: Two 25.4 x 27.9 x 45.7 cm (10 x 11 x 18”) acrylic reservoirs were connected to an acrylic bridge constructed by fusing two 47.5 x 1.3 x 12 cm (18 x 0.5 x 5”) acrylic pieces atop the sides of a base piece measuring 47.5 x 6.4 x 2.5 cm (18 x 2.5 x 1”), with a lid made to prevent evaporation. A grid with units of 1 cm x 0.5 cm was placed upon each bridge for measuring the dye migration distances. Each reservoir had a lid onto which a 12V computer fan was attached to create circulation (Figure 4.2). Mesh pouches with palladium-coated pellets were fitted atop the fans to capture any hydrogen gas produced. Each lid also had a center-cut hole accommodate the wire connections to the probes and its holders (Figure 4.2).

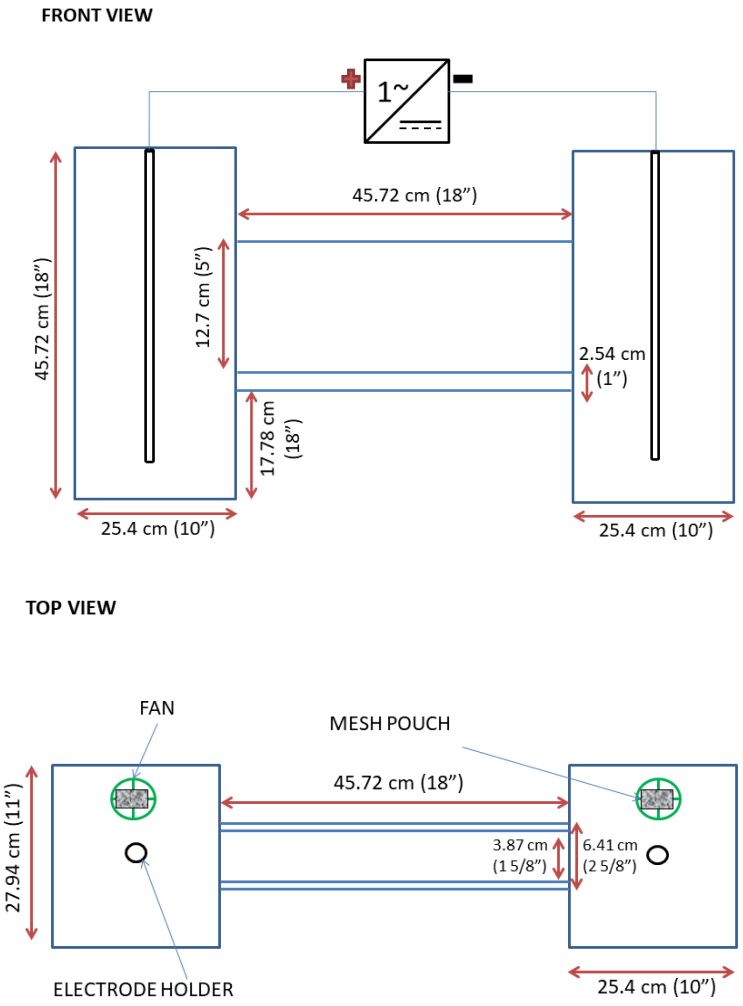

Figure 4.2 Schematics showing the top and bottom view of the electrokinetic apparatus used in these experiments.

The housing for the electrodes was constructed from clear PVC (Figure 4.3). Electrodes were 30 cm graphite rods with a 0.63 cm diameter. Power Supply was a commercial 30V output with a measured 9.36 ± 0.04 mA current output. The voltage gradient through the media was calculated to be 0.66 V/cm (0.45 V/cm between electrodes) and the current density was calculated to be .054 mA/cm^2. A confirmation experiment was performed for the migration of the green dye in sand at an identical

voltage but a slightly lower current output (0.040 mA/cm^2). A separate power supply was used for each system. Two systems were generally run in parallel.

For the green dye in sand, two sets of experiments were initially performed. Both experiment sets utilized two systems, designated as "System 1" and "System 2". The first experiment set functioned as a general determination, but control parameters were not put into place and many measurements were not taken. Based upon results of the first experiment set, a second experiment was conducted with strict monitoring and data collection.

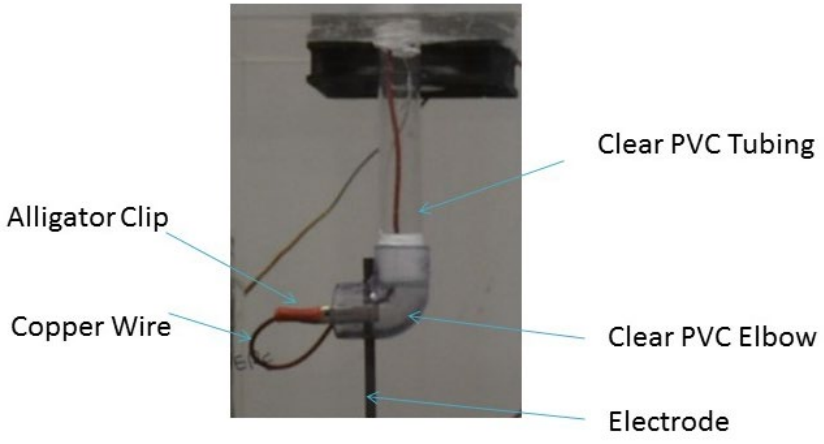

Figure 4.3 Diagram showing the electrode holder apparatus and connections.

4.2.2 Filling Techniques

For the tests using the red dye, a basic quality sand was used (Play Sand - Arena Natural, Sakrete®, Cincinnati, OH, USA), which was found to have a basic pH (8.5-9.0). Upon this discovery, the sand was switched to a higher quality very fine sand (FilPro® NJ 60 Filtration Sand (#000 size equivalent), U.S. Silica, Frederick, MD, USA). This new sand, which was used for the green dye, did not have any noted impact on the pH of the systems.

For filling the systems, sand was added to an empty system in the bridge area (see Figure 4.2) and filled to a height of about 10 cm. The sand was gently compacted and smoothed out to ensure uniformity. A solution of 1 g/L NaCl was prepared and mixed thoroughly. For the red dye tests, the NaCl was added directly to each reservoir and left to equilibrate so that the height of the liquid in the bridge was just below the sand surface (by ~2mm). For the first test utilizing the green dye (Set1), initially one of two systems was filled in this method while a second system employed a more ideal filling approach, where the NaCl solution was added to the anode reservoir (left) until it reached just below the sand surface. This allowed for proper distribution of the sodium chloride throughout the sand. The liquid was allowed to infiltrate and begin filling the cathode reservoir (right). As the level in the anode reservoir became lower, more NaCl solution was added periodically until it reached a level of 2 mm below the sand surface with both reservoir levels being equal. The system was allowed to equilibrate overnight. A confirmation experiment (also in duplicate) was additionally performed, utilizing only the latter filling method. Both experiment sets are reported in the data.

For the clay-based experiments, the clay media consisted of a 50/50 mixture of kaolin clay (EPK Kaolin (97% purity), Edgar Minerals, Hawthorne, FL, USA) and rock flour (fine-grained silt-sized granite, unknown source). For each setup, 1 kg of each soil type were mixed using a Classic™ heavy-duty mixer (KitchenAid, Benton Harbor, MI, USA) and then combined with 800 mL of tap water until a smooth consistency was achieved. (Tap water was used in order to approximately mimic groundwater in an in-situ environment). This corresponded to a 28.57% moisture content (w/w). A solution of 1 g/L NaCl was prepared and mixed thoroughly and added to each reservoir independently

until the liquid height was just above the clay, to ensure the clay would not become dry and crack. The final moisture content was 34.02 % and 30.43 %, respectively for the red dye experiment and 29.90 % and 29.20 %, respectively for the green dye experiment. Moisture contents were determined by weighing a sample prior to and following being dried overnight at 101.5°C. Final percentages were calculated by dividing the weight difference by the initial weight of the soil sample.

4.2.3 The Addition of Dyes

McCormick® Red Food Color (primarily FD&C red dye #40) was used as an anionic dye and Watkins® green Food Coloring was used as a dye with both anionic and cationic properties (Table 4.1). Herein, these dyes will be referred to as "red dye" and "green dye", respectively. The green dye was composed of turmeric and *Spirulina* Blue, with the latter component intended to be the migration substance of interest as the turmeric component was previously observed to remain behind (in both sand and clay media) and thus expected to remain in its place. In the sand experiments, for the red dye and the initial green dye experiments, approximately 2 mL of dye were injected via a 10 mL syringe just above the center height and in the red dye experiments, the dye was allowed to diffuse naturally overnight. Following any diffusion, the power was turned on and allowed to run until the edge of the visible sand area was reached (30-51 hours). In the initial green dye experiments, power was applied shortly after dye insertion and ran for about 50 hours. In order to confirm if the green dye would behave similarly were diffusion allowed to occur, in the second set of green dye experiments, the dye was allowed to diffuse naturally overnight. Once no more diffusion was detected, the power was supplied to the system. An addition difference between the initial and confirmation experiments was the use of

less dye to ensure a more controlled migration (although unlikely, this was necessary if any electroosmosis would occur). 1 mL of dye was injected via a 3 mL syringe into the justified center of the sand area. This confirmation experiment (ran in duplicate) was allowed to run until no more migration was detected (~65 h) plus an additional three days. The total duration of the second experiment set was approximately 7 days.

In all clay experiments, 2 mL of dye was inserted into each system by soaking one sheet of Kimwipe® into the dye to absorb it and the inserted via a small metal pole into the clay. A small amount of the dye washed up onto the surface of the clay prior to its insertion into the clay and thus the amount of dye estimated to reach the focal insertion point was `~1.5 mL. Dye was allowed to diffuse naturally overnight and subsequently the power was turned on and ran for about 6 days.

Table 4.1 Properties of Dyes Used in the Electrokinetic Experiments

Dye	Mol. Wt. (g/mol)	Dye Density (g/L)	Compound Density (g/L)	Charge	Volume inj. (mL)
Red Food Color. FD&C Red #40 (a.k.a. Allura Red AC)[1]	496.416[2]	1.0269[1]	0.8[2]	-2	2 mL*
Green Food Coloring. Spirulina Extract (C-phycocyanin)[3]	252000 [4]	1.15405[5]	0.96[6]	-2 to +18	1-2 mL*

*1.5 mL estimated for both dyes in clay as some dye was lost during injection, 2 mL is estimated for the first green dye experiment. 1 mL was used for the second green dye experiment.

[1]Red Food Color. Material Safety Data Sheet. McCormick and Company, Inc. 2010.
[2]FD&C Red No. 40. Compound Summary. PubChem. 2018.
[3]Kuddus, M. et al. 2015. Production of c-phycocyanin and its potential applications. *Biotechnology of bioactive compounds: sources and applications. Wiley-Blackwell Ltd*, p.283-299.
[4] C-Phycocyanin. Datasheet. AnaSpec. 2018.
[5]Natural Green Color. Safety Data Sheet. The J.R. Watkins Co. 2010.
[6]Organic Spirulina Extract WS. Material Safety Data Sheet. Natural Sourcing. 2011.
[7] Peptide Calculator. Bachem (alpha subunit). 2018. (Used to determine sequence)
[8] Protein Calculator. Sequence input. 2014.

4.3 Measurements

pH measurements for the large setups were conducted using the AquaShock pH meter (Sper Scientific®, Scottsdale, AZ, USA) and probe at two locations in each reservoir. One measurement was taken at the front corner, farthest away from the bridge of the apparatus (see Figure 4.2) and the other measurement was taken immediately adjacent to the beginning of the bridge, near the location of the electrode. In one of the systems (sand media, green dye – system 2), a polarity reversal (switching of anode and cathode) was performed in order to investigate the rate at which extreme pH values, generated by electrolytic phenomena (Equations 3.1 and 3.2), would be reversed (Figure 4.14).

Temperature was monitored as the electric current was hypothesized to raise a system's overall temperature. Temperatures values were also measured using the AquaShock pH meter, primarily at the first pH measurement location. Voltage and current were measured using the EX330 Multimeter (Extech® Instruments, Waltham, MA, USA) and measured with each probe at opposite ends of the media (anode-side and cathode-side) at about a 1/2 penetration depth. Salinity was measured using the YSI® Model 30 Salinity/ Conductivity/ Temperature meter (YSI Incorporated, Yellow Springs, OH, USA) and was measured in the center of each reservoir at about a mid-way depth.

4.4 Theory and Calculations

4.4.1 Electromigration in Sand

The migration of ions through sand is a relatively straightforward process. A direct current is applied to the system and a pair of electrode are established as anode and a cathode. Anions will migrate towards the anode and cations towards the cathode [340]. The speed at which they will migrate is dependent upon the ionic strength of the solution,

the ionic mobility and concentration of the contaminant, the grain size of the sand, and the voltage and current applied [296, 341].

4.4.2 Electromigration in Clay

Unlike electromigration in sand, which is relatively simple, due to the absence of significant charge on sand particles [70], electromigration in clay can be quite complex due to the nature of the clay and its chemical and electrical properties as well the type and concentrations of the ions in the relevant fluid (e.g., groundwater) [71]. Graphite rods (30 cm x 0.63 cm dia.) were submerged approximately 24 cm into each reservoir. Assuming a relevant surface of half the circumference, the area applied was 24.75 cm^2. The effective transport rate of ions via an EK system [342] is given by Equation 4.1:

$$v_i = \left(\frac{k_e}{\eta} \pm u_i^* \right) i_e \tag{4.1}$$

where v_i is the transport rate (m/s), k_e is the electroosmotic permeability ($cm^2\ V^{-1}s^{-1}$), η is the porosity, u_i^* is the effective ionic mobility ($cm^2\ V^{-1}s^{-1}$), and i_e is the voltage gradient (V/cm).

The electroosmotic permeability (k_e) for kaolin clay is 5.7 x 10^{-5} $cm^2\ V^{-1}s^{-1}$ and for rock flour is 4.5 x 10^{-5} $cm^2\ V^{-1}s^{-1}$ [71]. Therefore, for the 50:50 mixture of kaolin-rock flour mixture used in this experiment, the assumed value was the average of the above two values, which would be 5.1 x 10^{-5} $cm^2\ V^{-1}s^{-1}$. This value is similar to the k_e value of 5 x 10^{-5} $cm^2\ V^{-1}s^{-1}$ for clayey silt, which this mixture is meant to represent [343]. The porosity (η) of a clayey silt is approximated to be = 0.477 [344], the voltage gradient (i_e) applied in the electrokinetic systems was 0.667 V/cm, and the effective ionic mobility (u_i^*) value used was that of chloride (Cl^-), which is 1.66 x 10^{-4} $cm^2\ V^{-1}s^{-1}$ [345].

Inserting these values into Equation 4.1, the maximum transport rate would be $\left(\frac{5.1x10^{-5}}{.477}+1.66x10^{-4}\right).667=15.73$ cm/d for anionic compounds in this media due to electromigration. As tap water was used in this experiment, rather than de-ionized water, the maximum transport rate would be marginally higher than calculated as these calculations do not take into account the increased conductivity. The tap water had a conductivity of 280 µs/m and the 1 g/L NaCl solution created using this tap water had a final conductivity of approximately 2000 µs/m and a final salinity of 1.1 ± 0.1 g/L.

4.4.3 Flux Measurements and Calculations

The total mass flux is the sum of mass fluxes due to electromigration, diffusion, advection, and electroosmosis [299, 315]. The total Flux equation [346] (excluding electroosmotic flux) is shown in Equation 4.2 and includes three components, represented by the three terms. The first term is the migration flux (electromigration), the second term is the diffusion flux, and the third term is advective flux, which was zero in these experiments.

$$\boldsymbol{N_i} = -zu_iFc_i\nabla\phi - D\nabla c_i + c_iv \tag{4.2}$$

where N_i is the total flux (mol cm^{-2} d^{-1}) z is the molecular charge of the migrating species, F is Faraday's constant (C/eq), $\nabla\phi$ is the voltage gradient (V/cm), D is the effective diffusion coefficient (cm^2/s), ∇c_i is the change in concentration (mol/L), c_i is the overall concentration (mol/L) and v is the velocity of the fluid flow.

The absolute ionic mobility, a function of ionic mobility within a particular system can be calculated through a variety of different formulas. The formula chosen is seen in Equation 4.3. It was adapted from a paper by Mattson and Lindgren et al. [75] who

conducted multiple studies of EK transport in sand and soils. Alternative formulas are shown in Appendix B.1.

$$u_i^* = u_i \eta \tau^2 = u_i \eta \tau` \tag{4.3}$$

where u_i is the observed ionic mobility ($cm^2\ V^{-1}s^{-1}$), u_i^* is the absolute ionic mobility ($cm^2\ V^{-1}s^{-1}$), η is the typical porosity of the media used, τ is the tortuosity, and $\tau`$ is the tortuosity factor, defined as τ^2 [347].

As seen in Equation 4.2., diffusion flux is one of the two key components of the total flux. The diffusion term is $-D\nabla c$, where D is the effective diffusion coefficient (D_{eff}) which is difficult to calculate precisely due to the size of the molecule, the tortuosity, and the adsorption of the solute [348]. Therefore, D was assessed as an order of magnitude and compared with migrational mass flux to determine if negligible.

Rowe and Badv [349] report the average D_{eff} of chlorine (in a NaCl solution) in sand to be approximately 10^{-5} cm^2/s and in clay to be approximately 10^{-6} cm^2/s. Huweg [350] reports the diffusion of simple cations and anion in water within a porous media to be 10^{-5} - 10^{-6} cm^2/s. The diffusion of dyes in soil is reported to be two orders of magnitude lower (~10^{-8} cm^2/s), although this varies greatly upon the nature of the dye and the structure of the system [351].

4.5 Results

4.5.1 Sand – Red Dye ((FD&C #40 Red)

In order to determine an average migration rate of the red dye in sand, this experiment was run in duplicate. Both experiments utilizing the red dye showed very apparent electromigration over a short period of time. In System 1, the dye was inserted at a

distance of 22 cm from the left reservoir (anode chamber) and migrated 13 cm towards the anode in 30.5h (Figure 4.4 a-c), thus a velocity of 10.23 cm/d. In System 2, the dye was inserted at a distance of 29 cm from the left reservoir (anode chamber) and migrated 16.75 cm towards the anode in 50.16h (Figure 4.4 d-f), thus a velocity of 8.01 cm/d. The higher migration rate of System 1 was likely a product of systematic variability but may also be attributed to a lack of sufficient equilibration time prior to adding the dye (Figure 4.4 a-c).

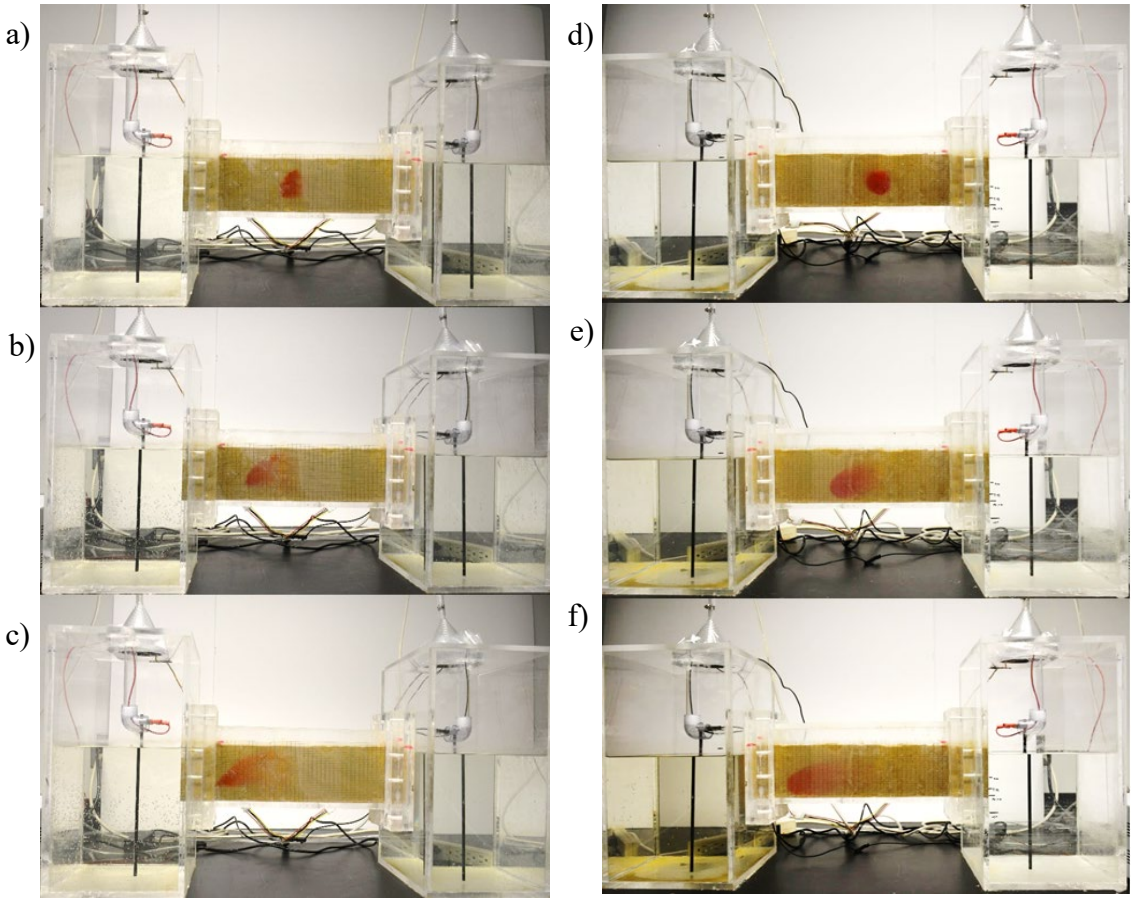

Figure 4.4 Electromigration of the red dye in sand.
System 1 at various times - a) 0h ; b) 24h ; c) 30h 30m
System 2 at various times - d) 0h ; e) 24h ; f) 50h 10m

4.5.2 Sand – Green Dye (*Spirulina* Blue / C-Phycocyanin)

Two sets of electrokinetic experiments were performed to investigate the migration of the green dye in sand. An initial experiment showed the general trend and a follow-up experiment was performed as a confirmation with better-controlled variables and additional measurements. The Initial experiment from this point forwards will be designated as "Set 1" and the confirmation experiment as "Set 2". Both experiments were run in duplicate using the convention System 1 and System 2. In Set 1, the green dye migrated to the left (towards the anode) (Figure 4.5), similar to the pattern exhibited by the red dye via electromigration. The same observation occurred for both filling methods (system 2 not shown). System 1 (which did not have the 1 g/L NaCl pass through the sand in order to fill the reservoirs) migrated 14.75 cm in 48 h or 6.88 cm/d (Figure 4.5), only slightly slower than System 2 (which *did* have the 1 g/L NaCl pass through the sand in order to fill the reservoirs), in which the dye migrated 16 cm in 50 h or 7.68 cm/d. No changes in hydraulic levels in either system were noticed.

As the initial set of experiments (Set 1) showed a quite rapid migration of the green dye (mostly the *Spirulina* blue) towards the anode, it was necessary to determine if this would occur under more controlled conditions. For Set 1, the exhibited migration pattern was different in both setups, as diffusion was not allowed to occur prior to the onset of power. As circumstances were uncertain, the experiment was replicated with modifications and under firmly monitored conditions. All diffusion was allowed to occur before turning on the power and power was turned on when no more diffusion was noticeable. Additionally, setups were run with opposite polarity (i.e., one system had the anode on the left, the other system had the anode on the right). This was done so as to eliminate any structural biases and thereby rule out any influence of hydrodynamics. In

both systems, a yellow trace (turmeric) was left behind, and the blue component moved towards the anode at (Figure 4.6) at a rate of 7.28 ± 0.57 cm/d (Table 4.2).

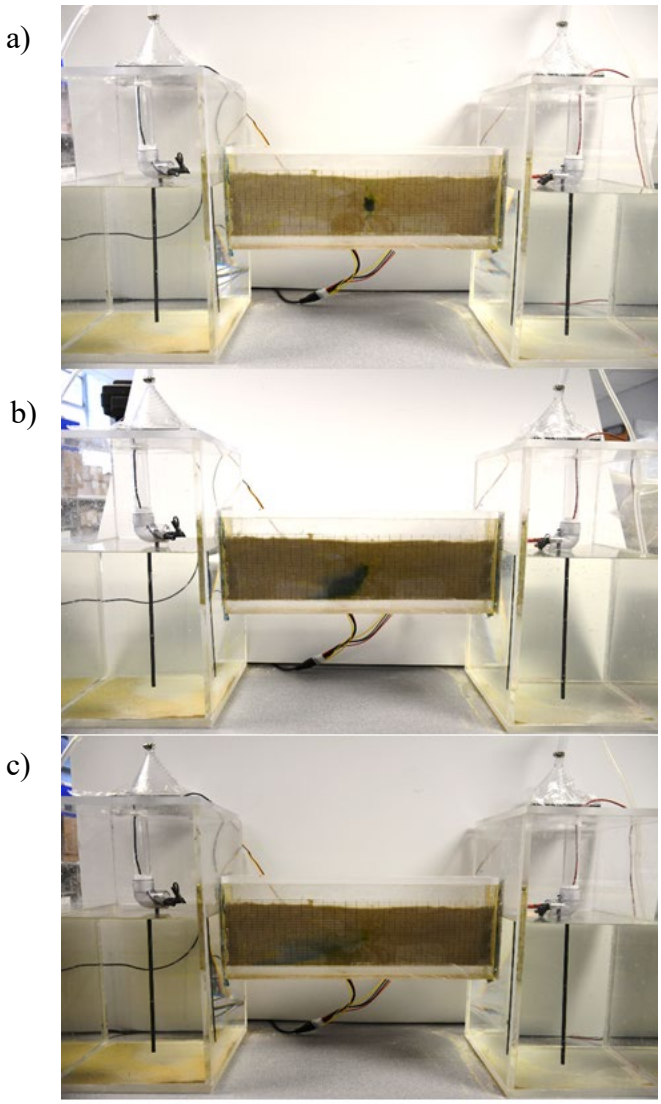

Figure 4.5 Electromigration of green dye in sand – system 1, at various times (anode on left): a) 0 h ; b) 27 h ; c) 48 h.

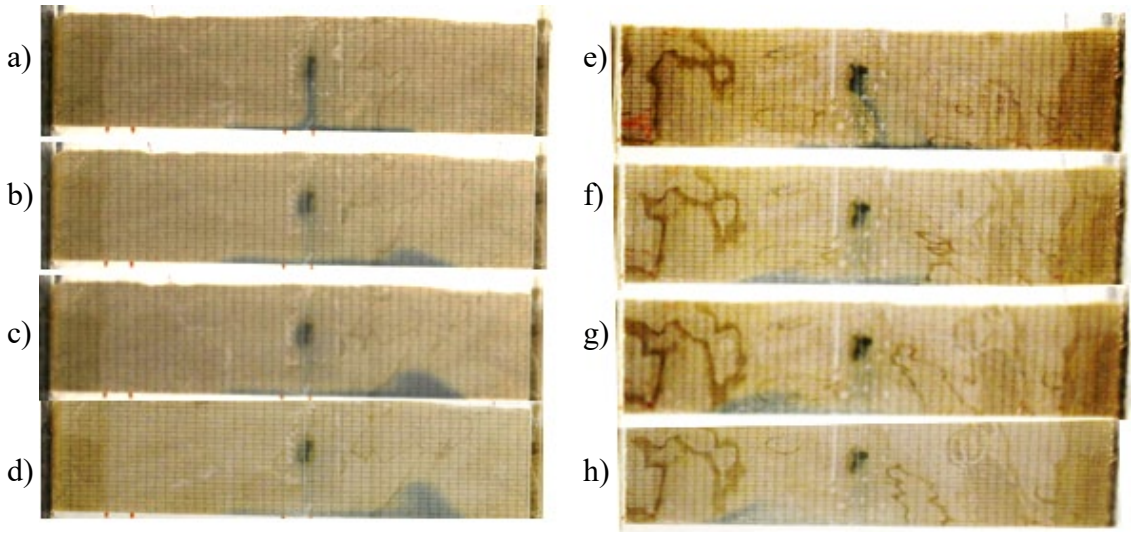

Figure 4.6 Electromigration of green dye in sand.
System 1 at various times (anode on right) - a) 0h ; b) 24h ; c) 48h ; d) 72h
System 2 at various times (anode on left) - e) 0h ; f) 24h ; g) 48h ; h) 72h

4.5.3 Clay – Red Dye (FD&C #40 Red)

To test the migration of the red dye in clay, setups were again run in duplicate. In both systems, the migration of suspended particles (electrophoresis) was observed shortly after turning on the power, causing small amounts of clay to migrate into the anode reservoirs (Figure 4.9). In negatively charged clay, such as kaolin, electrophoresis is known to occur in the anodic direction [352]. In System 1, the dye migrated 5.5 cm towards the anode in 161.5 h, providing an average speed of 0.82 cm/d (Figure 4.7). In System 2, the dye migrated 7 cm towards the anode in 161.5 h giving a speed of 1.04 cm/d (Figure 4.8). The migration of the dye in System 1 was also less noticeable than in System 2, probably because the dye in System 1 noticeably diffused away from the wall (y-direction) upon insertion and was therefore less visible from the exterior.

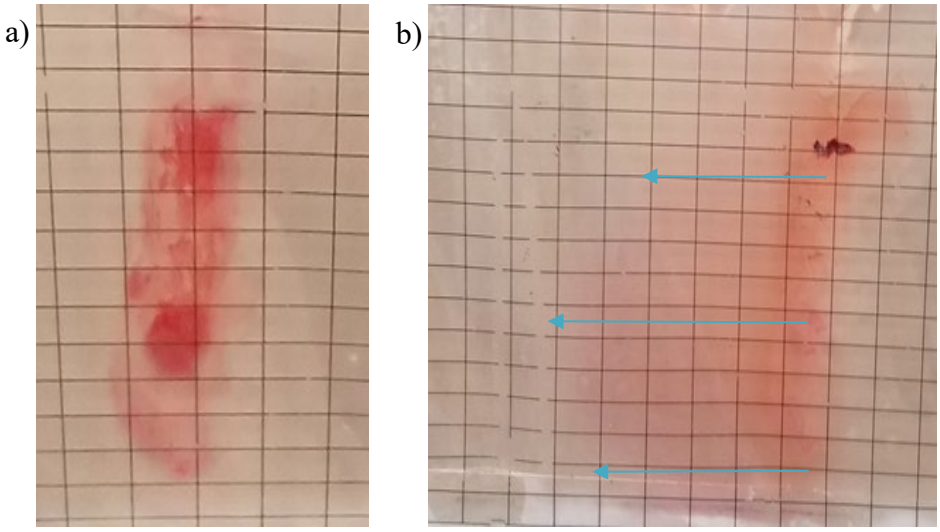

Figure 4.7 Electromigration of the red dye in clay - System 1 (close-up).
(Each grid rectangle = 1 cm length x 0.5 cm height)
After insertion of dye – pre-diffusion ; b) 96 h 50m

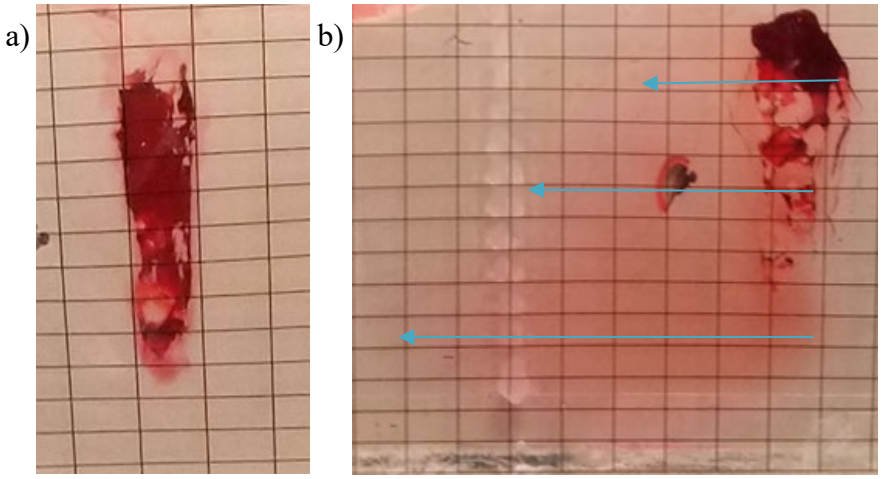

Figure 4.8 Electromigration of the red dye in clay - System 2 (close-up).
(Each grid rectangle = 1 cm length x 0.5 cm height)
a) After insertion of dye – pre-diffusion ; b) 96 h 50m

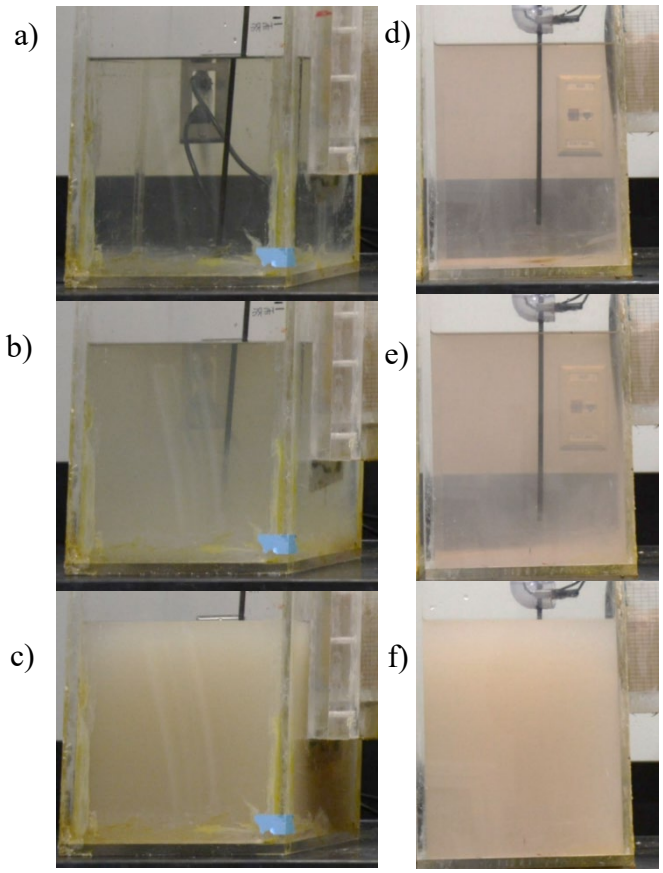

Figure 4.9 Demonstration of electrophoresis occurring in anode reservoirs.
System 1 at times: a) 0h b) 2h ; c) 24h ; System 2: d) 0h e) 2h f) 24h

4.5.4 Clay – Green Dye (*Spirulina* Blue / C-Phycocyanin)

To test the migration of the green dye in clay, setups were again run in duplicate. The insertion of dye was equally successful in both systems in the initial phases of the experiments. However, due to a significant leak in System 1, the reservoir had to be re-filled by adding 1 g/L NaCl to each side at its previous level, and a small (though non-negligible) wash-out of the dye occurred. Figure 4.10 shows a less pronounced blue/green color in System 1. Despite a colored migration pattern being less apparent, a change in shape of the dye area was noticeable in System 1, with the most pronounced effect being the migration of the blue (*spirulina*) dye component leaving behind only a yellow color

(turmeric). System 1 migrated 0.5 cm in 138 h or 0.09 cm/d but due to the presence of the errors, this value could not be validated. System 2 (Figure 4.11) operated properly and migrated 1 cm towards the anode in 140.67 h or 0.17 cm/d. (This was the value used for all subsequent calculations.) In both experiments, electrophoresis was observed shortly after turning on the power, causing small amounts of clay over time to migrate into the anode reservoir (see Figure 4.9).

Additionally, there was a very notable difference between the visual appearance of the dye prior-to and post- the re-filling of the reservoirs (Figure 4.10, a and b). Figure 4.13b shows several green "pockets" in the middle of the insertion area and more of the blue (*spirulina*) component apparent at the bottom. The initial dye movement prior to turning on the power was of a type of vertical diffusion, a function of the dye's density and gravity. Immediately following the insertion, the dye sank down towards the bottom of the sand are and spread out, and continued to spread, mostly vertically for a brief period of time, after which this "diffusion" ceased. Following the cessation of dye movement, the power was switched on and this was regarded as time "0" and referred to as "post-diffusion".

4.5.5 Migration Summaries

Electromigration was readily apparent with the red dye in both sand (9.12 ± 1.57 cm/d) and clay (0.93 ± 0.16) cm/d. It was also observed (Set 1) for the green dye in sand (7.28 ± 0.57 cm/d) but not in clay, probably due to amphoteric properties of the dye. The confirmation experiment (Set 2), which was performed at an identical voltage but a slightly lower current output (0.040 mA/cm^2), the migration rate was found to be similar, at 6.60 ± 0.20 cm/d. Values are summarized in Tables 4.2 and 4.3.

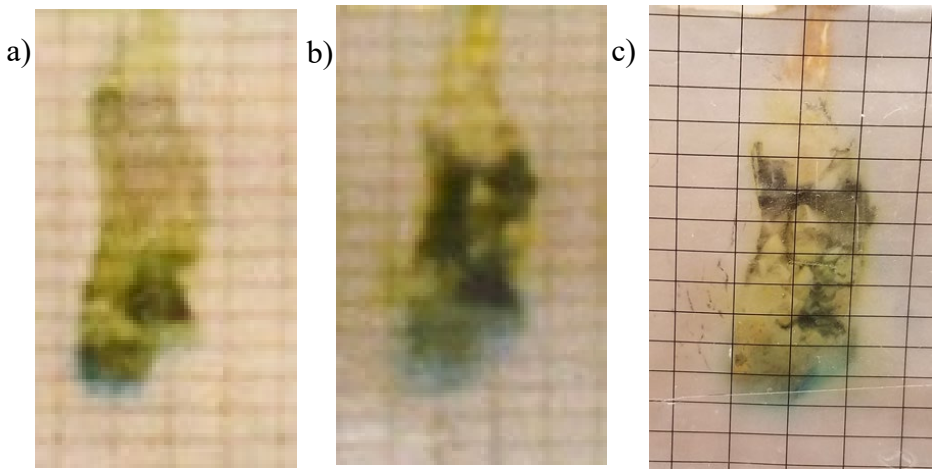

Figure 4.10 Electroosmosis of the green dye in clay - System 1 (close-up). a) Post-diffusion, prior to tank leak ; b) After refill of reservoir and additional dye added (post-diffusion) (t = 0h) ; c) At time t = 138 h *(Each grid rectangle = 1 cm length x 0.5 cm height)*

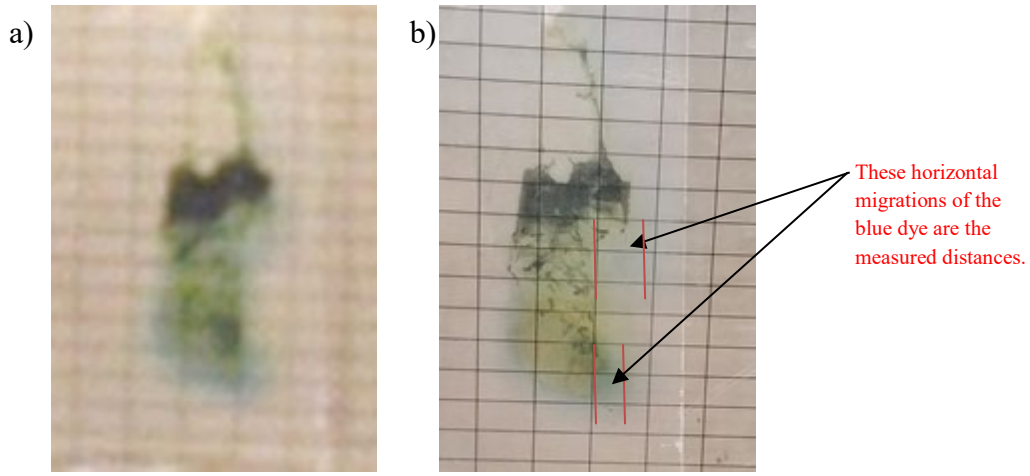

Figure 4.11 Electroosmosis of the green dye in clay - System 2 (close-up). a) after insertion of dye ; b) 140h 40m.

Table 4.2 Summary of Migration Rates in Sand for All Experiments

Dye	**Migration Distance 1** (cm)	**Time 1** (h)	**Migration Distance 2** (cm)	**Time 2** (h)	**Migration Rate 1** (cm/d)	**Migration Rate 2** (cm/d)	**Avg. Migration Rate** (cm/d)	**Voltage Gradient** (V/cm)	**Current Density** (mA/cm^2)
Red Dye	13 cm	30.5 h	16.75 cm	50.16 h	10.23	8.01	9.12 ± 1.57	0.667	0.054
Green Dye	14.75 cm	48 h	16 cm	50 h	6.88	7.68	7.28 ± 0.57	0.667	0.054
Green Dye	16 cm	60 h	17 cm	60 h	6.40	6.80	6.60 ± 0.20	0.667	0.040

Table 4.3 Summary of Migration Rates in Clay for All Experiments

Dye	**Migration Distance 1** (cm)	**Time 1** (h)	**Migration Distance 2** (cm)	**Time 2** (h)	**Migration Rate 1** (cm/d)	**Migration Rate 2** (cm/d)	**Avg. Migration Rate** (cm/d)	**Voltage Gradient** (V/cm)	**Current Density** (mA/cm^2)
Red Dye	5.5 cm	161.5 h	7 cm	161.5 h	0.82	1.04	0.93 ± 0.16	0.667	0.054
Green Dye	1 cm	140.7 h	N/A*	N/A*	0.17	N/A*	0.17	0.667	0.054

**Due to apparatus errors, values for system 2 are not reported. Only system 1 values are reported.*

4.5.6 Flux Values

The total mass flux in this experiment is a sum of the (electro)migration flux and the diffusion flux (Equation 4.2). The fluxes due to electromigration are reported in Table 4.4. Calculated values show that this flux in sand was approximately 30 times greater for the red dye than for the green dye. The migrational flux of the red dye in clay was three orders of magnitude greater than the calculated value for the green dye in clay. The diffusion flux in all experiments was negligible compared to the electromigration flux. Electroosmotic flux was only potentially relevant for the green dye in clay but was difficult to quantify due to the minimal migration observed and the high variability of the dye's amphoteric nature.

Table 4.4 Flux Values for All Dye Experiments

Experiment	**Migrational Mass Flux** (mol cm^{-2} d^{-1})	**Mig. Mass Flux range** (mol cm^{-2} d^{-1})	**Diffusion Flux** (mol cm^{-2} d^{-1})	**Electroosmotic Flux**** (mol cm^{-2} d^{-1})	**Total Flux** (mol cm^{-2} d^{-1})
Red Dye - sand	4.242	2.848-4.637	4.04×10^{-6}	N/A	-4.24 ± 0.56
Green Dye (exp1) - sand	0.109	0.103-0.115	1.43×10^{-8}	N/A	-0.11 ± 0.01
Green Dye (exp2) - sand	0.099	0.096-0.102	1.43×10^{-8}	N/A	-0.099 ± 0.004
Red Dye - clay	0.18	0.16-0.20	4.23×10^{-5}	N/A	-0.18 ± 0.02
Green Dye - clay	7.87×10^{-5}*	7.87×10^{-5}	6.22×10^{-7}	$\sim 10^{-8}$	$+7.93 \times 10^{-5}$

**Value for flux due to electromigration only, **Based upon calculations of system parameters*

4.5.7 pH and Other Values

In all systems, as there was no buffer, the pH in each reservoir quickly reached extreme values. The anode reservoir typically reached between a pH of 1-2, depending upon the duration of the experiment. A pH of near 2 was reached in less than 72 hours, and often 48 hours, and dropped near a value of 1 within about 70-90 hours. This was a result of the production of H^+ ions (Equation 3.1). The cathode reservoir typically reached a pH of 11-12, (a result of the production of OH^- ions). A pH of 11 was reached in as little as 40 hours and a value of 12 within 60-100 hours. The pH values reached their extremes in about 3 days and did not extend much farther, irrespective of the media being sand or clay (Figures 4.12 and 4.13)

A polarity reversal was performed in a parallel setup of the initial green dye sand experiment. The reversal was initiated at time 50 hour to see how quickly the pH extremes would invert. The trend reversed fully after an additional 70h in the anode and mostly in the cathode (Figure 4.14). The polarity reversal did cause a slight reverse migration of the dye which then stagnated. The reason for the stagnation is unknown. Despite the claim by Xu et al. [76] and others, that ionic species will flow in the opposite direction upon reversal in polarity, Mena et al. [353] found that in a study using an anionic surfactant in soil, that more of the surfactant concentrated towards the anodic end, despite polarity reversal.

In preliminary experiments, not reported in this article, similar trends were seen including the full inversion of pH extremes for both anode and cathode reservoirs. Voltage in reservoirs for all systems remained steady throughout all experiments at about 26 V

(Table 4.5). Current in the reservoirs for all systems was highly variable and could not accurately be measured. The current throughout the media, though, was constant at each measuring interval and had an overall average of 6.85 ± 2.93 mA (Table 4.6).

The average current density was calculated by dividing the average measured current in each setup by the relevant cross-sectional area (length (*x-direction*) x width (*y-direction*) of the porous media. The value measured in sand was calculated to be 0.49 ± 0.22 mA/cm^2 and the average current density measured in clay was calculated to be 0.63 ± 0.36 mA/cm^2. The power supply for System 2 of the clay media with the green dye had to be replaced during the course of the experiment and both the voltage and current in the system was unexpectedly reduced. These values were not factored into the overall averages for the experiment. Salinity values tended to increase slightly over each experiment although not uniformly (Table 4.7). Temperatures values did not change significantly during the experiment and any noticeable changes corresponded to changes in room temperature (Table 4.8). The average value was 21 ± 2°C and 20.92 ± 1.29°C for the sand and clay experiments, respectively.

Table 4.5 Average Potential (V) in Electrokinetic Setups

	Sand (red dye)	**Sand (green dye-Set1)**	**Sand (green dye-Set2)**	**Clay (red dye)**	**Clay (green dye)**
System 1	17.81 ± 0.32 V	20.82 V	NM	17.24 ± 0.97 V	22.05 ± 0.94 V
System 2	NM	20.38 ± 2.02 V	NM	21.98 ± 1.80 V	21.13 ± 0.47* / 18.06 ± 0.41 V

NM = Not Measured, *Power supply had to be replaced. Replacement not as efficient.

Table 4.6 Average Current (mA) in Electrokinetic Setups

	Sand (red dye)	**Sand (green dye – Set1)**	**Sand (green dye – Set2)**	**Clay (red dye)**	**Clay (green dye)**
System 1	4.19 ± 0.24 mA	5.42 mA	NM	7.40 ± 1.41 mA	5.14 ± 0.37 mA
System 2	NM	7.17 ± 1.70 mA	NM	11.04 ± 1.50 mA*	4.84 ± 0.08** / 4.05 ± 0.10 mA

NM = Not Measured, *Reported values higher than output, **Power supply had to be replaced. Replacement not as efficient.

Table 4.7 Salinity Levels Throughout the Experiment *(Values reported per Anode / Cathode reservoirs in g/L)*

	Sand (red dye)	**Sand (green dye – Set1)**	**Sand (green dye – Set2)**	**Clay (red dye)**	**Clay (green dye)**
System 1 – initial	NM	0.7 / 1.2	1.0 / 1.0	0.7 / 1.0	1.3 / 1.3
System 1 - final	NM	1.0 / 1.6	1.3 / 1.9	1.0 / 1.2	0.9 / 1.4
System 2 - initial	NM	1.1/1.0	0.9 / 1.0	0.9 / 0.9	NM
System 2 – final	NM	1.2/1.1	1.8 / 1.2	1.3 /1.1	1.5 / 1.3

NM = Not Measured

Table 4.8 Temperatures Throughout the Experiment *(Values report as Anode / Cathode reservoirs in °C)*

	Sand (red dye)	**Sand (green dye – Set1)**	**Sand (green dye – Set2)**	**Clay (red dye)**	**Clay (green dye)**
System 1	NM	NM	18.59 ± 0.92 / 17.79 ± 0.72	20.74 ± 0.75 / 20.46 ± 0.71	21.26 ± 1.29 / 20.76 ± 1.32
System 2	20.69 ± 1.39*	NM	18.38 ± 0.86 / 19.03 ± 1.34	21.33 ± 0.74 / 20.87 ± 0.81	21.03 ± 1.25 / 20.62 ± 1.29

NM = Not Measured, * Average of both reservoirs

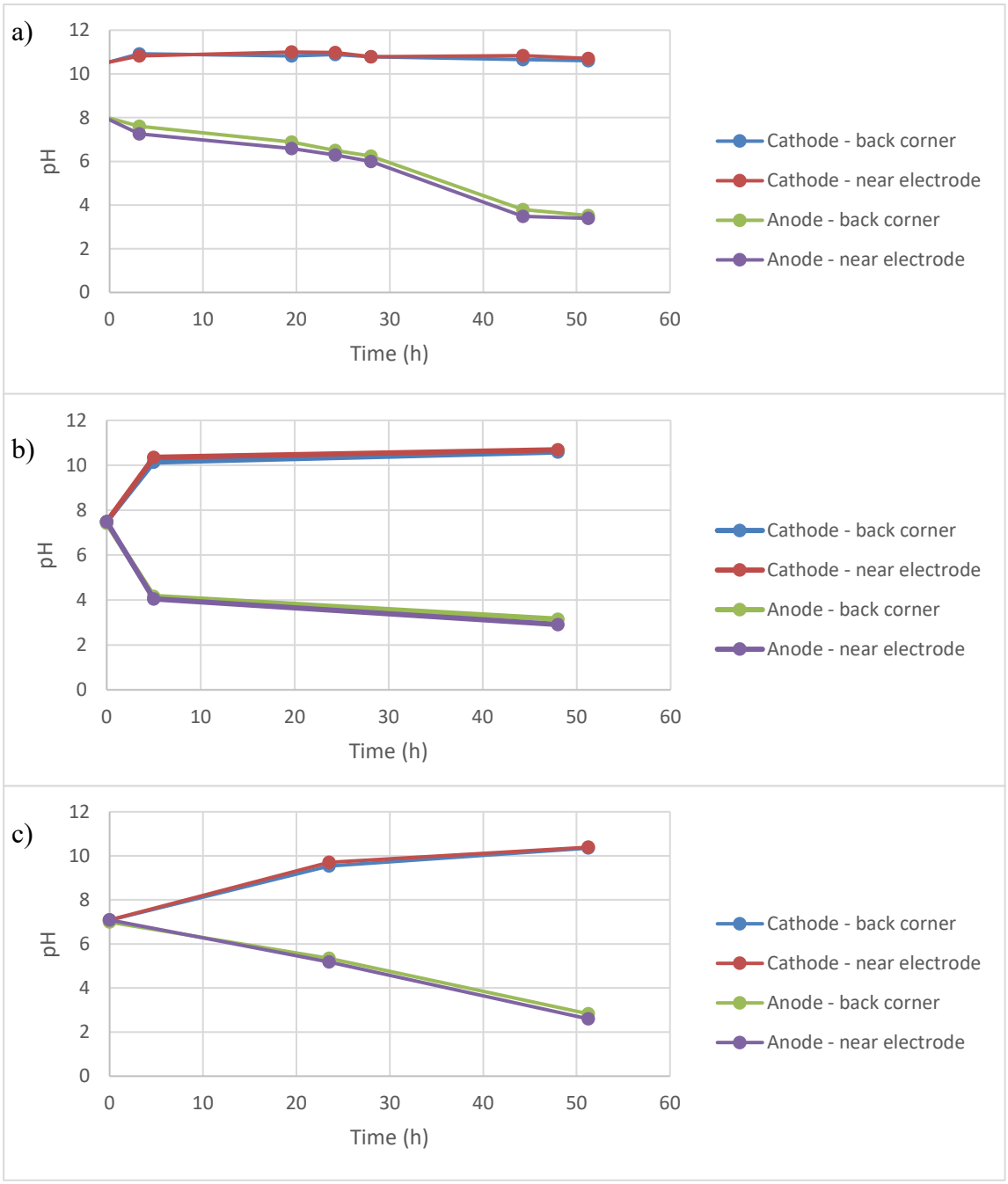

Figure 4.12 pH changes in reservoirs over time for sand media. a) red dye – exp. 2 (no data collected for exp. 1, *sand had basic pH initially) ; b) green dye – exp. 1 ; c) green dye – exp. 2

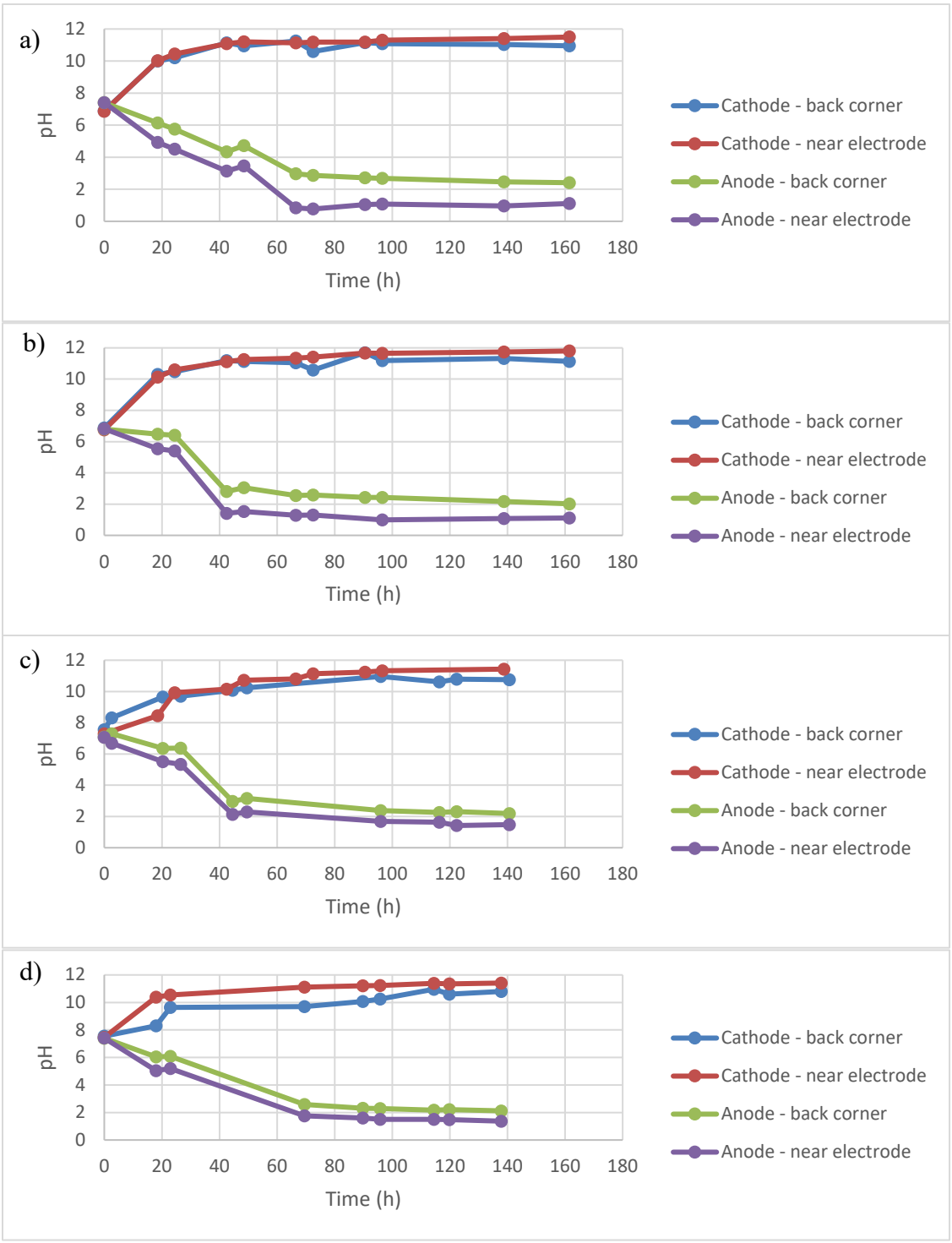

Figure 4.13 pH changes in reservoirs over time for clay media. a) red dye – exp. 1 ; b) red dye – exp. 2) c) green dye – exp. 1 ; d) green dye – exp. 2

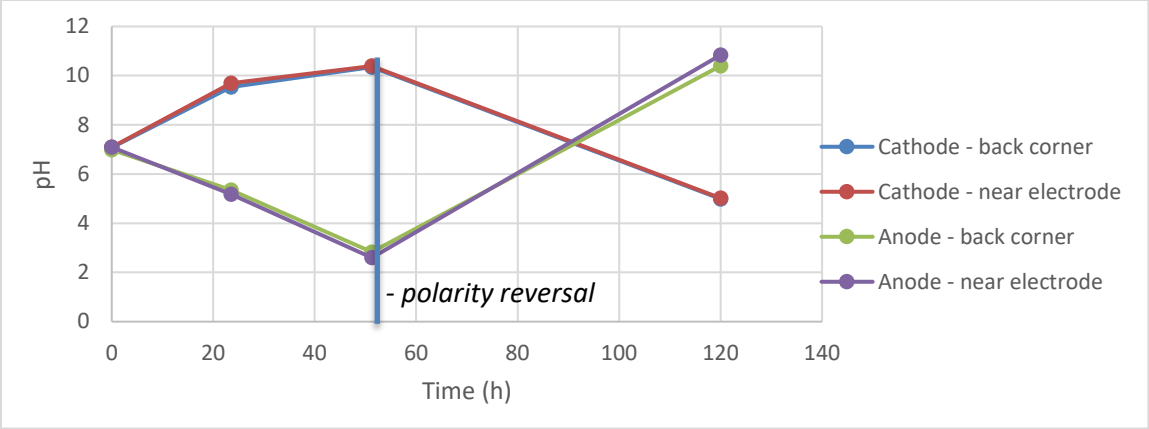

Figure 4.14 Demonstration of polarity reversal: Sand media with green dye (System 2).

4.6 Discussion

4.6.1 Migration Patterns and Comparisons

The primary objective of these experiments is to establish migration patterns in two media types (sand, clay) as a function of electromigration and/or electroosmosis. The migrational behaviors witnessed also are dependent upon the natures of the dyes used. The red dye in both sand and clay moved position through the respective media as a function of electromigration. Throughout all experiments, whether utilizing sand or clay, the ionic concentration and the current density were identical as well as constant. Therefore, any differences in electromigration rates must be a function of the grain size of the media and its effect on the ionic mobility. Thus, this can be defined as a function of the hydraulic permeability and porosity of a particular media, which are inversely related. As sand has a much larger grain size and a larger permeability than clay, it allows for greater ionic mobility and thus larger electromigration rates [342]. In addition, sand has a much lower surface charge density than clay, near zero, and thus, it does not affect electromigration

rates, whereas the greater charge density of clay may have been a hindrance for electromigration in the clay media [70].

However, zeta potential (the electric potential that between a charged particle's surface to the plane parallel to the particle surface), which is known to affect electroosmotic rates, does not appear to effect electromigration [296] and therefore the two processes should be independent in clay or soil. The migration of the red dye in clay can clearly be attributed to electromigration, rather than electroosmosis, as electroosmotic rates in clay are reported to be significantly lower than electromigration rates by a factor of one or two magnitudes [350].

Consequently, when comparing the rates of this dye in the two media, as the only two influential factors (permeability / ionic mobility and lack of charge inhibition) were greater in the sand than in the clay, it was reasonable to assume that electromigration in sand would occur at a much faster rate than in clay. This was indeed observed to be the case with migration rates of 6-10 cm/d in the sand versus less than 1 cm/d in the clay, an approximate ten-fold difference. Lindgren et al. [298] determined a rate of 11-12 cm/d for FD&C red dye #40, quite similar to the findings in this experiment, despite Lindgren et al., utilizing a higher voltage of 89-150 V and a greater current density of 0.35 mA/cm^2 (compared to 0.04-0.06 mA/cm^2 in these experiments). This may be indicative that in an efficient system, not as much current need be applied as initially thought.

With respect to experiments utilizing the green dye, the dye is seen to move rapidly towards the anode in sand while only minimally migrating towards the cathode, in clay. As sand carries minimal surface charge and is very poorly conductive, electroosmotic rates were assumed to be minimal, as concluded by Acar et al. [342] and others [57]. Acar et

al. [342] reports the effective transport rate (electromigration) of ammonium in fine-grained sand of 8.7 cm/d but an electromotic rate of only 0.7 cm/d, indicating that if electroosmosis does in fact occur in fine-grained sand, it would only be a fraction of the electromigration rate. This difference would be greatly enahnced for a dye, as it is molecularly much larger than an ammonia ion and thus cannot pass through sand as quickly. Therefore, for the approximate electromigration value of 8-10 cm/d as seen for the red dye, if the green dye's movement is due to electroosmosis, one would expect the electroosmotic rate to be far less than 1 cm/d. The results, which show a migration rate near 7 cm/d for the green dye, strongly indicate that its migration in sand is due to electromigration rather than electroosmosis.

It was determined that the migration component of the green dye, which is primarily C-phycocyanin [354], has a protein-like nature due to the presence of many terminal amine groups (Figure 4.1) and thus can become heavily positively or negatively charged as stated in Section 4.1. In both replicates of the green dye experiment (Sets 1 and 2), the dye was inserted roughly in the center of the sand media, horizontally. As the isoelectric curve is quite steep (Figure 4.15), at values not much below the pI, the C-phycocyanin molecule becomes strong positively charged (cationic) and slightly above the pI, the molecule becomes strongly negatively charged (anionic).

Figure 4.15 Illustration of an isoelectric curve of C-phycocyanin with respect to pH (obtained via ThermoFisher® Scientific's Peptide Analyzing Tool).

The pH profile across media is well established in the literature as being non-uniform [299, 355, 356] and although pH extremes of acidity and basicity are established in an electrokinetic system at the anode and cathode, respectively, there is a slow increase in the pH until shortly past the midway point of the media whereby the pH increases rapidly (see Figure 5.1). This would imply that at the point where the dye was, the pH values would be close to anodic pH. The isoelectric curve of C-phycocyanin (Figure 4.15) indicates that at this approximate pH value (~3), the molecule would be strongly positively charged, indicating that it should move strongly towards the cathode via electromigration. However, in these experiments, the dye is seen to move strongly towards the anode. Experiment Set 2 confirmed that after 5 days, the pH values in the center of a sand-based EK system are quite acidic (3 or less) and therefore more explanation is required. An additional study (Chapter 5) was conducted to analyze the changes in pH griadents over time, thus giving an inisght as to the green dye's migration patterns.

For the evaluation of the green dye in clay, as the dye migrated only 0.17 cm/d, it was initially uncertain if this migration was due to electroosmosis or due to the migrational flux (electromigration) in the cationic direction. It was also unknown is diffusion played a

role in this slow migration rate. Saichek and Reddy [357] report that both electromigration and electroosmosis are noticeably prevalent in a clay-based system provided there is a sufficient voltage gradient. Thus, in order to determine if this value of 0.17 cm/d could be attributed to electroosmotic flow, the theoretical rate must be estimated, and can be done using the Helmholz–Smoluchowski (H–S) equation [71] (4.4):

$$q = k_e \frac{V}{L} A \tag{4.4}$$

where k_e is the electroosmotic permeability (cm^2/V-s), V/L is the voltage gradient (V/cm) and A is the surface area (cm^2) of electrodes facing towards the media.

Applying the values given in Section 4.4.3 to Equation 4.4, the theoretical electroosmotic flow would be 8.08×10^{-4} cm^3/s. For this value of q, for the given cross-sectional area of the media, which was 188.71 cm^2 (18" x $1_{5/8}$"), the electroosmotic flow should be ~ 0.37 cm/d. This is relatively close to the migration value obtained for this experiment (0.17 cm/d), indicating that the dye migration is likely due to electroosmosis.

In order to confirm this both the theoretical electroosmotic flux and the migrational flux due to positively charged electromigration must be compared. To calculate total electroosmotic flux, q (obtained via Equation 4.4) per unit area, should be multiplied by the molar concentration of the dye divided by the molar concentration of water, which has a value of 1 [299]. This yields an electroosmotic flux value of 1.677×10^{-8} mol $cm^{-2}d^{-1}$

To calculate the theoretical distance the dye would migrate due to the positively charged electromigration, the absolute ionic mobility (u_i^*) is calculated via Equation 4.1, where the observed ionic mobility (u_i) is calculated by dividing the average migration rate by the voltage gradient and the diffusion tortuosity value (τ`) used is 0.42 [358]. u_i^* is calculated to be 1.24×10^{-6} cm^2 $V^{-1}s^{-1}$. When this value is converted from seconds to days

and multiplied by the voltage gradient, the expected maximum migration rate is determined to be 0.07 cm/d which is below the observed migration rate (0.17 cm/d). The difference between these values (0.07 cm/d and 0.17 cm/d) may not be truly significant as the migration rate was difficult to accurately measure due to the quite small increment that the dye moved over time. Moreover, the dye's partially faded nature made it difficult to accurately measure the distance migrated and thus, this migration rate must be regarded as a rough estimate. Additionally, the lack of a sound replicate, due to the leak in System 1 also reduces any rejection of the notion that this migration was not due to electromigration.

As a means of investigating this further, the theoretical migration flux due to cationic migration is calculated to be 7.88 x 10^{-5} mol $cm^{-2}d^{-1}$ (Equation 4.2), a value three orders of magnitude higher than the calculated electroosmotic flux. These values, contrary, to the findings of Equation 4.4, indicate a greater likelihood that the migration that occurred was due to cationic migration rather than electroosmosis. Alternative methods of calculating of u_i^* (as seen in Appendix B.1), however, yields substantially higher u_i^* values which in turn leads to values far above the observed migration rate, at values similar to those observed of the red dye in clay.

It was also essential to determine if this migration may have been largely due to diffusion, and hence the diffusion flux for this dye must be calculated. It was found to be on the order of 10^{-7} mol $cm^{-2}d^{-1}$, which is less than 1% of the migrational flux value and therefore regarded as insignificant.

4.6.2 Salinity Values

With respect to salinity values (Table 4.7), four of the eight measured experiments were noticeably different in the anode and cathode reservoirs, particularly at the end of each

experiment. Salinity is expected to increase over time as some evaporation as well as electrolysis occurred, thereby slightly increasing the salt-to-water ratio. It most instances, the higher salinity value occurred in the anode reservoir and thus could possibly be attributed to the faster migration rate of Cl^- than Na^+, as the chloride migrates towards the anode and sodium towards the cathode. The effective ionic mobilities of Cl^- and Na^+ are 1.66×10^{-4} cm^2 $V^{-1}s^{-1}$ and 1.09×10^{-4} cm^2 $V^{-1}s^{-1}$, respectively, and thus would translate to roughly a 1.5-fold difference in migration rate [345] .

The explanation for the initial saline imbalance for the green dye in sand – (Set1, System 1) was likely the result of the initial filling method, i.e., the omission of infiltrating the salt water through the sand when filling the system. In the final clay experiment (green dye), higher than expected salinity values were measured for both systems. It is hypothesized that this abnormality may be due to an increase in the tap water's salinity as new batches of tap water were used for each experiment set. (The tap water was measured the day following the creation of the reservoir solution and was found to be 0.1 g/L, identical to previous measurements, but a spike the previous day could have been possible as a momentary incident.) An additional possibility is if there were salt residual in the mixing bottle.

4.7 Conclusions

This experiment successfully highlighted the difference in migration rates for different media types and is most indicative for the red dye which demonstrated at ten-fold difference between migrations in sand vs clay. Values observed are similar to what were expected via calculations and what is found in the literature and is relevant to assessing a controlling the migration of ionic substances, primarily heavy metals, which can be often

mimicked by this type of anionic dye. For the green dye, electromigration was also readily apparent in sand, seemingly due to its' initial anionic nature (see Chapter 5) and at a rate close to that observed by the red dye. The minimal migration of the green dye in clay, however, was left unresolved if the phenomenon was as a result of cationic electromigration or electroosmosis, although diffusion was ruled out as a primary factor. The use of an amphoteric substance such as *Spirulina* Blue dye highlights an unforeseen obstacle that can take place in electrokinetic systems, namely the alteration of an added chemical due to the changes in pH values. In this experiment, the pH measured in the reservoirs hit extreme values in a very short period of time, indicating the need for buffers in any future or in-situ system. The use of polarity reversal was also demonstrated to be partially effective but is likely not practical as a sole tactic.

This study highlighted both the practical reliabilities of studying electrokinetic effects and its applications over different media types but also presented new findings and challenges not previously cited in the literature such as pH shifts affecting migration patterns and the difficulty in accurately maintaining static conditions (e.g., salinity, pH). Additional studies are needed to compare the migrations of other materials such as cationic dyes and actual contaminants, including metal complexes that may not behave uniformly. It would also be beneficial to determine how dye migrations may chance if the media used is of a composite nature, such as containing a high percentage of both sand and clay.

CHAPTER 5

THE ELECTROMIGRATION OF SPIRULINA BLUE DYE IN SAND AND THE DISCOVERY OF pH GRADIENT SHIFTS OVER TIME

5.1 Background

The green dye utilized in the previous experiment (Chapter 4) was found to have very unique properties due to the amphoteric nature of its migration component, *Spirulina* Blue. In both initial and conformational experiments (Set1 and Set2), a rapid migration of the dye in sand towards the anode was witnessed, at a rate near that observed by the red dye.

Due to the electrolysis that occurs in an electrokinetic system, a strong pH gradient is formed in a matter of no more than a few days, where the anodic pH can drop to below 2 and the cathodic pH increases to 12-13 [299]. It was thus necessary to determine how an amphoteric dye, greatly dependent upon pH values, would migrate in an electrokinetic system over time and how it related to the relative pH gradient formed.

Papers such as those by Acar and Alshawabkeh [299] and by Reddy and Chandhuri [359] show that across the media, pH gradually increases at a small increment until about 60-70% of the distance from the anode when the pH begins to rise sharply towards the value of the cathodic pH. An approximate illustration of this can be seen in Figure 5.1. This implies that the area at which the dye would be inserted (the horizontal center, i.e., ~50%), should have a pH value close to the anodic pH and therefore about 3-5. This acidic value is significantly below the pI value (~4.8) and consequently, it was expected that the C-phycocyanin (the predominant migrational component of the green dye) would become positively charged and move towards the cathode. Observations clearly demonstrated that

this was not the case and the confirmation experiment (Set2) verified that the dye migrated clearly towards the anode rather than cathode.

At the end of the second primary experiment (Set2), random pH values were taken across the sand at varying depths and all values were found to be less than 5, with most being 3 or less.

In an effort to explain what occurred, two hypotheses were set forth:

1) Only pH gradients in soil were found to be reported in the literature (e.g., Figure 5.1) and it may be that a different pH gradient would be established in sand.
2) The steep pH gradient mentioned in the literature was for experiments that took place over several days or longer and all sand-based migration experiments performed as part of this Dissertation's research had a duration of less than three days and thus perhaps a pH gradient could change over time. (The duration of the Set 2 experiments was approximately 7 days, however, migration ceased at about 65 h).

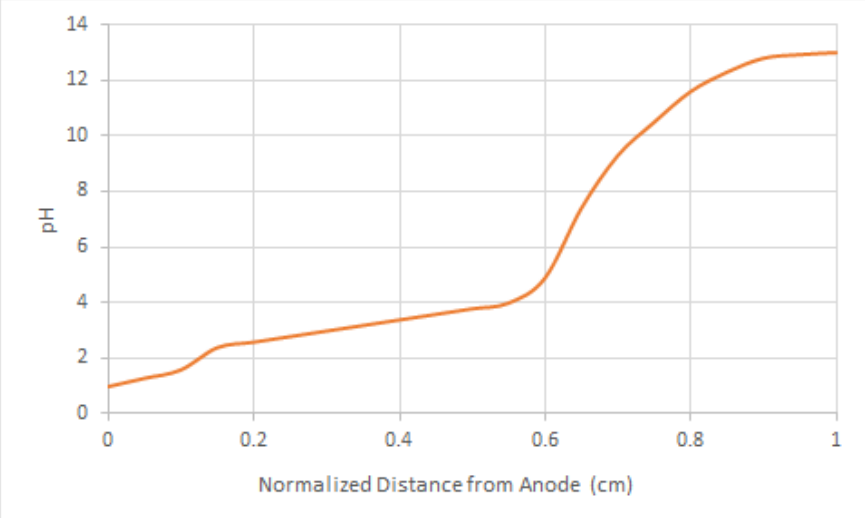

Figure 5.1 An estimation of a pH profile in an electrokinetic system based upon multiple literature reports.

5.2 Setups and Procedures

5.2.1 System Design

All initial experiments (Set1 and Set2) used a large-scale self-designed electrokinetic apparatus as described in Section 3.2. Following these experiments, in order to investigate both hypotheses, a mini-electrokinetic setup was constructed of two thin acrylic boxes and an acrylic bridge composed of 1.25 cm thick acrylic pieces (Figure 5.2). The boxes measured 9.5 x 9.5 x 12 cm (L x W x H) and the bridge area measured 20 x 3.8 x 6.5 cm. (These setups were arranged in a similar fashion to the larger setups (Figure 4.2). The chief purpose of these miniature setups was to determine the pH gradient as an independent variable over time (without experimental bias). Electrodes used were 15 cm graphite rods (of identical composition to those used in the larger setups) with a 0.63 cm diameter. The voltage gradient was adjusted to a 13.33 V output with a measured 2.91 ± 0.02 mA current output. The voltage gradient was applied over a distance of 20 cm calculated to be 0.667 V/cm and the current density was calculated to be 0.038 mA/cm^2. This voltage and current density were meant to match those used in the latter larger experiment (Section 3.5.2), which had a voltage gradient of 0.667 V/cm and current density of 0.040 mA/cm^2. This experiment was run in triplicate in additional to a preliminary study, run in duplicate, which studied the pH gradients in sand at 0.50 V/cm and 0.028 mA/cm^2. A grid with units of 1 cm x 0.5 cm was placed upon each bridge for measuring the distances from the anode. In order to compare the observed pH values over time in sand to those formed in soil, a supplement study was conducted and can be seen in Appendix C.

Of the two sets of studies were conducted. The initial study, which had fewer sampling points and sampling times is hereby labeled as the “preliminary experiment” and

the second study, which had more sampling points and more frequent sampling times, is labeled as the “primary experiment”.

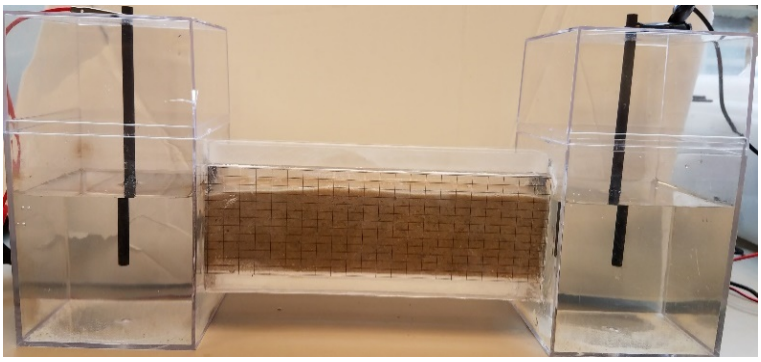

Figure 5.2 Photograph of one of the miniature electrokinetic setups.

5.2.2 Filling Technique

The systems used in the initial experiments (Set1 and Set2) were filled according to the method described in Section 3.2.2. Miniature setups were setup in an identical manner to most of the larger setups, namely: A solution of 1 g/L NaCl was prepared by adding 1g of anhydrous sodium chloride per liter of de-ionized water (as a batch of 20 liters) and allowed to mix on a stir plate for at least one hour. Once mixed, the NaCl solution was added directly to the anode reservoir until it reached the sand surface. The liquid was allowed to infiltrate and begin filling the cathode reservoir. As the level in the anode reservoir became lower, more NaCl solution was added periodically until it reached a level of 2 mm below the sand surface with both reservoir levels ultimately being equal. The system was allowed to equilibrate overnight. The height of the sand in these setups was 6.25 cm, close to the top of the bridge (6.5 cm).

5.2.3 Absence of Dye Addition

Watkins® green food coloring (Table 4.1) was used in the initial experiments (Set1 and Set2) but no dye was used in the miniature setups as their sole function was to analyze pH gradients rather than dye migration.

5.3 Measurements

pH and temperature measurements for the larger setups were conducted using the AquaShock pH meter (Sper Scientific®, Scottsdale, AZ, USA) and accompanying probe at two locations in each reservoir. Voltage and current were measured using the EX330 Multimeter (Extech® Instruments, Waltham, MA, USA) and measured with each probe at opposite reservoir ends at about a mid-way depth. Salinity and conductivity were measured using the YSI® Model 30 Salinity/ Conductivity/ Temperature meter (YSI Incorporated, Yellow Springs, OH, USA) and was measured in the center of each reservoir at about a mid-way depth. For the miniature setups**,** only pH measurements were taken. pH values in the reservoirs were measured with AquaShock pH meter and probe in the center of each reservoir and pH values in the sand were determined via Fisherbrand® Paper pH strips (Fisher Scientific). A slightly curved steel spatula was inserted in the sand at marked regular intervals (Figure 5.3) and placed upon a pH strip for determination. Previous use of these strips helped to identify slight discrepancies and matchup with the color-identification guide, however, due to lack of overall accuracy, pH values reported have an error of 0.5-1.0.

5.4 Results

Images from the preliminary experiment are shown in Figure 5.3. The results from this experiment found that the pH profile formed in sand was indeed similar to those found in the literature, but it was discovered that each system only reached that point over the course of time (Figure 5.3). From about 24 hours, the pH profile was actually quite linear and only reached the type of pH profile noted in the literature after about 72 hours. (System 2 had a power interruption for about 10 hours, and therefore System 1 is a better representation). For the primary experiment, setups were run in triplicate (Figure 5.5 a-c) and labelled as Systems1-3, accordingly. Systems 1 and 2 ran for 118 h, while System 3 ran for 144 h, but encountered a problem with one of the electrodes at 72h, and hence all data sets from the point forward are omitted. Another replicate (Figure 5.5 d) was also conducted but was prone to a crack in the acrylic, yielding a slight leak which impacted the results prior to day 48. Results for this replicate, labeled as "System 4", is placed in Figure 5.5 as a comparison for the pH gradient at 6h and 24h.

Although voltage remained constant throughout the experiment (13.3V), the current in each system fluctuated, each in a particularly different manner. For Systems 1 and 2, the current in the reservoir was measured at 24 h and at 118 h and a notable decline in current can be seen in Table 5.1. Reasons for the substantial drop in current over time are not known and was not readily seen in Systems 3 and 4 (Figure 5.4). In Systems 3 and 4, the measured current fluctuated over the course of the experiment, averaging 2.38 ± 0.14 mA and 2.29 ± 0.14 mA, respectively, but no significant drop in current values was seen.

System results from the primary experiments were compared at specific time intervals as seen in Figure 5.6. A lag time in the pH gradient shift was noted in system 2, likely due to the lower current density in the system. Problems associated with System 4

can already be seen at 24 h (Figure 5.6b), even though no discrepancy is noted at time 6 h (Figure 5.6a), and thus Systems 1 and 3's results offer the best illustration of the pH gradient shift over time.

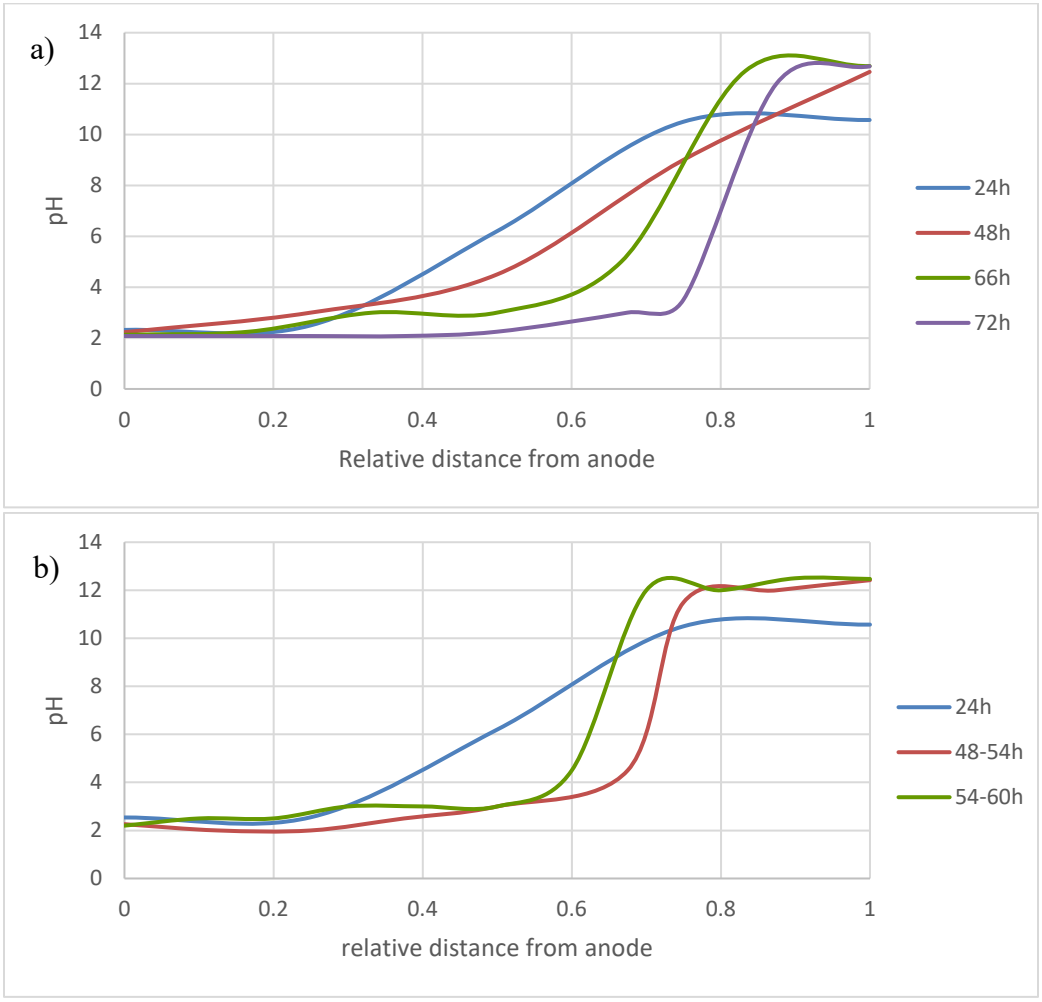

Figure 5.3 pH gradients relative to the anode for the preliminary experiment in the miniature EK setups. a) System 1 ; b) System 2

Table 5.1 Decrease in Current Observed in Systems 1 and 2 of the Primary Experiment

System	Current Output (mA)	Measured Current in the Reservoirs (mA)		
		Initial	24 h	118 h
1	2.89	NM	2.29	1.55
2	2.90	NM	1.95	1.28

NM = Not Measured

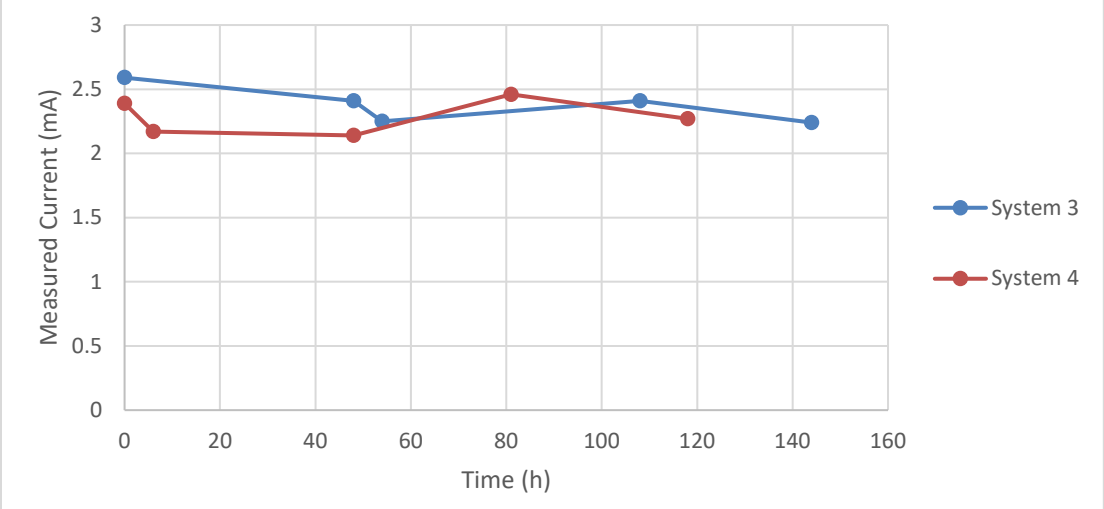

Figure 5.4 Current fluctuations observed in Systems 3 and 4 of the primary experiment.

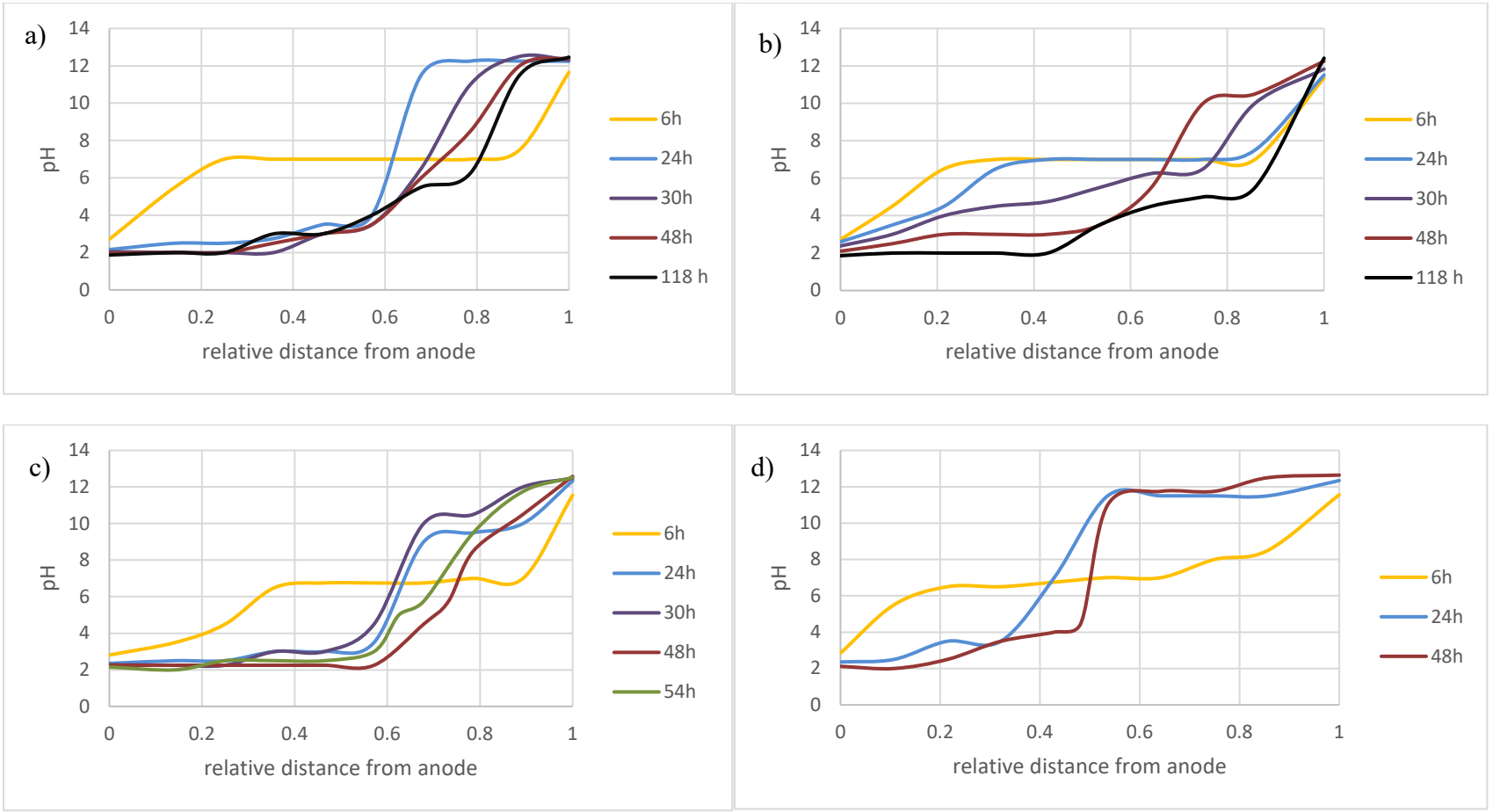

Figure 5.5 pH gradients relative to the anode for the primary experiment in the miniature EK setups.
a) System 1 ; b) System 2 ; c) System 3 ; d) System 4

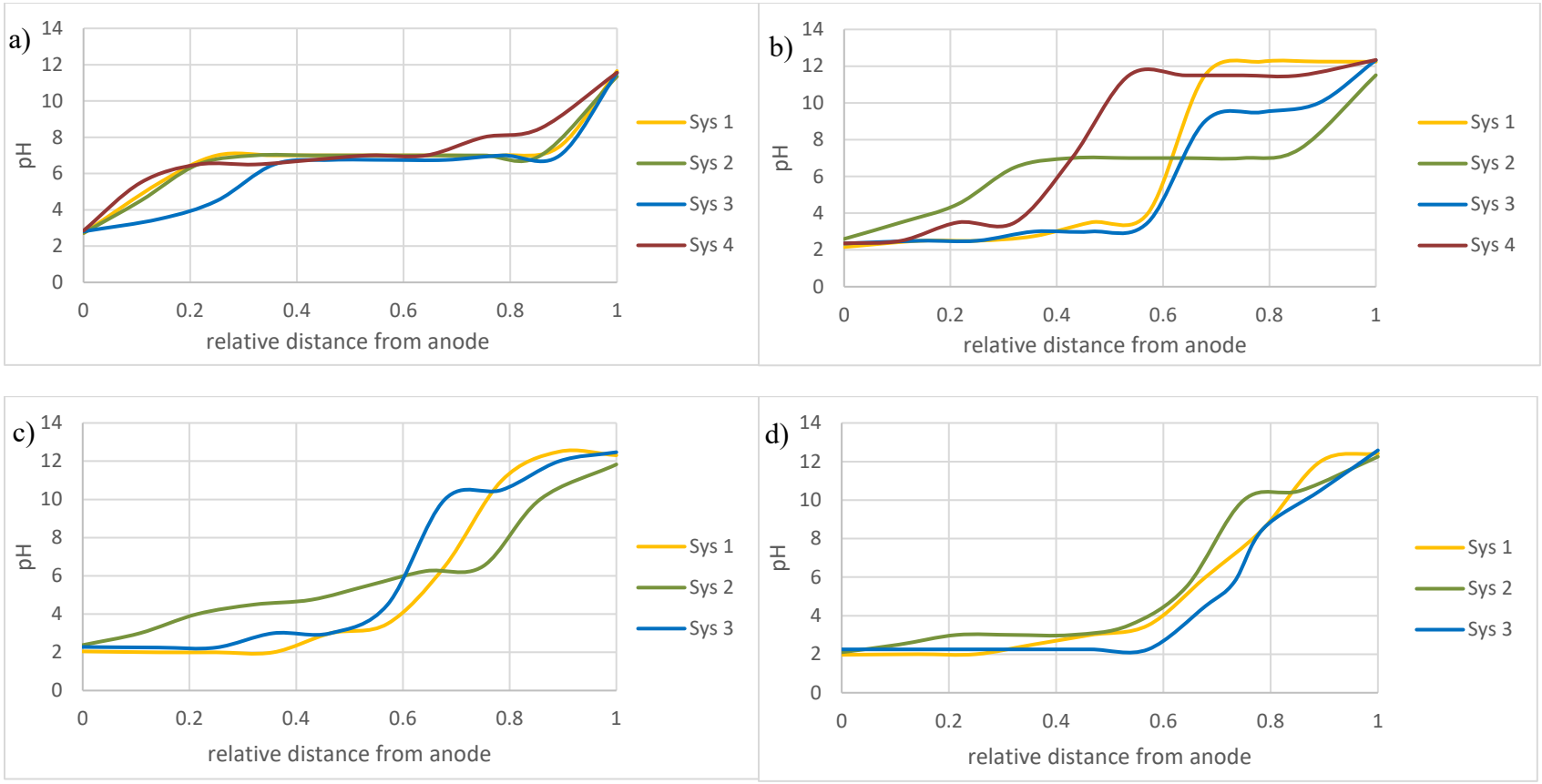

Figure 5.6 Comparative pH gradients relative to the anode at specific time intervals for the primary experiment in miniature EK setups. a) 6 h ; b) 24 h ; c) 30 h ; d) 48 h

5.5 Discussion

The preliminary results strongly indicated a shift in the shape of the pH gradient over time. At a period of 24 hours, the trend was almost linear, with a mid-point value of about 6. After an additional 24 hours, System 1 (Figure 5.3a) indicated a slight acidic shift, while System 2, which had a 5-10 h power interruption, shifted more quickly, for reasons unknown. The curve depicted for System 2 at 54h (including the interruption time) more closely resembles the curve shown for System 1 at 66 h. By 72 h, a pH profile in System 1 was reached that closely resembled the steep anode-biased curve shown in the literature (see Figure 5.1).

The primary results, particularly Systems 1 and 3, which were not prone to any errors, showed that at with a slightly increased voltage gradient (0.67 V/cm rather than 0.50 V/cm) and output current density (0.038 mA/cm^2 rather than 0.028 mA/cm^2), the pH gradient shifted at almost double the rate. At 6 h (Figure 5.6a), the pH in the central regions of the sand had not begun to shift much but by 24 h (Figure 5.6b), an acidic pH near the anodic value was seen until shortly past the mid-point distance from the anode to the cathode. The shift in pH at the measured points adjacent to the sand's center can be seen to increase quickly in Figure 5.7. The similar trend with lag time can be seen in Figure 5.8.

Systems 1 and 3, which were operated at voltage gradients and current densities akin to those used in the larger setup, illustrate that the central point in the sand where the green dye was inserted would have initially been above the dye's (i.e., C-phycocyanin's) isoelectric point of ~ 5.8. For up to 24 hours, or if taking into the account the preliminary results, up to 48 hours, the green dye would have been anionic and thus been prone to migrate towards the anode. This theory can thus explain why, in the confirmational green dye experiment (Set2), migration towards the anode slowed and stopped after about 3 days,

as the pH would have the dropped well below the isoelectric point and thus the dye molecules would have become positively charged.

The results from the miniature setup, however, indicate that migration should have stopped or slowed significantly by 24-48 hours into the experiment (Figure 5.9). Although the voltages and current densities were similar in the miniature setup, the specific construction of the EK apparatus was not identical. The overall designs of the two sizes were similar but the height of the bridge relative to the position of the reservoirs was different. In the larger setups (Figure 4.2), the bottom of the sand (bridge) was located at 39% of the reservoir height and the fill height (i.e., the top of the sand) was located at 64% of the reservoir height. In contrast, for the miniature setup, the bottom of the sand was located at 33% of the reservoir height and the fill height was located at 75% of the reservoir height. This indicates that a larger portion of the reservoir liquid (42% by height) came in contact with the sand bridge in the miniature setups than in the larger setups (25% by height). More study is needed, but this larger contact area may have led to a faster shift in the pH gradient, and therefore for the larger setups, the pH may have only dropped below the isoelectric point after 48 hours.

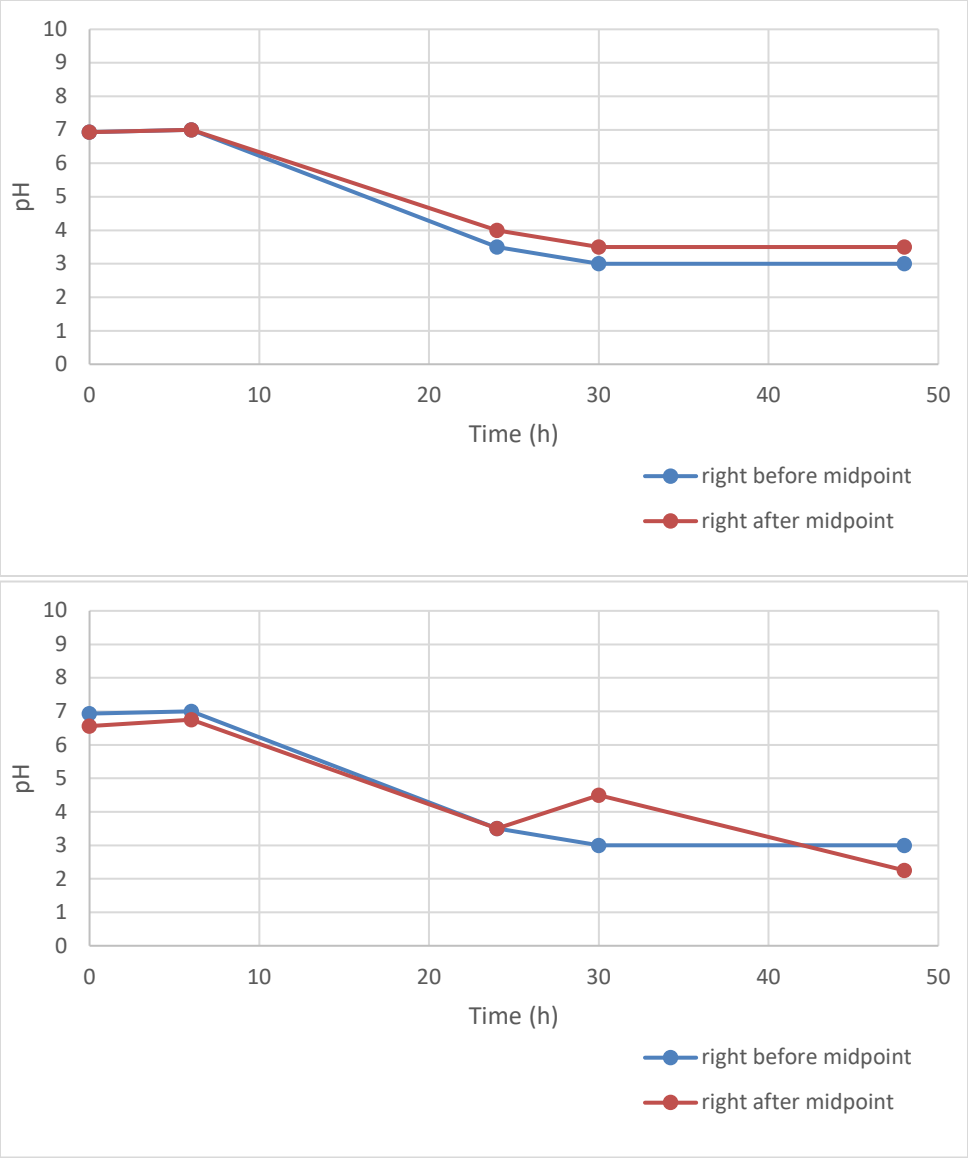

Figure 5.7 Decline in measured pH values adjacent to the midpoint* in sand.
a) System 1 ; b) System 3

*"Midpoint" is defined as 50% of the distance from the anode to the cathode. For both graphs, the measured points were located at 46.4% and 57.1% distances from the anode, respectively.

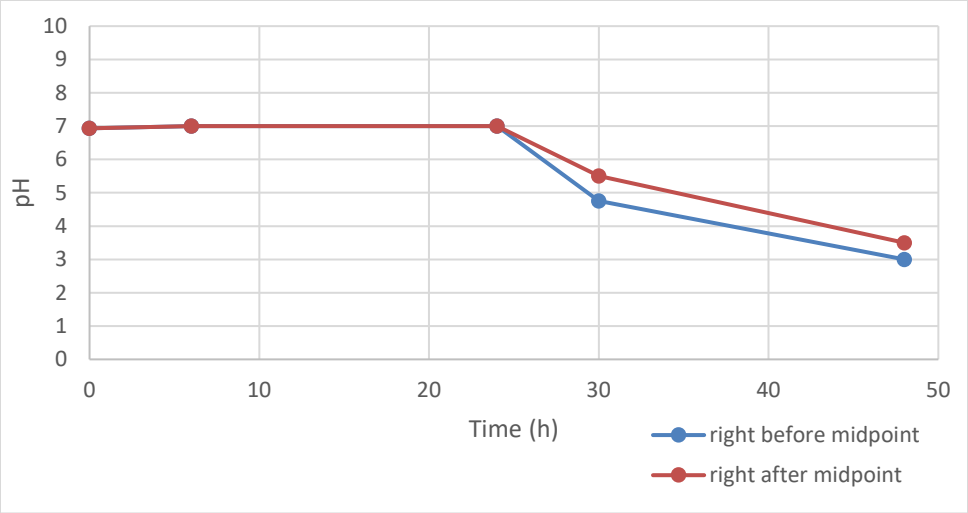

Figure 5.8 Decline in measured pH values adjacent to the midpoint* in sand for System 2. Lag time was due to decreased current density.

*The measured points in this graph were located at 42.9% and 53.6% distances from the anode, respectively.

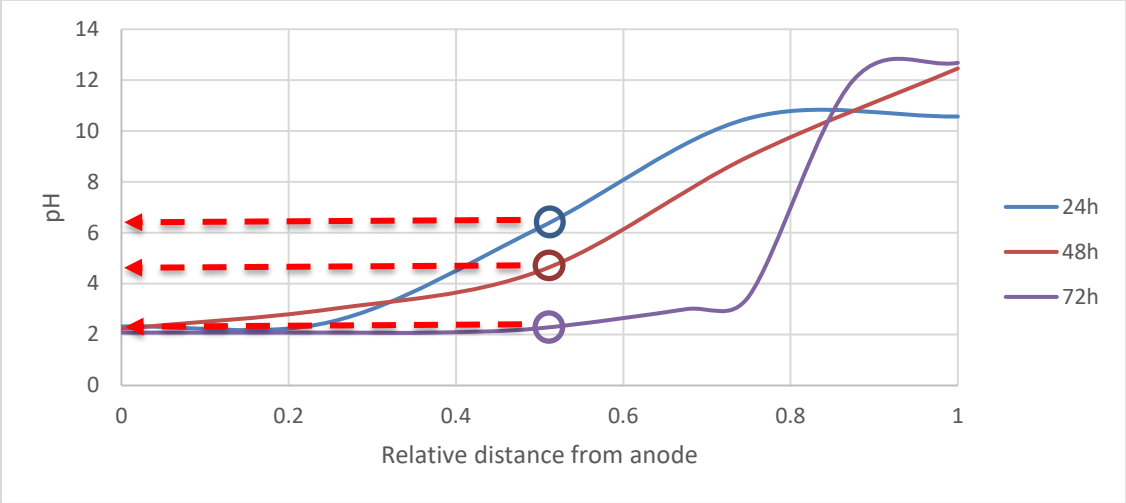

Figure 5.9 Relative pH values of gradients at approximate dye insertion location. Values shown for System 1.

5.6 Conclusion

This experiment yields profound implications as it may be assumed in the literature that a pH gradient in an electrokinetic system should have the form indicated in Figure 5.1. The discovery that a pH does not initially take this profile may be relevant for any contaminants that have strong ionic qualities but that are capable of migrating in a short period of time. It is also conceivable that an effort which would involve a lower current and voltage than the one applied would have a longer period until which the typical profile would take shape. This seems to be a unique phenomenon not cited in the literature and may have other ramifications not yet seen. Future studies may include how pH profiles change over time in other media such as sandy soil and clayey soil and how this may be relevant, especially towards amphoteric contaminants including certain toxic dyes and other industrial products.

CHAPTER 6

ENHANCED BIODEGRADATION OF LOW MOLECULAR WEIGHT PAHs BY ELECTROKINETICS

6.1 Introduction

Once the electrokinetic process and its mechanisms were understood, it was investigated to see if this technology could be used to enhance biodegradation. An experiment was conducted to determine the degree to which electrokinetics could effectively deliver electron donors and nutrients to the target organisms. The three compounds (fluorene, phenanthrene, fluoranthene) were chosen due to their presence on the EPA priority PAH list [360] and their similar chemical structures. Fluorene contains two benzene rings fused to a five-membered ring. Phenanthrene contains three benzene rings, and fluoranthene contains three benzene rings and a five-membered ring (Figure 6.1)

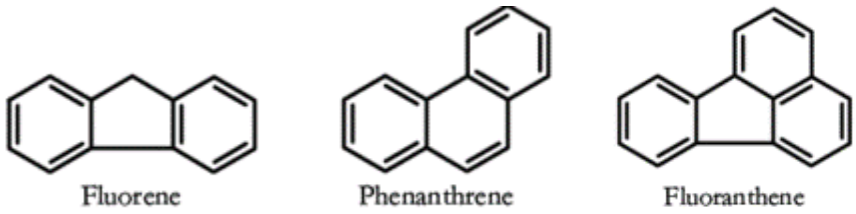

Figure 6.1 Structural images of the three PAH compounds tested in this experiment. *Source:* [361].

Phenanthrene has a unique angular structure that may make it easier for microbes to attack [362, 363] due to its strong bay and k-regions [10, 364]. and has many proposed pathways for biodegradation to occur [365]. Fluorene degradation also has many proposed pathways [39] although it is not noted in the literature as frequently as phenanthrene [39, 366]. Wammer and Peters [367] imply that the order of degradation is such as the number

of rings is the greatest factor with respect to degradation and therefore phenanthrene and fluorene should be more readily degraded. They posit that perhaps the slightly non-polar 5-membered ring found in fluorene may be more difficult for enzymes to access leading to a preference toward phenanthrene degradation.

The overall goal of this experiment was to determine the efficiency of electrokinetic technology to deliver nutrients and provide increased bioavailability for the biodegradation of 3-ringed PAHs. If successful, these results could help guide applied uses of electrokinetic systems. An additional objective was to at the comparison of degradation rates of the PAHs and how they vary based upon their structure and conformation.

6.2 Materials and Methods

6.2.1 System Design

Three identical self-designed electrokinetic (EK) apparatuses (Figures 4.2-4.3) were utilized in this experiment and are the same apparatuses used in the dye migration experiments (Chapters 4 and 5). Electrodes were 30 cm graphite rods with a 0.63 cm diameter. Power Supply was a commercial 30V output with a measured 9.36 ± 0.04 mA current output. The voltage gradient was calculated to be 0.667 V/cm and the current density was calculated to be .054 mA/cm^2. A separate power supply was used for each system.

6.2.2 Soil Sampling

Soil used in this experiment was taken from the grounds of an NJIT construction site. It was analyzed via ASTM method D2487 and found to be SW (Well-graded sandy soil). Grain size ranged from 0.08 – 6 mm and the moisture content was 14.47 ± 1.19 % (w/w).

The pH of the soil was approximately 8.24 and the density was found to be 1.15 ± 0.07 kg/L. Density was determined following 24 hours of drying at room temperature and the removal of large and medium-sized stones. Soil was collected several months prior to initiation of the study and was stored at room temperature until commencement of experiment. Soil was analyzed via GC-MS (gas chromatograph with mass spectrometry) to ensure no background levels of any relevant contaminants. A Most Probable Number (MPN) procedure (Wrenn, 2012) was used to verify the presence of alkane-degrading and PAH-degrading bacteria prior to the onset of the experiment (Figure 6.2). Background metal and some nutrient measurements of the soil were measured via XRF and it was found to be fairly representative of an urban soil. No inhibitory concentrations of any metals were found (Table 6.1). All large and obvious stones were removed prior to the performance of all tests.

a) b)

Figure 6.2 Images of MPN plates showing positive identification of : a) Alkane-degrading bacteria, b) PAH-degrading bacteria.

Table 6.1 Soil Properties

Density (kg/L)	pH	Moisture Content	Arsenic (ppm)	Cadmium	Mercury	Lead (ppm)	Cobalt (ppm)	Copper (ppm)
1.13 ± 0.07	8.24	14.47 ± 1.19%	11.18 ± 6.13	ND	ND	57.02 ± 7.67	166.6 ± 88.2	49.12 ± 16.38

ND = Not Detected

6.2.3 Soil Spiking Setup

6.2.3.1 Preparation of Soil. The inner chamber of each EK apparatus was measured to be 2000 cm^3 or 2L by volume. Density was determined to be approximately 1.15 kg/L and therefore 2.3 kg of soil was to be added to each system. Accordingly, for three apparatuses (duplicates plus control), 6L of soil, or 6.9 kg was needed. 10 kg of spiked soil was prepared as a contingency. Prior to weighing, soil was allowed to air dry overnight so as to easily remove all obvious stones.

6.2.3.2 Preparation of PAH Mixture. A stock solution of fluorene, phenanthrene, and fluoranthene in methanol was prepared in order to yield a final concentration of 100mg/kg of each PAH compound in the soil.

6.2.3.3 Spiking of Soil. Due to lack of accessible machinery, the PAH solution was poured gently into several containers containing the soil and mixed thoroughly by hand. Residues of the gloves were eventually scraped into the mixture to minimize any losses. Four equal portions of 2.3 kg each (corresponding to 2L) of the spiked soil by weight were separated. Each portion of the PAH-laced soil was left in a chemical hood overnight to allow all residual methanol to evaporate. The resulting soil in each portion was assumed to have an average concentration of 100 mg/kg of each parent PAH compound. Glassware

used in this experiment were acid-washed with 1:1 HCl, cleaned with distilled water and dried at 110°C before each experiment.

6.2.4 Nutrient Medium

Bushnell-Haas (B-H) medium was prepared in a 5L Erlenmeyer flask by dissolving the dry medium obtained from Difco Products (Detroit, MI) in deionized medium according to the manufacturer's instructions. 0.6 g of yeast extract was added. The solution was stirred and heated until all particulates dissolved.

6.2.5 Filling Method

In each EK apparatus, 2.3 kg (equivalent to 2L) of spiked soil was placed in layers in the inner chamber of each of the three EK apparatuses. The soil was lightly compressed with a self-made acyclic pressing tool to eliminate any large cracks or air-pockets showing. In all systems, both reservoirs were filled with a 1 g/L NaCl solution up to the bottom of the soil level. The NaCl solution was created by dissolving 1g of NaCl granulated power in water for each L of water needed. As one of the purposes of this experiment was to mimic underground scenarios, tap water was chosen as the source of water rather than de-ionized water. This would provide additional electrolytes that may be found in in-situ environments and could increase electrical conductivity and possibly microbial growth. The tap water was taken from the laboratory sink at the New Jersey Institute of Technology and was found to have following characteristics: Conductivity was reported to be 271.6 ± 10 µS/cm and the salinity of the water was 0.1 g/L. The final 1 g/L NaCl solution was found to have following characteristics: Conductivity was reported to be 2068 µS/cm and the salinity was 1.1 g/L. 500 mL of 10% sodium azide solution (final system concentration of 1.5 g/L) was added to the control system as a biocide. Additional 1 g/L NaCl solution

was then added to each reservoir of all systems to bring the liquid levels to meet the soil surface levels. The liquid was then allowed to infiltrate into the soil. As the liquid passed into the soil, the soil area was periodically flattened and compressed and again a best effort was put forth to ensure a lack of any large cracks or air-pockets.

6.2.6 Adding the Nutrients

After the system equilibrated, 500 mL of the nutrient medium and 100mL of 0.1 M phosphate buffer (pH 7.4) was added to each reservoir. A large stirring rod was used to mix thoroughly but briefly. The lids with electrodes were then placed atop the reservoirs and 1h was allowed for the system to settle.

6.2.7 Extractions and Analysis

All systems liquids were taken from each reservoir and stored separately for analysis. When all liquid was removed, the soil was carefully removed from the inner part of each system and stored in sealed bags. A vigorous rinse with de-ionized water (4.5 L per system) was performed to remove any additional soil particles adhering to the acrylic surface and any residues in the reservoir chambers. This liquid was stored separately for each system for analysis. Soil extraction was performed based upon a modified version of Khodadoust et al. [368] with the following steps:

For each system's soil, the soil was mixed within its sealed bag and then sampled at various locations to collect 50g of sample. This was performed in order to achieve a more representative sample on the final soil's concentrations. Each system was sampled with two 50g portions of soil for analysis. The initial solvent utilized for the extraction was comprised of 85% Ethyl alcohol (mixture of Fisher Scientific®, ACS Grade (200 proof) and Fisher Scientific®, Reagent Grade, denatured, 95% purity), 10% de-ionized water, and

5% Methanol (Fisher Scientific® ACS Grade, 99.8% Purity). Solvent was added to soil in a 1:4 mL ratio, or 200 mL total per soil sample. Mixture was shaken on a MaxQ 2000 orbital shaker (ThermoFisher®) for 1h and intermittent speeds between 30-125 rpm. The mixture was then centrifuged at 2600g for 30 minutes (ThermoFisher® ST16 Model) and the supernatant set aside. This procedure was performed a total of three times, each time adding 200 mL additional solvent mixture (after the removal and storage of the previous liquid). Each extraction liquid was stored separately. In order to prepare samples for GC-MS (gas chromatograph with mass spectrometry) analysis, the extraction liquid necessitated a second extraction into a more appropriate solvent and to remove the presence of water from the sample. A modified version of EPA Method 3510C, utilizing hexane rather than methylene chloride was performed, and all sets of extract were set aside for analysis. Any samples not measured immediately were placed at -20°C for future analysis. This method of extraction was also used to extract from the reservoir and rinse liquid samples.

A Gas Chromatograph equipped with Mass Spectrometry (GC-MS) was used for the quantification of the three parent PAH compounds (fluorene, phenanthrene, and fluoranthene) and the qualification of any metabolites. The column used was a SPB-5 30m x 0.53mm x 1.5 um Film Thickness. Inlet flow rate set at 42.9 mL/min, Column flow rate at 1.5 mL/min, Helium carrier and makeup. Oven: Temp 1 = 120°C, (no hold), Temp 2 = 320°C (66.7 min), Rate 1 = 3°C/min, hold at 320°C (5 min). Injector Temp = 250°C, Detector Temp = 320°C, Splitless.

To test the efficiency of the extraction method, a mock extraction with identically spiked soil and identical extraction procedure was performed and the PAH recoveries were

reported as: 78.36 ± 0.63 % for fluorene, 81.06 ± 0.91% for phenanthrene, and 96.27 ± 2.16% for fluoranthene.

6.3 Measurements

pH measurements were conducted using the Sper® Model #850052 pH Pen (Sper Scientific®, Scottsdale, AZ, USA) at two locations in each reservoir. One measurement was taken at the front corner, farthest away from the bridge of the apparatus (Figure 4.2) and the other measurement was taken immediately adjacent to the beginning of the bridge, near the location of the electrode. Temperature was monitored as the electric current was hypothesized to raise a system's overall temperature. Temperatures values were also measured using the Sper Scientific® Model #850052 pH Pen, primarily at the first pH measurement location.

Conductivity and Salinity measurements were taken via the YSI® Model 30 Handheld Salinity/Conductivity/Temperature Meter (YSI Incorporated, Yellow Springs, OH, USA) and accompanying probe. For measurements, the probe was inserted into the center of each reservoir.

6.4 Results

6.4.1 PAH Recovery and Degradation Rates

Initial findings indicated as much as 89.47% degradation of the PAHs (phenanthrene) occurred in one of the systems. Yet, as extraction procedures are not always efficient, percent recovery must be normalized against the control. Only 40.06 ± 6.84%, 41.27 ± 4.76%, and 47.44 ± 4.83%, of fluorene, phenanthrene, and fluoranthene, respectfully, was recovered for the Control system. This was a stark contrast in comparison to the mock

extraction results. This implies likely either a flaw in the subsequent extraction or that a very high percentage of the PAHs became adsorbed strongly to the acrylic surface, thereby impeding recovery. The summary for all results (Table 6.2) shows the diminished recovery for the control systems but that Systems 1 and 2 did show further diminished yields, indicating the likely presence of biodegradation.

Systems 1 and 2 were meant to function as duplicates and their voltage and current values were similar. However, there was a structural problem with System 2 and it was prone to slight leaking during the course of the experiment. It is not known how much of the PAHs were lost due to this process, but it was estimated that up to 40% of the original reservoir liquid was lost. Despite this, the trace amount PAHs detected in the reservoir liquids indicates that at most only a very minor fraction of the total PAHs may have been lost due to this phenomenon. Thus, the decreased recovery may have been primarily due to variations in microbial activity and possibly more effective biodegradation.

Analysis of the reservoir liquids for all three systems showed nearly no traces of PAH or their metabolites with the exception of minimal (<<0.01%) traces of phenanthrene and several soil components. Each individual system after removal of the soil and reservoir liquids was rinsed with 4.5 liters of de-ionized water and then extracted via liquid-liquid extraction (EPA Method 3510C). The percent recovered via the rinsing process, which included a small remainder of the soil, is reported in Table 6.3.

Table 6.2 Percent PAH Recovery and Overall Degradation

FLUORENE	% Recovered	Average % Degraded	% Degraded minus Control	Relative % Degraded
Test Extraction	78.36 ± 0.63%	-	-	-
Control	40.06 ± 6.84%	59.94%	-	-
System 1	24.71 ± 1.04%	76.29%	16.35%	26.61%
System 2	11.07 ± 0.54%	88.93%	28.99%	48.37%
PHENANTHRENE	**% Recovered**	**Average % Degraded**	**% Degraded minus Control**	**Relative % Degraded**
Test Extraction	81.06 ± 0.91%	-	-	-
Control	41.27 ± 4.76%	58.73%	-	-
System 1	29.76 ± 13.09%	70.24%	11.51%	19.60%
System 2	10.91 ± 0.05%	89.09%	30.36%	51.70%
FLUORANTHENE	**% Recovered**	**Average % Degraded**	**% Degraded minus Control**	**Relative % Degraded**
Test Extraction	96.27 ± 2.16%	-	-	-
Control	47.44 ± 4.83%	52.56%	-	-
System 1	33.84 ± 6.39%	66.16%	13.61%	26.89%
System 2	23.94 ± 0.70%	76.06%	23.51%	44.72%

Table 6.3 Percent PAH Recovery by System Rinsing

FLUORENE	% Recovered	Avg % From System	Avg % From Rinse	Rel % in Rinse
Control	40.06 ± 6.84%	99.28%	0.72%	0.73%
System 1	24.71 ± 1.04%	98.78%	1.22%	1.23%
System 2	11.07 ± 0.54%	97.23%	2.77%	2.84%
PHENANTHRENE	**% Recovered**	**Avg % From System**	**Avg % From Rinse**	**Rel % in Rinse**
Control	41.27 ± 4.76%	16.80%	0.64%	0.65%
System 1	29.76 ± 13.09%	9.24%	0.82%	0.82%
System 2	10.91 ± 0.05%	3.81%	2.21%	2.26%
FLUORANTHENE	**% Recovered**	**Avg % From System**	**Avg % From Rinse**	**Rel % in Rinse**
Control	47.44 ± 4.83%	17.38%	0.55%	0.55%
System 1	33.84 ± 6.39%	10.24%	0.88%	0.89%
System 2	23.94 ± 0.70%	4.41%	1.45%	1.48%

6.4.2 System Changes Over Time

When initially pouring the liquid into reservoirs, some soil particulates were flushed out into the reservoir liquid, initially giving the reservoirs a brownish color. However, within a day the soil particulates settled at the bottom of the reservoir as a thin blanket (Figure 6.3).

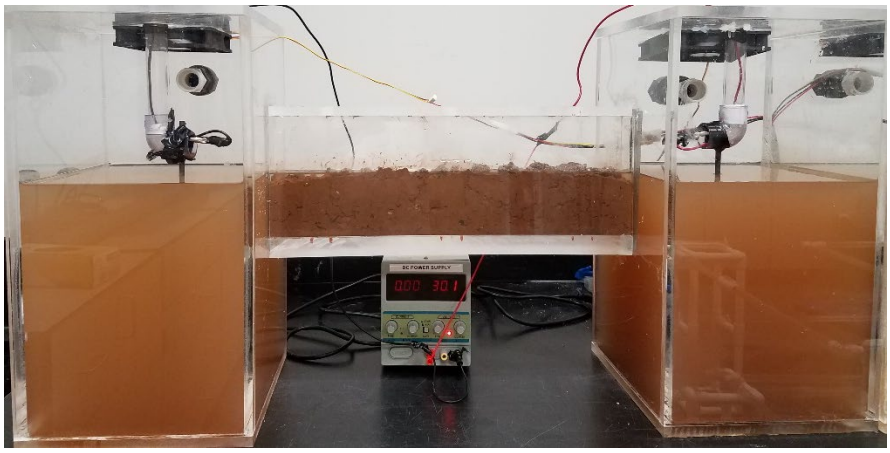

Figure 6.3 Image showing brownish color in reservoirs due to soil particles being flushed out when adding liquid.

On days 3-5 from when the power supplies were turned on, a large amount of white precipitate was noted covering much of the cathode electrode and a slight blanket of white covered the bottom of the tank in the cathode chamber (Figure 6.4). Precipitate was easily disturbed and upon very light agitation, immediately was disrupted throughout the reservoir. This precipitate was noted in all three systems and was thought to be of a calcium or carbonate nature. Precipitate was greater on day 5 than day 3 and at that point all precipitate amounts in all systems appeared equal, despite still only being present in the cathode reservoirs, which had a basic pH.

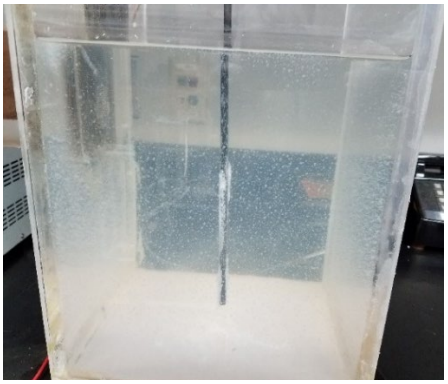

Figure 6.4 Image taken of white precipitate forming on cathode electrode and in its reservoir.

After seven days, it was noted that the amount of phosphate buffer initially added was insufficient as extreme pH values were observed in all systems. An additional 200 mL of 1M phosphate buffer (pH 7.4) was added to each reservoir and each reservoir was briefly mixed. Shortly following the addition of the phosphate buffer and polarity reversal, pH values stabilized in both reservoirs of all systems and initially remained stable at neutral pH values. On day 14 of the experiment, the non-control reservoirs (i.e., Systems 1 and 2) began to grow dark and small bits of biofilm appeared on the reservoir liquid surfaces. By day 17, a relatively thick biofilm was apparent on the entire cathode reservoir surface of both systems and a partial biofilm was observed in the anode reservoirs. No biofilm was apparent on either day in the control system. Despite a basic lid on the systems, a decrease in liquid levels was noted in all system reservoirs due to evaporation in addition to any water lost due to electrolysis. As noted previously, System 2 also had a slight leak and therefore required even greater replenishment. De-ionized water would be added to all systems when needed beginning on day 19 but in the interim (day 17), 200 mL of 1 g/L NaCl was added to each reservoir of System 2 to compensate for the estimated leak-related losses.

On day 19, a thick biofilm was observed in System 1, especially in the cathode reservoir. A sheen rather than a biofilm was observed in System 2, primarily in the anode reservoir. No sheen or biofilm was observed in the Control. As previously noted, on day 19, de-ionized water only was added to all systems to restore reservoirs to previous water levels (aligned with top of soil). 3L was added to each reservoir of System 1, 3.5 L was added to each reservoir of System 2 and 2.7 L was added to each reservoir of the Control. Water was added slowly so as not to disturb the bottom layer, although it was in fact

disturbed in cathode reservoir of System 1 and to a lesser extent in both of the control reservoirs.

On day 24, a biofilm was once again observed in System 1, covering most of the surface in the cathode reservoir, with some floating biofilm pieces. The anode reservoir had a thick and fully expansive biofilm and the entire reservoir was cloudy as well as filled with biofilm pieces (note: The increased biofilm and cloudiness may have been due to the disruption of the bottom layer 5 days prior). In System 2, only a sheen rather than a thick biofilm was observed and was more prominent in the anode reservoir. There was no sheen, biofilm, or cloudiness observed in the Control. Both reservoirs appeared identical and clear although with a slight brownish color due to the disruption of the bottom layer.

After a polarity-reversal was performed on Day 24, both reservoirs of System 1 were found to be dark and cloudy on Day 26, with a significant biofilm presence. The left reservoir of System 2 (now functioning as the cathode) had a thin biofilm covering most of the surface and the right reservoir (now functioning as the anode) had a sheen and traces of a biofilm. Both reservoirs were dark, and similar in appearance to those of System 1. Control reservoirs still were both clear and identical and maintained a minor brownish color with no indication of a sheen or biofilm. On Day 31, both reservoirs of System 1 had a relatively thick biofilm covering the entire surface and were dark and cloudy with many biofilm pieces. The cathode (left) reservoir had a moderate biofilm covering all of its surface but had no noticeable biofilm pieces despite being quite dark and relatively cloudy. The anode reservoir (right) had now a thin biofilm covering most of its surface, and was dark but not cloudy, yet a few biofilm pieces were noted. No changes were observed in the Control. Additional de-ionized water was added to each system as levels were once

again decreasing. 1.5 L was added to each reservoir of System1 and the Control, and 2 L to each reservoir was needed for System 2. Polarity in all systems was reversed again as pH values began to shift. As the upper level of soil had now become fairly dry, a very thin layer of moist (unspiked) soil was added atop the soil in all three systems, in order to allow for the entire spiked soil area to be subject to biodegradation.

On Day 38, both reservoirs of System 1 had a medium biofilm covering most of surface, and the reservoirs were dark and cloudy with many biofilm pieces. (This was significant considering the prior disruptions.) The left (now anode) reservoir of System 2 had a light-to-moderate biofilm covering most of the surface with substantial biofilm pieces (while not as numerous as System 1) and was cloudy and dark. The right reservoir (cathode) had a slight biofilm or sheen covering the surface and the reservoir was dark but not cloudy, and only a few biofilm pieces were observed. No changes were observed in the Control. The addition of more de-ionized water was again necessary. For System 1, 2 L was added to the left reservoir, and 1.5L to the right. For System 2, 2 L was added to each reservoir, and for the Control, 2 L was added to the left reservoir, and 1.7 L to the right.

On Day 45, the left reservoir of System 1 (cathode – polarity reversal was performed on Day 40) had a very thick biofilm covering the entire surface although the right (anode) reservoir only had a sheen on its surface despite appearing cloudier than the left reservoir (both were substantially dark and cloudy). The left reservoir of System 2 (cathode) had a thin biofilm covering most of its surface and the right reservoir (anode) had only a minor sheen. Biofilm pieces were present in both reservoirs, with a greater prevalence in the right (anode) reservoir. Both reservoir was dark but only slightly cloudy. No changes were observed in the Control.

On Day 49, the left reservoir of System 1 (cathode) only had a thin biofilm covering most of the surface and many biofilm pieces were observed. The right reservoir (anode) surprisingly had no noticeable biofilm or sheen, though some biofilm pieces were observed. The left reservoir was very cloudy, and the right was slightly cloudy. The left reservoir of System 2 (cathode) had light-to-moderate biofilm covering about half of its surface, was relatively cloudy and a moderate amount of biofilm pieces were observed. The right reservoir was slightly darker albeit less cloudy and less biofilm pieces were observed. A thin sheen was observed over half of the surface. No changes were observed in the Control. The addition of more de-ionized water was again necessary. For System 1, 2 L was added to the left reservoir, and 2.4 L to the right. For System 2.6 L was added to the left reservoir and 3.4 L to the right, and for the Control, 2 L was added to the left reservoir, and 2.2 L to the right.

On Day 52 (post polarity-reversal), the left reservoir of System 1 (anode) was much darker than before, fully opaque, and very cloudy. A thin biofilm covered most of the surface. The same was noted for the right reservoir (cathode) with exception of a lesser degree of cloudiness. Both reservoirs of System 2 appeared identically to those of System 1, except not fully opaque in appearance. No changes were observed in the Control.

On Day 54, a foam (Figure 6.5) appeared around the top of the electrodes in both Systems 1 and 2. It was very rigid, and the bubbles did not burst easily upon pressure. The foam was collected for analysis, but no reasonable results were achieved. It was concluded that the bubbles were likely hydrogen or other gases formed and trapped within the biofilm to create the foam. (This same foam appeared multiple times in future biological experiments.)

Figure 6.5 Examples of the foam that formed around the electrode on the reservoir surface.

On Day 56 (after polarity-reversal on Day 54), both reservoirs of System 1 had a thin biofilm covering most of its surface with a moderate amount of biofilm pieces observed. The left reservoir (cathode) also had a thin biofilm covering most of its surface with a few biofilm pieces observed. The right reservoir (anode) had a thin biofilm covering nearly the entire surface with many biofilm pieces observed. No changes were observed in the Control.

On Day 60, the final day of the experiment, the left (cathode) reservoir of System 1 had only a very thin biofilm, a small amount of foam, and a moderate amount of biofilm pieces was observed. The right (anode) reservoir had no noticeable biofilm despite the observation of light-to-moderate biofilm pieces. However, a multi-color (oil-like) sheen covered the majority of the surface. All reservoirs of Systems 1 and 2 were dark and fully opaque (Figure 6.6). No changes were observed in the Control. Not very long (2-3 weeks) after the initiation of the experiment, a white color was seen atop the uppermost level of the soil. It was assumed initially to be due do dryness, but this white color never appeared

in the Control system. A possible hypothesis is that this white color might be indicative of a fungus which could not grow in the presence of sodium azide, even though there would only be minimal amount by the soil surface.

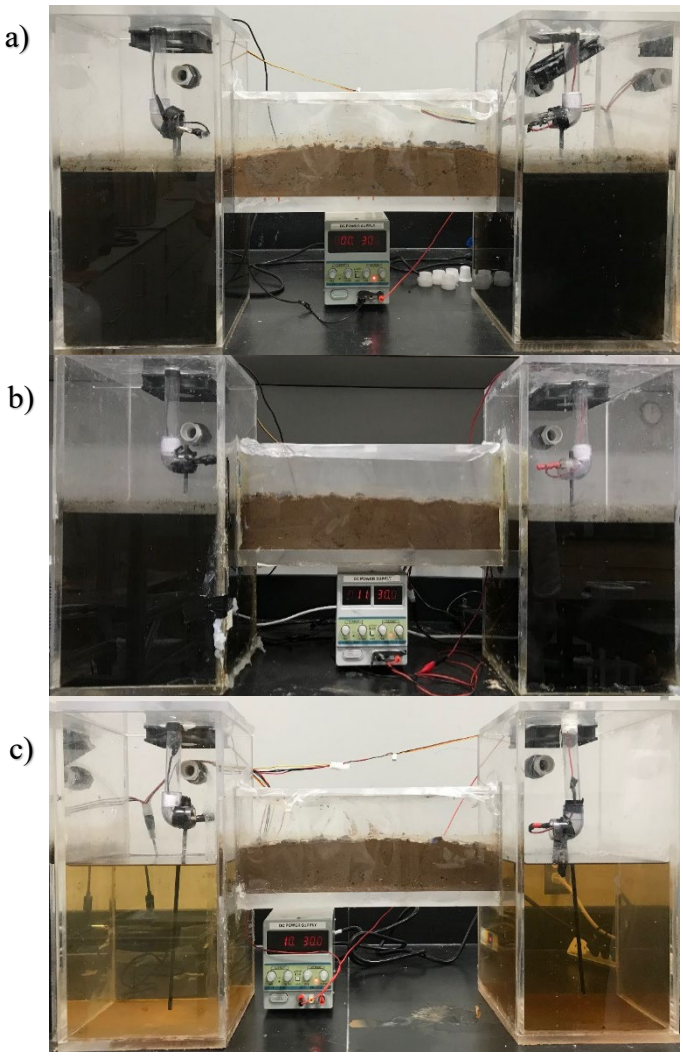

Figure 6.6 Visual Comparison of All Systems at the End of the Experiment (day 60). a) System 1 ; b) System 2 ; c) Control System

(Note: The image for System 2 contains a strong reflection of other materials in the lab but visually appeared near-identical to the darkened reservoirs of System 1).

6.4.3 Current and Voltage

Current and Voltage throughout all systems remained relatively constant in all systems. A potential of 30V was applied for the entire duration of the experiment to all three systems. At the electrodes, voltages were measured to be 30.04 ± 0.06 V, 29.01 ± 1.02 V, 29.52 ± 0.38 for systems 1, 2, and Control, respectively. In the reservoirs, minor losses were observed as the voltages measured 26.79 ± 0.36 V, 26.40 ± 1.65 V, 26.98 ± 0.65, for systems 1, 2, and Control, respectively. The power supply utilized for System 2 was slightly older than the other two and was prone to slight decreases in both current and voltage over parts of the duration of the experiment.

Current was expected to fluctuate but remained relatively stable for the duration of the experiment. At the electrodes, current values were measured to be 7.41 ± 0.82 mA, 6.83 ± 0.18 mA, 7.06 ± 0.79 mA for systems 1, 2, and control, respectively. In the reservoirs, measured adjacent to the soil, current values were measured to be 6.74 ± 0.94 mA, 6.02 ± 0.37 mA, 6.55 ± 0.38 mA for systems 1, 2, and control, respectively. Previous usage of these power supplies in addition to the initial values observed in this experiment showed a current output of 9.36 ± 0.04 mA for a set output of 30V. Yet, perhaps due to the quality of these economic power systems or perhaps due to a greater buildup of resistance over time, power and current output diminished.

6.4.4 pH and other Values

pH values were monitored over time. Previous electrokinetic experiments conducted indicated that extremes as low of 1 and high as 13 could be reached without the addition of a buffer. The phosphate buffer initially added (100 mL of 0.1M) proved to be insufficient as after 7 days extreme pH values of about 2 and 10 were observed (Figure 6.7). pH values

were not as extreme in the control system as the sodium azide may have provided a slight buffering effect. On day 7, 200mL of 1M potassium phosphate buffer (calibrated for pH 7.4) was added to each reservoir of all systems. A polarity reversal was conducted to re-establish neutral pH levels and on day 10, pH levels were observed to neutral and even in both cathode and anode reservoirs.

As the experiment progressed, the effectiveness of the buffer, primarily in Systems 1 and 2, began to dissipate, indicating the possible consumption of phosphate by the bacteria present. Polarity reversal was employed numerous times as indicated in Figures 6.7 and 6.8. The Control system, following the addition of the buffer initially actually destabilized, with respect to pH and then re-stabilized at an elevated basic pH (9-11). At this point, not only was the pH elevated but the salinity and conductivity rose greatly as well (Figure 6.8). For System 1, salinity values ranged from 1.6 to 2.2 g/L with an average value of 1.8 ± 0.2 g/L. For System 2, salinity values ranged from 1.6 to 2.2 g/L with an average value of 1.9 ± 0.2 g/L. For the Control, salinity values ranged from 2.7-3.5 g/L with an average value of 3.21 ± 0.25 g/L. For System 1, conductivity values ranged from 2818 to 3978 μS/cm with an average value of 3475 ± 294 μS/cm. For System 2, conductivity values ranged from 3052 to 4207 μS/cm with an average value of 3590 ± 336 μS/cm. For the Control, conductivity values ranged from 4820 to 6470 μS/cm with an average value of 5817 ± 531 μS/cm.

Salinity and conductivity values reported are for experimental days 14-60, after the addition of the phosphate buffer and time for stabilization. (System 2 values were slightly higher than System 1 values for both salinity and conductivity due to the leak present in System 2 and therefore a marginally greater salt % of the total liquid volume.) During the

period of time when the salinity and conductivity values were far greater in the Control system, a much-enhanced production of bubbles (hydrogen and oxygen for the cathode and anode, respectively) was observed being produced along the electrodes. The production of these gases as well as the salinity and conductivity began to decrease slightly beginning on Day 52. This could be indicative of chemical changes in the system, or perhaps an occurrence of biological activity. It was presumed that the levels (1.5 g/L) of sodium azide in the system would be sufficient to curb any bacterial growth, however, subsequent MPN results (Figure 6.9) confirmed a moderate presence of bacteria in both the soil and reservoir samples from the Control system.

6.4.5 Temperature

Temperature was monitored as the electric current was hypothesized to raise a system's overall temperature, though, temperature values did not change significantly during the experiment and any noticeable variations corresponded to changes in room temperature. The average temperatures measured were 19.3 ± 1.2 °C, 19.2 ± 1.2 °C, and 19.2 ± 1.2 °C, for systems 1, 2, and Control, respectively, with an overall range of 16.8 – 21.7 °C.

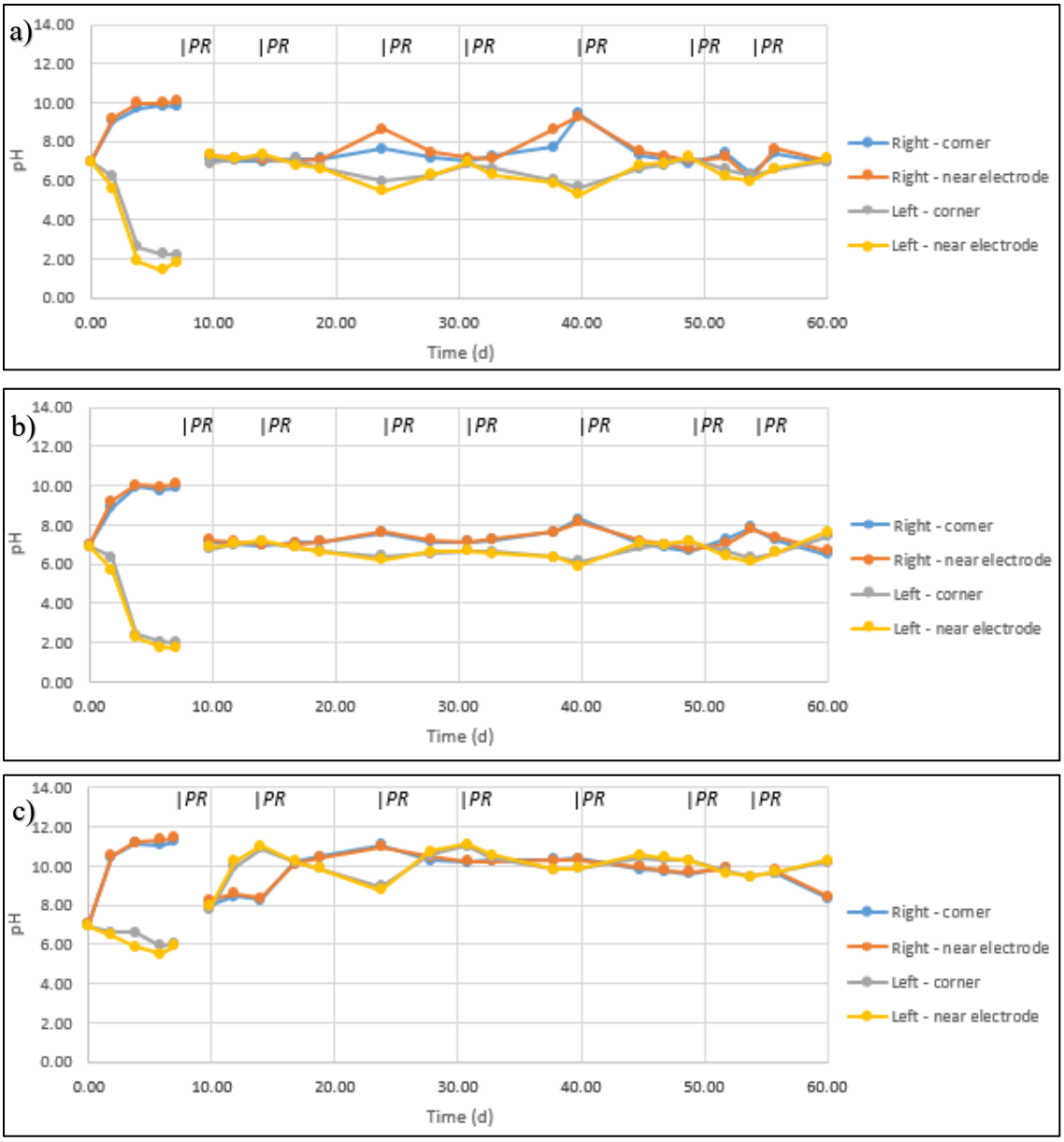

Figure 6.7 pH in Electrokinetic Systems Over the Duration of the Experiment.
a) System 1 ; b) System 2 ; c) Control (PR = Polarity Reversal)

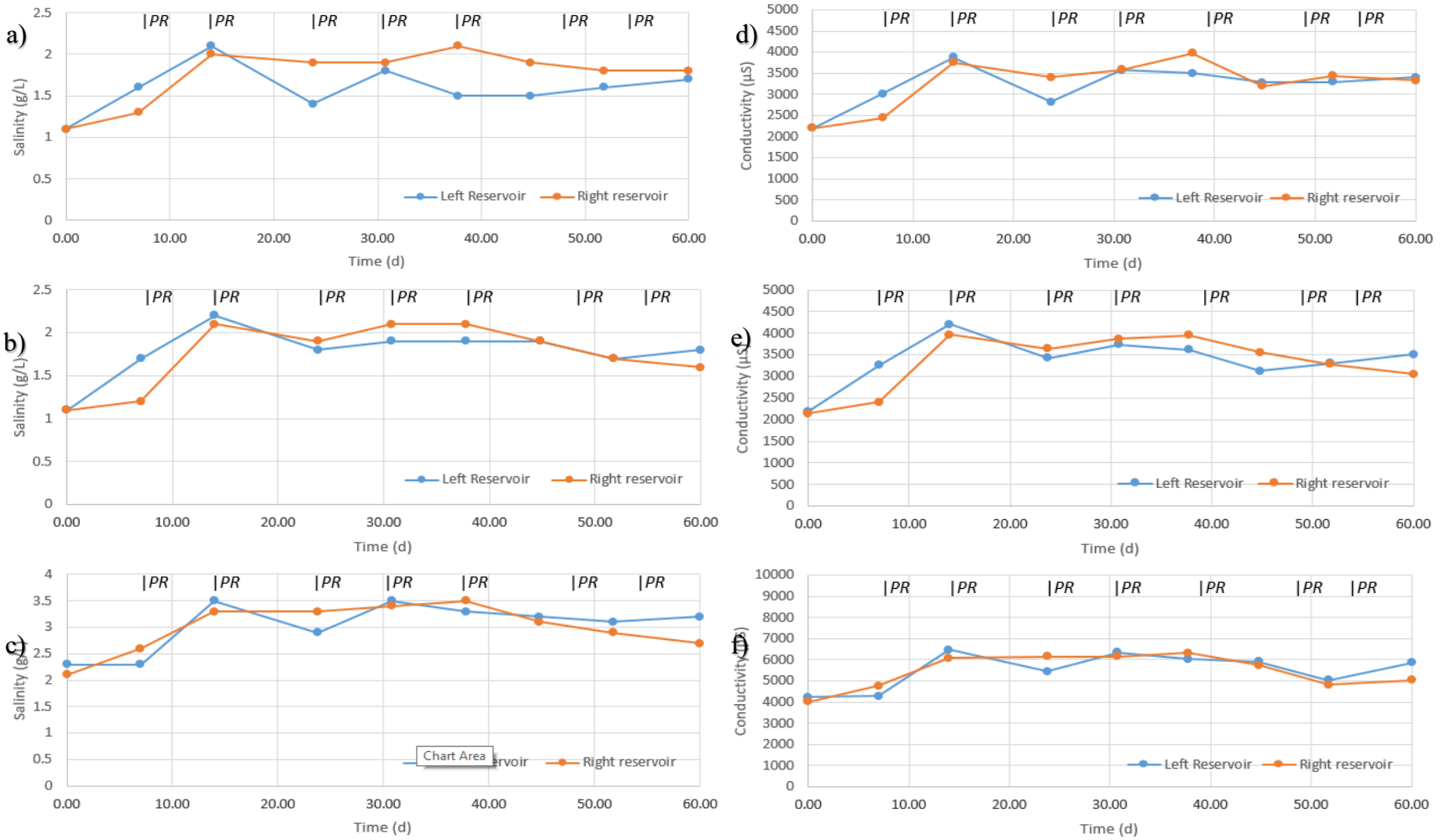

Figure 6.8 Salinity and Conductivity Changes in Electrokinetic Systems Over the Duration of the Experiment (PR = Polarity Reversal):
Salinity Measurements versus Time: a) System 1 ; b) System 2 ; c) Control
Conductivity Measurements versus Time: d) System 1 ; e) System 2 ; f) Control

a)

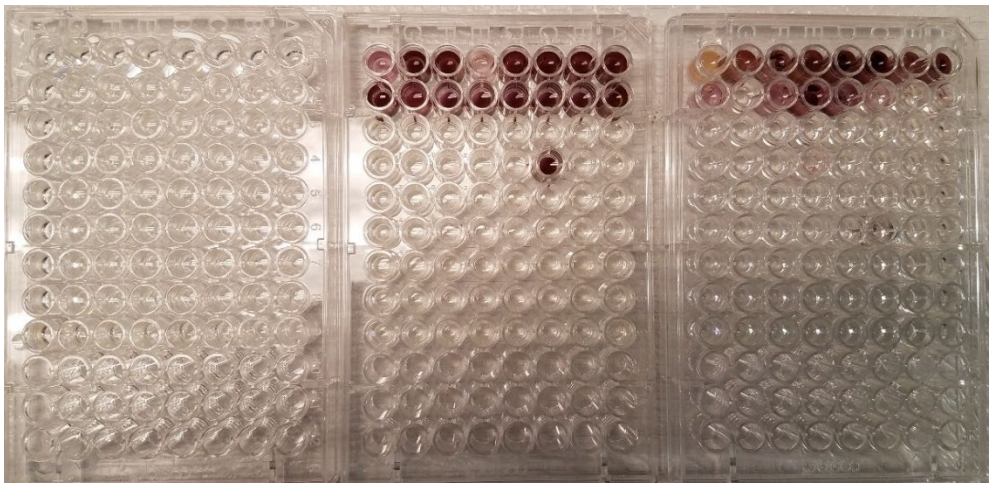

b)

Figure 6.9 Images of MPN plates showing positive identification of
a) Alkane-degrading bacteria ; b) PAH-Degrading Bacteria
(both images left-to-right: De-ionized water only, Control reservoir liquid, Control soil)

6.5 Discussion

6.5.1 Degradation Analysis

Given an assumption that all PAHs not recovered were degraded, relative to the Control, Systems 1 and 2 showed a sizeable increase in degradation rates. In System 1, when compared to the Control, fluorene showed the greatest degradation (16.35 ± 1.04 %) although this was within the standard deviations of both phenanthrene (11.51 ± 13.09 %) and fluoranthene (13.61 ± 6.39 %). In System 2, which had a much lower degree of PAH recovery, and thus increased degradation, when compared to the Control, phenanthrene showed the greatest degradation (30.36 ± 0.05 %), followed by fluorene (28.99 ± 0.54 %), and then fluoranthene (23.51± 0.70 %). With respect to total recovery, however, the Control did not have a high overall yield, thus implying possible degradation occurring in that system. In the Control, only 40.06 ± 6.84 %, 41.27 ± 4.76 %, and 47.44 ± 4.83 % of fluorene, phenanthrene, and fluoranthene, respectively were covered. This would imply an average degradation of 59.94%, 58.73%, and 52.56%, for fluorene, phenanthrene, and fluoranthene, respectively (Table 6.2). If these results are indicative of degradation, then it can be concluded that fluorene and phenanthrene degraded to near-identical degrees with slightly less degradation taking place for fluoranthene. For Systems 1 and 2, fluorene and phenanthrene had the lowest overall recoveries, and thus higher potential degradation rates than fluoranthene. Though, for System 1, the deviation in measurements obtained for phenanthrene overlapped with both fluorene and fluoranthene recoveries. Relative to the Control, System 1 had average degradation rates of 0.588 mg/d, 0.441 mg/d, 0.522 mg/d, and System 2 had average degradation rates of 1.111 mg/d, 1.164 mg/d, and 0.901 mg/d for fluorene, phenanthrene, and fluoranthene, respectively.

Corresponding to the recoveries seen from the mock extraction (Table 6.2), phenanthrene in all systems had substantially lower yields than the other two compounds and thus a greater potential degradation. The mock extraction demonstrated, though, that it a far higher yield could be obtained for fluoranthene than fluorene, and thus when comparing true potential degradation, these may be not statistical difference between these two compounds. Of the three compounds studied, phenanthrene should be most readily degradable by aerobic organisms [369, 370], and was suggested by the data in this study. It was also observed that in all systems, fluoranthene was potentially degraded to a greater degree than fluorene. Although highly dependent upon pathway availability and the respective organisms, fluorene is reported to be more readily degradable on average than fluoranthene [371]. Weissenfels et al. [369] found that phenanthrene, fluorene and fluoranthene could be each be used a sole carbon source. In contrast, it is has also been reported that for some strains, fluorene cannot be utilized as a sole carbon source [372]. This experiment contained yeast extract and thus had an additional carbon source. Researchers claim that phenanthrene and fluoranthene can inhibit fluorene degradation [77] but other researchers claim that the presence of fluorene can inhibit fluoranthene degradation [373]. It is uncertain whether either of these phenomena occurred in this study. Yet, it is possible that due to the particular strains present it may have been more favorable to degrade one compound over another.

The purpose of the Control system was to provide an abiotic reference to compare against the biological systems (1 and 2). It was assumed that the addition of sodium azide would be sufficient to curb any potential microbial growth. However, PAH recoveries for the Control were also low, indicating that significant degradation may have taken place. A

most-probable number (MPN) test was performed and some biological presence was confirmed in the Control system. Rozycki and Bartha [374] report that the effectiveness of azide as a biocide is reduced as pH increases, and especially so under very basic conditions. As the sodium azide appears to have raised the pH of the Control, this implies a possible decreased biocidal effect of the azide chemical and hence the possibility of biodegradation within the system.

Despite the determination of biological presence in the Control system, the absence of biofilm or other visual evidence of significant bacterial growth (such as that observed in Systems 1 and 2) indicates there may be other reasons for lack of PAH recovery. It was hypothesized that the majority of the PAH compounds perhaps still adhered to the acrylic surface of the setups. Prior to this determination, a solvent rinse was used for cleaning the setups but was not captured in order to test this hypothesis. A later experiment (Section 6.2.7) determined that a thorough solvent rinse of the systems yielded a 1-2% recovery of the parent PAH compounds, and thus it appeared unlikely that the bulk loss of PAHs was due to adsorption or adherence.

Using the theoretical assumption that lack of yield in the Control systems was due to biodegradation, maximum degradation rates in the Control would be found to range from 1.83 – 2.52 mg/d, with System 1 ranging from 2.19 – 3.19 mg/d and System 2 from 2.89 – 3.43 mg/d. Though, as the Control was non-functional as per its design, any results or theories in this experiment must be dismissed as inconclusive.

6.5.2 Biofilm

Biofilm presence was greater in System 1 than System 2 and formed at a slightly earlier point in time. The thickness of the biofilm can be indicative of a greater biological activity

and cooperation [375] or of greater stress on the particular organisms involved [376]. However, as the turbidity and opaqueness of System 1 for most of the experiment was greater than that of System 2, one may conclude that the increased presence of biofilm as well as the turbidity and opaqueness indicate a stronger bacterial presence in System 1. Therefore, additional degradation noted for System 2 is assumed to be due to losses that occurred during leakage.

6.5.3 Possible Metabolites and Degradation Products

Despite indications that biodegradation took place in Systems 1 and 2, there was no significant difference in metabolites observed in comparison to the Control. A full spectrum of both soil and reservoir water was analyzed via GC-MS and the only stark difference between the biological systems and the Control system was the presence of 1,2-Benzenedicarboxylic acid, mono(2-ethylhexyl) which was found in significant yet still minimal quantities in System 2 reservoir waters. Only traces of this compound were found in System 1 and Control reservoir waters. Various dicarboxylic acid compounds are known to be metabolic products in the degradation pathway for fluorene, phenanthrene, and fluoranthene [39, 377]. Nevertheless, this particular compound does not seem to appear in the literature except with respect to photooxidation of phenanthrene in the presence of titanium dioxide [378], which does not seem likely, despite average levels of titanium being present in the soil. Terephthalic acid, which was present in all reservoir samples, was present in double the concentration in System 1 than in System 2 or the Control which were relatively comparable to each other. No indication of terephthalic acid was found in the literature as a degradation product of any of the PAH compounds and thus its source is unknown and may have been an undetected soil impurity.

Benzoic acid, 4-ethoxy-ethyl ester was seen in very low levels (0.003-0.1% total makeup) in System 2 and Control soils but not in System 1. One of the two extractions for System 2 soil found a peak with RT of 21.06 that best matches p-terphenyl (86% match that was not found in any other samples and was present in noticeable concentrations (0.729%). Compounds observed in the soil that were assumed not be impurities were found in all three Systems and included the following: Benzoic acid, ethyl ester (0.2-0.5%);), two similar compounds with primary peak 228, possibly identified as benz[a]anthracene and triphenylene (this was also found in pre-experimental spiked soil after several months and may be either an undetected impurity or a non-biological degradation product); three compounds with primary peak 252 (RT 26.79, 26.30, 26.40) which most closely resembled perylene, although poorly. 9-fluorenone (specifically 9H-Fluoren-9-one) was detected in most samples but was confirmed to be an impurity of the fluorene initially added. Concentrations of this compound varied but did not suggest their presence as a metabolite due to their very small peak areas relative to the fluorene and the absence of 9-hydroxyfluorene, and 1-indanone, which are noted to be concurrent metabolites [372].

6.5.4 Monitoring of Conductivity and Salinity

In this and previous studies, the observation that the salinity increased mildly over time was noted, largely due to evaporation. Initial values were measured at 1.1 g/L yet trended near or slightly above 2 g/L by the end of the experiment. Much of the increase was attributed to the addition of a highly concentrated buffer (1M), with added to the salinity primarily via the contribution of potassium ions. The meter and probe used to measure salinity and conductivity values determined the salinity based upon the conductivity relative to the temperature, and thus the salinity was a function of all salts that contribute

conductivity, including the potassium added from the buffer. The rise in conductivity of lead to values between 3000-4500 µS/cm, although the values fluctuated without a regular pattern due to changing variable within the systems.

In the Control, the addition of sodium azide, due to the presence of the sodium, increased the salinity further towards values of 2-2.5 g/L and ultimately peaked at 3.7 g/L before beginning to slightly decline. The corresponding increase in conductivity initially lead to values between 4200-4800 µS/cm but rose to over 6000 µS/cm upon the addition of the buffer. Towards the end of the experiment (days 44-60), the conductivity began to decrease yet still elevated in comparison to Systems 1 and 2, with values near 5000 µS/cm (Figure 6.8).

6.5.5 pH And Polarity Reversal

One of the key difficulties in maintaining an electrokinetic system is keeping the pH balanced. Electrolysis creates extreme pH shifts in a very short time frame. The second addition of phosphate buffer mitigated the pH shift effect, but polarity reversal was still needed. Additionally, a decreasing effectiveness of the buffer was observed in the biological systems, likely indicating consumption by the microorganisms present. This is important to take into consideration when utilizing electrokinetics in field studies or other in-situ remediation projects. A series of overlapping or rotating electrodes may prove to be most effective [379], nonetheless the use of buffers is still a beneficial option.

Additional increases in salinity and conductivity in the Control system were expected, but prior to this experiment, increases in pH due to sodium azide were not foreseen. Researching pertaining to this matter is extremely limited but a paper by Rozycki and Bartha [374] indicates that the addition of sodium azide to soil can greatly increase the

soil's pH, and presumably this could be true in other media as well. This is echoed in a recently published paper by Lees et al.[380].

6.6 Conclusion

This experiment demonstrated the possibility that electrokinetic technology may effectively enhance biodegradation rates of fluorene, phenanthrene, and fluoranthene, although the extent of effectiveness and a confirmation of its occurrence at all could not be determined. This experiment also highlighted the difficulties of trying to emulate electrokinetic technology in a laboratory setting rather than an in-situ setting. Perhaps more questions were yielded from the experiment than satisfactory answers, but it adds much investigative potential for future work, including the study of pH gradients and changes in microbial communities.

CHAPTER 7

SURFACTANT-ENHANCED BIODEGRADATION OF LOW MOLECULAR WEIGHT PAHs BY ELECTROKINETICS

7.1 Background

The success of electrokinetic technology can often be limited for strongly recalcitrant compounds such as PAHs [13]. The addition of surfactants such as Brij 35 has been shown to be enhance the bioavailability of PAHs to the degrading microorganisms [88]. Brij 35 and similar non-ionic surfactants can not only increased biodegradation rates but also reduce the time of biodegradation (mineralization) [87]. Nonionic surfactants, such as Brij, are often utilized as they are less toxic to organisms than cationic or anionic surfactants [85]. An additional benefit of the use of surfactants is that is resolves the issue of microbes tending to attach to sediment and organic matter particles (which can reduce bacterial transport) [57]. Yet, surfactant efficiency for the desorption of PAHs is highly dependent upon soil composition, PAH properties, and the surfactant's structure [96].

Due to complications and possible lack of success in the first biodegradation experiment (Chapter 6), the experiment was repeated, this time also utilizing the addition of the Brij 35 surfactant.

7.2 Materials and Methods

The same three electrokinetic apparatuses used in the previous biodegradation experiment (Chapter 6) and the dye migration experiments (Chapters 4-5) were used in this experiment. Electrodes were 30 cm graphite rods with a 0.63 cm diameter. Power Supply was a commercial 30V output with a measured 7.05 ± 0.01 mA current output. The voltage

gradient was 0.67 V/cm and the current density was calculated to be .040 mA/cm^2. A separate power supply was used for each system.

7.2.1 Soil Sampling

Soil used in this experiment was taken from the grounds of an NJIT construction site and was found to be similar in nature to the soil used in the previous biodegradation experiment (Chapter 6) with the exception of the moisture content. The soil was analyzed via ASTM method D2487 and found to be either SW-MC or SW-SC (Well-graded sand with silt and/or clay). Grain size ranged from 0.08 – 8 mm and the moisture content was 9.02 ± 0.07 % (w/w). The pH of the soil was approximately 7.98 and the density was found to be 1.17 ± 0.01 kg/L. Soil was collected about a month prior to initiation of the study and was stored at room temperature until commencement of experiment. Soil was analyzed via GC-MS (gas chromatograph with mass spectrometry) to ensure no background levels of any relevant contaminants. A Most Probable Number (MPN) procedure (Wrenn, 2012) was used to verify the presence of alkane-degrading and PAH-degrading bacteria prior to the onset of the experiment. Background metal and some nutrient measurements of the soil were measured via XRF and it was found to be fairly representative of an urban soil. No inhibitory levels of any metals were found (Table 7.1). All large and obvious stones were removed prior to the performance of all tests.

Table 7.1 Soil Properties

Density (kg/L)	pH	Moisture Content	Arsenic (ppm)	Cadmium	Lead (ppm)	Cobalt (ppm)	Copper (ppm)
1.17 ± 0.01	7.98	9.02 ± 0.07%	ND	ND	104.10 ± 3.82	ND	1.15 ± 31.15

ND = Not Detected

7.2.2 Soil Spiking Setup

7.2.2.1 Preparation of Soil. The inner chamber of each EK apparatus was measured to be approximately 2L by volume. Density was determined to be 1.17 ± 0.01 kg/L and therefore 2.34 kg of soil was to be added to each system. Accordingly, for three apparatuses (duplicates plus control), 6L of soil, or 7.02 kg was needed. 10 kg of spiked soil was prepared as a contingency.

7.2.2.2 Preparation of PAH Mixture. A stock solution of fluorene, phenanthrene, and fluoranthene in methanol was prepared in order to yield a final concentration of 100 mg/kg of each PAH compound in the soil. The resultant concentration was 117 ± 2 mg/L of each PAH compound per system soil.

7.2.2.3 Spiking of Soil. 10 kg of soil was weighed out weighted out on an industrial scale after passing through a 12.5 mm sieve and placed within a 5-gallon (18.93 L) plastic bucket. The PAH solution was poured carefully atop the soil and mixed immediately with a Nordstrand PWTPM01 Pro Mixer Stirring Tool and 140mm mixing paddle for 5 minutes. Soil was allowed to air dry for about 24 hours to let the methanol evaporate.

7.2.3 Nutrient Medium

3L of Bushnell-Haas (B-H) medium was prepared in a 5L Erlenmeyer flask by dissolving the dry medium obtained from Difco Products (Detroit, MI) in deionized medium according to the manufacturer's instructions. 0.6 g of yeast extract was added. The solution was stirred and heated until all particulates dissolved.

7.2.4 Buffer Solution

1.5 L of 1M potassium phosphate buffer (pH 7.6) was created to be added to each reservoir to help mitigate extreme pH gradients formed during the electrolytic process.

7.2.5 Sodium Azide

A solution of sodium azide (NaN_3) was prepared for use a biocide in the control system. The desired concentration was 5 g/L in the soil and therefore 10g of sodium azide dissolved in 300 mL of de-ionized water was prepared to be added to the soil. A sodium azide solution was not prepared for the reservoir but rather the powder was added directly to the reservoir liquid.

7.2.6 Filling Method

The soil was poured carefully via a funnel into the bridge areas of each EK system and filled until a predetermined 2L fill line. Soil was pressed lightly to ensure uniformity. In all systems, both reservoirs were filled with a 1 g/L NaCl solution up to the bottom of the soil level prior to the addition of the soil. The NaCl solution was created by dissolving 1g of NaCl granulated power in de-ionized water for each L of water needed (created in 20 L batches). The final 1 g/L NaCl solution was found to have following characteristics: Conductivity was reported to be 2100 ± 100 µS/cm and the salinity was 1.0 ± 0.1 g/L.

When the reservoirs of each system were approximately half-filled, 500 mL of the nutrient medium and 250 mL of 1M phosphate buffer (pH 7.6) were added to each reservoir. To maintain uniformity, buffer and nutrient medium were also added to the control system. A metal rod was used to mix thoroughly but briefly. Additional 1 g/L NaCl solution was then added to each reservoir of all systems to bring the liquid levels just above the soil surface levels. The liquid was then allowed to infiltrate into the soil and a slight

additional amount of 1 g/L NaCl was added to reestablish the liquid level just above the soil surface.

In the control system, the sodium azide solution was poured gently into the soil area and allowed to infiltrate. 52.7 g of sodium azide was then added to each control reservoir and stirred briefly. (For a reservoir fill volume of about 19.7 L, this yields a concentration of approximately 2.7 g NaN_3/L.) In all reservoirs, 10 g/L of Brij-35 (19.05 mL at a density of 1.05 g/mL) was added to the soil via injection by a 10 mL syringe and fine-tipped needle. Brij-35 was injected on the anodic side 4 cm from the edge and at approximately a 2/3 depth. The lids with electrodes were then placed atop the reservoirs and the system was allowed to settle overnight.

7.2.7 Extractions and Analysis

All systems liquids were taken from each reservoir and stored separately for analysis. Liquid was removed to well beneath soil level and the soil was then carefully removed from the inner part of each system and stored in glass jars other than those set aside for immediate analysis and stored initially at 4°C and then -12°C. For analysis, approximately 75g of soil in duplicate was taken from each system and placed within Thermo Scientific™ Centrifugation Polypropylene Bio-Bottles. Soil extraction was performed based upon a modified version of Khodadoust et al. [368] with the following steps:

For each system's soil, the soil was mixed thoroughly with a metal spatula and spoon for about five minutes. It was then sampled at various locations to collect approximately 75g of sample. (Each sample's exact weight was noted and factored into the recovery calculations.) The sample from multiple locations was performed in order to achieve a more representative sample of the final soil's concentrations. The initial

extraction solvent was comprised of 85% Ethyl alcohol (Fisher Scientific®, ACS Grade (200 proof), 10% de-ionized water, and 5% Methanol (Fisher Scientific® ACS Grade, 99.8% Purity). Solvent was added to soil in a 1:4 mL ratio, or 300 mL total per soil sample. The mixture was shaken on a MaxQ 2000 orbital shaker (ThermoFisher®) for 24h at intermittent speeds between 150-200 rpm, with an average speed of 175 rpm. The mixture was then centrifuged at 2600g for 30 minutes (ThermoFisher® ST16 Model) and the supernatant set aside. After adding 200 mL more solvent mixture, the same procedure repeated with the exception of a duration of 1h on the orbital shaker rather than 24h. Based upon recoveries, a third extraction was not deemed necessary. Each extraction liquid was stored separately.

In order to prepare samples for GC-MS (gas chromatograph with mass spectrometry) analysis, the extraction liquid necessitated a second extraction into a more appropriate solvent and to remove the presence of water from the sample. A modified version of EPA Method 3510C (liquid-liquid extraction), utilizing hexane rather than methylene chloride was performed, and all sets of extract were set aside for analysis. A vigorous rinse with de-ionized water (3.5 L per system) was performed to remove additional soil particles adhering to the acrylic surface and any residues in the reservoir chambers. This liquid was stored separately for each system for analysis and analyzed via the liquid-liquid extraction method mentioned above. The results from the prior experiment (Chapter 6) indicated that much of the PAH balance may have adhered to the acrylic surface and therefore a solvent rinse of each system was required. For each system, 1L (approximately 850 mL total volume) of hexane was applied upon all inner surfaces of the apparatus, with particular focus upon the inner bridge chamber where the soil was

located. The hexane rinse was collected and stored in 1L vapor-tight glass bottles. A liquid-liquid extraction (identical to above) was then performed on each rinse sample. A Gas Chromatograph equipped with Mass Spectrometry (GC-MS) was used for the quantification of the three parent PAH compounds (fluorene, phenanthrene, and fluoranthene) and qualification of any metabolites. The column used was a SPB-5 30m x 0.53mm x 1.5 um Film Thickness. Inlet flow rate set at 55.2 mL/min, Column flow rate at 1.8 mL/min, Helium carrier and makeup. Oven: Temp 1 = 70°C, (4 min), Temp 2 = 300°C (23 min), Rate 1 = 10°C/min, hold at 300°C (10 min). Injector Temp = 300°C, Detector Temp = 320°C, Splitless.

In order to verify proper performance of the GC-MS, a stock solution of all three PAH compounds was created at a concentration of 50 mg/L. Accounting for impurities, the GC-MS results yielded 49.8 mg/L for fluorene, 47.4 mg/L for phenanthrene, and 47.9 mg/L for fluoranthene. A mock extraction of the spiked soil with identical extraction procedure was performed and the PAH recoveries were: 79.09 ± 7.73 % for fluorene, 90.39 ± 4.48% for phenanthrene, and 81.63 ± 2.28% for fluoranthene.

7.3 Measurements

pH measurements for the large setups were conducted using the AquaShock pH meter (Sper Scientific®, Scottsdale, AZ, USA) and probe at two locations in each reservoir. One measurement was taken at the front corner, farthest away from the bridge of the apparatus and the other measurement was taken immediately adjacent to the beginning of the bridge, near the location of the electrode (see Figure 4.2). Voltage and current were measured using the EX330 Multimeter (Extech® Instruments, Waltham, MA, USA) and measured with each probe at opposite reservoir ends at about a mid-way depth. Salinity, conductivity, and

temperature were measured using the YSI® Model 30 Salinity/ Conductivity/ Temperature meter (YSI Incorporated, Yellow Springs, OH, USA) with accompanying probe and was measured in the center of each reservoir at about a mid-way depth.

7.4 Results

7.4.1 PAH Recovery and Degradation Rates

In comparison, to the earlier similar experiment (Chapter 6), a decent PAH yield was recovered in this experiment (Table 7.2). A major difference between the two experiments was the relative similarity between the biological systems and the Control, indicating a lack of biodegradation. The recovery for System 1 was 57.92 ± 7.64%, 78.15 ± 10.90%, and 75.77 ± 9.35% for fluorene, phenanthrene, and fluoranthene, respectively. System had slightly lower recoveries reported as 47.61 ± 1.32%, 65.06 ± 2.04%, and 62.29 ± 1.66% for fluorene, phenanthrene, and fluoranthene, respectively. In comparison, the Control yielded even lower PAH levels, with a recovery of 39.30 ± 0.21%, 55.33 ± 1.02%, and 55.26 ± 0.12% for fluorene, phenanthrene, and fluoranthene, respectively (Figure 7.1).

The rinses of each System with water and solvent (hexane) are reported in Table 7.2 and although a small contributor to the total, the amount recovered from the rinses was not insignificant (Figure 7.2). Maximum contribution of the rinses was 1.93% and 4.42% of the total amount recovered for the water and solvent rinses respectively. No metabolites could be detected in any of the extraction samples, and the only few notable peaks detected other than the parent PAH compounds were typical organic compounds found in soil and plant matter.

7.4.2 Changes over Time

When initially pouring the liquid into reservoirs, as well as when adding additional water to the systems, some soil particulates were flushed out into the reservoir liquids. For the Biological systems, this initially gave the reservoirs a brownish color but quickly became an opaque black as biological activity increased. In the control, only minimal soil was flushed into the reservoirs during the initial fill and the reservoirs remained relatively clear up until several weeks into the duration of the experiment where the pouring of additional water inadvertently stirred up soil and the reservoirs became a brownish color. Most instances after this point when water was added to the Control system, the color in the reservoir became darker until it was nearly black and relatively opaque by the end of the experiment. There were black-colored pools atop the middle of the soil, indication that the source of the black-like color was in fact from the soil. Despite similarities in the ultimately appears of the reservoirs, the Control system has no indication of any biofilm or any semblance of biological activity, whereas the blacked color that appeared in Systems 1 and 2 was apparent earlier and across the entire soil in a thicker form (in comparison to the blackened area atop the soil in the Control which was only located in the middle, had no solidity, and appeared at a much later time). Additionally, no white precipitate was observed in any system in contrast to the previous experiment (Figure 6.4).

Table 7.2 PAH Recovery Values

FLUORENE	**% Total Recovery**		**% Recovery from Water Rinse**	**% Recovery from Solvent Rinse**	
	Avg	St Dev	Avg	Avg	St Dev
Test Extraction	79.09%	7.73%	N/A	N/A	N/A
Ctrl	39.30%	0.21%	0.37%	1.48%	0.02%
Sys 1	57.92%	7.64%	1.10%	1.45%	0.04%
Sys 2	47.61%	1.32%	0.25%	1.61%	0.01%
PHENANTHRENE	**% Total Recovery**		**% Recovery from Water Rinse**	**% Recovery from Solvent Rinse**	
	Avg	St Dev	Avg	Avg	St Dev
Test Extraction	90.39%	4.48%	N/A	N/A	N/A
Ctrl	55.33%	1.02%	0.46%	1.94%	0.09%
Sys 1	78.15%	10.90%	0.75%	1.64%	0.07%
Sys 2	65.06%	2.04%	0.24%	1.55%	0.03%
FLUORANTHENE	**% Total Recovery**		**% Recovery from Water Rinse**	**% Recovery from Solvent Rinse**	
	Avg	St Dev	Avg	Avg	St Dev
Test Extraction	81.63%	2.28%	N/A	N/A	N/A
Ctrl	55.26%	0.12%	0.11%	2.44%	0.03%
Sys 1	75.77%	9.35%	0.37%	1.29%	0.02%
Sys 2	62.29%	1.66%	0.10%	1.08%	0.00%

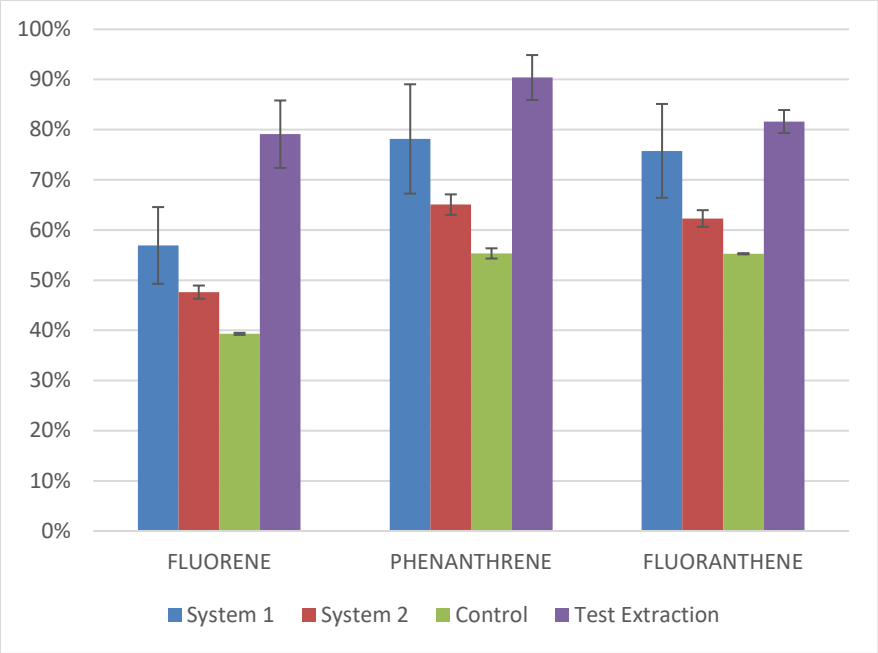

Figure 7.1 Extraction yield comparisons for three PAH compounds.

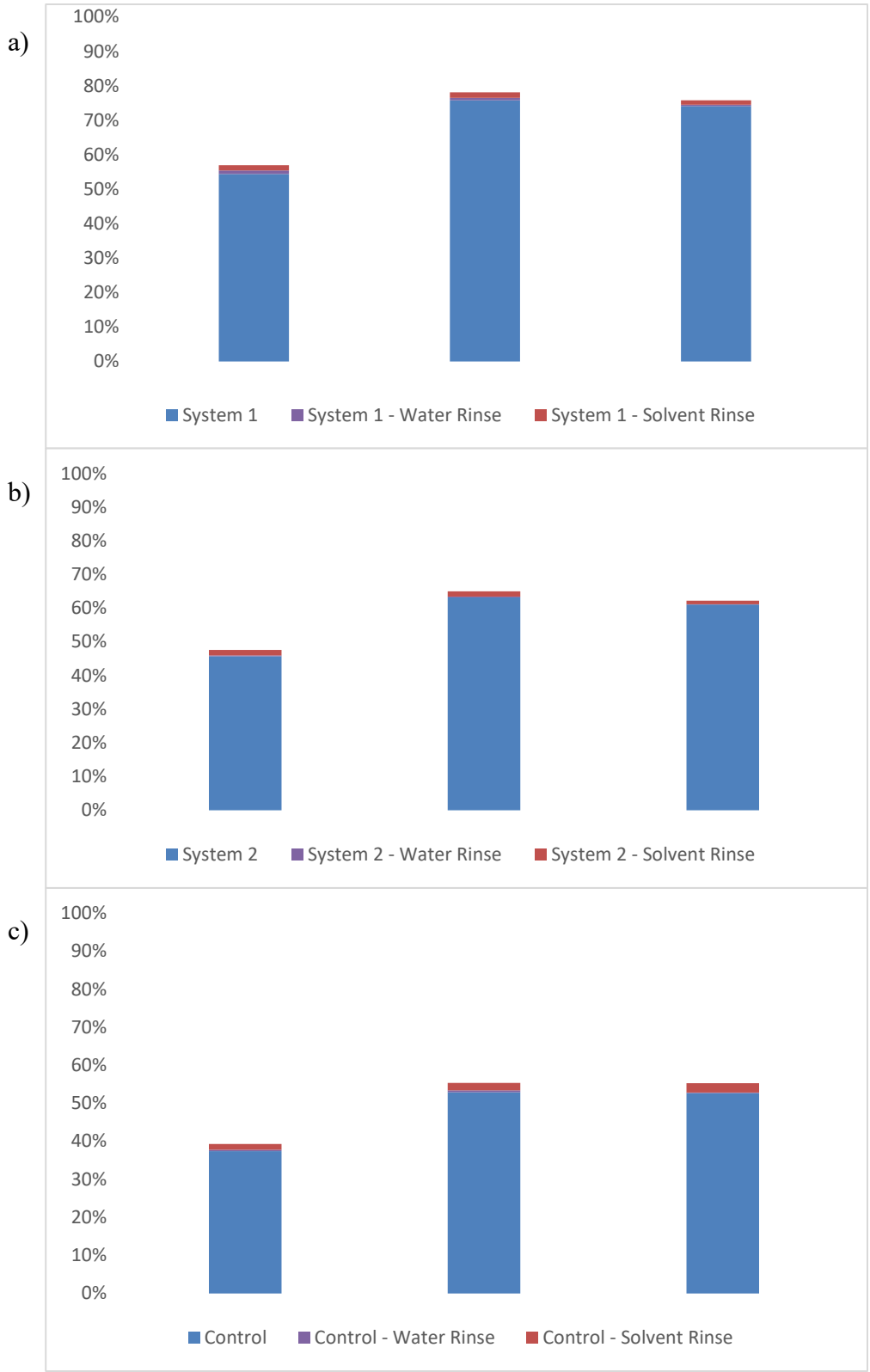

Figure 7.2 Relative percent yield from rinses for the three PAH compounds. a) System 1 ; b) System 2; c) Control

On Day 4 of the experiment, strong biological activity was seen in both System 1 and System 2 and there was no indication of any biological activity in the Control, which appeared exactly the same as it did just following the onset of the experiment. System 1's left reservoir (functioning as the anode) appeared stratified, with the top half of the liquid a pale brown and bottom half relatively colorless (Figure 7.3a). System 1's right reservoir (functioning as the cathode) had a yellowish color, was a bit cloudy and had a thin film on the liquid surface (Figure 7.3a). Numerous film-pockets were noted in this reservoir, seemingly of a biological nature and with the appearance of portions of a plastic bag (not shown). Both System 2 reservoirs appeared relatively identical, with a pale-yellow color and of a very cloudy nature (Figure 7.3b). Many biofilm pieces were seen floating both in and atop the reservoir liquids.

In both Systems 1 and 2, a white mucousy layer, assumed to the beginning of a biofilm was seen atop the soil (Figure 7.4), although this was more pronounced in System 1. The Control system (Figure 7.5a) did not have any layer apparent on its soil surface (Figure 7.5b). As seen in previous experiments, the addition of sodium azide created an increase in conductivity of the Control system (see Section 5.5) and a turbulent stream of bubbles was generated on both electrodes but was more pronounced on the left (anodic) electrode (Figure 7.6a). As this side was proximal to the area where the surfactant (Brij-35) was inserted, a thick sudsy blanket began to appear atop the reservoir liquid (Figure 7.6b). Over the next several days, this soapy foam grew but diminished when polarity was then reversed.

a)

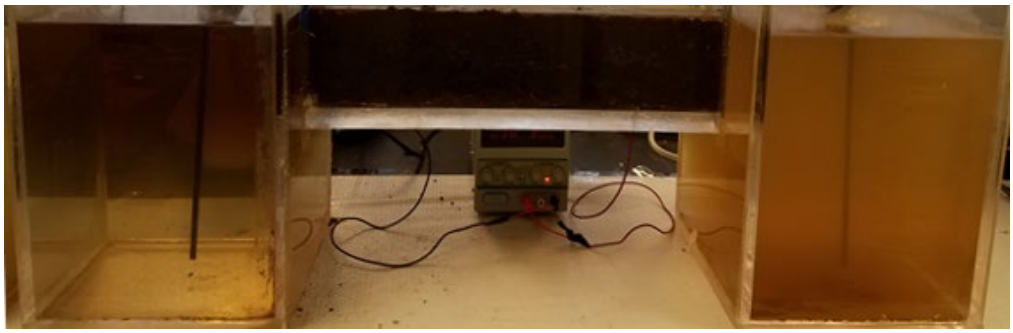

b)

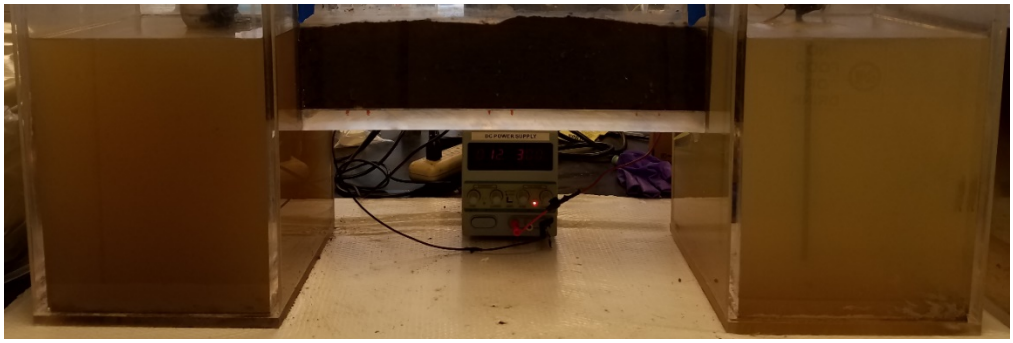

Figure 7.3 Images at Day 4. a) System 1 ; b) System 2

Figure 7.4 Close-up image of the mucousy layer that appeared atop the soil in Systems 1 and 2.

a) 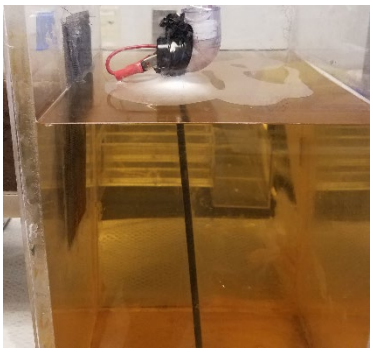 b) 

Figure 7.5 Images of Control system at Day 4 . a) Reservoir ; b) Soil

a) 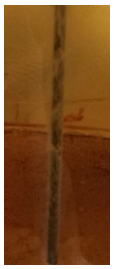 b) 

Figure 7.6 Influences of Increased Current in Control system (Day 4). a) Increased electrolysis (seen on electrode) ; b) Foam generated by agitation of surfactant

On Day 6, the biofilm began to take on a modified appearance in System 1 and grew thicker in System 2. No change in the Control was observed. As pH values began reaching extreme values, a polarity reversal of all systems was performed (see Section 7.4.4). On Day 8, System 1's left reservoir (now functioning as the cathode) had a thick biofilm on its surface and a greater presence of the plastic-resembling film-pockets than noted earlier. Stratification was again noticed, with the upper portion a medium brown and the lower portion a brownish yellow color. There was a slightly opacity seen in this reservoir and a small amount of soapy foam was noted on top of the reservoir liquid, indicating some leaching of the surfactant, an expected occurrence. System 1's right

reservoir (now functioning as the anode) took on a strong black appearance and was fairly opaque but without a biofilm presence seen on the liquid surface. A thin, solid biofilm was still present atop System 1's soil as the water level began to diminish (due to unavoidable evaporation and electrolysis) and just barely reached above the soil. System 2's left reservoir appeared brown and very cloudy with a thin biofilm covering all of its surface, the right reservoir was fairly cloudy a had blackish tint which a thicker biofilm on its surface. No noticeable changes in the Control were observed other than a lesser presence of surfactant-related foam.

On Day 11, both of System 1's reservoirs were fully black. The left reservoir was opaque other than the bottom third and there was a moderate biofilm on the liquid surface. System 1's right reservoir was essentially fully opaque with no noticeable biofilm on its surface. The biofilm atop the soil was somewhat thinner than observed on Day 8 as the water level diminished slightly. System 2's left reservoir was brown in appearance and very cloudy with a thin biofilm on most of its surface. The right reservoir had a far thicker biofilm, and its color was black and mostly opaque. No biofilm was seen on the soil as the water level dropped just below the soil surface. The only notable change in the Control, other than slightly lower water levels was a darker tint to the right reservoir and the appearance of some soapy foam on its surface.

On Day 14, A small amount of soapy foam was seen in System 1's reservoir but the gaseous foam (as seen in Figure 6.5), to hereby be designated as "biological foam", was noted in the right reservoir. Both reservoirs were now fully black and opaque and remained so until the end of the experiment. A light-to-medium biofilm was seen atop both reservoirs. System 2's left was brown but with a grayish tint (possibly due to a piece

of corroded alligator clip that fell to the bottom of the reservoir which had disintegrated). A medium biofilm was apparent atop the reservoir and a large quantity of biofilm pieces were observed throughout the reservoir. The right reservoir contained an ample but slightly thinner biofilm and moderate biofilm pieces. No chance in the Control was observed other than a slightly darker appearance to the right reservoir. Water levels in System 2 had dropped to a point where it necessitated more be required. Although having dropped from its initial point, it was determined that it was not quite yet necessary to add water to System 1 (water was later added on Day 18). 4L of de-ionized water was added to System 2, but due to a noted salinity imbalance, all water was added to the left reservoir (which has a higher salinity) and allowed to flow into the right reservoir. 1.3L of de-ionized water was added to each reservoir of the Control system (2.6 L total) in order to reach identical levels to Systems 1 and 2. Reservoir lids were then sealed with packaging tape and in the bridge area, a silicon sealant was used so as to reduce the evaporation rate occurring.

On Day 18, Systems 1 and 2, for the past week had a strong garbage-like odor emanating from the reservoirs when opened for measurements. This odor now resembled a sewage-like smell. Only a minor biofilm was seen on the surface of both System 1 reservoir but there were many biofilm pieces apparent within the reservoir. No more biofilm was seen atop the soil and the water level had decreased slightly since Day 14 and thus it was deemed necessary to add 0.8L of de-ionized water to each reservoir of System 1. System 2's left reservoir was highly cloudy but still not fully opaque. Color was a medium-dark brown rather than black and there was a light biofilm on the reservoir surface with a moderate amount of biofilm pieces within. The right reservoir had a thick, well-formed biofilm on its surface and the reservoir was fully black and opaque (it remained so

for the duration of the experiment). The appearance of the Control, since the addition of water, had changed. The left reservoir now appeared a dark brown (semi-opaque) and many microbubbles were seen within the reservoir liquid. A moderately thick soapy foam was seen on top of the reservoir liquid. The right reservoir appeared nearly identical to that of Day 14, except minimally darker. No changes in water level for System 2 or the Control were noticed.

On Day 20, both reservoirs of System 1 had both types of foam (soapy, biological) present on their surface with a very thin biofilm on both surfaces. System 2's left reservoir was darker than on Day 18 but still not fully black. A light biofilm covered half of its surface. In contrast, the right reservoir had a very thick biofilm as well as some foam (both types) and appeared very similar to System 1's reservoirs. Control's left reservoir became a darker brown and grew more opaque, a medium soapy blanket was seen atop the reservoir. The right reservoir appeared identical to Day 18.

On Day 22, no significant change was seen in System 1 or System 2since Day 20 other than a decrease in the amount of foam (both types). No notable changes to the Control. On Day 25, both System 1 reservoirs still had a light biofilm but now only on parts of the surfaces and the water level in the System had greatly decreased. Despite the lack of a strong biofilm atop the reservoirs, the reservoir liquid had a greater presence of biofilm pieces. Additionally, no odor was detected. System 2's left reservoir now appeared fully opaque and almost black but with a brownish tint. A moderate biofilm was seen on its surface. The right reservoir also had a moderate biofilm covering most of the surface, in contrast to Day 22, on which a thick biofilm and full surface coverage was observed. The water level in System 2 had also diminished significantly but not quite to

the extent of System 1. A strong sewage-like odor was detected. Control's left reservoir was now fully opaque (dark brown) and no change was noted for the right reservoir. Some water loss was detected. More de-ionized water was needed in each system: 1.95 L was added to each reservoir of System 1, 2.4 L and 1.25 L was added to System 2's left and right reservoir, respectively (salinity imbalance still noted), and 1 L and 1.4 L was added to the Control's left and right reservoirs, respectfully (slight salinity imbalance).

On Day 28, only traces of the biofilm remained in either System 1 reservoir with very few notable biofilm pieces. No odor was apparent. Both System 2 reservoirs had a light-to-moderate biofilm with a moderate amount of biofilm pieces. Strong odor still apparent. Right reservoir of the Control now also dark brown and fairly opaque. Soapy foam still present on both reservoirs. On Day 32, System 1 had only faint traces of the biofilm on its surfaces and very few biofilm pieces were apparent. Water level had diminished slightly in all reservoir but was slightly lower in system 1 than in other systems. System 2's left reservoir had a moderate biofilm covering half of the surface but with a different appearance that on prior days. Many biofilm pieces were observed in the reservoir. The right reservoir had a moderate-to-thick biofilm on most of its surface but fewer biofilm pieces. Only the right reservoir was odorous and less pungent than on previous days. No significant change was noted in the Control. The addition of more de-ionized water in each system was needed: 1.4 L was added to each reservoir of System 1, 2 L was added to System 2's left reservoir (no water added to right), (salinity imbalance less but still prominent), and 1 L was added to each reservoir of the Control.

On Day 34, System 1 had no biofilm apparent on either surface, although the right reservoir contained many biofilm pieces as well as some biological foam on its surface.

System 2 had no significant changes in appearance since Day 32 other than some biological foam. No change was observed in the Control other than a slightly darker appearance in the left reservoir. On Day 36, Systems 1 and 2 appeared identical to Day 34. Control was identical other than the presence of increased (soapy) foam.

On Day 39, some biofilm re-appeared on the surfaces, scattered and thin on the right reservoir and minimal traces on the left reservoir. Some soapy foam was seen in the left reservoir, but none appeared in the right reservoir. Water level had dropped significantly (about 1.5 cm below soil). System 2's left reservoir had a light-to-moderate biofilm covering most of its surface, and the right reservoir had a slightly thicker biofilm on most of its surface. Odor was no longer apparent in either reservoir. Moderate biofilm pieces were seen in the left reservoir, fewer in the right. Water level had diminished but to a lesser extent than in System 1. No changes were observed in the Control. The addition of more de-ionized water in each system was needed: 1.8 L and 1.2 L was added to System 1's left and right reservoirs, respectively, 1.9 L and 1.1 L was added to System 2's left and right reservoirs, respectively, 0.525 L and 0.725 L was added to the Control's left and right reservoirs, respectfully.

On Day 42, all traces of surface biofilm in System 1 had disappeared, although moderate biofilm pieces were noted in the left reservoir and few in the right reservoir. A small amount soapy foam was observed in the right reservoir. System 2 had a very light biofilm on only a small portion of each reservoir's surface. This system was once again odorous but to a lesser extent than previously and predominant in the right reservoir. Both Control reservoirs were now slightly darker due to some soil flushing that occurred in the last water addition. On Day 46, System 1 had no observable biofilm on its surface, no

biofilm pieces in the left reservoir and very few in the right reservoir. In addition, the water level had dropped again considerably. System 2 had a trace of biofilm scattered along both reservoir surfaces. Very few biofilm pieces were noted in the left reservoir, but many were seen in the right. Water level had also diminished but to lesser extent than System 1. Both reservoirs of the Control were now fully dark brown and opaque and water levels were slightly diminished. (The higher rate of water loss was likely to due to increased evaporation, as the temperature in the laboratory was several degrees warmer.) Additional de-ionized water was added to each system as follows: 3 L was added to System 1, only in the right reservoir (new salinity imbalance), 1.4 L was added to each reservoir in System 2 (salinity imbalance greatly diminished), respectively, 1 L and 0.775 L was added to the Control's left and right reservoirs, respectfully.

On Day 48, a sparse biofilm re-appeared atop the right reservoir liquid, though none was apparent in the left reservoir. No biofilm pieces were seen in the left reservoir and very few in the right. System 2 had a small amount of scattered biofilm atop both reservoirs and both reservoir contained few-to-moderate biofilm pieces. Control reservoirs grew darker still, almost black in appearance and a small amount of black-toned liquid was seen atop the center of the soil, indicating the dark color likely rooted from soil leachate.

On Day 54, both reservoirs of System 1 now had traces of biofilm, yet no biofilm pieces were seen in either. A substantial amount of soapy foam was seen in the left reservoir and some biological foam was seen atop the right reservoir. System 2 had a thin, scattered biofilm atop both reservoirs, although more prominent on the right reservoir. The left reservoir had many biofilm pieces, greater in number than previously noted but smaller in size. The right reservoir's biofilm pieces were also this size but far fewer in number.

Due to air conditioning issues, the temperature in the laboratory was quite warm and therefore, the systems were more prone to evaporation. The water level in systems 1 and 2 had diminished greatly (70% of the soil height). The water level in the Control was less diminished (80% of the soil height) but otherwise no change was observed. Laboratory temperature was. Additional de-ionized water was added to each system as follows: 2 L was added to each reservoir in System 1 (lower salinity imbalance), 2 L and 1.8 L was added to the left and right reservoirs in System 2, respectfully (salinity imbalance again prominent), 2 L and 0.4 L was added to the Control's left and right reservoirs, respectfully (increased salinity imbalance noted).

On Day 56, no biofilm was seen in either System 1 reservoir and no biofilm pieces were observed in the left reservoir and very few in the right. System 2's left reservoir had a light scattered biofilm and only traces of a biofilm atop the right reservoir. Many very small biofilm pieces were observed in both reservoirs. No changes were observed in the Control other than the absence of foam. On Day 59, in System 1, water levels had diminished somewhat but a thick biofilm residue remained where the water level was previously. A thin, scattered biofilm re-appeared in the left reservoir and no biofilm was seen on the right reservoir. No biofilm pieces were observed in the left reservoir, but an abundant amount of small biofilm pieces was seen in the right reservoir. In system 2, a light, scattered biofilm was seen in the right reservoir and only traces were seen in the right. Relatively few biofilm pieces were seen in either reservoir. A small amount of soapy foam was in the left reservoir but only biological foam in the right reservoir. No changes were observed in the Control. On Day 62, at the end of the experiment, a very thin, scattered biofilm reappeared on both reservoir surfaces of System 1 and was the same for System 2.

No changes were observed in the Control. Water levels were diminished to about 75% of the soil heights in Systems 1 and 2 but only marginally (90-95%) in the Control.

7.4.3 Current and Voltage

Current and Voltage throughout all systems remained relatively constant in all systems. A potential of 30V was applied for the entire duration of the experiment to all three systems. At the electrodes, voltages were measured to be 29.44 ± 0.33 V, 29.91 ± 0.19 V, 29.40 ± 0.85 for Systems 1, 2, and Control, respectively. In the reservoirs, minor losses were observed as the voltages measured 27.04 ± 0.16 V, 27.75 ± 0.32 V, 27.44 ± 0.82, for Systems 1, 2, and Control, respectively.

Current was expected to fluctuate but remained relatively stable for the duration of the experiment. At the electrodes, current values were measured to be 7.90 ± 0.04 mA, 7.99 ± 0.08 mA, 7.87 ± 0.22 mA for Systems 1, 2, and Control, respectively. In the reservoirs, measured at the corner farthest from the soil, current values were measured to be 7.06 ± 0.06 mA, 7.26 ± 0.07 mA, 7.16 ± 0.11 mA for Systems 1, 2, and Control, respectively. The power supply utilized for the Control was slightly older than the other two and was more prone to fluctuations in both current and voltage over parts of the duration of the experiment.

7.4.4 pH and other Values

pH values were monitored over time. Previous electrokinetic experiments conducted indicated that extremes as low of 1 and high as 13 could be reached without the addition of a buffer. Phosphate buffer was added to mitigate sharp changes in pH values. It was clearly observed (as was in the previous experiment, see Chapter 6), that effectiveness of the buffer diminished over time in Systems 1 and 2 but not significantly in the Control.

This is assumed to be due to the consumption of the phosphate buffer by the biological organisms present. No buffer consumption seemingly occurred in the Control due to the presence of (increased) sodium azide.

Polarity reversals were conducted at multiple intervals, when pH values were determined to be unfavorable for microbial growth. This technique was employed on Days 6, 18, 28, 35, 42, 48, 54, and 59 as indicated in Figures 7.7 and 7.8. A summary of pH values can be seen in Tables 7.3-7.5.

Table 7.3 Summary of pH Values Reported for System 1

	Left Reservoir (far corner)	Left Reservoir (near soil)	Right Reservoir (near soil)	Right Reservoir (far corner)
Min	3.29*	3.27*	5.50	7.24
Max	11.39	11.49	11.35	11.30
Avg	7.64 ± 1.85	7.71 ± 1.83	8.08 ± 1.69	8.18 ± 1.60

Table 7.4 Summary of pH Values Reported for System 2

	Left Reservoir (far corner)	Left Reservoir (near soil)	Right Reservoir (near soil)	Right Reservoir (far corner)
Min	7.78	7.74	7.27	7.55
Max	10.20	10.11	11.13	10.99
Avg	7.51 ± 0.70	7.43 ± 0.71	8.48 ± 1.53	8.46 ± 1.49

Table 7.5 Summary of pH Values Reported for Control

	Left Reservoir (far corner)	Left Reservoir (near soil)	Right Reservoir (near soil)	Right Reservoir (far corner)
Min	7.41	7.28	7.46	7.46
Max	12.19	12.28	12.90	12.42
Avg	9.99 ± 1.59	10.01 ± 1.64	10.48 ± 1.42	10.53 ± 1.35

**Min values correspond to one incident (day 6). Next Min values were 7.15 (both left reservoir locations).*

For System 1, salinity values ranged from 2.1 to 3.2 g/L with an average value of 2.7 ± 0.3 g/L. For System 2, salinity values ranged from 1.9 to 4.0 g/L with an average value of 2.7 ± 0.5 g/L. For the Control, salinity values ranged from 4.5 to 7.5 g/L with an average value of 5.2 ± 0.5 g/L. Conductivity values for all systems were found to be at consistent relativity to the salinity in a system's reservoir at a given time. For System 1, conductivity values ranged from 3919 to 5870 µS/cm with an average value of 4997 ± 478 µS/cm. For System 2, conductivity values ranged from 3626 to 7170 µS/cm with an average value of 5048 ± 926 µS/cm. For the Control, conductivity values ranged from 8060 to 11440 µS/cm with an average value of 9284 ± 815 µS/cm. The ratio of conductivity-to-salinity was found to be 1865 ± 34, 1868 ± 66, and 1780 ± 17 µS/cm per g/L for Systems 1, 2, and Control, respectively. The meter and probe used to calculate the values based salinity values upon conductivity relative to temperature. As temperature was generally slightly greater in the Control system, the conductivity-to-salinity ratio was not identical to Systems 1 and 2.

As in the previous experiment (Chapter 6), the pH of the Control system initially destabilized following the addition of the buffer and then re-stabilized at an elevated basic pH (9-12) (Figure 7.7c). At this point, not only was the pH elevated but the salinity and conductivity rose greatly as well, although salinity and conductivity rose instantaneously upon the addition of the sodium azide (Figure 7.8 e and f).

7.4.5 Temperature

Temperature was monitored as the electric current was hypothesized to raise a system's overall temperature, however, temperature values did not change significantly during the experiment and any noticeable variations often corresponded to changes in room

temperature. Minor increases were sometimes seen for the Control. The average temperatures measured were 23.1 ± 1.2 °C, 22.8 ± 1.0 °C, and 23.7 ± 0.9 °C, for Systems 1, 2, and Control, respectively, with an overall range of 20.4 – 27.2 °C.

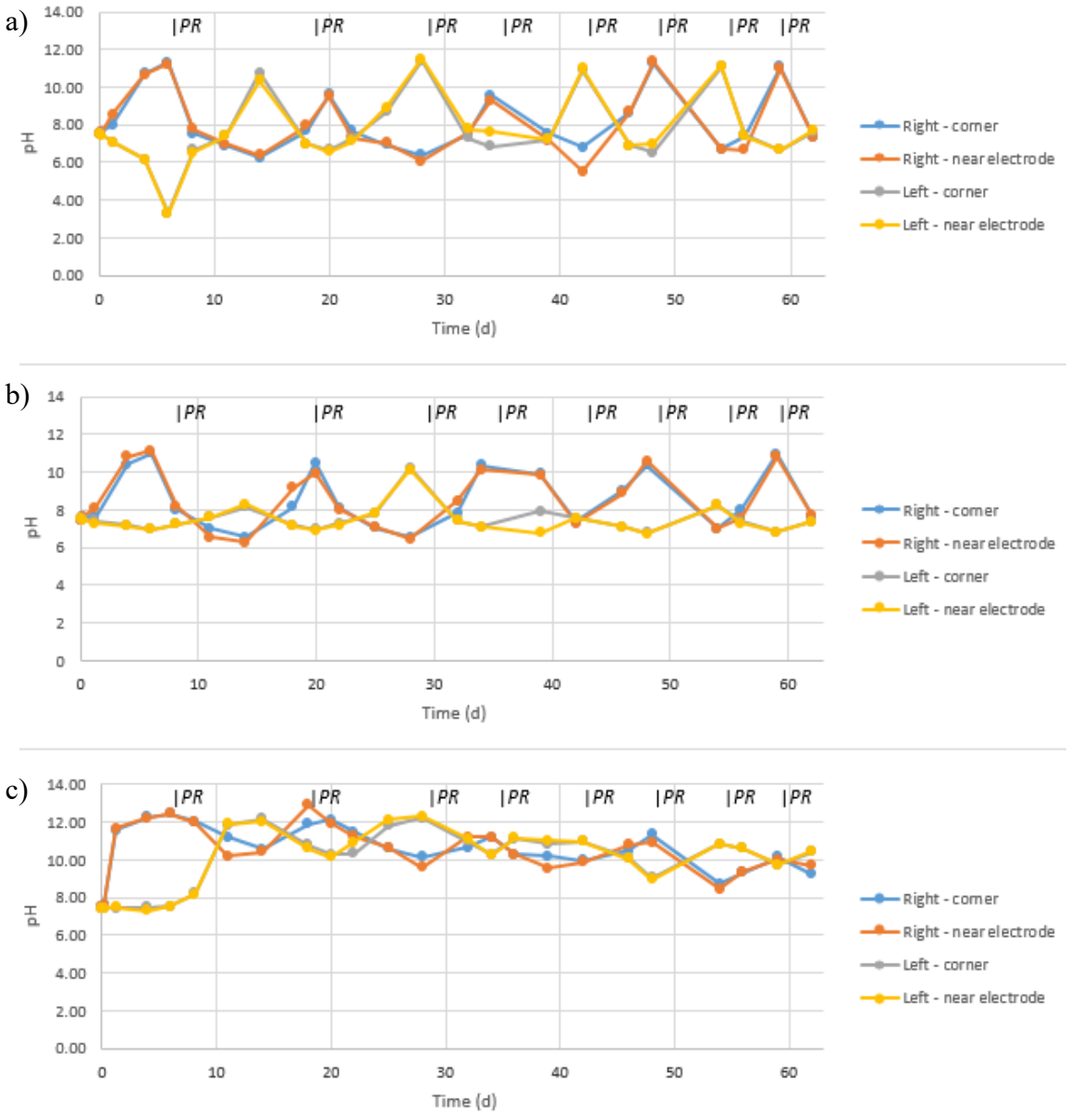

Figure 7.7 Changes in pH Over Time. a) System 1 ; b) System 2 ; c) Control

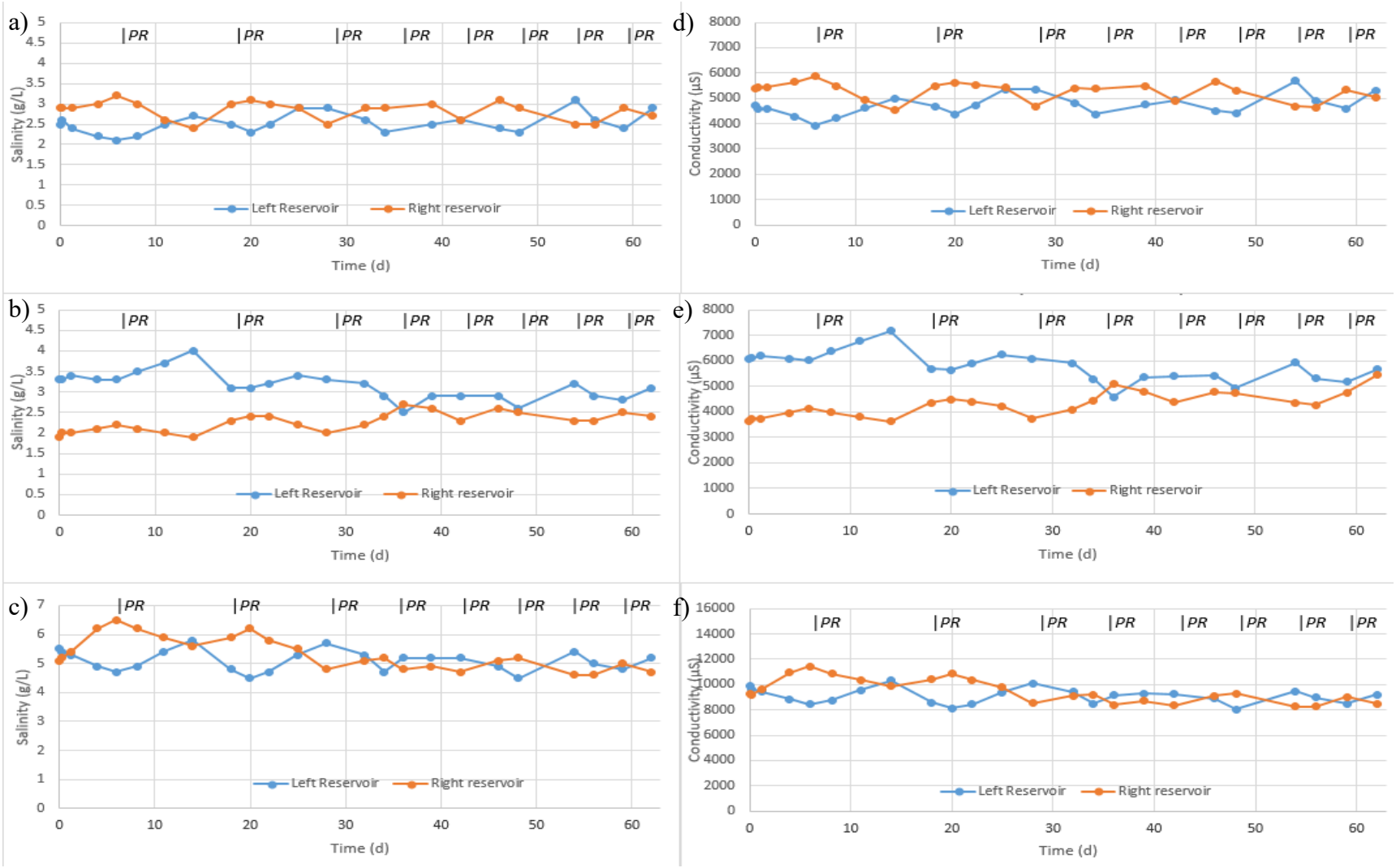

Figure 7.8 Changes in Salinity and Conductivity over Time. a-b) System 1 ; c-d) System 2 ; e-f) Control

7.5 Discussion

7.5.1 Degradation Analysis

Despite much biological activity in the non-control systems no PAH degradation was apparent in this experiment. No metabolites were found in any of the extractions (soil, water rinse, or solvent rinse) for any of the systems. Any non-PAH peaks were fairly small, and all determined to be soil or plant-based and none outstanding with respect to the control were found with the exception of one very small peak in one extraction, which was also a compound found in grass plants (likely from the organic matter in the soil).

It was expected that the addition of the surfactant in this experiment would increase bioavailability and thus biodegradation rates. Though it was not confirmed due to errors present in the Control system, the previous experiment (Chapter 6) indicated that some degradation was occurring using this type of electrokinetic approach, as PAH recovery was less than those reported in the Control (Table 6.2). However, not only did the presence of the surfactant not increase degradation rates, but it may have retarded it. The concentration of Brij 35 utilized in this study was well above the critical micelle concentration (CMC). Numerous studies have shown that Brij-35 levels well above the CMC can be inhibitory towards the biodegradation of PAHs, including phenanthrene [85, 155]. Yet, other studies have shown that many non-ionic surfactants, including Brij 30 and Brij 35 are not only non-inhibitory but can increase PAH degradation, even at levels well above the CMC [87, 88, 381]. Much of the effectiveness seen has been documented for PAHs containing 4 rings or more but this was not exclusive. As a result, many researchers have claimed that there is an inherent contradiction in the literature and that more study is needed to determine in what cases a particular surfactant may be inhibitory [382] [383].

As no metabolites were found and any of the system extractions, it appears as though no degradation occurred. The potential metabolites found in the previous experiment (Section 5.5.3) were not found in this experiment, despite the suggestion that they may have been impurities. The type of soil used in this experiment was similar in nature and sampled from a nearby location to the soil used in the earlier experiment (Chapter 6), although it was not known if the majority of microorganisms present were similar in the two experiments. MPN tests (Figure 7.9) confirmed the presence of PAH degraders in the soil and the abundance of PAH degraders seemingly surpassed those observed in original soil used (Figure 6.9). The presence of heavy biological activity in both Systems 1 and 2 was quite similar in nature to that observed in the initial experiment (Chapter 6) and while this experiment contained yeast extract and thus a carbon source other than the PAHs, the yeast extract was also present in similar concentration in the initial experiments and used when incubating the MPN plates for PAH degraders. Further analysis would be needed to determine if the amount of yeast extract supplied could sustain the amount of biological growth that took place in System 1 and 2, yet it also may be possible, that although no significant amount of carbon-based compounds were detected via GC-MS analysis, that there may have been other carbon-rich compounds (e.g., organic matter) in the soil that was capable of sustaining the biological growth present.

Data collected from the earlier experiment (Chapter 6) found that the Control, while having a higher PAH recovery than the biological systems, had a relatively small overall yield. The disappearance of the majority of the PAH compounds was attributed to biological presence in the Control and possible adsorption to the acrylic surfaces (see Section 5.5). However, neither explanation sufficiently seemed to account for the greatly

diminished yield. In this experiment, though, PAH recoveries were substantial and within target range of the test extraction results (Table 7.2). The rinsing methods contributed no more than 3% of the total yield and therefore it was not clear why recoveries were far stronger in this experiment than in the previous one.

Hypotheses for this include:

- Less or no biological presence in the Control, as a higher dose of sodium azide was implemented, in addition to its injection directly into the soil and not merely the reservoirs.
- The use of the surfactant prevented much adherence to the acrylic, of which the solvent rinse alone would not be sufficient to remove most of the adsorbed PAHs.
- Possible physical and chemical differences in the soil used and hence a greater efficiency of the extraction process.
- A potential loss of PAHs during the mixing phase (prior to addition to EK setups) via undetected residues in mixing containers as this was not measured in the first study.

a) b)

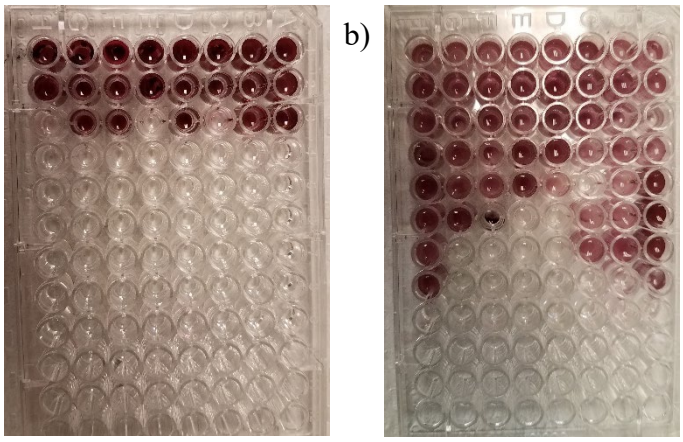

Figure 7.9 MPN Test Showing the Presence of a) Alkane-degrading and b) PAH-degrading microorganisms in the soil prior to the experiment.

7.5.2 Salinity and Conductivity Levels

Fluctuations in salinity and conductivity were expected due to shifts in pH gradients, minor current fluctuations, and evaporation. Water losses in the system yielded a relatively higher amount of salt present per total volume and thus increased salinity and conductivity. Upon the addition of de-ionized water restore levels, these values were once again reduced (see Figure 7.8). Initial salinity levels of System 1 and System 2 were 1 g/L, as the NaCl solution was created in such a concentration prior to the addition of the NaCl solution (i.e., 1 g NaCl per L of de-ionized water). The addition of the potassium phosphate buffer increased the salinity and conductivity more than twofold. The meter and probe used to measure these values determined the salinity based upon the conductivity relative to the temperature, and thus the salinity was a function of all salts that contribute conductivity, and therefore the potassium added from the buffer was incorporated into the salinity measurements.

Additional increases in salinity and conductivity in the Control system were expected as sodium azide contains sodium, a basic contributor to total salinity. Prior to the initial experiment (Chapter 6), however, increases in pH due to sodium azide was not foreseen. Researching pertaining to this matter is extremely limited but a paper by Rozycki and Bartha [374] indicates that the addition of sodium azide to soil can greatly increase the soil's pH, and presumably this could be true in other media as well. This is echoed in a recently published paper by Lees et al.[380]. The former paper also sheds light on the biological activity that was present in the Control in the earlier experiment. Rozycki and Bartha [374] report that the effectiveness of azide as a biocide is reduced as pH increases, and especially under very basic conditions. As the pH of the Control system was elevated

and thus nearly always in the basic range, this implies a possible decreased biocidal effect of the azide chemical.

7.5.3 Biofilm

The appearance of a thick biofilm in Systems 1 and 2, in addition to a quick transformation of the reservoir liquids to an opaque, black appearance, indicate a very strong biological presence. After reaching a maximum thickness mid-way through the experiment (although earlier for System 1), the biofilm became thinner and more sparse over the experiment's duration. It is unclear why biofilm and their respective pieces disappeared and reappeared but was likely a function of stress caused by increasing fluctuations in system variables, primarily pH values. No biofilm or film-like traces were seen in the Control system other than a small area revealed at bottom of the right reservoir upon emptying the apparatus. The minimal size of this area and the lack of noticeably undiminished effect of the buffer indicated that any biological activity would have been likely insignificant. This is despite the uncertainty of how the biological presence in the Control in this experiment compared to the control in the previous experiment (Chapter 6). The use of an MPN or other means of determining biological presence post-experiment was not employed. This was due to time and financial consideration, as it was deemed unnecessary as no degradation seemingly took place in any part of the experiment.

7.5.4 pH And Polarity Reversal

The use of the buffer in this experiment, while initially partially effective, became less effective over time and the use of a polarity reversal was needed increasingly throughout the experiment. The amount of buffer used in this experiment was greater than the amount employed in the previous experiment (Chapter 6) and a greater concentration would

possibly have become detrimental to the system due to increased chemical interactions. Though the use of buffer can slightly mitigate strong pH shifts, in an in-situ environment, a system employing automatic polarity reversals or the use of a series of overlapping or rotating electrodes may prove to be most effective [379].

7.5.5 System Discrepancies

As seen in Table 7.2, the yields of all PAH compounds for all three systems were largely different from one another. The recovery values for System 1 ranged from 72-93% of the test extraction values and two of the three compounds (Phenanthrene, Fluoranthene) fit within the overlap of the test extraction's standard deviations. Minor losses and system variability were expected, and therefore the recovery values for System 2 (assuming no degradation took place) are within reason. Yet, for fluoranthene, the difference in recovery between System 2 and the Control is relatively minor, for fluorene and phenanthrene, it is more pronounced. This is in addition to the fact that for all three PAH compounds, the Control yielded the lowest recovery values. No explanation for this seems logical at first introspection and more analysis may be required in order to determine why precisely this phenomenon took place.

7.6 Conclusion

Despite reports of the use of electrokinetic technology to successfully increase biodegradation rates and capability, the particular design utilized in these experiments (Chapters 6 and 7) was shown not to be effective but the limitation may not have been solely with the design but also the approaches. More study is needed to determine an effective approach that will yield significant degradation and minimize system-based conflicts such as leakages, evaporation, and contaminant adsorption to system surfaces. It

may be necessary to acclimate the soil bacteria to the PAHs prior to this type of study or allow the experiment to run for a much longer duration. MPN tests, which indicated the ability of these organisms to utilize PAHs, has the PAH compounds as the only carbon source other than yeast extract. This is in distinction to the biodegradation study, where a large amount of soil was present containing significant organic matter, and therefore a much more favorable carbon source for the bacteria. With respect to the apparatus used in this study, if future studies will determine a tendency of PAHs to adhere to acrylic surface, an alternative material might be needed such as other hard plastics or borosilicate glass. Additionally, a different material might be needed that would be easier to ensure proper construction, thereby reducing the chance of leakages. An ideal design would consist of interchangeable and quick-assembly parts in order to modify design parameters as well as have the option to install a pumping system, a component present in most successful EK tests in the literature.

The use of electrokinetic technology to promote the growth of microorganisms via nutrient delivery could not be confirmed in this experiment as most biological activity was seen in the reservoirs, in which the nutrient medium was directly added. The effort to improve bioavailability was fully inconclusive as it was unknown as to the reason why biodegradation did not take place. Any additional studies must have greater characterization of the soil, the microorganisms present, and the potential toxicity of Brij 35 towards those microorganisms. Despite the lack of successful biodegradation, other observational data obtained in this experiment may be beneficial for other uses such as pH gradient shift, improvements for future studies, and changes in genomics and population dynamics.

CHAPTER 8

CONCLUSIONS AND FUTURE WORK

8.1 Purpose and Goals

The overarching goal of all research contained within this document is to better understand methods of hydrocarbon remediation, primarily PAHs, and means of improving degradation efficiencies. Secondary goals are to firmly understand the benefits, applications, and also limitations of electrokinetic technology. This includes investigating the transport of charged and non-charged species in different media types and the use of this technology towards biological and chemical degradation efforts. The PAHs of focus are three-to-four-ringed hydrocarbons of a similar nature and it is of interest to determine how structural configurations may affect biodegradability and to extrapolate these findings to larger PAHs, which are often more toxic, and often mutagenic or carcinogenic in nature.

An additional focus aims at studying whether the addition of a chemical surfactant (Brij-35) will have any impact on biodegradation rates, as is indicated positively by the literature.

8.2 Summary of Research Sections and Their Implications

8.2.1 Chapter 2: A Review of the Effect of Multiple Variables on the Anaerobic Degradation of Hydrocarbons.

This chapter focuses on approaches to improve biodegradation rates of hydrocarbons (primarily PAHs) under anaerobic conditions. As complex hydrocarbons tend to be recalcitrant under these conditions (largely due to the reduced ability or efficiency of anaerobic microorganisms to utilize or degrade them), it is important to understand all

variables relevant to a particular case. Anaerobic degradation can take place under a variety of different conditions and every environment, therefore, presents a unique challenge. Electron acceptors, electron donors, temperature, salinity, pH all play key roles in determining the possibility effective of effective degradation occurring. Additionally, the use of co-substrates or techniques such as bioaugmentation may greatly enhance this capability. All data and research pertaining to these matters was obtained from the literature but is a matter that is constantly updated.

8.2.2 Chapters 4 and 5: A Study in Electrokinetic Migration Rates in Sand and Clay; The Electromigration of *Spirulina* Blue Dye in Sand and The Discovery of pH Gradient Shifts over Time

Four unique electrokinetic experiments researching dye migration patterns are reported in these chapters. This is comprised of analyzing the behavior of an anionic dye as well as a dye with both anionic and cationic properties in two different media: sand and clay. Following this, a confirmation experiment of the green dye in sand and a subsequent measurement of a developing pH gradient is investigated. These studies are based upon multiple objectives: Comparing migration rates of identical dye types in different media (i.e., sand, clay), and the comparative behaviors of dyes with different ionic properties in each media type. The observation of the green (*Spirulina* Blue) dye in sand leads to indications that it is operating as an anionic dye, despite indications that it should have cationic properties. An additional study shows that the pH gradient demonstrated in the literature is not immediate and that the pH gradient, in fact, shifts over time, allowing for an explanation of the observations.

8.2.3 Chapters 6 and 7: Enhanced Biodegradation of Low Molecular Weight PAHs by Electrokinetics With and Without the Use of a Surfactant

These chapters investigate the potential of electrokinetic technology to enhance biodegradation rates. Using natural soil bacteria, shown to be capable of growing on low-molecular-weight PAHs, the hope is that electrokinetic phenomena (electromigration, electroosmosis, and electrophoresis) would increase bioavailability in addition to enhance nutrient transport thereby augmenting bacterial growth rates. The first study indicates the potential of increased biodegradation, but it appears that this biodegradation may also be occurring in the Control system, due to a lack of effectiveness of the biocide used. This, in addition to concerns about adsorbance and adherence to the acrylic surfaces leads the results of this study to be fully inconclusive. The second study, in an effort to conclusively show the presence of significant biodegradation and to enhance it further via the use of a surfactant (Brij-35), is unfortunately quite unsuccessful. Surprisingly, no degradation under these conditions takes place and various theories are put forward including inhibition by the surfactant, excess carbon sources, or genus/species discrepancies.

8.3 Future Research and Objectives

When performing the experiments contained in this dissertation, perhaps the most novel discovery is that notion of a changing pH gradient in an electrokinetic system over time. This is a phenomenon that is seemingly unmentioned in the literature in addition to the fact that pH gradients described in research articles pertain only to clay or soil media, and not to sand. While the use of electrokinetics in sand is often not a cost-effective approach, it

can have some applications such as when contaminated with particularly heavy oil where flushing is not an option or in deep anaerobic environments. Efforts to better understand both potential differences in media types as well as pH-sensitive applications may benefit from additional studies. The behaviors observed of an amphoteric substance such as the green dye utilized in these studies can also potentially be applicable for researching the removal of emerging contaminants such as certain hormones and pharmaceuticals which can have similar properties. Flushing of these compounds via electromigration can be accomplished at lower pH levels as protonation and thus ionization occurs, allowing for ionic transport to occur.

With respect to the aerobic experiments, despite the lack of success of confirmed biodegradation, it is clear from the literature that there should be a stronger occurrence and therefore this may lead to efforts to improve or modify current techniques. It is also important to understand the microbial communities and how they react to not only the contaminants but to the stresses and nutrient levels within the examined environment. As the bacteria utilized in these experiments are seemingly typical bacteria, further exploration of the families, genera, and, species may be researched and even if not fully applicable for biodegradation purposes, this may be of keen interest for biologists. Of a particular interest may be biological community factors, such as biofilm development and breakup over time. In future studies, efforts can be made to understand the type and nature of the microorganisms involved and their sensitivities to surfactants such as Brij 35 and potential PAH toxicity at the studied concentrations. This is in addition to a potential acclimation period of the bacterial species towards the PAHs or at the very least, having biodegradation experiments proceed for a duration far longer than 60 days. Fluctuations in salinity and

conductivity and complex pH gradient shifts in the reservoirs may also prove to be helpful in maintaining biological or chemical degradation experiments in an in-situ environment.

A comprehensive study should also be performed as to determine the sorption capacity of the PAHs studied to the acrylic material used in both biodegradation studies. Although there appears to be no indication in the literature of a tendency of hydrocarbons to adsorb or adhere to an acrylic surface, it may also have not truly been studied. A theoretical design for this study would include storing the spiked soil at identical PAH concentrations in an acrylic box matching the dimensions of the acrylic bridge utilized in the biodegradation studies. Soils would be stored with an identical moisture contest and be examined both with and without the present of the Brij-35 surfactant. After a 60-day period, the soil would be removed, and the acrylic boxes each given a brief rinse with de-ionized water. Following this, the boxes would be disassembled, and each set of acrylic pieces soaked in hexane for a period not exceeding five minutes. This hexane would then be analyzed via GC-MS for potential PAH recovery.

APPENDIX A

ATTEMPTED EXPERIMENTS AND LESSONS LEARNED: THE CONVERSION OF ANAEROBIC CONDITIONS TO AEROBIC CONDITIONS IN SAND VIA THE ADDITION OF PEROXIDE IN AN ELECTROKINETIC SYSTEM

A.1 Introduction

Crude oil spills are fairly common in coastal areas [384] and can penetrate deeply within sand columns of a beach or sandy soils [105]. Many crude oil components, including polycyclic aromatic hydrocarbons (PAHs), have been found to be toxic to aquatic life, and potentially carcinogenic or mutagenic humans and higher organisms [18]. Most PAHs can readily biodegrade under aerobic conditions (i.e., in the presence of oxygen), provided there are sufficiently high concentration of nutrients available [37, 38], however, deeply buried oil could reside in an anaerobic environment (i.e., lacking oxygen) for decades or longer [42]. The organisms present in deep sediments and sands are largely anaerobic bacteria and archaea, and research has shown that they have the ability to degrade certain oil components (alkanes, single ring aromatics, and some two-ring aromatics). Nonetheless, they have not been shown to readily biodegrade most polycyclic aromatic hydrocarbons (PAHs) [43].

Aerobic environments contaminated with PAHs can become anaerobic due to a variety of factors including geochemical reaction as well as the stimulation of the in-situ microbial community, which leads to depletion of molecular oxygen during aerobic respiration. As the oxygen is not replenished at the same rate as it is depleted, anaerobic zones are formed proximal to the contaminant source. Without the presence of molecular oxygen, alternative electron acceptors such as nitrate, ferrous iron and sulfate could be used

by the microbial community to oxidize the PAHs [34]. In many environments, especially marine sediments, sulfate-reduction is typically for more predominant as an anaerobic process than other processes such as nitrate-reduction [122].

Boufadel et al. [5] performed an experiment analyzing beaches in Prince William Sound, Alaska, where oil from the Exxon Valdez spill, highly contaminated with PAHs, had persisted for more than 20 years. Low oxygen concentrations were determined to be the major factor causing the persistence of the oil and they conducted a study utilizing a deep injection of hydrogen peroxide (and nutrients) into four beaches in the area. Their results showed very good efficiency of oxygen and nutrient delivery to the contaminated areas of the beach. As injection of peroxide through a large area can be difficult and costly [5], an experiment was designed to determine whether an anaerobic sand-based environment can be converted to an aerobic environment via the addition of hydrogen peroxide and system-generated oxygen in an electrokinetic system. Ramirez et al. [79] successfully migrated oxygen through a similarly designed electrokinetic setup. They showed success in sandy and silty soils but could not migrate oxygen through clay. However, they only utilized the oxygen generated through the electrolytic process and not via the addition of an oxygenating substance. They suggest that the oxygen generated via electrolysis can create dissolved oxygen concentrations of 4-9 mg O_2/L. This experiment was designed to confirm these results and look at the added effect of peroxide (H_2O_2). Reddy and Chandhuri [359] successfully delivered a 5-10% H_2O_2 solution through clayey (kaolin) soil, primarily enhanced by electroosmotic flow. Although electroosmotic flow would not be present in this experiment, as it utilized sand media, there is some indication that electric potential can increase diffusion rates of the peroxide.

A.2 Materials and Methods

This experiment utilized three electrokinetic apparatuses with different variables. Two setups had power provided from an external power supply, and one of those also had hydrogen peroxide added at the onset of the experiment. The system utilizing both power and electrical power was designated “PE” and the system utilizing electrical power only was designated as “E”. The third setup (designated as “C”) functioned as a control where no peroxide nor electrical power was provided. The setups were self-designed electrokinetic (EK) apparatuses made of fused acrylic parts and constructed at the New Jersey Institute of Technology. Each EK apparatus consisted of an anode chamber, a cathode chamber, and a bridge between housed the media (i.e., sand). It was fitted with a pressure-release valve in the rear of each reservoir along with palladium-coated pellets to convert any hydrogen produced to water vapor (Figure A.1). Mesh pouches containing these pellets were also inserted towards the top of each reservoir to reduce oxygen levels further by catalyzing the reaction of oxygen with the hydrogen gas used in purging.

Three specially-designed porous tubes (ultra-high-molecular-weight polyethylene 2.54cm (1”) OD x 1.91cm (1") ID x 22.86 cm (9") Long, hydrophilic, with 50 µm pore size) (Scientific Commodities, Inc., Lake Havasu City, AZ), were setup within the sand that allowed water in the system to pass through unobstructed while preventing sand from infiltrating (Figure A.1). This allowed for analysis by a dissolved oxygen probe which was inserted via air-tight sampling ports fitting into an acrylic lid atop the bridge housing the sand. A solution of 1 g/L NaCl (de-ionized water plus granulated sodium chloride) was created in 20L batches and added to fill each chamber to ensure proper cation and anion flow. The sand (very fine, #000 grade) was poured carefully into the bridge area to a fill and packed fairly densely. Two graphite electrodes were inserted into both the anode and

cathode chambers to distribute the electric current as a gradient across the system (Figure A.1).

Prior to purging, all components of the system were sealed air-tight with both silicone and a waterproof adhesive and check for both air and water leakage. Once ensuring each system was both water-tight and air-tight, each entire system was purged initially with pure nitrogen (100%) followed by a second purge with a 95% nitrogen: 5% hydrogen gas mixture. This was done in each reservoir and all three bridge ports. System was allowed to equilibrate overnight and checked for anaerobic conditions before and after this period. Several attempts at reaching anaerobic oxygen levels were made and additional sealing and time was required. Eventually, very low oxygen levels (< 0.5 mg O_2 /L) were reached and (briefly) maintained. At this point, the power supply was turned on for two of the systems ("PE" and "E"). A potential of 30V (0.667 V/cm) was applied with an initial current output of 7.00 ± 0.04 mA. In the system designated as "PE", 3 mL of 30% hydrogen peroxide was added via a plastic syringe and long-tipped needle into the anode reservoir. In was ensured that all systems were fully sealed and dissolved oxygen levels were periodically motored. Dissolved oxygen levels at all points were measured using the HI2040 Edge® Multiparameter DO meter (Hanna Instruments, Woonsocket, RI) with HI764080 Dissolved Oxygen electrode. Prior to initiation, pH was measured in all systems and temperature was measured both at the onset and conclusion of the experiment. Both pH and temperature were measured using the AquaShock pH meter (Sper Scientific®, Scottsdale, AZ, USA) and accompanying probe. The duration of the experiment was 14 days.

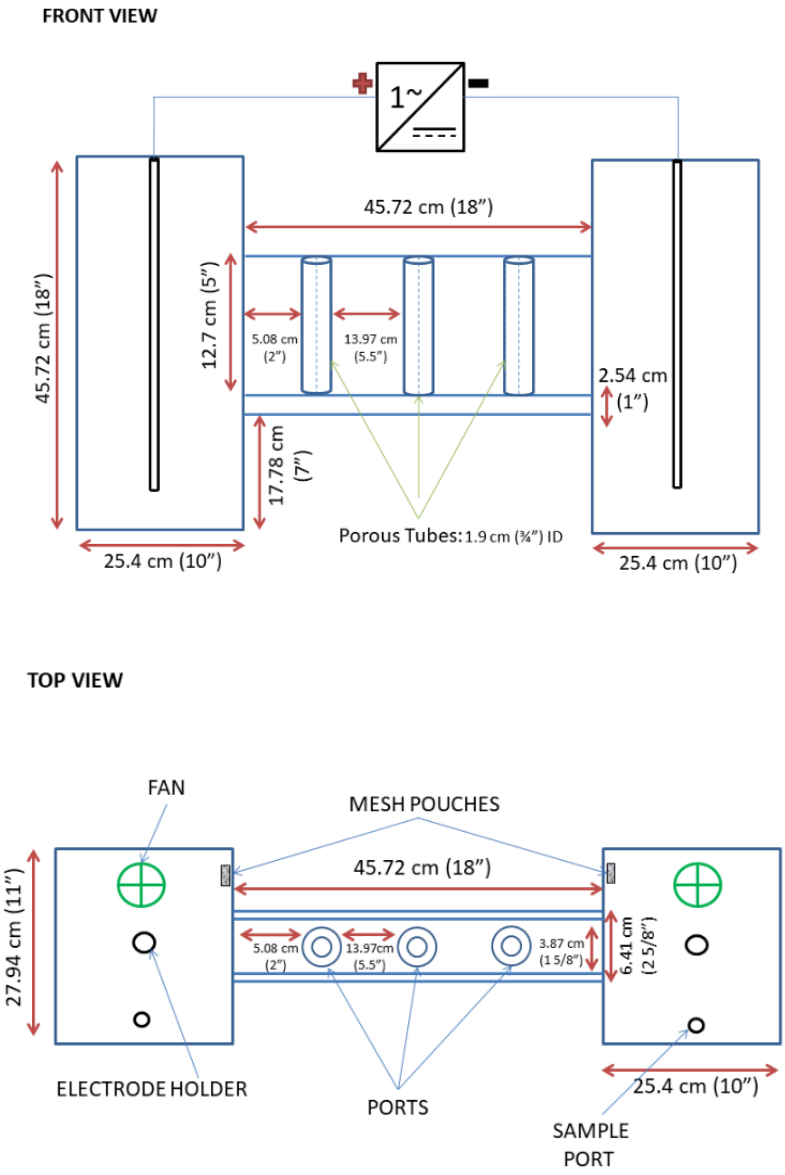

Figure A.1 Schematic of modified electrokinetic apparatus with oxygen sample ports. Front view (top) and view from above (bottom).

A.3 Results

Being able to maintain anaerobic or even anoxic conditions was more difficult than anticipated and after prolonged trials, the experiment was forced to begin with part of each system having levels slightly above 0.5 mg O_2/L. This appears to be due the nature of the large apparatus and its numerous parts. Having many micro-areas through which oxygen could infiltrate despite proper sealing, this system design was shown not to be well-suited for this type of experiment. Per each sampling period, dissolved oxygen levels were measured at five points in each system: Both reservoirs and the three sampling ports within the sand area. At the onset of the experiment, dissolved oxygen levels (in mg O_2 /L) were measured and reported in Table A.1

The anodic reservoir where the peroxide was injected (system PE) quickly became hyperoxic and the sand area adjacent to the anode reservoir gradually became fully oxic. However, oxygen levels, relative to the control, did not rise significantly in any of the other sampling areas, noting the absence of electrically-enhanced diffusion (Figure A.2). System E, which produced oxygen only through the electrolytic process, showed a gradual and more uniform increase in oxygen levels. Increases in this system at most points were notably greater than the control system (C), noting a benefit of added oxygen from the electrolytic process over permeation from system flaws alone. This was primarily apparent towards the anodic side of the system, where O_2 was generated via the electrolytic process. At day 14, all power systems were turned off and systems were let to stand an additional three days (75 hours) for to monitor the effect of diffusion in the systems (Table A.2). The changes in the central sand area are noticeably striking and perhaps the best comparison versus the control, as System E showed a very strong contrast in oxygen levels (Table A.3).

Table A.1 Dissolved Oxygen Levels at Onset of Experiment (mg O_2 /L)

System	Cathode	Sand (towards Cathode)	Sand (Center)	Sand (towards Anode)	Anode
PE	0.14	0.21	0.32	0.16	1.16
E	0.54	0.45	0.05	0.53	0.57
C	0.72	0.52	0.11	0.34	0.65

Table A.2 Dissolved Oxygen Levels (mg O_2 /L) 75 Hours After Conclusion of Experiment

System	Cathode	Sand (towards Cathode)	Sand (Center)	Sand (towards Anode)	Anode
PE	4.33	2.64	1.64	12.16	22.04
E	5.23	4.12	3.28	4.28	5.47
C	5.44	4.38	1.26	2.06	4.11

Table A.3 Minimum and Maximum Oxygen Levels (mg O_2 /L) [Excluding Diffusion Values]

System	Cathode			Sand (towards Cathode)			Sand (Center)			Sand (towards Anode)			Anode		
	Min	Max	Δ	Min	Max	Δ	Min	Max	Δ	Min	Max	Δ	Min	Max	Δ
PE	0.14	4.02	+3.88	0.21	3.38	+3.17	0.17	3.73	+3.56	0.16	10.71	+10.55	1.16	21.01	+19.85
E	0.51	4.42	+3.91	0.45	3.78	+3.33	0.05	3.97	+3.92	0.53	5.25	+4.72	0.51	5.58	+5.07
C	0.71	5.18	+4.47	0.33	3.62	+3.29	0.11	1.11	+1.00	0.34	2.73	+2.39	0.59	3.90	+3.31

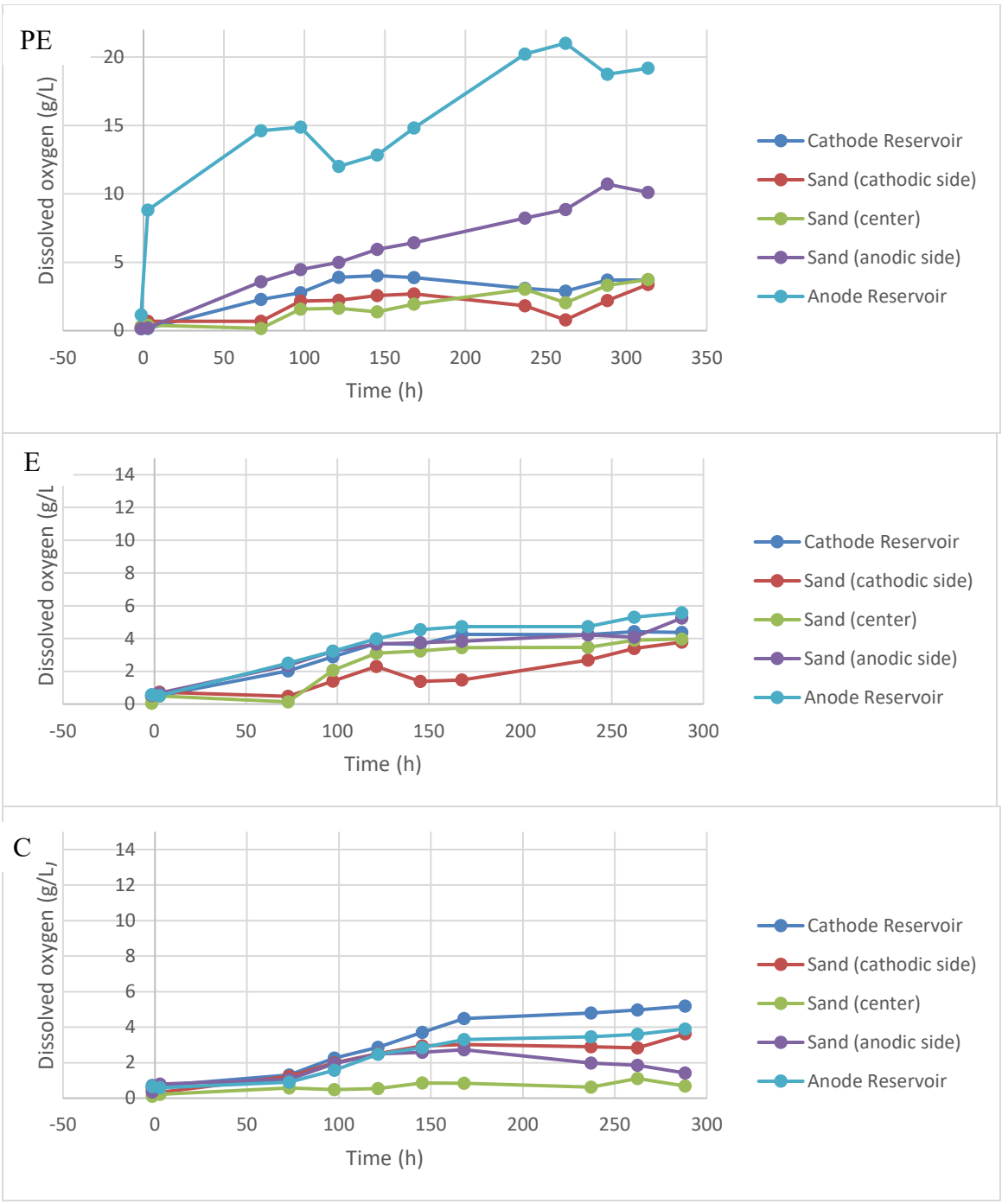

Figure A.2 Graphs depicting the changes in dissolved oxygen levels over the duration of the experiment. PE = Peroxide + Electric Power, E = Electric Power only, C = Control*

**(For the Control, designations of "cathode" and "anode" are arbitrary as there was no power applied to this system. Terms were applied to match convention used for other systems.)*

A.4 Discussion and Conclusion

Two important matters were ascertained through this attempted experiment. One realization is that the ability to create an anaerobic environment in a complex system has many challenges, and that acrylic material may not be at all feasible to conduct such an experiment. The inability of these setups to maintain even anoxic levels calls all results into question and any potential revision of this experiment would require substantially different materials. The second realization is that it may not be possible to transport peroxide via sand due to the lack of any electric charge and subsequent carrying process. Peroxide can be pumped into sand in order to facilitate the creation of aerobic environments, but it appears that the use of electrokinetic technology cannot be used to enhance its delivery. A summary of items that could be concluded from this experiment but not confirmed were the following:

- Neither electrokinetic phenomena nor the presence of a strong voltage gradient succeeded in enhancing the diffusion of the peroxide-based oxygen through the sand.
- The generation of oxygen from the electrolytic process was significant compared to oxygen that permeated into the system.
- Permeation of oxygen into the reservoirs was far greater than permeation into the sand

APPENDIX B

ALTERNATIVE METHODS FOR CALCULATING IONIC MOBILITY (u_i^*) AND ITS RAMIFICATIONS

B.1 Method 1 - Theory

A method (Equation B.1) of calculating absolute ionic mobility utilizing the system's ionic strength is derived from Xu et al. [385]:

$$u_i = u_i^* \exp\left(-\eta\sqrt{zI}\right) \tag{B.1}$$

Where u_i is the ionic mobility (based upon observational data), u_i^* is the absolute ionic mobility, z is the molecular charge, η is the correction coefficient (if z = 1, η = 0.5, if z = >2, η = 0.77), I is the ionic strength of the liquid (e.g., salt water).

The ionic strength (I) must be calculated (Equation B.2), which necessitates the calculation of the dye concentration (Equation B.3).

$$I = 0.5\sum c_i z_i^2 \tag{B.2}$$

$$c_i = \frac{\left[\frac{Volume\,injected\,(mL)}{sand\_volume(L)} * density\left(\frac{g}{mL}\right)\right]}{molecular\,weight\left(\frac{g}{mol}\right)} \tag{B.3}$$

B.2 Method 1 – Calculations

$$c_i = 2\frac{mL}{L}\,at\,density\,of\,0.8\frac{g}{mL} = 1.6\frac{g}{L} / \left(496.416\frac{g}{mol}\right) = .003224\frac{mol}{L}$$

$$I = 0.5\sum c_i z_i^2 = 0.5(.003224)(-2)^2 = .006448$$

The observed u_i value is calculated via diving the average migration rate by the voltage gradient:

$$u_i = \frac{9.12\frac{cm}{d}}{0.667\frac{V}{cm}} = 13.6732\frac{cm^2}{dV} = 1.58x10^{-4}\frac{cm^2}{sV}$$

Plugging all values into Equation B.1: $u_i^* = 8.6x10^{-5}\frac{cm^2}{sV} = 7.43\frac{cm^2}{dV}$

B.3 Method 2 - Theory

An alternative means of calculating u_i^* is via Equation B.4 [386], which takes into account the approximate diffusivity in a system and the environmental variables.

$$u_i^* = \frac{D_i^* z_i F}{RT} \tag{B.4}$$

Where D_i^* is the typical max diffusivity, z_i is the molecular charge, F is Faraday's constant, R is the universal gas constant, T is the temperature of the system.

B.4 Method 2 - Calculations

Using the higher possible value of diffusion through sand obtained from the literature, (10^{-6} cm^2/s):

$$u_i^* = \frac{D_i^* z_i F}{RT} = \frac{10^{-6}(2)(96500)}{(8.314)(294.15)} = 7.89x10^{-5}\frac{cm^2}{sV} = 6.82\frac{cm^2}{dV}$$

B.5 Conclusions

It would be expected the first alternative method (Equation B.1) would more closely resemble the originally calculated absolute ionic mobility than the second alternative method (Equation B.4). This was expected particularly as Equation B.1 utilized the observed migration rate and also included the ionic strength, which was assumed to be essential. Equation B.4 did not include the migration rate nor the ionic strength.

However, calculated values for both alternative methods were near identical (Table B.1), and although within an order of magnitude, were far close to each other than via the original method. For comparison, these methods were also employed for the all dye experiments (using appropriate values) and are reported in Table B.2.

Table B.1 Comparison of Absolute Ionic Mobility (u_i^*) Values via Various Methods for Red Dye in Sand

Original Method (Eq. 4.5) ($cm^2\ V^{-1}\ s^{-1}$)	**Alternative Method 1 (Eq. B.1)** ($cm^2\ V^{-1}\ s^{-1}$)	**Alternative Method 2 (Eq. B.4)** ($cm^2\ V^{-1}\ s^{-1}$)
2.53×10^{-5}	8.60×10^{-5}	7.89×10^{-4}

Table B.2 Comparison of Absolute Ionic Mobility (u_i^*) Values via Various Methods for all Other Dye Experiments

	Original Method (Eq. 4.5) ($cm^2\ V^{-1}\ s^{-1}$)	**Alternative Method 1 (Eq. B.1)** ($cm^2\ V^{-1}\ s^{-1}$)	**Alternative Method 2 (Eq. B.4)** ($cm^2\ V^{-1}\ s^{-1}$)
Green Dye in Sand	2×10^{-5}	NC	7.10×10^{-4}
Red Dye in Clay	6.76×10^{-6}	NC	7.89×10^{-5} -7.89×10^{-7}
Green Dye in Clay	1.24×10^{-6}	NC	7.89×10^{-5} -7.89×10^{-7}

NC = Not Calculated

APPENDIX C

THE INVESTIGATION OF pH GRADIENT SHIFTS IN AN ELETROKINETIC SYSTEM IN A SANDY SOIL OVER TIME AND HOW IT COMPARES TO pH SHIFTS IN SAND

C.1 Objective

After investigating how in an electrokinetic system, the pH profile changed over time, it was hypothesized that the same trend would be observed in a sandy soil, albeit at a different rate. Using the same miniature setups described in Section 4.2.1, a study identical to that conducted in Chapter 5 was performed. In this variation of the study, a sandy soil, of the same type and sampling used in Chapter 7 was used in place of sand.

C.2 Materials and Methods

The soil used in this experiment was taken from the grounds of an NJIT construction site and determined via ASTM method D2487 o be either SW-MC or SW-SC (Well-graded sand with silt and/or clay). The grain size ranged from 0.08 – 8 mm and the moisture content, after the removal of obvious stones was 9.02 ± 0.07 % (w/w). Medium-size stones were not removed for the experiment in an effort to more closely simulate an *in-situ* environment. The pH of the soil was previously measured to be 7.98 but was not verified and slight infiltration of the soil into the reservoirs appeared to have no effect on pH values. Density of the soil when previously measured was found to be 1.17 ± 0.01 kg/L.

The setups used in this study are described in Section 5.2.1 and are meant to parallel those constructed and used in Chapter 5. The voltage gradient applied was a 13.33 V output with a measured 2.91 ± 0.02 mA current output, yielding a voltage gradient of 0.667 V/cm

and current density of 0.038 mA/cm^2. This experiment was done as single setup followed by three replicates and were filled according to the technique described in Section 5.2.2. These setups are hereby referred to as Systems 1-4, respectively. System 1 ran for a total of 7 days (168 h) and System 2-4 ran for a total of 6 days (144 h).

C.3 Measurements

pH measurements were conducted in an identical fashion to those noted in Chapter 6, namely: pH values in the reservoirs were measured with AquaShock pH meter (Sper Scientific®, Scottsdale, AZ, USA) and accompanying probe in the center of each reservoir and pH values in the sand were determined via Fisherbrand® Paper pH strips (Fisher Scientific). A slightly curved steel spatula was inserted in the sand at marked regular intervals and placed upon a pH strip for determination. Due to the variability of this method, pH values reported have an error of 0.5-1.0.

C.4 Results and Discussion

The results from this experiment can be seen in Figure C.2. The initial setup and the three replicates (Systems 1-4) all showed quite similar pH gradients at time 6h. At this point, only the areas of the sand near the anode and cathode shifted dramatically from the original pH value. Over the course of all experiments a trend indicated a growing bias towards the cathodic pH, the precise inverse of what was described in the literature (Figure C.1). The profiles of Systems 2 and 4 most closely resemble each other, particularly at times 24h and 48h. System 3 had slightly higher water levels, peaking just above the soil and became strongly basic at a faster rate than Systems 2 or 4. System 1, the initial setup, overall match

the findings of the other three setups and its gradients over time appeared to be somewhat of a hybrid between Systems 1-3. All systems showed an increase in pH values at the central sand regions (Figure C.3) and were somewhat linear, particularly for Systems 2 and 4. pH values at the anode and cathode reached extreme values of 1.80 and 13.00, respectively but neared these values already by 48h.

Current values in the reservoirs of the initial setup was 2.36 mA at the onset of the experiment but had dropped to 1.99 mA by 168h. Systems 2-4 did not have a noticeable drop in current but rather fluctuated regularly with averages values of 2.04 ± 0.20, 2.16 ± 0.08, and 2.20 ± 0.17 mA, respectively. System 2 had a lower measured current of 1.70 mA at 120h and may have been symptomatic of a loose connection to the electrode, as it was seen to have risen to 2.25 mA at 144h and upon contact with the connector, fluctuations in the current readings were seen. This was the same physical setup used for the initial setup (System 1) and therefore the drop in current may have been due to the connection issue.

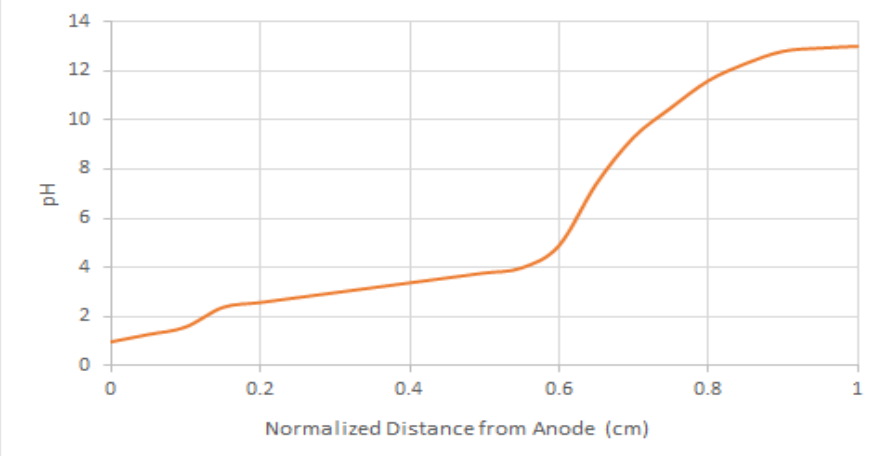

Figure C.1 An estimation of a pH profile in an electrokinetic system based upon multiple literature reports.

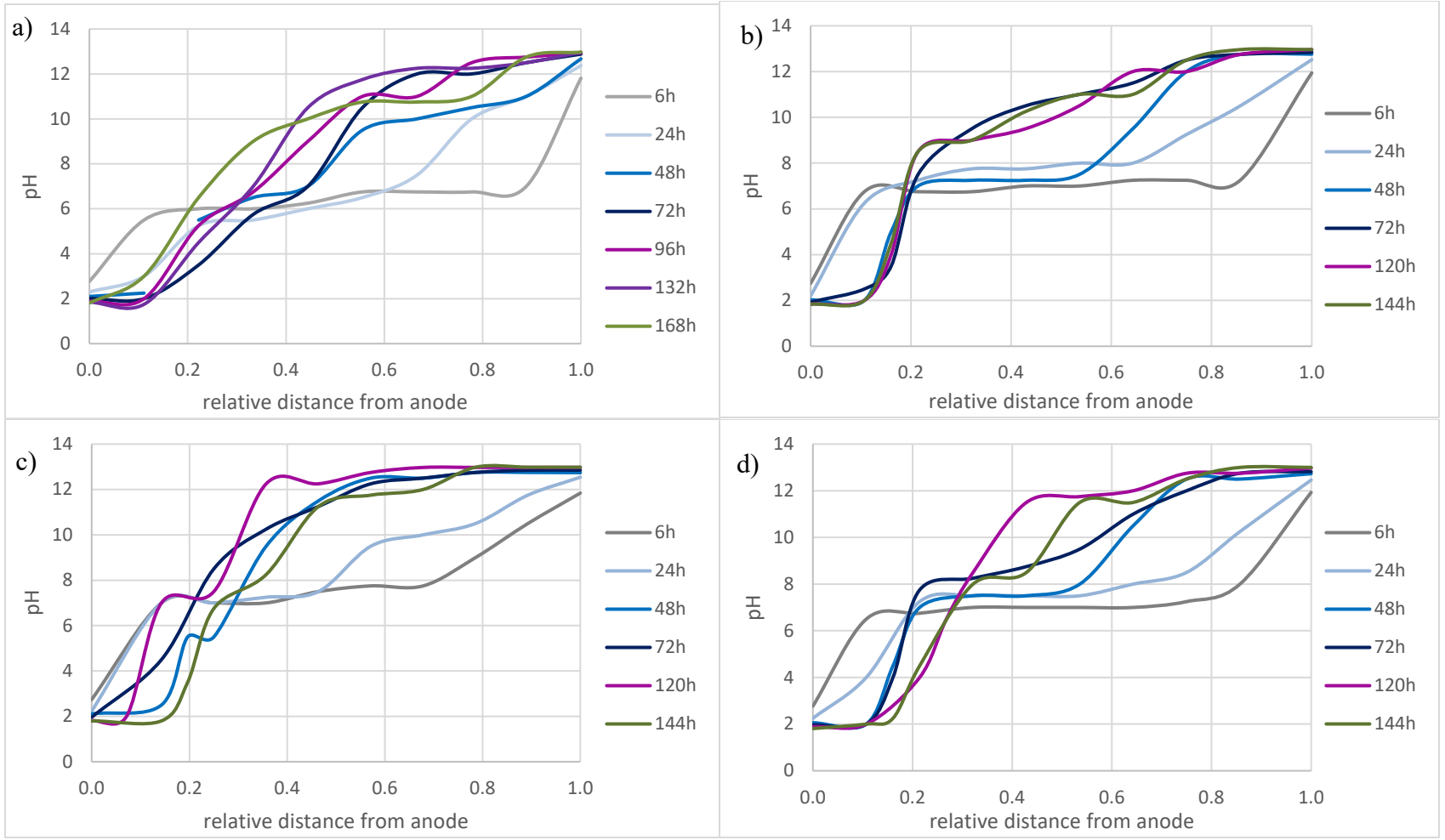

Figure C.2 pH gradients relative to the anode for soil in the miniature EK setups. a) System 1; b) System 2; c) System 3; d) System 4

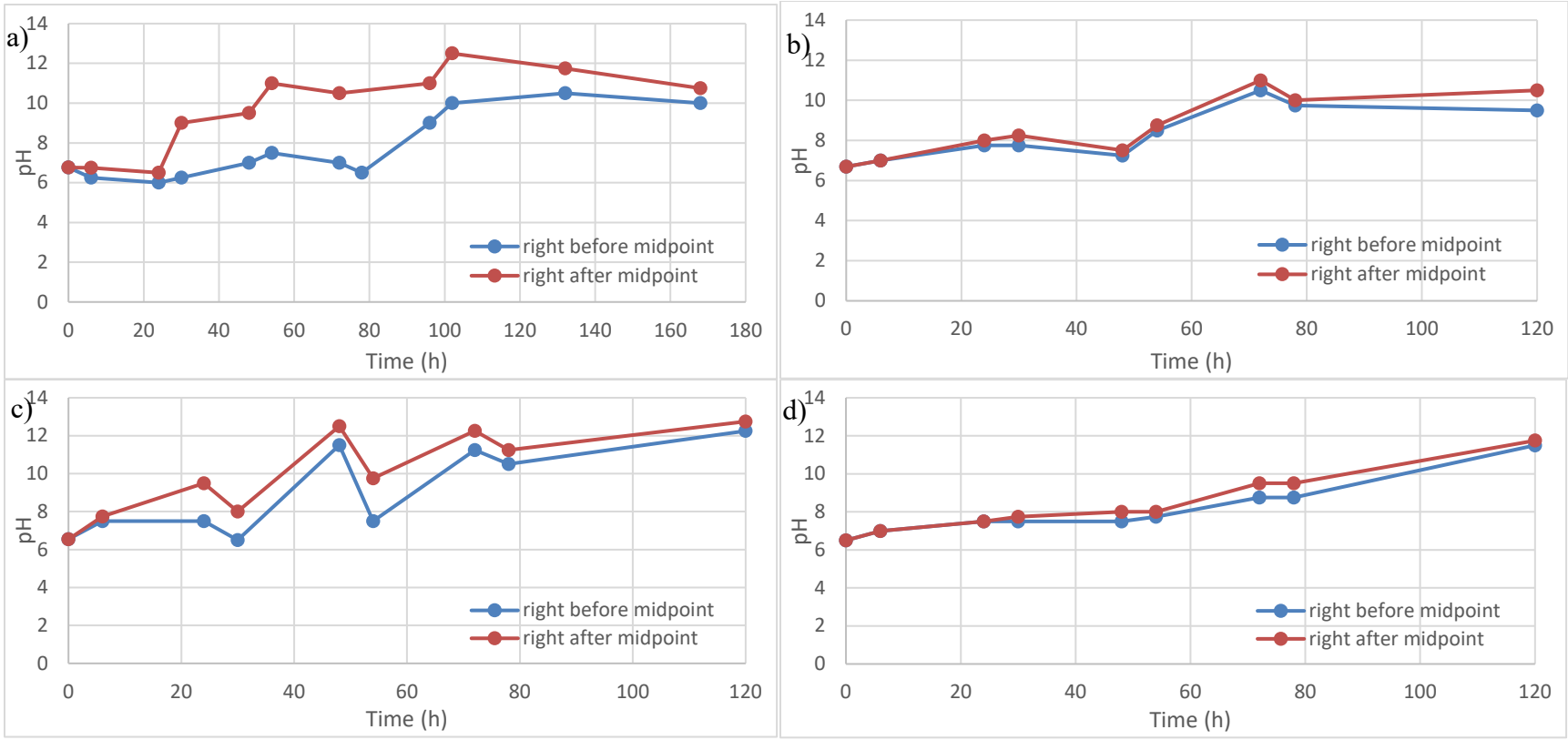

Figure C.3 Increase in measured pH values adjacent to the midpoint* in sand. a) System 1; b) System 2; c) System 3; d) System 4

*"Midpoint" is defined as 50% of the distance from the anode to the cathode. For Systems 1, 3, and 4, the measured points were located at 42.9% and 53.6% distances from the anode, respectively. For System 2, the measure points were located at 46.4% and 57.1% distances from the anode, respectively.

C.5 Conclusions

The notion of a highly dynamic shift in pH profile across media over time appears to be a novel finding not reported in the literature. Although pH gradients for the duration of an experiment are reported in most experiments involving an electrokinetic (EK) setup, rarely, if at all, are all pH point in the media shown over time and the change in the overall gradient over time is not something that is yet seen. Complexities such as the makeup of a particular soil and the characteristics a particular EK design make a prediction of pH shifts in a real-time system difficult to model, yet with sufficient data and modeling, this may become entirely possible.

REFERENCES

[1] D.A. Gill, J.S. Picou, L.A. Ritchie, The Exxon Valdez and BP oil spills: A comparison of initial social and psychological impacts, American Behavioral Scientist, 56 (2012) 3-23.

[2] I. Onwurah, V. Ogugua, N. Onyike, A. Ochonogor, O. Otitoju, Crude oil spills in the environment, effects and some innovative clean-up biotechnologies, International Journal of Environmental Research, 1 (2007) 307-320.

[3] B. Laffon, E. Pásaro, V. Valdiglesias, Effects of exposure to oil spills on human health: updated review, Journal of Toxicology and Environmental Health, Part B, 19 (2016) 105-128.

[4] Y. Gong, X. Zhao, Z. Cai, S. O'reilly, X. Hao, D. Zhao, A review of oil, dispersed oil and sediment interactions in the aquatic environment: influence on the fate, transport and remediation of oil spills, Marine Pollution Bulletin, 79 (2014) 16-33.

[5] M.C. Boufadel, X. Geng, J. Short, Bioremediation of the Exxon Valdez oil in Prince William Sound Beaches, Marine Pollution Bulletin, 113 (2016) 156-164.

[6] J. Beyer, H.C. Trannum, T. Bakke, P.V. Hodson, T.K. Collier, Environmental effects of the Deepwater Horizon oil spill: a review, Marine Pollution Bulletin, (2016).

[7] M. Fingas, The Basics of Oil Spill Cleanup, CRC press, Boca Raton, FL, 2012.

[8] X.C. Kretschmer, R.R. Chianelli, Bioremediation of environmental contaminants in soil, water, and air, Dekker Encyclopedia of Nanoscience and Nanotechnology, 1 (2004) 331.

[9] L.W. Perelo, In situ and bioremediation of organic pollutants in aquatic sediments, Journal of Hazardous Materials, 177 (2010) 81-89.

[10] D. Ghosal, S. Ghosh, T.K. Dutta, Y. Ahn, Current state of knowledge in microbial degradation of polycyclic aromatic hydrocarbons (PAHs): a review, Frontiers in Microbiology, 7 (2016) 1369.

[11] S. Kuppusamy, P. Thavamani, K. Venkateswarlu, Y.B. Lee, R. Naidu, M. Megharaj, Remediation approaches for polycyclic aromatic hydrocarbons (PAHs) contaminated soils: Technological constraints, emerging trends and future directions, Chemosphere, 168 (2017) 944-968.

[12] X. Li, P. Li, X. Lin, C. Zhang, Q. Li, Z. Gong, Biodegradation of aged polycyclic aromatic hydrocarbons (PAHs) by microbial consortia in soil and slurry phases, Journal of Hazardous Materials, 150 (2008) 21-26.

[13] F.Z. Mesbaiah, F. Mansour, K. Eddouaouda, A. Badis, Surfactant effects on biodegradation of polycyclic aromatic hydrocarbons, Desalination and Water Treatment, 57 (2016) 5995-6000.

[14] M. Sherafatmand, H.Y. Ng, Using sediment microbial fuel cells (SMFCs) for bioremediation of polycyclic aromatic hydrocarbons (PAHs), Bioresource Technology, 195 (2015) 122-130.

[15] A.L. Juhasz, R. Naidu, Bioremediation of high molecular weight polycyclic aromatic hydrocarbons: a review of the microbial degradation of benzo [a] pyrene, International Biodeterioration and Biodegradation, 45 (2000) 57-88.

[16] J. Meador, J. Stein, W. Reichert, U. Varanasi, Bioaccumulation of polycyclic aromatic hydrocarbons by marine organisms, Reviews of Environmental Contamination and Toxicology, Springer, New York, NY, 1995, pp. 79-165.

[17] A.F. Wick, N.W. Haus, B.F. Sukkariyah, K.C. Haering, W.L. Daniels, Remediation of PAH-contaminated soils and sediments: a literature review, Virginia Polytechnic Institute and State University, Dept. of Crop and Soil Environmental Sciences, Blacksburg, VA, 2011.

[18] D. Pampanin, M. Sydnes, Polycyclic aromatic hydrocarbons a constituent of petroleum: Presence and influence in the aquatic environment, Intech, 2013, p. 83-118.

[19] E.W. Liebeg, T.J. Cutright, The investigation of enhanced bioremediation through the addition of macro and micro nutrients in a PAH contaminated soil, International Biodeterioration and Biodegradation, 44 (1999) 55-64.

[20] J.G. Mueller, P.J. Chapman, P.H. Pritchard, Creosote-contaminated sites. Their potential for bioremediation, Environmental Science & Technology, 23 (1989) 1197-1201.

[21] C.S. Van Zuydam, Determination of polycyclic aromatic hydrocarbons (PAHs) resulting from wood storage and wood treatment facilities for Electricity transmission in Swaziland, Environmental Science, University of South Africa, 2009.

[22] R. Harvey, Polycyclic Aromatic Hydrocarbons., Wiley-VCH Verlag, Weinheim, Germany, 1997.

[23] S.C. Wilson, K.C. Jones, Bioremediation of soil contaminated with polynuclear aromatic hydrocarbons (PAHs): a review, Environmental Pollution, 81 (1993) 229-249.

[24] R. Dabestani, I.N. Ivanov, A compilation of physical, spectroscopic and photophysical properties of polycyclic aromatic hydrocarbons, Photochemistry and Photobiology, 70 (1999) 10-34.

[25] J. Wang, C. Wang, Q. Huang, F. Ding, X. He, Adsorption of PAHs on the sediments from the yellow river delta as a function of particle size and salinity, Soil and Sediment Contamination: An International Journal, 24 (2015) 103-115.

[26] Y. Zhou, R. Liu, H. Tang, Sorption interaction of phenanthrene with soil and sediment of different particle sizes and in various CaCl2 solutions, Journal of Colloid and Interface Science, 270 (2004) 37-46.

[27] J. Jimenez, E. Gonidec, J.A.C. Rivero, E. Latrille, F. Vedrenne, J.-P. Steyer, Prediction of anaerobic biodegradability and bioaccessibility of municipal sludge by coupling sequential extractions with fluorescence spectroscopy: towards ADM1 variables characterization, Water Research, 50 (2014) 359-372.

[28] J.D. Stokes, G. Paton, K.T. Semple, Behaviour and assessment of bioavailability of organic contaminants in soil: relevance for risk assessment and remediation, Soil Use and Management, 21 (2005) 475-486.

[29] J. Harmsen, Measuring bioavailability: from a scientific approach to standard methods, Journal of Environmental Quality, 36 (2007) 1420-1428.

[30] M.J. Riding, K.J. Doick, F.L. Martin, K.C. Jones, K.T. Semple, Chemical measures of bioavailability/bioaccessibility of PAHs in soil: fundamentals to application, Journal of Hazardous Materials, 261 (2013) 687-700.

[31] T.N. Bosma, H. Harms, A.J. Zehnder, Biodegradation of xenobiotics in environment and technosphere, Biodegradation and Persistence, Springer, 2001, p. 163-202.

[32] M. Alexander, Aging, bioavailability, and overestimation of risk from environmental pollutants, Environmental Science & Technology, 34 (2000) 4259-4265.

[33] D. Delille, E. Pelletier, A. Rodriguez-Blanco, J.-F. Ghiglione, Effects of nutrient and temperature on degradation of petroleum hydrocarbons in sub-Antarctic coastal seawater, Polar Biology, 32 (2009) 1521-1528.

[34] S.M. Bamforth, I. Singleton, Bioremediation of polycyclic aromatic hydrocarbons: current knowledge and future directions, Journal of Chemical Technology and Biotechnology, 80 (2005) 723-736.

[35] J.L. Sims, R.C. Sims, J.E. Matthews, Approach to bioremediation of contaminated soil, Hazardous Waste and Hazardous Materials, 7 (1990) 117-149.

[36] A.L.C. Lima, J.W. Farrington, C.M. Reddy, Combustion-derived polycyclic aromatic hydrocarbons in the environment—a review, Environmental Forensics, 6 (2005) 109-131.

[37] M. Boufadel, P. Reeser, M. Suidan, B. Wrenn, J. Cheng, X. Du, T.L. Huang, A. Venosa, Optimal nitrate concentration for the biodegradation of n-heptadecane in a variably-saturated sand column, Environmental Technology, 20 (1999) 191-199.

[38] A.D. Venosa, X. Zhu, Biodegradation of crude oil contaminating marine shorelines and freshwater wetlands, Spill Science & Technology Bulletin, 8 (2003) 163-178.

[39] J.-S. Seo, Y.-S. Keum, Q.X. Li, Bacterial degradation of aromatic compounds, International Journal of Environmental Research and Public Health, 6 (2009) 278-309.

[40] M. Kronenberg, E. Trably, N. Bernet, D. Patureau, Biodegradation of polycyclic aromatic hydrocarbons: Using microbial bioelectrochemical systems to overcome an impasse, Environmental Pollution, 231 (2017) 509-523.

[41] S. Harayama, H. Kishira, Y. Kasai, K. Shutsubo, Petroleum biodegradation in marine environments, Journal of Molecular Microbiology and Biotechnology, 1 (1999) 63-70.

[42] J.W. Farrington, Oil pollution in the marine environment II: Fates and effects of oil spills, Environment: Science and Policy for Sustainable Development, 56 (2014) 16-31.

[43] C. Berdugo-Clavijo, Methanogenic biodegradation of crude oil and polycyclic aromatic hydrocarbons, Biological Sciences, University of Calgary, Calgary, Alberta, 2015.

[44] R.U. Meckenstock, M. Boll, H. Mouttaki, J.S. Koelschbach, P. Cunha Tarouco, P. Weyrauch, X. Dong, A.M. Himmelberg, Anaerobic degradation of benzene and polycyclic aromatic hydrocarbons, Journal of Molecular Microbiology and Biotechnology, 26 (2016) 92-118.

[45] X.-Y. Lu, B. Li, T. Zhang, H.H. Fang, Enhanced anoxic bioremediation of PAHs-contaminated sediment, Bioresource Technology, 104 (2012) 51-58.

[46] L. Lei, A. Khodadoust, M. Suidan, H. Tabak, Biodegradation of sediment-bound PAHs in field-contaminated sediment, Water Research, 39 (2005) 349-361.

[47] J. Sabaté, M. Viñas, A.M. Solanas, Bioavailability assessment and environmental fate of polycyclic aromatic hydrocarbons in biostimulated creosote-contaminated soil, Chemosphere, 63 (2006) 1648-1659.

[48] A.J. Stams, F.A. De Bok, C.M. Plugge, M.H. Van Eekert, J. Dolfing, G. Schraa, Exocellular electron transfer in anaerobic microbial communities, Environmental Microbiology, 8 (2006) 371-382.

[49] D.R. Van Stempvoort, K. Millar, J.R. Lawrence, Accumulation of short-chain fatty acids in an aquitard linked to anaerobic biodegradation of petroleum hydrocarbons, Applied Geochemistry, 24 (2009) 77-85.

[50] S. Kümmel, F.-A. Herbst, A. Bahr, M. Duarte, D.H. Pieper, N. Jehmlich, J. Seifert, M. von Bergen, P. Bombach, H.H. Richnow, Anaerobic naphthalene degradation

by sulfate-reducing Desulfobacteraceae from various anoxic aquifers, FEMS Microbiology Ecology, 91 (2015) 1-13.

[51] J.-C. Tsai, M. Kumar, J.-G. Lin, Anaerobic biotransformation of fluorene and phenanthrene by sulfate-reducing bacteria and identification of biotransformation pathway, Journal of Hazardous Materials, 164 (2009) 847-855.

[52] A. Bahr, A. Fischer, C. Vogt, P. Bombach, Evidence of polycyclic aromatic hydrocarbon biodegradation in a contaminated aquifer by combined application of in situ and laboratory microcosms using 13C-labelled target compounds, Water Research, 69 (2015) 100-109.

[53] S. Gupta, B. Pathak, M. Fulekar, Molecular approaches for biodegradation of polycyclic aromatic hydrocarbon compounds: a review, Reviews in Environmental Science and Bio/Technology, 14 (2015) 241-269.

[54] Z. Zhang, I.M. Lo, Biostimulation of petroleum-hydrocarbon-contaminated marine sediment with co-substrate: involved metabolic process and microbial community, Applied Microbiology and Biotechnology, 99 (2015) 5683-5696.

[55] W. Liamleam, A.P. Annachhatre, Electron donors for biological sulfate reduction, Biotechnology Advances, 25 (2007) 452-463.

[56] Y.T. He, C. Su, Use of Additives in Bioremediation of Contaminated Groundwater and Soil, Advances in Bioremediation of Wastewater and Polluted Soil, InTech, 2015.

[57] R. Gill, M.J. Harbottle, J. Smith, S. Thornton, Electrokinetic-enhanced bioremediation of organic contaminants: A review of processes and environmental applications, Chemosphere, 107 (2014) 31-42.

[58] J.D. Coates, J. Woodward, J. Allen, P. Philp, D.R. Lovley, Anaerobic degradation of polycyclic aromatic hydrocarbons and alkanes in petroleum-contaminated marine harbor sediments, Applied and Environmental Microbiology, 63 (1997) 3589-3593.

[59] R. Ambrosoli, L. Petruzzelli, J.L. Minati, F.A. Marsan, Anaerobic PAH degradation in soil by a mixed bacterial consortium under denitrifying conditions, Chemosphere, 60 (2005) 1231-1236.

[60] J.K.C. Nieman, R.C. Sims, J.E. McLean, J.L. Sims, D.L. Sorensen, Fate of pyrene in contaminated soil amended with alternate electron acceptors, Chemosphere, 44 (2001) 1265-1271.

[61] Y. Wang, R. Wan, S. Zhang, S. Xie, Anthracene biodegradation under nitrate-reducing condition and associated microbial community changes, Biotechnology and Bioprocess Engineering, 17 (2012) 371-376.

[62] J. Dai, X. Zuo, M. Wang, Y. Yao, Z. Zhou, Effect of nitrate amendment on soil denitrification activity and anthracene anaerobic degradation, Chinese Journal of Environmental Science (Huanjing Kexue), 39 (2018) 422-429.

[63] W. Qin, F. Fan, Y. Zhu, X. Huang, A. Ding, X. Liu, J. Dou, Anaerobic biodegradation of benzo (a) pyrene by a novel *Cellulosimicrobium cellulans* CWS2 isolated from polycyclic aromatic hydrocarbon-contaminated soil, Brazilian Journal of Microbiology, 49 (2018) 258-268.

[64] W. Qin, F. Fan, Y. Zhu, Y. Wang, X. Liu, A. Ding, J. Dou, Comparative proteomic analysis and characterization of benzo (a) pyrene removal by Microbacterium sp. strain M. CSW3 under denitrifying conditions, Bioprocess and biosystems engineering, 40 (2017) 1825-1838.

[65] W. Qin, Y. Zhu, F. Fan, Y. Wang, X. Liu, A. Ding, J. Dou, Biodegradation of benzo (a) pyrene by Microbacterium sp. strain under denitrification: degradation pathway and effects of limiting electron acceptors or carbon source, Biochemical Engineering Journal, 121 (2017) 131-138.

[66] Z. Yan, N. Song, H. Cai, J.-H. Tay, H. Jiang, Enhanced degradation of phenanthrene and pyrene in freshwater sediments by combined employment of sediment microbial fuel cell and amorphous ferric hydroxide, Journal of Hazardous Materials, 199 (2012) 217-225.

[67] B. Chang, L. Shiung, S. Yuan, Anaerobic biodegradation of polycyclic aromatic hydrocarbon in soil, Chemosphere, 48 (2002) 717-724.

[68] S.Y. Yuan, B.V. Chang, Anaerobic degradation of five polycyclic aromatic hydrocarbons from river sediment in Taiwan, Journal of Environmental Science and Health Part B, 42 (2007) 63-69.

[69] K.R. Reddy, C. Cameselle, Electrochemical remediation technologies for polluted soils, sediments and groundwater, John Wiley & Sons, 2009.

[70] Y.B. Acar, R.J. Gale, A.N. Alshawabkeh, R.E. Marks, S. Puppala, M. Bricka, R. Parker, Electrokinetic remediation: basics and technology status, Journal of Hazardous Materials, 40 (1995) 117-137.

[71] K. Alaydi, The Application of Electroosmosis in Clay Improvement, Infastructure and Environmental Engineering, Chalmers University of Technology, Gothenburg, Sweden, 2016.

[72] Á.V. Delgado, Interfacial Electrokinetics and Electrophoresis, CRC Press, 2001.

[73] U.N. Da Rocha, M.R. Tótola, D.M.M. Pessoa, J.T.A. Júnior, J.C.L. Neves, A.C. Borges, Mobilisation of bacteria in a fine-grained residual soil by electrophoresis, Journal of hazardous materials, 161 (2009) 485-491.

[74] P. Carter, Coupled electrokinetic - bioremediation: applied aspects, C.C. Krishna R. Reddy (Ed.) Electrochemical Remediation Technologies for Polluted Soils, Sediments and Groundwater, John Wiley & Sons, 2009, p. 389.

[75] E.D. Mattson, R.S. Bowman, E.R. Lindgren, Electrokinetic ion transport through unsaturated soil: 1. Theory, model development, and testing, Journal of Contaminant Hydrology, 54 (2002) 99-120.

[76] W. Xu, C. Wang, H. Liu, Z. Zhang, H. Sun, A laboratory feasibility study on a new electrokinetic nutrient injection pattern and bioremediation of phenanthrene in a clayey soil, Journal of Hazardous Materials, 184 (2010) 798-804.

[77] X.-Y. Lu, T. Zhang, H.H.-P. Fang, Bacteria-mediated PAH degradation in soil and sediment, Applied Microbiology and Biotechnology, 89 (2011) 1357-1371.

[78] Y.J. Tang, S.D. Carpenter, J.W. Deming, B. Krieger-Brockett, Depth-related influences on biodegradation rates of phenanthrene in polluted marine sediments of Puget Sound, WA, Marine Pollution Bulletin, 52 (2006) 1431-1440.

[79] E.M. Ramírez, J.V. Camacho, M.R. Rodrigo, P.C. Cañizares, Feasibility of electrokinetic oxygen supply for soil bioremediation purposes, Chemosphere, 117 (2014) 382-387.

[80] I. Hassan, E. Mohamedelhassan, E.K. Yanful, Z.-C. Yuan, A Review article: Electrokinetic bioremediation Current knowledge and new prospects, Advances in Microbiology, 6 (2016) 57.

[81] K.J. Rockne, S.E. Strand, Biodegradation of bicyclic and polycyclic aromatic hydrocarbons in anaerobic enrichments, Environmental Science & Technology, 32 (1998) 3962-3967.

[82] I. Zawierucha, G. Malina, Effects of oxygen supply on the biodegradation rate in oil hydrocarbons contaminated soil, Journal of Physics: Conference Series, 289 (2011) 012035.

[83] B. Kumari, S. Rajput, P. Gaur, S. Singh, D. Singh, Biodegradation of pyrene and phenanthrene by bacterial consortium and evaluation of role of surfactant, Cellular & Molecular Biology, 60 (2014) 22-28.

[84] L.F. Bautista, R. Sanz, M.C. Molina, N. González, D. Sánchez, Effect of different non-ionic surfactants on the biodegradation of PAHs by diverse aerobic bacteria, International Biodeterioration & Biodegradation, 63 (2009) 913-922.

[85] Y.-T. Chang, C.-H. Hung, H.-L. Chou, Effects of polyethoxylate lauryl ether (Brij 35) addition on phenanthrene biodegradation in a soil/water system, Journal of Environmental Science and Health, Part A, 49 (2014) 1672-1684.

[86] G.A. Husseini, W.G. Pitt, Micelles and nanoparticles for ultrasonic drug and gene delivery, Advanced Drug Delivery Reviews, 60 (2008) 1137-1152.

[87] S. Boonchan, M.L. Britz, G.A. Stanley, Surfactant-enhanced biodegradation of high molecular weight polycyclic aromatic hydrocarbons by Stenotrophomonas maltophilia, Biotechnology and Bioengineering, 59 (1998) 482-494.

[88] A.C. Adrion, J. Nakamura, D. Shea, M.D. Aitken, Screening nonionic surfactants for enhanced biodegradation of polycyclic aromatic hydrocarbons remaining in soil after conventional biological treatment, Environmental Science & Technology, 50 (2016) 3838-3845.

[89] K.A. Bourbonais, G.C. Compeau, L.K. MacClellan, Evaluating effectiveness of in situ soil flushing with surfactants, ACS Publications, 1995.

[90] N. Cicek, R. Govind, Micellar enhanced electrokinetic remediation of contaminated soils, Water Environment Federation (WEFTEC) Conference Proceedings, 70th Annual Conf. Exposition Chicago, 1997, p. 89-100.

[91] R.E. Saichek, K.R. Reddy, Electrokinetically enhanced remediation of hydrophobic organic compounds in soils: a review, Critical Reviews in Environmental Science and Technology, 35 (2005) 115-192.

[92] J.-L. Niqui-Arroyo, J.-J. Ortega-Calvo, Effect of electrokinetics on the bioaccessibility of polycyclic aromatic hydrocarbons in polluted soils, Journal of environmental quality, 39 (2010) 1993-1998.

[93] D.G. Brown, P.R. Jaffé, Effects of nonionic surfactants on bacterial transport through porous media, Environmental Science & Technology, 35 (2001) 3877-3883.

[94] L.Y. Wick, P.A. Mattle, P. Wattiau, H. Harms, Electrokinetic transport of PAH-degrading bacteria in model aquifers and soil, Environmental Science & Technology, 38 (2004) 4596-4602.

[95] A. Jamshidi-Zanjani, A. Khodadadi Darban, A review on enhancement techniques of electrokinetic soil remediation, Pollution, 3 (2017) 157-166.

[96] J. de Boer, M. Wagelmans, Polycyclic aromatic hydrocarbons in soil–practical options for remediation, CLEAN–Soil, Air, Water, 44 (2016) 648-653.

[97] I.B. Ivshina, M.S. Kuyukina, A.V. Krivoruchko, A.A. Elkin, S.O. Makarov, C.J. Cunningham, T.A. Peshkur, R.M. Atlas, J.C. Philp, Oil spill problems and sustainable response strategies through new technologies, Environmental Science: Processes & Impacts, 17 (2015) 1201-1219.

[98] P. Eckle, P. Burgherr, E. Michaux, Risk of large oil spills: a statistical analysis in the aftermath of Deepwater Horizon, Environmental Science & Technology, 46 (2012) 13002-13008.

[99] Science for Environment Policy: Highest risk for severe oil spills from exploration and production, T.U.o.t.W.o.E. SCU, Bristol (Ed.), European Commision DG, Environment News Alert Service, 2013.

[100] J. Xue, Y. Yu, Y. Bai, L. Wang, Y. Wu, Marine oil-degrading microorganisms and biodegradation process of petroleum hydrocarbon in marine environments: a review, Current Microbiology, 71 (2015) 220-228.

[101] L. Cheng, S. Shi, Q. Li, J. Chen, H. Zhang, Y. Lu, Progressive degradation of crude oil n-alkanes coupled to methane production under mesophilic and thermophilic conditions, PLOS One, 9 (2014) e113253.

[102] A.J. Kuhl, J.A. Nyman, M.D. Kaller, C.C. Green, Dispersant and salinity effects on weathering and acute toxicity of South Louisiana crude oil, Environmental Toxicology and Chemistry, 32 (2013) 2611-2620.

[103] B. Thapa, A.K. Kc, A. Ghimire, A review on bioremediation of petroleum hydrocarbon contaminants in soil, Kathmandu University Journal of Science, Engineering and Technology, 8 (2012) 164-170.

[104] E.Z. Ron, E. Rosenberg, Enhanced bioremediation of oil spills in the sea, Current Opinion in Biotechnology, 27 (2014) 191-194.

[105] Y. Xia, M.C. Boufadel, Beach geomorphic factors for the persistence of subsurface oil from the Exxon Valdez spill in Alaska, Environmental Monitoring and Assessment, 183 (2011) 5-21.

[106] D.S. Page, P.D. Boehm, J.S. Brown, E.R. Gundlach, J.M. Neff, Fate of oil on shorelines, Oil in the Environment: Legacies and Lessons of the Exxon Valdez Oil Spill, (2013) 116-143.

[107] R.C. Prince, Petroleum spill bioremediation in marine environments, Critical Reviews in Microbiology, 19 (1993) 217-240.

[108] R.U. Meckenstock, H. Mouttaki, Anaerobic degradation of non-substituted aromatic hydrocarbons, Current opinion in biotechnology, 22 (2011) 406-414.

[109] E.B. Overton, T.L. Wade, J.R. Radović, B.M. Meyer, M.S. Miles, S.R. Larter, Chemical composition of Macondo and other crude oils and compositional alterations during oil spills, Oceanography, 29 (2016) 50-63.

[110] O.O. Alegbeleye, B.O. Opeolu, V.A. Jackson, Polycyclic aromatic hydrocarbons: a critical review of environmental occurrence and bioremediation, Environmental Management, 60 (2017) 758-783.

[111] K.Y. Maillacheruvu, I.A. Pathan, Biodegradation of naphthalene, phenanthrene, and pyrene under anaerobic conditions, Journal of environmental science and health. Part A, Toxic/hazardous Substances & Environmental Engineering, 44 (2009) 1315-1326.

[112] J. Heider, A.M. Spormann, H.R. Beller, F. Widdel, Anaerobic bacterial metabolism of hydrocarbons, FEMS Microbiology Reviews, 22 (1998) 459-473.

[113] M.E. Caldwell, R.M. Garrett, R.C. Prince, J.M. Suflita, Anaerobic biodegradation of long-chain n-alkanes under sulfate-reducing conditions, Environmental Science & Technology, 32 (1998) 2191-2195.

[114] J. Foght, Anaerobic biodegradation of aromatic hydrocarbons: pathways and prospects, Journal of Molecular Microbiology and Biotechnology, 15 (2008) 93-120.

[115] A. Greene, M. Wright, H. Aldosary, Bacterial diversity and metal reducing bacteria in Australian thermal environments, Microbes in the Spotlight: Recent Progress in the Understanding of Beneficial and Harmful Microorganisms, (2016) 32.

[116] A.R. Johnsen, L.Y. Wick, H. Harms, Principles of microbial PAH-degradation in soil, Environmental Pollution, 133 (2005) 71-84.

[117] F. Widdel, R. Rabus, Anaerobic biodegradation of saturated and aromatic hydrocarbons, Current opinion in biotechnology, 12 (2001) 259-276.

[118] R. Karthikeyan, A. Bhandari, Anaerobic biotransformation of aromatic and polycyclic aromatic hydrocarbons in soil microcosms: a review, Journal of Hazardous Substance Research, 3 (2001) 3.

[119] U. Jaekel, J. Zedelius, H. Wilkes, F. Musat, Anaerobic degradation of cyclohexane by sulfate-reducing bacteria from hydrocarbon-contaminated marine sediments, Frontiers in Microbiology, 6 (2015) 116.

[120] A. Haritash, C. Kaushik, Biodegradation aspects of polycyclic aromatic hydrocarbons (PAHs): a review, Journal of Hazardous Materials, 169 (2009) 1-15.

[121] J. Chen, H. Zhang, H. Huang, X. Li, S. Shi, F. Liu, L. Chen, Impact of anaerobic biodegradation on alkylphenanthrenes in crude oil, Organic Geochemistry, 61 (2013) 6-14.

[122] L.A. Hayes, K.P. Nevin, D.R. Lovley, Role of prior exposure on anaerobic degradation of naphthalene and phenanthrene in marine harbor sediments, Organic Geochemistry, 30 (1999) 937-945.

[123] E. Díaz, Bacterial degradation of aromatic pollutants: a paradigm of metabolic versatility, International Microbiology, 7 (2004) 173-180.

[124] H.L. Bohn, R.A. Myer, G.A. O'Connor, Soil chemistry, John Wiley & Sons, 2002.

[125] N. Abu Laban, D. Selesi, C. Jobelius, R.U. Meckenstock, Anaerobic benzene degradation by Gram-positive sulfate-reducing bacteria, FEMS Microbiology Ecology, 68 (2009) 300-311.

[126] J. Dou, X. Liu, Z. Hu, D. Deng, Anaerobic BTEX biodegradation linked to nitrate and sulfate reduction, Journal of Hazardous Materials, 151 (2008) 720-729.

[127] J.-C. Tsai, M. Kumar, S.-M. Chang, J.-G. Lin, Determination of optimal phenanthrene, sulfate and biomass concentrations for anaerobic biodegradation of phenanthrene by sulfate-reducing bacteria and elucidation of metabolic pathway, Journal of Hazardous Materials, 171 (2009) 1112-1119.

[128] C.J. Plante, Importance of the sedimentary matrix for anaerobic oil degradation by marine bacterial assemblages, Bioremediation Journal, 11 (2007) 155-163.

[129] J.M. Yagi, J.M. Suflita, L.M. Gieg, C.M. DeRito, C.-O. Jeon, E.L. Madsen, Subsurface cycling of nitrogen and anaerobic aromatic hydrocarbon biodegradation revealed by nucleic acid and metabolic biomarkers, Applied and Environmental Microbiology, 76 (2010) 3124-3134.

[130] J. Zedelius, R. Rabus, O. Grundmann, I. Werner, D. Brodkorb, F. Schreiber, P. Ehrenreich, A. Behrends, H. Wilkes, M. Kube, Alkane degradation under anoxic conditions by a nitrate-reducing bacterium with possible involvement of the electron acceptor in substrate activation, Environmental Microbiology Reports, 3 (2011) 125-135.

[131] A.A. Langenhoff, A.J. Zehnder, G. Schraa, Behaviour of toluene, benzene and naphthalene under anaerobic conditions in sediment columns, Biodegradation, 7 (1996) 267-274.

[132] S.M. Burland, E.A. Edwards, Anaerobic benzene biodegradation linked to nitrate reduction, Applied and Environmental Microbiology, 65 (1999) 529-533.

[133] R. Rabus, F. Widdel, Anaerobic degradation of ethylbenzene and other aromatic hydrocarbons by new denitrifying bacteria, Archives of Microbiology, 163 (1995) 96-103.

[134] S.A. Weelink, M.H. Van Eekert, A.J. Stams, Degradation of BTEX by anaerobic bacteria: physiology and application, Reviews in Environmental Science and Bio/Technology, 9 (2010) 359-385.

[135] X. Lu, T. Zhang, H.H.-P. Fang, K.M. Leung, G. Zhang, Biodegradation of naphthalene by enriched marine denitrifying bacteria, International Biodeterioration & Biodegradation, 65 (2011) 204-211.

[136] X. Yang, J. Ye, L. Lyu, Q. Wu, R. Zhang, Anaerobic biodegradation of pyrene by Paracoccus denitrificans under various nitrate/nitrite-reducing conditions, Water, Air, & Soil Pollution, 224 (2013) 1-10.

[137] X. Yang, Z. Chen, Q. Wu, M. Xu, Enhanced phenanthrene degradation in river sediments using a combination of biochar and nitrate, Science of The Total Environment, 619 (2018) 600-605.

[138] S. Yuan, C. Yu, B. Chang, Biodegradation of nonylphenol in river sediment, Environmental Pollution, 127 (2004) 425-430.

[139] Z. Wang, Y. Yang, Y. Dai, S. Xie, Anaerobic biodegradation of nonylphenol in river sediment under nitrate-or sulfate-reducing conditions and associated bacterial community, Journal of Hazardous Materials, 286 (2015) 306-314.

[140] J.P. De Weert, M. Vinas, T. Grotenhuis, H.H. Rijnaarts, A.A. Langenhoff, Degradation of 4-n-nonylphenol under nitrate reducing conditions, Biodegradation, 22 (2011) 175-187.

[141] C. Dorer, C. Vogt, T.R. Neu, H. Stryhanyuk, H.H. Richnow, Characterization of toluene and ethylbenzene biodegradation under nitrate-, iron(III)- and manganese(IV)-reducing conditions by compound-specific isotope analysis, Environmental Pollution, 211 (2016) 271-281.

[142] J.D. Coates, R.T. Anderson, J.C. Woodward, E.J. Phillips, D.R. Lovley, Anaerobic hydrocarbon degradation in petroleum-contaminated harbor sediments under sulfate-reducing and artificially imposed iron-reducing conditions, Environmental Science & Technology, 30 (1996) 2784-2789.

[143] U. Kunapuli, T. Lueders, R.U. Meckenstock, The use of stable isotope probing to identify key iron-reducing microorganisms involved in anaerobic benzene degradation, The ISME journal, 1 (2007) 643-653.

[144] L.M. Gieg, S.J. Fowler, C. Berdugo-Clavijo, Syntrophic biodegradation of hydrocarbon contaminants, Current Opinion in Biotechnology, 27 (2014) 21-29.

[145] N. Abu Laban, D. Selesi, T. Rattei, P. Tischler, R.U. Meckenstock, Identification of enzymes involved in anaerobic benzene degradation by a strictly anaerobic iron-reducing enrichment culture, Environmental Microbiology, 12 (2010) 2783-2796.

[146] L. Zhuang, J. Tang, Y. Wang, M. Hu, S. Zhou, Conductive iron oxide minerals accelerate syntrophic cooperation in methanogenic benzoate degradation, Journal of Hazardous Materials, 293 (2015) 37-45.

[147] R. Kleemann, R.U. Meckenstock, Anaerobic naphthalene degradation by Gram-positive, iron-reducing bacteria, FEMS Microbiology Ecology, 78 (2011) 488-496.

[148] S. Marozava, H. Mouttaki, H. Müller, N.A. Laban, A.J. Probst, R.U. Meckenstock, Anaerobic degradation of 1-methylnaphthalene by a member of the Thermoanaerobacteraceae contained in an iron-reducing enrichment culture, Biodegradation, 29 (2018) 23-39.

[149] J.B. Müller, D.T. Ramos, C. Larose, M. Fernandes, H.S. Lazzarin, T.M. Vogel, H.X. Corseuil, Combined iron and sulfate reduction biostimulation as a novel approach to enhance BTEX and PAH source-zone biodegradation in biodiesel blend-contaminated groundwater, Journal of Hazardous Materials, 326 (2017) 229-236.

[150] W. Villatoro-Monzón, A. Mesta-Howard, E. Razo-Flores, Anaerobic biodegradation of BTEX using Mn (IV) and Fe (III) as alternative electron acceptors, Water Science & Technology, 48 (2003) 125-131.

[151] W.R. Villatoro-Monzón, M.G. Morales-Ibarria, E.K. Velázquez, H. Ramírez-Saad, E. Razo-Flores, Benzene biodegradation under anaerobic conditions coupled with metal oxides reduction, Water, Air, and Soil Pollution, 192 (2008) 165-172.

[152] C.W. Yeung, D.R. Van Stempvoort, J. Spoelstra, G. Bickerton, J. Voralek, C.W. Greer, Bacterial community evidence for anaerobic degradation of petroleum hydrocarbons in cold climate groundwater, Cold Regions Science and Technology, 86 (2013) 55-68.

[153] X. Li, X. Wang, L. Wan, Y. Zhang, N. Li, D. Li, Q. Zhou, Enhanced biodegradation of aged petroleum hydrocarbons in soils by glucose addition in microbial fuel cells, Journal of Chemical Technology & Biotechnology, 91 (2016) 267-275.

[154] A. Paulo, A.F. Salvador, J. Alves, R. Castro, A. Langenhoff, A.J.M. Stams, A.J. Cavaleiro, Enhancement of methane production from 1-hexadecene by additional electron donors, Microbial Biotechnology, 11 (2018) 657-666.

[155] S. Yuan, S. Wei, B. Chang, Biodegradation of polycyclic aromatic hydrocarbons by a mixed culture, Chemosphere, 41 (2000) 1463-1468.

[156] B.-V. Chang, I. Chang, S. Yuan, Anaerobic degradation of phenanthrene and pyrene in mangrove sediment, Bulletin of Environmental Contamination and Toxicology, 80 (2008) 145-149.

[157] J.D. Coates, K.A. Cole, R. Chakraborty, S.M. O'Connor, L.A. Achenbach, Diversity and ubiquity of bacteria capable of utilizing humic substances as electron donors for anaerobic respiration, Applied and Environmental Microbiology, 68 (2002) 2445-2452.

[158] T.-W. Cheng, L.-H. Lin, Y.-T. Lin, S.-R. Song, P.-L. Wang, Temperature-dependent variations in sulfate-reducing communities associated with a terrestrial hydrocarbon seep, Microbes and Environments, 29 (2014) 377.

[159] Y. Higashioka, H. Kojima, M. Fukui, Temperature-dependent differences in community structure of bacteria involved in degradation of petroleum hydrocarbons under sulfate-reducing conditions, Journal of Applied Microbiology, 110 (2011) 314-322.

[160] C. Cravo-Laureau, R. Matheron, J.-L. Cayol, C. Joulian, A. Hirschler-Rea, Desulfatibacillum aliphaticivorans gen. nov., sp. nov., an n-alkane-and n-alkene-degrading, sulfate-reducing bacterium, International Journal of Systematic and Evolutionary Microbiology, 54 (2004) 77-83.

[161] R. Alex, Bioremediation of Hydrocarbons by Lysinibacillus fusiformis BTTS10, Cochin University of Science and Technology, 2012.

[162] E.G. Roussel, B.A. Cragg, G. Webster, H. Sass, X. Tang, A.S. Williams, R. Gorra, A.J. Weightman, R.J. Parkes, Complex coupled metabolic and prokaryotic community responses to increasing temperatures in anaerobic marine sediments: critical temperatures and substrate changes, FEMS Microbiology Ecology, 91 (2015) fiv084.

[163] L. Michaud, A.L. Giudice, M. Saitta, M. De Domenico, V. Bruni, The biodegradation efficiency on diesel oil by two psychrotrophic Antarctic marine bacteria during a two-month-long experiment, Marine Pollution Bulletin, 49 (2004) 405-409.

[164] C. Knoblauch, B.B. Jørgensen, Effect of temperature on sulphate reduction, growth rate and growth yield in five psychrophilic sulphate-reducing bacteria from Arctic sediments, Environmental Microbiology, 1 (1999) 457-467.

[165] S.M. Powell, S.H. Ferguson, I. Snape, S.D. Siciliano, Fertilization stimulates anaerobic fuel degradation of Antarctic soils by denitrifying microorganisms, Environmental science & technology, 40 (2006) 2011-2017.

[166] X.B. Wang, C.Q. Chi, Y. Nie, Y.Q. Tang, Y. Tan, G. Wu, X.L. Wu, Degradation of petroleum hydrocarbons (C6-C40) and crude oil by a novel Dietzia strain, Bioresource Technology, 102 (2011) 7755-7761.

[167] O. Lefebvre, S. Quentin, M. Torrijos, J. Godon, J. Delgenes, R. Moletta, Impact of increasing NaCl concentrations on the performance and community composition of two anaerobic reactors, Applied Microbiology and Biotechnology, 75 (2007) 61-69.

[168] L. Liang, X. Song, J. Kong, C. Shen, T. Huang, Z. Hu, Anaerobic biodegradation of high-molecular-weight polycyclic aromatic hydrocarbons by a facultative anaerobe Pseudomonas sp. JP1, Biodegradation, 25 (2014) 825-833.

[169] D.M. Al-Mailem, M. Eliyas, S.S. Radwan, Ferric sulfate and proline enhanced heavy-metal tolerance of halophilic/halotolerant soil microorganisms and their

bioremediation potential for spilled-oil under multiple stresses, Frontiers in Microbiology, 9 (2018) 394.

[170] T. Brusa, S. Borin, F. Ferrari, C. Sorlini, C. Corselli, D. Daffonchio, Aromatic hydrocarbon degradation patterns and catechol 2,3-dioxygenase genes in microbial cultures from deep anoxic hypersaline lakes in the eastern Mediterranean sea, Microbiological Research, 156 (2001) 49-58.

[171] V. Grossi, C. Cravo-Laureau, R. Guyoneaud, A. Ranchou-Peyruse, A. Hirschler-Réa, Metabolism of n-alkanes and n-alkenes by anaerobic bacteria: a summary, Organic Geochemistry, 39 (2008) 1197-1203.

[172] R. Rabus, M. Boll, J. Heider, R.U. Meckenstock, W. Buckel, O. Einsle, U. Ermler, B.T. Golding, R.P. Gunsalus, P.M. Kroneck, Anaerobic microbial degradation of hydrocarbons: from enzymatic reactions to the environment, Journal of Molecular Microbiology and Biotechnology, 26 (2016) 5-28.

[173] S. Kleindienst, F.-A. Herbst, M. Stagars, F. Von Netzer, M. Von Bergen, J. Seifert, J. Peplies, R. Amann, F. Musat, T. Lueders, Diverse sulfate-reducing bacteria of the Desulfosarcina/Desulfococcus clade are the key alkane degraders at marine seeps, The ISME Journal, 8 (2014) 2029.

[174] W. Huang, C. Kao, Bioremediation of petroleum-hydrocarbon contaminated groundwater under sulfate-reducing conditions: effectiveness and mechanism study, Journal of Environmental Engineering, 142 (2015) 04015089.

[175] A.G. Dickson, C. Goyet, Handbook of methods for the analysis of the various parameters of the carbon dioxide system in sea water, ORNL/CDIAC-74, 107 (1994).

[176] Y. Chen, J.J. Cheng, K.S. Creamer, Inhibition of anaerobic digestion process: a review, Bioresource Technology, 99 (2008) 4044-4064.

[177] E. Beauchamp, J. Trevors, J. Paul, Carbon sources for bacterial denitrification, Advances in Soil Science, Springer, 1989, p. 113-142.

[178] S. Ge, Y. Peng, S. Wang, C. Lu, X. Cao, Y. Zhu, Nitrite accumulation under constant temperature in anoxic denitrification process: The effects of carbon sources and COD/NO3-N, Bioresource Technology, 114 (2012) 137-143.

[179] T. Bregnard, A. Haner, P. Hohener, J. Zeyer, Anaerobic degradation of pristane in nitrate-reducing microcosms and enrichment cultures, Applied and Environmental Microbiology, 63 (1997) 2077-2081.

[180] S. Atashgahi, B. Hornung, M.J. Waals, U.N. Rocha, F. Hugenholtz, B. Nijsse, D. Molenaar, R. Spanning, A.J. Stams, J. Gerritse, A benzene-degrading nitrate-reducing microbial consortium displays aerobic and anaerobic benzene degradation pathways, Scientific Reports, 8 (2018) 4490.

[181] A. Aburto-Medina, A.S. Ball, Microorganisms involved in anaerobic benzene degradation, Annals of Microbiology, 65 (2015) 1201-1213.

[182] A.H. Keller, S. Kleinsteuber, C. Vogt, Anaerobic benzene mineralization by nitrate-reducing and sulfate-reducing microbial consortia enriched from the same site: Comparison of community composition and degradation characteristics, Microbial Ecology, 75 (2018) 941-953.

[183] M.J. van der Waals, S. Atashgahi, U.N. Da Rocha, B.M. van der Zaan, H. Smidt, J. Gerritse, Benzene degradation in a denitrifying biofilm reactor: activity and microbial community composition, Applied Microbiology and Biotechnology, 101 (2017) 5175-5188.

[184] R. Chakraborty, J. Coates, Anaerobic degradation of monoaromatic hydrocarbons, Applied Microbiology and Biotechnology, 64 (2004) 437-446.

[185] J. Heider, M. Szaleniec, K. Sünwoldt, M. Boll, Ethylbenzene dehydrogenase and related molybdenum enzymes involved in oxygen-independent alkyl chain hydroxylation, Journal of Molecular Microbiology and Biotechnology, 26 (2016) 45-62.

[186] M. Boll, Dearomatizing benzene ring reductases, Journal of Molecular Microbiology and Biotechnology, 10 (2005) 132-142.

[187] M. Sperfeld, G. Diekert, S. Studenik, Community dynamics in a nitrate-reducing microbial consortium cultivated with p-alkylated vs. non-p-alkylated aromatic compounds, FEMS Microbiology Ecology, (2018).

[188] A.-E. Rotaru, C. Probian, H. Wilkes, J. Harder, Highly enriched Betaproteobacteria growing anaerobically with p-xylene and nitrate, FEMS Microbiology Ecology, 71 (2010) 460-468.

[189] S. Herrmann, C. Vogt, A. Fischer, A. Kuppardt, H.H. Richnow, Characterization of anaerobic xylene biodegradation by two-dimensional isotope fractionation analysis, Environmental Microbiology Reports, 1 (2009) 535-544.

[190] R.U. Meckenstock, R.J. Warthmann, W. Schäfer, Inhibition of anaerobic microbial o-xylene degradation by toluene in sulfidogenic sediment columns and pure cultures, FEMS Microbiology Ecology, 47 (2004) 381-386.

[191] R. Ambrosoli, L. Petruzzelli, J. Luis Minati, F. Ajmone Marsan, Anaerobic PAH degradation in soil by a mixed bacterial consortium under denitrifying conditions, Chemosphere, 60 (2005) 1231-1236.

[192] A. Langenhoff, Biodegradation of toluene, benzene and naphthalene under anaerobic conditions, Laboratory of Microbiology, (1997) 131.

[193] J. Dou, X. Liu, A. Ding, Anaerobic degradation of naphthalene by the mixed bacteria under nitrate reducing conditions, Journal of Hazardous Materials, 165 (2009) 325-331.

[194] J.R. Mihelcic, R.G. Luthy, Microbial degradation of acenaphthene and naphthalene under denitrification conditions in soil-water systems, Applied and Environmental Microbiology, 54 (1988) 1188-1198.

[195] C. Anyika, Z.A. Majid, Z. Ibrahim, M.P. Zakaria, A. Yahya, The impact of biochars on sorption and biodegradation of polycyclic aromatic hydrocarbons in soils—a review, Environmental Science and Pollution Research, 22 (2015) 3314-3341.

[196] S. Chen, A.-E. Rotaru, P.M. Shrestha, N.S. Malvankar, F. Liu, W. Fan, K.P. Nevin, D.R. Lovley, Promoting interspecies electron transfer with biochar, Scientific reports, 4 (2014) 5019.

[197] M. Zwolinski, R. Harris, W. Hickey, Microbial consortia involved in the anaerobicdegradation of hydrocarbons, Biodegradation, 11 (2000) 141-158.

[198] B. Chang, J. Chang, S. Yuan, Degradation of phenanthrene in river sediment under nitrate-reducing conditions, Bulletin of Environmental Contamination and Toxicology, 67 (2001) 898-905.

[199] M. Elliott, Polycyclic Aromatic Hydrocarbons and Redox Parameters in a Creosote-Contaminated Aquifer, Master's Thesis. Virginia Tech, 2001.

[200] K. Hidaka, K. Miyanaga, Y. Tanji, The presence of nitrate-and sulfate-reducing bacteria contributes to ineffectiveness souring control by nitrate injection, International Biodeterioration & Biodegradation, (2018).

[201] S.J. Varjani, Microbial degradation of petroleum hydrocarbons, Bioresource Technology, 223 (2017) 277-286.

[202] T.P.A. Bregnard, P. Höhener, J. Zeyer, Bioavailability and biodegradation of weathered diesel fuel in aquifer material under denitrifying conditions, Environmental Toxicology and Chemistry, 17 (1998) 1222-1229.

[203] J.P. Pietroski, J.R. White, R.D. DeLaune, J.J. Wang, S.K. Dodla, Fresh and weathered crude oil effects on potential denitrification rates of coastal marsh soil, Chemosphere, 134 (2015) 120-126.

[204] F. Musat, H. Wilkes, A. Behrends, D. Woebken, F. Widdel, Microbial nitrate-dependent cyclohexane degradation coupled with anaerobic ammonium oxidation, The ISME journal, 4 (2010) 1290-1301.

[205] Q. He, Z. He, D.C. Joyner, M. Joachimiak, M.N. Price, Z.K. Yang, H.-C.B. Yen, C.L. Hemme, W. Chen, M.M. Fields, Impact of elevated nitrate on sulfate-

reducing bacteria: a comparative study of Desulfovibrio vulgaris, The ISME Journal, 4 (2010) 1386.

[206] T.P. Van den Brand, K. Roest, G.-H. Chen, D. Brdjanovic, M.C. van Loosdrecht, Effects of chemical oxygen demand, nutrients and salinity on sulfate-reducing bacteria, Environmental Engineering Science, 32 (2015) 858-864.

[207] C. Hubert, G. Voordouw, Oil field souring control by nitrate-reducing Sulfurospirillum spp. that outcompete sulfate-reducing bacteria for organic electron donors, Applied and Environmental Microbiology, 73 (2007) 2644-2652.

[208] K. Londry, J. Suflita, Use of nitrate to control sulfide generation by sulfate-reducing bacteria associated with oily waste, Journal of Industrial Microbiology & Biotechnology, 22 (1999) 582-589.

[209] C.M. Callbeck, A. Agrawal, G. Voordouw, Acetate production from oil under sulfate-reducing conditions in bioreactors injected with sulfate and nitrate, Applied and Environmental Microbiology, (2013) AEM. 01251-01213.

[210] S. Dev, A.K. Patra, A. Mukherjee, J. Bhattacharya, Suitability of different growth substrates as source of nitrogen for sulfate reducing bacteria, Biodegradation, 26 (2015) 415-430.

[211] M. Schaechter, Encyclopedia of Microbiology, Academic Press, 2009.

[212] T.J. Boyd, D.C. Smith, J.K. Apple, L.J. Hamdan, C.L. Osburn, M.T. Montgomery, Evaluating PAH biodegradation relative to total bacterial carbon demand in coastal ecosystems: Are PAHs truly recalcitrant?, Microbial Ecology Research Trends, (2008) 1-38.

[213] M.A. Robinson-Lora, R.A. Brennan, The use of crab-shell chitin for biological denitrification: batch and column tests, Bioresource Technology, 100 (2009) 534-541.

[214] B.-T. Wong, D.-J. Lee, Sulfide enhances methanogenesis in nitrate-containing methanogenic cultures, Bioresource Technology, 102 (2011) 2427-2432.

[215] Z. Zhang, I.M. Lo, D.Y. Yan, An integrated bioremediation process for petroleum hydrocarbons removal and odor mitigation from contaminated marine sediment, Water research, 83 (2015) 21-30.

[216] D.R. Lovley, Dissimilatory metal reduction: from early life to bioremediation, ASM News, 68 (2002) 231-237.

[217] O.V. Singh, Bio-pigmentation and Biotechnological Implementations, John Wiley & Sons, 2017.

[218] D. Jun, M. Xiaolan, L. Jingjie, Removal of aromatic hydrocarbons from aquifers by oxidation coupled with dissimilatory bacterial reduction of iron, Chemistry and Technology of Fuels and Oils, 49 (2013) 70-80.

[219] Y.N. Vodyanitskii, Iron compounds and oil biodegradation in overmoistened contaminated soils: a review of publications, Eurasian Soil Science, 44 (2011) 1250.

[220] D.R. Lovley, D.J. Lonergan, Anaerobic oxidation of toluene, phenol, and p-cresol by the dissimilatory iron-reducing organism, GS-15, Applied and Environmental Microbiology, 56 (1990) 1858-1864.

[221] D.R. Lovley, S.J. Giovannoni, D.C. White, J.E. Champine, E. Phillips, Y.A. Gorby, S. Goodwin, Geobacter metallireducens gen. nov. sp. nov., a microorganism capable of coupling the complete oxidation of organic compounds to the reduction of iron and other metals, Archives of Microbiology, 159 (1993) 336-344.

[222] T. Zhang, T.S. Bain, K.P. Nevin, M.A. Barlett, D.R. Lovley, Anaerobic benzene oxidation by Geobacter species, Applied and Environmental Microbiology, (2012) AEM. 02469-02412.

[223] J.D. Coates, V.K. Bhupathiraju, L.A. Achenbach, M. Mclnerney, D.R. Lovley, Geobacter hydrogenophilus, Geobacter chapellei and Geobacter grbiciae, three new, strictly anaerobic, dissimilatory Fe (III)-reducers, International Journal of Systematic and Evolutionary Microbiology, 51 (2001) 581-588.

[224] U. Kunapuli, M.K. Jahn, T. Lueders, R. Geyer, H.J. Heipieper, R.U. Meckenstock, Desulfitobacterium aromaticivorans sp. nov. and Geobacter toluenoxydans sp. nov., iron-reducing bacteria capable of anaerobic degradation of monoaromatic hydrocarbons, International Journal of Systematic and Evolutionary Microbiology, 60 (2010) 686-695.

[225] S.A. Weelink, W. van Doesburg, F.T. Saia, W.I. Rijpstra, W.F. Roling, H. Smidt, A.J. Stams, A strictly anaerobic betaproteobacterium Georgfuchsia toluolica gen. nov., sp. nov. degrades aromatic compounds with Fe(III), Mn(IV) or nitrate as an electron acceptor, FEMS Microbiology Ecology, 70 (2009) 575-585.

[226] D.E. Holmes, C. Risso, J.A. Smith, D.R. Lovley, Anaerobic oxidation of benzene by the hyperthermophilic archaeon Ferroglobus placidus, Applied and Environmental Microbiology, (2011) AEM. 05452-05411.

[227] K.L. Straub, M. Benz, B. Schink, F. Widdel, Anaerobic, nitrate-dependent microbial oxidation of ferrous iron, Applied and Environmental Microbiology, 62 (1996) 1458-1460.

[228] U. Kunapuli, C. Griebler, H.R. Beller, R.U. Meckenstock, Identification of intermediates formed during anaerobic benzene degradation by an iron-reducing enrichment culture, Environmental Microbiology, 10 (2008) 1703-1712.

[229] M.E. Caldwell, J.M. Suflita, Detection of phenol and benzoate as intermediates of anaerobic benzene biodegradation under different terminal electron-accepting conditions, Environmental Science & Technology, 34 (2000) 1216-1220.

[230] C.H. Li, Y.S. Wong, N.F. Tam, Anaerobic biodegradation of polycyclic aromatic hydrocarbons with amendment of iron(III) in mangrove sediment slurry, Bioresource Technology, 101 (2010) 8083-8092.

[231] A.M. Gounot, Microbial oxidation and reduction of manganese: consequences in groundwater and applications, FEMS Microbiology Reviews, 14 (1994) 339-349.

[232] P.-L. Tremblay, T. Zhang, Functional genomics of metal-eeducing microbes degrading hydrocarbons, Anaerobic Utilization of Hydrocarbons, Oils, and Lipids, (2017) 1-21.

[233] A.A. Langenhoff, D.L. Brouwers-Ceiler, J.H. Engelberting, J.J. Quist, J.G. Wolkenfelt, A.J. Zehnder, G. Schraa, Microbial reduction of manganese coupled to toluene oxidation, FEMS Microbiology Ecology, 22 (1997) 119-127.

[234] Y. Xie, H. Dong, G. Zeng, L. Tang, Z. Jiang, C. Zhang, J. Deng, L. Zhang, Y. Zhang, The interactions between nanoscale zero-valent iron and microbes in the subsurface environment: a review, Journal of Hazardous Materials, 321 (2017) 390-407.

[235] N. Jiménez, B.E.L. Morris, M. Cai, F. Gründger, J. Yao, H.H. Richnow, M. Krüger, Evidence for in situ methanogenic oil degradation in the Dagang oil field, Organic Geochemistry, 52 (2012) 44-54.

[236] E.N. Chirwa, Y.-T. Wang, Simultaneous chromium (VI) reduction and phenol degradation in an anaerobic consortium of bacteria, Water Research, 34 (2000) 2376-2384.

[237] M.E. Khayat, M.F.A. Rahman, M.S. Shukor, S.A. Ahmad, N.A. Shamaan, M.Y. Shukor, Characterization of a molybdenum-reducing Bacillus sp. strain khayat with the ability to grow on SDS and diesel, Rendiconti Lincei, 27 (2016) 547-556.

[238] M.J. McInerney, J.R. Sieber, R.P. Gunsalus, Syntrophy in anaerobic global carbon cycles, Current opinion in biotechnology, 20 (2009) 623-632.

[239] A. Nzila, Biodegradation of high-molecular-weight polycyclic aromatic hydrocarbons under anaerobic conditions: Overview of studies, proposed pathways and future perspectives, Environmental Pollution, 239 (2018) 788-802.

[240] T. Sayara, M. Čvančarová, T. Cajthaml, M. Sarrà, A. Sánchez, Anaerobic bioremediation of PAH-contaminated soil: assessment of the degradation of contaminants and biogas production under thermophilic and mesophilic conditions, Environmental Engineering & Management Journal (EEMJ), 14 (2015).

[241] S. Zhang, Q. Wang, S. Xie, Molecular characterization of phenanthrene-degrading methanogenic communities in leachate-contaminated aquifer sediment, International Journal of Environmental Science and Technology, 9 (2012) 705-712.

[242] A. Callaghan, B. Morris, I. Pereira, M. McInerney, R.N. Austin, J.T. Groves, J. Kukor, J. Suflita, L. Young, G. Zylstra, The genome sequence of Desulfatibacillum alkenivorans AK-01: a blueprint for anaerobic alkane oxidation, Environmental Microbiology, 14 (2012) 101-113.

[243] C.R. Toth, L.M. Gieg, Time Course-Dependent Methanogenic Crude Oil Biodegradation: Dynamics of Fumarate Addition Metabolites, Biodegradative Genes, and Microbial Community Composition, Frontiers in Microbiology, 8 (2018) 2610.

[244] Q. Ye, Z. Zhang, Y. Huang, T. Fang, Q. Cui, C. He, H. Wang, Enhancing electron transfer by magnetite during phenanthrene anaerobic methanogenic degradation, International Biodeterioration & Biodegradation, 129 (2018) 109-116.

[245] F. Beolchini, L. Rocchetti, F. Regoli, A. Dell'Anno, Bioremediation of marine sediments contaminated by hydrocarbons: experimental analysis and kinetic modeling, Journal of Hazardous Materials, 182 (2010) 403-407.

[246] T. Sayara, E. Borràs, G. Caminal, M. Sarrà, A. Sánchez, Bioremediation of PAHs-contaminated soil through composting: influence of bioaugmentation and biostimulation on contaminant biodegradation, International Biodeterioration & Biodegradation, 65 (2011) 859-865.

[247] X. Li, X. Wang, L. Wan, Y. Zhang, N. Li, D. Li, Q. Zhou, Enhanced biodegradation of aged petroleum hydrocarbons in soils by glucose addition in microbial fuel cells, Journal of Chemical Technology and Biotechnology, 91 (2016) 267-275.

[248] A. Paulo, A.F. Salvador, J. Alves, R. Castro, A. Langenhoff, A. Stams, A.J. Cavaleiro, Enhancement of methane production from 1-hexadecene by additional electron donors, Microbial Biotechnology, (2017).

[249] Q. Bach, S. Kim, S. Choi, Y. Oh, Enhancing the intrinsic bioremediation of PAH-contaminated anoxic estuarine sediments with biostimulating agents, Journal of Microbiology, Seoul, Korea, 43 (2005) 319.

[250] O. Adelaja, T. Keshavarz, G. Kyazze, The effect of salinity, redox mediators and temperature on anaerobic biodegradation of petroleum hydrocarbons in microbial fuel cells, Journal of Hazardous Materials, 283 (2015) 211-217.

[251] C. Quantin, E.J. Joner, J.M. Portal, J. Berthelin, PAH dissipation in a contaminated river sediment under oxic and anoxic conditions, Environmental Pollution, 134 (2005) 315-322.

[252] D.R. Lovley, J.D. Coates, E.L. Blunt-Harris, E.J. Phillips, J.C. Woodward, Humic substances as electron acceptors for microbial respiration, Nature, 382 (1996) 445.

[253] M. Karr, Using Humic Substances in the Bioremediation of Petroleum Polluted Soils. Personal Publication 2011.

[254] D.R. Lovley, J.L. Fraga, J.D. Coates, E.L. Blunt-Harris, Humics as an electron donor for anaerobic respiration, Environmental Microbiology, 1 (1999) 89-98.

[255] T. Sayara, M. Pognani, M. Sarrà, A. Sánchez, Anaerobic degradation of PAHs in soil: Impacts of concentration and amendment stability on the PAHs degradation and biogas production, International Biodeterioration & Biodegradation, 64 (2010) 286-292.

[256] A.S. Abdul, T.L. Gibson, D.N. Rai, Use of humic acid solution to remove organic contaminants from hydrogeologic systems, Environmental Science & Technology, 24 (1990) 328-333.

[257] D. Van Stempvoort, K. Biggar, Potential for bioremediation of petroleum hydrocarbons in groundwater under cold climate conditions: A review, Cold Regions Science and Technology, 53 (2008) 16-41.

[258] A.I. Okoh, Biodegradation alternative in the cleanup of petroleum hydrocarbon pollutants, Biotechnology and Molecular Biology Reviews, 1 (2006) 38-50.

[259] R. Bargiela, F. Mapelli, D. Rojo, B. Chouaia, J. Tornés, S. Borin, M. Richter, M.V. Del Pozo, S. Cappello, C. Gertler, Bacterial population and biodegradation potential in chronically crude oil-contaminated marine sediments are strongly linked to temperature, Scientific Reports, 5 (2015).

[260] J. Dolfing, S.R. Larter, I.M. Head, Thermodynamic constraints on methanogenic crude oil biodegradation, The ISME journal, 2 (2008) 442-452.

[261] L. Cheng, L. Dai, X. Li, H. Zhang, Y. Lu, Isolation and characterization of Methanothermobacter crinale sp. nov., a novel hydrogenotrophic methanogen from the Shengli oil field, Applied and Environmental Microbiology, 77 (2011) 5212-5219.

[262] R. Margesin, F. Schinner, Biodegradation and bioremediation of hydrocarbons in extreme environments, Applied Microbiology and Biotechnology, 56 (2001) 650-663.

[263] D. Nedwell, Effect of low temperature on microbial growth: lowered affinity for substrates limits growth at low temperature, FEMS Microbiology Ecology, 30 (1999) 101-111.

[264] A. Rodríguez-Blanco, V. Antoine, E. Pelletier, D. Delille, J.-F. Ghiglione, Effects of temperature and fertilization on total vs. active bacterial communities exposed to crude and diesel oil pollution in NW Mediterranean Sea, Environmental Pollution, 158 (2010) 663-673.

[265] D. Van Stempvoort, J. Armstrong, B. Mayer, Bacterial sulfate reduction in biodegradation of hydrocarbons in low-temperature, high-sulfate groundwater, western Canada, Proc. 2002 Petroleum Hydrocarbons and Organic Chemicals in Ground Water: Prevention, Detection, and Remediation, 19th Annual Conference and Exposition (NGWA/API), 2002, p. 244-259.

[266] M. Eriksson, E. Sodersten, Z. Yu, G. Dalhammar, W.W. Mohn, Degradation of polycyclic aromatic hydrocarbons at low temperature under aerobic and nitrate-reducing conditions in enrichment cultures from northern soils, Applied and Environmental Microbiology, 69 (2003) 275-284.

[267] A.L. Giudice, V. Bruni, M. De Domenico, L. Michaud, Psychrophiles-cold-adapted hydrocarbon-degrading microorganisms, Handbook of Hydrocarbon and Lipid Microbiology, Springer, 2010, p. 1897-1921.

[268] R.L. Dias, L. Ruberto, E. Hernández, S.C. Vázquez, A.L. Balbo, M.T. Del Panno, W.P. Mac Cormack, Bioremediation of an aged diesel oil-contaminated Antarctic soil: Evaluation of the “on site” biostimulation strategy using different nutrient sources, International Biodeterioration & Biodegradation, 75 (2012) 96-103.

[269] F. Espínola, H.M. Dionisi, S. Borglin, C.J. Brislawn, J.K. Jansson, W.P. Mac Cormack, J. Carroll, S. Sjöling, M. Lozada, Metagenomic analysis of subtidal sediments from polar and subpolar coastal environments highlights the relevance of anaerobic hydrocarbon degradation processes, Microbial Ecology, 75 (2018) 123-139.

[270] D.S. Sampaio, J.R.B. Almeida, H.E. de Jesus, A.S. Rosado, L. Seldin, D. Jurelevicius, Distribution of anaerobic hydrocarbon-degrading bacteria in soils from King George Island, Maritime Antarctica, Microbial Ecology, 74 (2017) 810-820.

[271] R. Malavenda, C. Rizzo, L. Michaud, B. Gerçe, V. Bruni, C. Syldatk, R. Hausmann, A.L. Giudice, Biosurfactant production by Arctic and Antarctic bacteria growing on hydrocarbons, Polar Biology, 38 (2015) 1565-1574.

[272] P.M. Domingues, A. Almeida, L.S. Leal, N.C. Gomes, Â. Cunha, Bacterial production of biosurfactants under microaerobic and anaerobic conditions, Reviews in Environmental Science and Bio/Technology, 16 (2017) 239-272.

[273] F. Zhao, F. Ma, R. Shi, J. Zhang, S. Han, Y. Zhang, Production of rhamnolipids by Pseudomonas aeruginosa is inhibited by H2S but resumes in a co-culture with P. stutzeri: applications for microbial enhanced oil recovery, Biotechnology Letters, 37 (2015) 1803-1808.

[274] S.E. Lowe, M.K. Jain, J.G. Zeikus, Biology, ecology, and biotechnological applications of anaerobic bacteria adapted to environmental stresses in temperature, pH, salinity, or substrates, Microbiological Reviews, 57 (1993) 451-509.

[275] R. Lepik, Biodegradability of phenolic compounds as single and mixed substrates by ctivated ludge, 2011.

[276] G.A. Hambrick, R.D. DeLaune, W. Patrick, Effect of estuarine sediment pH and oxidation-reduction potential on microbial hydrocarbon degradation, Applied and Environmental Microbiology, 40 (1980) 365-369.

[277] A.N. Roychoudhury, Sulfate respiration in extreme environments: a kinetic study, Geomicrobiology Journal, 21 (2004) 33-43.

[278] L.L. Barton, F.A. Tomei, Characteristics and activities of sulfate-reducing bacteria, Sulfate-Reducing Bacteria, Springer, 1995, p. 1-32.

[279] D. Fortin, B. Davis, T. Beveridge, Role of Thiobacillus and sulfate-reducing bacteria in iron biocycling in oxic and acidic mine tailings, FEMS Microbiology Ecology, 21 (1996) 11-24.

[280] V. O'Flaherty, T. Mahony, R. O'Kennedy, E. Colleran, Effect of pH on growth kinetics and sulphide toxicity thresholds of a range of methanogenic, syntrophic and sulphate-reducing bacteria, Process Biochemistry, 33 (1998) 555-569.

[281] C.-H. Li, Y.-S. Wong, H.-Y. Wang, N.F.-Y. Tam, Anaerobic biodegradation of PAHs in mangrove sediment with amendment of NaHCO3, Journal of Environmental Sciences, 30 (2015) 148-156.

[282] R. Brunet, L. Garcia-Gil, Sulfide-induced dissimilatory nitrate reduction to ammonia in anaerobic freshwater sediments, FEMS Microbiology Ecology, 21 (1996) 131-138.

[283] I. Koike, A. Hattori, Denitrification and ammonia formation in anaerobic coastal sediments, Applied and Environmental Microbiology, 35 (1978) 278-282.

[284] D. Minai-Tehrani, S. Minoui, A. Herfatmanesh, Effect of salinity on biodegradation of polycyclic aromatic hydrocarbons (PAHs) of heavy crude oil in

soil, Bulletin of Environmental Contamination and Toxicology, 82 (2009) 179-184.

[285] O. Lefebvre, Z. Tan, S. Kharkwal, H.Y. Ng, Effect of increasing anodic NaCl concentration on microbial fuel cell performance, Bioresource Technology, 112 (2012) 336-340.

[286] C.A. Nicholson, Biodegradation of petroleum hydrocarbons by halophilic and halotolerant microorganisms, in, Oklahoma State University, 2005.

[287] S. Le Borgne, D. Paniagua, R. Vazquez-Duhalt, Biodegradation of organic pollutants by halophilic bacteria and archaea, Journal of Molecular Microbiology and Biotechnology, 15 (2008) 74-92.

[288] X. Li, X. Wang, Y. Zhang, Q. Zhao, B. Yu, Y. Li, Q. Zhou, Salinity and conductivity amendment of soil enhanced the bioelectrochemical degradation of petroleum hydrocarbons, Scientific Reports, 6 (2016) 32861.

[289] L. Tremblay, S.D. Kohl, J.A. Rice, J.-P. Gagné, Effects of temperature, salinity, and dissolved humic substances on the sorption of polycyclic aromatic hydrocarbons to estuarine particles, Marine Chemistry, 96 (2005) 21-34.

[290] J. Means, Influence of salinity upon sediment-water partitioning of aromatic hydrocarbons, Marine Chemistry, 51 (1995) 3-16.

[291] L. Ke, W. Bao, L. Chen, Y.S. Wong, N.F. Tam, Effects of humic acid on solubility and biodegradation of polycyclic aromatic hydrocarbons in liquid media and mangrove sediment slurries, Chemosphere, 76 (2009) 1102-1108.

[292] F.I. Khan, T. Husain, R. Hejazi, An overview and analysis of site remediation technologies, Journal of Environmental Management, 71 (2004) 95-122.

[293] H.K. Hansen, L.M. Ottosen, A.B. Ribeiro, Electrokinetic soil remediation: an overview, Electrokinetics Across Disciplines and Continents, Springer, 2016, p. 3-18.

[294] S. Shin, G.V. Chilingar, M. Haroun, B. Ghosh, N. Meshkati, S. Pamukcu, J.K. Wittle, M. Al Badawi, The effect of generated chlorine gas on electroremediation of heavy metals from offshore muds, Journal of Environmental Protection, 3 (2012) 363.

[295] M. Masi, Electrokinetic remediation of heavy metal-contaminated marine sediments: experiments and modelling, Doctoral Dissertation. ISBN 978-88-90228-92-6. University of Pisa, 2017.

[296] J. Virkutyte, M. Sillanpää, P. Latostenmaa, Electrokinetic soil remediation—critical overview, Science of the Total Environment, 289 (2002) 97-121.

[297] S. Pamukcu, J. Kenneth Wittle, Electrokinetic removal of selected heavy metals from soil, Environmental Progress, 11 (1992) 241-250.

[298] E. Lindgren, M. Kozak, E. Mattson, Electrokinetic remediation of contaminated soils: an update, Sandia National Lab.(SNL-NM), Albuquerque, NM (United States), 1991.

[299] Y.B. Acar, A.N. Alshawabkeh, Principles of electrokinetic remediation, Environmental Science & Technology, 27 (1993) 2638-2647.

[300] A.N. Alshawabkeh, Theoretical and experimental modeling of removing contaminants from soils by an electric field, Agricultural and Mechanical College, Louisiana State University, 1994.

[301] R. Lageman, Electroreclamation. Applications in the netherlands, Environmental science & technology, 27 (1993) 2648-2650.

[302] S.V. Ho, C. Athmer, P.W. Sheridan, B.M. Hughes, R. Orth, D. McKenzie, P.H. Brodsky, A. Shapiro, R. Thornton, J. Salvo, The Lasagna technology for in situ soil remediation. 1. Small field test, Environmental Science & Technology, 33 (1999) 1086-1091.

[303] V. Boeva, Distribution of ammonium nitrate as nitrogen containing nutrient for in-situ biodegradation by means of electrokinetics, Master's Thesis. Concordia University, Montreal, Canada. 1995.

[304] S. Thevanayagam, T. Rishindran, Injection of nutrients and TEAs in clayey soils using electrokinetics, Journal of Geotechnical and Geoenvironmental Engineering, 124 (1998) 330-338.

[305] M. Pazos, E. Rosales, T. Alcántara, J. Gómez, M. Sanromán, Decontamination of soils containing PAHs by electroremediation: a review, Journal of Hazardous Materials, 177 (2010) 1-11.

[306] J. Gómez, M. Alcántara, M. Pazos, M. Sanromán, A two-stage process using electrokinetic remediation and electrochemical degradation for treating benzo [a] pyrene spiked kaolin, Chemosphere, 74 (2009) 1516-1521.

[307] C. Wang, Z. Zhang, W. Xu, H. Sun, Electrokinetic-assisted bioremediation of field soil with historic polycyclic aromatic hydrocarbon contamination, Environmental Engineering Science, 33 (2016) 44-52.

[308] T. Li, Y. Wang, S. Guo, X. Li, Y. Xu, Y. Wang, X. Li, Effect of polarity-reversal on electrokinetic enhanced bioremediation of Pyrene contaminated soil, Electrochimica Acta, 187 (2016) 567-575.

[309] D. Huang, Z. Ai, J. Tan, Y. Zhao, J. Fu, Degradation of benzo [a] pyrene (BaP) in clay soil by electro-bioremediation, Green Building, Environment, Energy and

Civil Engineering: Proceedings of the 2016 International Conference on Green Building, Materials and Civil Engineering (GBMCE 2016), April 26-27 2016, Hong Kong, PR China, CRC Press, 2016, p. 175.

[310] M. Alcántara, J. Gómez, M. Pazos, M. Sanromán, Electrokinetic remediation of PAH mixtures from kaolin, Journal of Hazardous Materials, 179 (2010) 1156-1160.

[311] A.N. Alshawabkeh, R.M. Bricka, D.B. Gent, Pilot-scale electrokinetic cleanup of lead-contaminated soils, Journal of Geotechnical and Geoenvironmental Engineering, 131 (2005) 283-291.

[312] A. Colacicco, G. De Gioannis, A. Muntoni, E. Pettinao, A. Polettini, R. Pomi, Enhanced electrokinetic treatment of marine sediments contaminated by heavy metals and PAHs, Chemosphere, 81 (2010) 46-56.

[313] A.N. Alshawabkeh, Y.B. Acar, Electrokinetic remediation. II: Theoretical model, Journal of Geotechnical Engineering, 122 (1996) 186-196.

[314] A.N. Alshawabkeh, Electrokinetic soil remediation: challenges and opportunities, Separation Science and Technology, 44 (2009) 2171-2187.

[315] R. Azzam, W. Oey, The utilization of electrokinetics in geotechnical and environmental engineering, Transport in Porous Media, 42 (2001) 293-314.

[316] Q. Luo, X. Zhang, H. Wang, Y. Qian, The use of non-uniform electrokinetics to enhance in situ bioremediation of phenol-contaminated soil, Journal of Hazardous Materials, 121 (2005) 187-194.

[317] M. Pazos, M. Ricart, M. Sanromán, C. Cameselle, Enhanced electrokinetic remediation of polluted kaolinite with an azo dye, Electrochimica Acta, 52 (2007) 3393-3398.

[318] K.R. Reddy, U.S. Parupudi, S.N. Devulapalli, C.Y. Xu, Effects of soil composition on the removal of chromium by electrokinetics, Journal of Hazardous Materials, 55 (1997) 135-158.

[319] E. Lindgren, E. Mattson, M. Kozak, Electrokinetic remediation of unsaturated soils, ACS Publications, 1994.

[320] E. Lindgren, M. Kozak, E. Mattson, Electrokinetic Remediation of Contaminated Soils, Sandia National Labs., Albuquerque,,NM. 1992.

[321] E. Lindgren, E. Mattson, M. Kozak, Electrokinetic remediation of unsaturated soils, ACS symposium series (USA), 1994.

[322] K.R. Reddy, U.S. Parupudi, Removal of chromium, nickel and cadmium from clays by in-situ electrokinetic remediation, Soil and Sediment Contamination, 6 (1997) 391-407.

[323] K.R. Reddy, S. Chinthamreddy, Effects of initial form of chromium on electrokinetic remediation in clays, Advances in Environmental Research, 7 (2003) 353-365.

[324] M. Pazos, C. Cameselle, M. Sanromán, Remediation of dye-polluted kaolinite by combination of electrokinetic remediation and electrochemical treatment, Environmental Engineering Science, 25 (2008) 419-428.

[325] A. Özcan, Ç. Ömeroğlu, Y. Erdoğan, A.S. Özcan, Modification of bentonite with a cationic surfactant: an adsorption study of textile dye Reactive Blue 19, Journal of hazardous materials, 140 (2007) 173-179.

[326] J. Subhashini, S. Mahipal, G. Reddy, P. Reddanna, C-Phycocyanin, a biliprotein from Spirulina platensis: anti-oxidant, anti-inflammatory and, Traditional Systems of Medicine, (2006) 395.

[327] D. Stanic-Vucinic, S. Minic, M.R. Nikolic, T.C. Velickovic, Spirulina phycobiliproteins as food components and complements, IntechOpen. (2018). 130-149

[328] L. Sala, F. Figueira, G. Cerveira, C. Moraes, S. Kalil, Kinetics and adsorption isotherm of C-phycocyanin from Spirulina platensis on ion-exchange resins, Brazilian Journal of Chemical Engineering, 31 (2014) 1013-1022.

[329] F. Wang, Y.-H. Liu, Y. Ma, Z.-G. Cui, L.-L. Shao, Application of TMA-PEG to promote C-phycocyanin extraction from S. platensis in the PEG ATPS, Process Biochemistry, 52 (2017) 283-294.

[330] A.M.S. Solano, S. Garcia-Segura, C.A. Martínez-Huitle, E. Brillas, Degradation of acidic aqueous solutions of the diazo dye Congo Red by photo-assisted electrochemical processes based on Fenton's reaction chemistry, Applied Catalysis B: Environmental, 168 (2015) 559-571.

[331] K. Hunger, Industrial dyes: chemistry, properties, applications, John Wiley & Sons, 2007.

[332] A. Białk-Bielińska, J. Kumirska, P. Stepnowski, What do we know about the chronic and mixture toxicity of the residues of sulfonamides in the environment?, Organic Pollutants-Monitoring, Risk and Treatment, InTech, 2013.

[333] C. Rendal, K.O. Kusk, S. Trapp, Optimal choice of pH for toxicity and bioaccumulation studies of ionizing organic chemicals, Environmental Toxicology and Chemistry, 30 (2011) 2395-2406.

[334] Y. Zhao, J. Geng, X. Wang, X. Gu, S. Gao, Tetracycline adsorption on kaolinite: pH, metal cations and humic acid effects, Ecotoxicology, 20 (2011) 1141-1147.

[335] A.M. Pereira, L.J. Silva, L.M. Meisel, A. Pena, Fluoroquinolones and tetracycline antibiotics in a Portuguese aquaculture system and aquatic surroundings: occurrence and environmental impact, Journal of Toxicology and Environmental Health, Part A, 78 (2015) 959-975.

[336] D. Ren, S. Zhou, Q. Li, C. Wang, S. Zhang, H. Zhang, Enhanced electrokinetic remediation of quinoline-contaminated soils, Toxicological & Environmental Chemistry, 98 (2016) 585-600.

[337] N. Reynier, J.F. Blais, G. Mercier, S. Besner, Decontamination of metals, pentachlorophenol, and polychlorined dibenzo-p-dioxins and dibenzofurans polluted soil in alkaline conditions using an amphoteric biosurfactant, Environmental technology, 35 (2014) 177-186.

[338] V. Vyskocil, J. Barek, Electroanalysis of nitro and amino derivatives of polycyclic aromatic hydrocarbons, Current Organic Chemistry, 15 (2011) 3059-3076.

[339] M. Muz, J.P. Dann, F. Jäger, W. Brack, M. Krauss, Identification of Mutagenic Aromatic Amines in River Samples with Industrial Wastewater Impact, Environmental Science & Technology, 51 (2017) 4681-4688.

[340] Z. Li, J.-W. Yu, I. Neretnieks, Removal of Pb (II), Cd (II) and Cr (III) from sand by electromigration, Journal of Hazardous Materials, 55 (1997) 295-304.

[341] L. Van Cauwenberghe, Electrokinetics, Ground-Water Remediation Technology Analysis Center, (1997) 97-103.

[342] Y.B. Acar, M.F. Rabbi, E.E. Ozsu, Electrokinetic injection of ammonium and sulfate ions into sand and kaolinite beds, Journal of Geotechnical and Geoenvironmental Engineering, 123 (1997) 239-249.

[343] C. Cameselle, Enhancement of electro-osmotic flow during the electrokinetic treatment of a contaminated soil, Electrochimica Acta, 181 (2015) 31-38.

[344] D.G. Tarboton, Rainfall-runoff processes, Utah State University, (2003).

[345] K.-J. Kim, J.-M. Cho, K. Baek, J.-S. Yang, S.-H. Ko, Electrokinetic removal of chloride and sodium from tidelands, Journal of Applied Electrochemistry, 40 (2010) 1139-1144.

[346] G. Prentice, Electrochemical Engineering Principles, Prentice Hall. 1991.

[347] M. Abderrahmene, B. AbdelIllah, G. Fouad, Electrical prediction of tortuosity in porous media, Energy Procedia, 139 (2017) 718-724.

[348] M. Boufadel, Personal Communication.

[349] R.K. Rowe, K. Badv, Chloride migration through clayey silt underlain by fine sand or silt, Journal of Geotechnical Engineering, 122 (1996) 60-68.

[350] A.F.S. Huweg, Modelling of electrokinetic phenomena in soils, Doctoral Dissertation, University of Southern Queensland, 2013.

[351] M. Rauf, S. Bukallah, F. Hamour, A. Nasir, Adsorption of dyes from aqueous solutions onto sand and their kinetic behavior, Chemical Engineering Journal, 137 (2008) 238-243.

[352] T. Paillat, E. Moreau, P. Grimaud, G. Touchard, Electrokinetic phenomena in porous media applied to soil decontamination, IEEE Transactions on Dielectrics and Electrical Insulation, 7 (2000) 693-704.

[353] E. Mena, J. Villaseñor, M.A. Rodrigo, P. Cañizares, Electrokinetic remediation of soil polluted with insoluble organics using biological permeable reactive barriers: effect of periodic polarity reversal and voltage gradient, Chemical Engineering Journal, 299 (2016) 30-36.

[354] G. Martelli, C. Folli, L. Visai, M. Daglia, D. Ferrari, Thermal stability improvement of blue colorant C-Phycocyanin from Spirulina platensis for food industry applications, Process Biochemistry, 49 (2014) 154-159.

[355] M.M. Page, C.L. Page, Electroremediation of contaminated soils, Journal of Environmental Engineering, 128 (2002) 208-219.

[356] K. Beddiar, T. Fen-Chong, A. Dupas, Y. Berthaud, P. Dangla, Role of pH in electro-osmosis: experimental study on NaCl–water saturated kaolinite, Transport in Porous Media, 61 (2005) 93-107.

[357] R.E. Saichek, K.R. Reddy, Surfactant-enhanced electrokinetic remediation of polycyclic aromatic hydrocarbons in heterogeneous subsurface environments, Journal of Environmental Engineering and Science, 4 (2005) 327-339.

[358] J. Blewett, W. McCarter, T. Chrisp, G. Starrs, An experimental study on ionic migration through saturated kaolin, Engineering Geology, 70 (2003) 281-291.

[359] K.R. Reddy, K.S. Chandhuri, Fenton-like oxidation of polycyclic aromatic hydrocarbons in soils using electrokinetics, Journal of Geotechnical and Geoenvironmental Engineering, 135 (2009) 1429-1439.

[360] S.A. Wise, L.C. Sander, M.M. Schantz, Analytical methods for determination of polycyclic aromatic hydrocarbons (PAHs)—a historical perspective on the 16 US EPA priority pollutant PAHs, Polycyclic Aromatic Compounds, 35 (2015) 187-247.

[361] S. Lundstedt, Analysis of PAHs and their transformations products in contaminated soil and remedial processes. Doctoral Thesis, Department of Chemistry, Umea University, Kemi, 2003.

[362] S. Mallick, S. Chatterjee, T.K. Dutta, A novel degradation pathway in the assimilation of phenanthrene by Staphylococcus sp. strain PN/Y via meta-cleavage of 2-hydroxy-1-naphthoic acid: formation of trans-2, 3-dioxo-5-(2′-hydroxyphenyl)-pent-4-enoic acid, Microbiology, 153 (2007) 2104-2115.

[363] A. Gupte, A. Tripathi, H. Patel, D. Rudakiya, S. Gupte, Bioremediation of polycyclic aromatic hydrocarbon (PAHs): a perspective, Open Biotechnology Journal, 10 (2016) 363-378.

[364] I.D. Bossert, R. Bartha, Structure-biodegradability relationships of polycyclic aromatic hydrocarbons in soil, Bulletin of Environmental Contamination and Toxicology, 37 (1986) 490-495.

[365] S. Gao, J.-S. Seo, J. Wang, Y.-S. Keum, J. Li, Q.X. Li, Multiple degradation pathways of phenanthrene by Stenotrophomonas maltophilia C6, International Biodeterioration & Biodegradation, 79 (2013) 98-104.

[366] S.K. Samanta, A.K. Chakraborti, R.K. Jain, Degradation of phenanthrene by different bacteria: evidence for novel transformation sequences involving the formation of 1-naphthol, Applied Microbiology and Biotechnology, 53 (1999) 98-107.

[367] K.H. Wammer, C.A. Peters, Polycyclic aromatic hydrocarbon biodegradation rates: a structure-based study, Environmental Science & Technology, 39 (2005) 2571-2578.

[368] A.P. Khodadoust, R. Bagchi, M.T. Suidan, R.C. Brenner, N.G. Sellers, Removal of PAHs from highly contaminated soils found at prior manufactured gas operations, Journal of Hazardous Materials, 80 (2000) 159-174.

[369] W.D. Weissenfels, M. Beyer, J. Klein, Degradation of phenanthrene, fluorene and fluoranthene by pure bacterial cultures, Applied Microbiology and Biotechnology, 32 (1990) 479-484.

[370] X.-X. Zhang, S.-P. Cheng, Z. Cheng-Jun, S. Shi-Lei, Microbial PAH-Degradation in Soil: Degradation Pathways and Contributing Factors1, Pedosphere, 16 (2006) 555-565.

[371] H.W. Zhou, T.G. Luan, F. Zou, N.F.Y. Tam, Different bacterial groups for biodegradation of three-and four-ring PAHs isolated from a Hong Kong mangrove sediment, Journal of Hazardous Materials, 152 (2008) 1179-1185.

[372] B. Boldrin, A. Tiehm, C. Fritzsche, Degradation of phenanthrene, fluorene, fluoranthene, and pyrene by a Mycobacterium sp, Applied and Environmental Microbiology, 59 (1993) 1927-1930.

[373] R.-H. Peng, A.-S. Xiong, Y. Xue, X.-Y. Fu, F. Gao, W. Zhao, Y.-S. Tian, Q.-H. Yao, Microbial biodegradation of polyaromatic hydrocarbons, FEMS Microbiology Reviews, 32 (2008) 927-955.

[374] M. Rozycki, R. Bartha, Problems associated with the use of azide as an inhibitor of microbial activity in soil, Applied and Environmental Microbiology, 41 (1981) 833-836.

[375] J.W. Costerton, Z. Lewandowski, D.E. Caldwell, D.R. Korber, H.M. Lappin-Scott, Microbial biofilms, Annual Reviews in Microbiology, 49 (1995) 711-745.

[376] A. Spormann, Physiology of microbes in biofilms, Bacterial Biofilms, Springer, 2008, p. 17-36.

[377] R.L. Stingley, A.A. Khan, C.E. Cerniglia, Molecular characterization of a phenanthrene degradation pathway in Mycobacterium vanbaalenii PYR-1, Biochemical and Biophysical Research Communications, 322 (2004) 133-146.

[378] Y. Zhang, J. Wong, P. Liu, M. Yuan, Heterogeneous photocatalytic degradation of phenanthrene in surfactant solution containing TiO2 particles, Journal of Hazardous Materials, 191 (2011) 136-143.

[379] Q. Luo, H. Wang, X. Zhang, X. Fan, Y. Qian, In situ bioelectrokinetic remediation of phenol-contaminated soil by use of an electrode matrix and a rotational operation mode, Chemosphere, 64 (2006) 415-422.

[380] K. Lees, M. Fitzsimons, J. Snape, A. Tappin, S. Comber, Soil sterilisation methods for use in OECD 106: How effective are they?, Chemosphere, (2018).

[381] M. Bueno-Montes, D. Springael, J.-J. Ortega-Calvo, Effect of a nonionic surfactant on biodegradation of slowly desorbing PAHs in contaminated soils, Environmental science & technology, 45 (2011) 3019-3026.

[382] D. Jin, X. Jiang, X. Jing, Z. Ou, Effects of concentration, head group, and structure of surfactants on the degradation of phenanthrene, Journal of Hazardous Materials, 144 (2007) 215-221.

[383] R.S. Makkar, K.J. Rockne, Comparison of synthetic surfactants and biosurfactants in enhancing biodegradation of polycyclic aromatic hydrocarbons, Environmental Toxicology and Chemistry: An International Journal, 22 (2003) 2280-2292.

[384] D. Schmidt-Etkin, Spill occurrences: a world overview, Oil spill science and technology, Elsevier, 2011, p. 7-48.

[385] Y.J. Xu, S. Li, W. Zhang, L.Y. Fan, J. Shao, C.X. Cao, Moving reaction boundary and isoelectric focusing: IV. Systemic study on Hjertén's pH gradient mobilization, Journal of Separation Science, 32 (2009) 585-596.

[386] A.N. Alshawabkeh, Theoretical and experimental modeling of removing contaminants from soils by an electric field, Doctoral Dissertation, Louisiana State Univeristy and Agricultural & Mechanical College. (1994).